Three Essays in Quantitative Finance

Dissertation
submitted to the
Faculty of Business, Economics and Informatics
of the University of Zurich

to obtain the degree of
Doktor der Wirtschaftswissenschaften, Dr. oec.
(corresponds to Doctor of Philosophy, PhD)

presented by

Felix Matthys

from Zürich, Switzerland

approved in October 2014 at the request of

Prof. Dr. Markus Leippold
Prof. Dr. Loriano Mancini

The Faculty of Business, Economics and Informatics of the University of Zurich hereby authorizes the printing of this dissertation, without indicating an opinion of the views expressed in the work.

Zurich, October 22, 2014.

The Chairman of the Doctoral Committee: Prof. Dr. Josef Zweimüller.

Acknowledgements

I dedicate this thesis to my beloved parents, my mother Evelyne who unexpectedly passed away on January 13th 2009, and father Felix, who passed away on December 20th 2015.

I want to express my gratitude to Prof. Dr. Markus Leippold, my thesis supervisor, for his support, encouragement and advice, and for the great work atmosphere I could benefit from. It was a great pleasure to work with him during my PhD studies. I would like to further thank my co-supervisor Prof. Dr. Loriano Mancini for accepting to be on my PhD committee.

Furthermore, I am also very grateful to Prof. Dr. Yacine Aït-Sahalia who invited me to come to Princeton University and gave me the great opportunity to work with him on a very interesting topic. His comments and suggestions have improved my papers substantially and I am very glad to be given this chance to collaborate with him.

I would also like to thank Prof. Dr. Walter Farkas and Prof. Dr. Marc Paolella for always being encouraging and for the career advice they gave me.

Furthermore, I would like to thank all the faculty members at the Bendheim Center for Finance and the Woodrow Wilson School of Economics for giving me valuable feedback for all my projects, most notably Yacine Aït-Sahalia, Christopher Sims, Markus Brunnermeier, Valentin Haddad, Oleg Itskhoki, Wei Xiong and Jakub Jurek.

Additionally, I would like to thank Jan Homann and Gabriel Tenorio for proofreading my thesis.

Furthermore, I am very thankful to be given the chance to work in such a wonderful chair and I have enjoyed my time as a team member throughout my entire PhD studies. Special thanks to my colleagues and friends Nikola Vasiljevic, Olivier Darmouni, Michael Sockin, Chris Moser, Gabriele La Spada, Lujing Su, Ji Huang, Jeong Ho John Kim, Chris Bardgett and Meriton Ibraimi, for always being ready to help, for all the insightful and entertaining conversations we shared and for all the good times we had together.

Finally I wish to express my deep gratitude to my wonderful wife Fernanda Marquez, who always supported me in both the good and bad times.

Princeton NJ, August 2014 Felix Matthys

Contents

Chapter 1

Introduction and Summary of Research Results

This doctoral thesis entitled "Three Essays in Quantitative Finance" comprises three independent papers.

In *Chapter 1*, we study the impact of economic policy uncertainty on the term structure of nominal interest rates. We develop a general equilibrium model, in which the real side of the economy is driven by government policy uncertainty and the central bank sets money supply endogenously following a Taylor rule. We analyze the impact of government and monetary policy uncertainty on nominal yields, short rates, bond risk premia, and the term structure of bond yield volatility. Our affine yield curve model is able to capture both the shape of the interest rate term structure as well as the hump-shape of bond yield volatilities. Our empirical analysis shows that higher government policy uncertainty leads to a decline in yields and an increase in bond yield volatility, whereas monetary policy uncertainty has no significant contemporaneous effect on yields nor volatilities. However, it is an important predictor for bond risk premia.

In *Chapter 2*, we study the consumption-portfolio allocation problem in continuous time when asset prices follow Lévy processes and the investor is concerned about potential model

misspecification. We derive optimal portfolio holdings in closed form under model uncertainty, incorporating perturbations to the reference model affecting both the drift and jump intensity. We then present a method for calculating error-detection probabilities by means of Fourier inversion of the conditional characteristic function in the case when the measure change follows a jump-diffusion process.

In *Chapter 3*, we present a novel method in analyzing microstructure noise of high-frequency data as a measurement error problem. In particular, we study the estimation of endogenous Markov-switching regression models, in which the regression disturbance and the latent state variable controlling the regime are correlated. We show infill asymptotic results and prove that under endogeneity the popular realized variance estimator is biased and no longer converges to the integrated regime dependent volatility. Exploring high-frequency intraday return data on foreign exchange rates, we find that the state variable is indeed endogenous. Similar to the popular volatility signature plot, we propose an endogeneity plot which indicates as to which sampling frequency the assumption of exogeneity of the state variable controlling the regime remains valid.

Part I

Research Papers

Chapter 2

Economic Policy Uncertainty and the Yield Curve

Felix Matthys[1]

I have presented this paper at:

- Finance and Math Seminar ETH and University of Zurich, May 2013
- 12th Doctorial Workshop in Finance at Gerzensee, June 2013
- The Princeton Student Research Workshop, December 2013 and November 2014
- PhD Defense, Zurich, September 2014
- Bank of England Macro Financial Analysis Division, London, December 2014

[1]This paper benefited greatly from discussions with Yacine Aït-Sahalia, Caio Almeida, Markus Brunnermeier, Jérôme Detemple, Itamar Drechsler, Darell Duffie, Fabio Trojani, Valentin Haddad, Oleg Itskhoki, Jakub Jurek, Philippe Mueller, Jean-Charles Rochet, Christopher Sims, David Srear, Adi Sunderam, Josef Teichmann, and Wei Xiong. For helpful comments we would like to thank the seminar participants of the 2015 SAFE Asset Pricing Workshop in Frankfurt, the Finance and Math Seminar ETH and University of Zurich, the 12th Doctorial Workshop in Finance at Gerzensee, the Princeton Student Research Workshop, Financial Mathematics Seminar at ORFE Princeton University, Bank of England, Central Bank of Mexico, and ITAM. Financial support from the Swiss Finance Institute (SFI), Bank Vontobel, the Swiss National Science Foundation and the National Center of Competence in Research "Financial Valuation and Risk Management" is gratefully acknowledged.

Abstract

We study the impact of economic policy uncertainty on the term structure of nominal interest rates. We develop a general equilibrium model, in which the real side of the economy is driven by government policy uncertainty and the central bank sets money supply endogenously following a Taylor rule. We analyze the impact of government and monetary policy uncertainty on nominal yields, short rates, bond risk premia, and the term structure of bond yield volatility. Our affine yield curve model is able to capture both the shape of the interest rate term structure as well as the hump-shape of bond yield volatilities. Our empirical analysis shows that higher government policy uncertainty leads to a decline in yields and an increase in bond yield volatility, whereas monetary policy uncertainty has no significant contemporaneous effect on yields nor volatilities. However, it is an important predictor for bond risk premia.

2.1 Introduction

Economic policy is driven by government and central banking actions. Governments define fiscal policy and impose regulations, while central banks manage the money supply and set nominal short rates. These policies have a fundamental impact on financial markets. However, despite good intentions their effectiveness remains uncertain at best. In this paper, we explore the impact of such policy uncertainty on the term structure of interest rates, its corresponding volatility curve, and on bond risk premia. We develop a general equilibrium model, in which the real side of the economy is subject to government policy uncertainty and the nominal side of the economy is affected by monetary policy shocks. Our model setup allows us to derive an approximate analytical solution for the general equilibrium in the case where the representative agents has CRRA-utility. A key model device is the assumption of the central bank following a Taylor rule, which links the real with the nominal side of the economy and turns out to be crucial in reproducing the salient features of the nominal term structure and its volatility curve.

Our general equilibrium framework builds upon Buraschi & Jiltsov (2005). However, the key distinction is that for our representative agent we depart from the log-utility assumption and impose a constant relative risk aversion (CRRA) utility. It is well known that for such a utility specification, no closed-form solution for the term structure of interest rates can be obtained. Using perturbation methods, we find that the agents' optimal controls remain affine in the state variables up to a first order approximation in the risk aversion coefficient. This result allows us to study the effect of changing risk aversion on the term structure of interest rates and the yield volatility curve, which previous papers such as Buraschi & Jiltsov (2005) or Ulrich (2013*a*) were not able to do, and which turn out to be non-trivial.

In our model, both government and monetary policy uncertainty are affecting nominal yields, the term structure of volatility, and bond risk premia in a fundamentally different way. An increase in government policy uncertainty adversely affects the trend component of real output growth. Therefore, it renders capital investments more risky, which will eventually induce investors to favor safe assets such as government bonds. Such a flight-to-quality behavior will raise government bond prices and therefore drives down its yields. This observation is in line with Bloom (2009), who argues that productivity growth falls, because higher uncertainty causes firms to temporarily pause their investment. Moreover, in our model economy higher government policy uncertainty will not only negatively affect the long run growth path of production. It also increases its volatility and therefore leads to a worsening of economic growth prospects, which are fundamental to the agents consumption-investment allocation problem.[2]

Not only does government policy uncertainty play an important role in determining the level of interest rates, but it has also a crucial impact on the level and shape of the term

[2]Our model is similar in style to the long run risk model of Bansal & Yaron (2004). However, the key distinctive difference is that the long run growth component and the market price of output risk are both driven by the same underlying risk factor, namely government policy uncertainty. Furthermore, our setting can also be compared to the literature on real business cycle analysis. For instance, shocks to trend growth exhibit fundamentally different effects on the (real) economy as opposed to transitory fluctuations. The agents or county's reaction to temporary shocks is to borrow in the short run to smooth out consumption. However, if the shock is more persistent, the long run consumption level has to be adjusted as borrowing for an infinite time horizon is not longer possible.

structure of bond yield volatilities. Although our model belongs to the class of affine models as introduced by Duffie & Kan (1996), we can replicate the typical hump-shape of the volatility term structure, caused by the empirical observation that volatility tends to be highest around the two-year maturity bucket. The key mechanism leading to this result is that government policy uncertainty negatively affects the long run growth path of productivity, which translates into a hump-shaped curve at a higher volatility level. With this amplification mechanism we can also explain the 'excess bond yield volatility puzzle' that empirical bond yields, especially at the long end of the term structure, cannot be reproduced by standard affine models of the term structure of interest rates (see Shiller (1979) and Piazzesi & Schneider (2006)).[3]

Dealing wit policy uncertainty, a fundamental question that arises in this context is: What is an appropriate measure for government and monetary policy uncertainty? As starting point, we use the economic policy uncertainty (EPU) index developed by Baker et al. (2012). According to their definition, the EPU index contains uncertainty related to both government and monetary policy. Hence, we aggregate the corresponding EPU constituents into a government (GPU) and a monetary policy uncertainty (MPU) index.

[Figure A.1 about here]

In Figure A.1 we plot the relationship between U.S. treasury bond yields and volatilities together with the EPU, GPU, and MPU index for the period of 1990 to 2014. The first two prominent spikes of the EPU index are related to the terrorist attacks on the World Trade Center and the 2nd Gulf War. By the end of 2003 and until the outbreak of the financial crisis in 2008, the US economy entered a steady economic growth phase. Both, the EPU and GPU show similar patterns. They declined in the pre-crisis period and started to peak at the onset of the financial crisis. The EPU and GPU index remain at a high level ever since, exhibiting highly volatile behavior. In contrast, the MPU index slowly reversed to its pre-

[3] A possible solution to this problem is to introduce heterogeneous agents who have different prior beliefs about some fundamental economic variable, such as for instance inflation as in Xiong & Yan (2010) or to introduce time-varying risk preference as in Buraschi & Jiltsov (2007), which are however analytically less tractable.

crisis level. We attribute this observation to the fact that the EPU and GPU index captures political uncertainty, which was especially high during the debt-ceiling crisis of 2011 and lasted until late 2013 where some governmental authorities were even forced to suspend their services temporarily.

Figure A.1 also shows that both the EPU and GPU index exhibit a countercyclical pattern with nominal yields. When the EPU or GPU index is high, yields tend to go down. This apparent negative relationship is also confirmed by computing the sample correlation coefficient, which ranges from -0.544 (EPU, 1 year) to -0.32 (GPU, 10 years) for the period January 1990 until June 2014.[4] These numbers suggest that higher economic or government policy uncertainty leads to lower treasury bond yields. Thus, as political risk increases, investors seek safer assets and therefore start to shift from stocks to (government) bonds, which is in line with the predictions in Pastor & Veronesi (2013).[5]

The discussion above suggests that government and monetary policy uncertainty may have different effects on yields and volatilities. Therefore, we not only split economic uncertainty into these two different components, but we allow government policy uncertainty to play a role for interest rate policy. The empirical analysis of the model confirms our theoretical prediction in that government policy uncertainty is the main driver in contemporaneous movements in the term structure of interest rates and its volatility curve.

There is increasing evidence that policy uncertainty leads to direct reactions of the central bank authority (see for instance David & Veronesi (2014)). To motivate a link between government policy uncertainty and yields for our model design, we estimate pairwise Vector Auto

[4]The time series correlation between the EPU and GPU (MPU) is 0.857 (0.657) and 0.572 between the GPU and MPU index. As can be inferred from Figure A.1, the monetary policy uncertainty index appears to have no link with contemporaneous movements in nominal yields. Indeed, the estimated time series correlation is roughly zero along the entire term structure. We collect the all empirical sample correlation of treasury bond yields and the EPU, GPU and MPU indexes in Table A.1 as well as realized volatility and EPU, GPU and MPU indexes in Table A.2 in Appendix A.6. Furthermore, the sample correlation between the EPU and the VIX index is 0.44 for the same period.

[5]Using also the EPU index of Baker et al. (2012), they show that political uncertainty raises not only the equity risk premium but also the volatilities and correlations of stock returns.

Regressions (VAR) for the GPU and MPU with the three-month T-bill rate, which we take as proxy for monetary policy.

[Figure A.2 about here]

Figure A.2 reports the resulting impulse responses for the time period from January 1995 to June 2014. Panel A reveals that a shock to the GPU index leads to a sustained negative impact on the short-term rate and hence on future monetary policy. This impact remains highly significant up to a time horizon of more than 20 months. In contrast, from Panel B we observe that a shock to the short-term rate has no significant impact on the GPU index.[6] This suggests that government policy uncertainty shocks drives monetary policy actions, but not the other way around. Hence, the central bank conducts its monetary policy taking into account uncertainty shocks from the real side whereas the central banks interest rate policy does not seem to affect fiscal uncertainty.

We provide a theoretical explanation for the empirical results above. In our model economy, higher real uncertainty lowers productivity growth, which feeds into the monetary policy through our assumption that the central bank controls the money supply growth following a Taylor rule. Hence, the monetary authority's efforts to stabilize growth (and inflation) causes it to react to real uncertainty by lowering the cost of capital. Moreover, since we assume money neutrality, nominal shocks do not have an impact on the real side of the economy. However, the converse is not true. The equilibrium price level growth is driven by the capital accumulation growth, which implies that the nominal side is also driven by shocks from the real side, namely government policy shocks. Through these two transmission channels, inflation and capital accumulation growth targeting, the money supply growth becomes a function of government policy uncertainty. Therefore, by letting the central bank react endogenously to deviations from long

[6]Further analyzing the impulse responses from our VAR model, we find that the MPU index has a similar behavior as the GPU index in that it does (negatively) influence monetary policy, but the MPU does not respond to a shock in the short rate. Furthermore, the response of the short rate from a MPU shock is less pronounced than from a GPU shock. Finally, the MPU and GPU responses to GPU and MPU shocks are negligible and become insignificant after four to five months. We do not report these graphs here, but they can be obtained on request.

run capital growth and inflation targets establishes an important link between the real and the nominal side of the economy that allows government policy shocks to affect nominal quantities. This link proves to be essential in order to simultaneously match both the term structure of interest rates and its corresponding volatility curve.

Finally, we allow both monetary and government policy shocks to carry a risk premium. Hence, our model accommodates a time-varying risk premia in bond returns, which implies that monetary and government policy uncertainty are priced risk factors and the equilibrium inflation process exhibits heteroskedastic time-variation in both variables.

While our paper belongs to the class of equilibrium finance models of the term structure, it is specifically related to the following strands of literature.[7] Traditional work on asset pricing usually abstracts from modeling government uncertainty and its impact on asset prices. However, especially since the European debt crisis starting in 2010 and the 2011 Congress debate about raising the fiscal debt ceiling in the US, policy uncertainty has recently attracted interest from academia. For instance, Pastor & Veronesi (2012) and Pastor & Veronesi (2013) develop a general equilibrium model, in which the profitability of firms is driven by government policy, and discuss the impact of policy risk on stock prices. Several empirical papers have shown that uncertainty about political outcomes has a significant effect on asset returns and corporate decisions.[8] There is also a large strand of literature trying to infer political risk from government

[7]Equilibrium term structure models include, among many others, Wachter (2006), Piazzesi & Schneider (2006), Buraschi & Jiltsov (2007), Gallmeyer et al. (2007), Bekaert et al. (2009), and Bansal & Shaliastovich (2013). Recently, macro-finance term structure models have been critisized for their failure to accomodate for the presence of "unspanned macroeconomic risk," see Joslin, Priebsch & Singleton (2014). However, there is support for spanned macro-finance term structure models. Basically, Bauer & Rudebusch (2015) claim to have resolved the unspanning puzzle. Although our model belongs to the spanned model class, we do not delve further into this discussion but refer the interested reader to the two cited papers above.

[8]For instance, early studies include Rodrik (1991) or Pindyck & Solimano (1993). They show empirically that uncertainty about political factors can lead to lower investment expenditures, especially when investment is irreversible. More recently, Durnev (2010) and Julio & Yook (2012) document that firms tend to withhold their investment activity prior to national elections. Gulen & Ion (2012) argue, based on the newly developed policy index by Baker et al. (2012), that policy uncertainty reduces firm and industry level investment and that the magnitude of reduction is substantial. Boutchkova et al. (2012) take the analysis further and show that some industries are more sensitive to political uncertainty than others. Some further related articles analyzing the relationship between political uncertainty and asset returns include Belo et al. (2013), Bialkowski et al. (2008) or Bond & Goldstein (2012).

bond yields such as, e.g., Huang et al. (2013) who empirically study the relationship between political risk and government bond yields. For an overview of this literature, we refer to Bekaert et al. (2012).

While the literature on government policy impacts is sparse but growing, the fundamental link between monetary policy and the term structure of interest rates and volatilities has been studies more extensively. For the yield effects we refer to, e.g., Kuttner (2001), Piazzesi (2005), Fleming & Piazzesi (2005), Gürkaynak et al. (2005*a*), and Wright (2012). For the volatility effects see, e.g., Balduzzi et al. (2001), Piazzesi (2005) or de Goeij & Marquering (2006), among others. The literature on the link between monetary policy and bond risk premia is surveyed in Buraschi et al. (2014). In an empirical study, they find that monetary shocks are indeed an important source of priced risk, helping to explain the risk premia in bond markets. Using a standard predictability regression of excess bond returns, they find that monetary policy shocks account for a substantial part of the variance of bond excess returns, which is in line with our empirical results.

Despite the recent attention brought to modeling the impact of policy uncertainty on asset prices, the papers mentioned above either address the empirical link between government bond yields and policy uncertainty or focus on the theoretical impact that a given government policy has on stock returns. Our paper provides a theoretical framework for studying the impact of both government and monetary policy uncertainty on the nominal yield curve and its implications for the term structure of bond yield volatility.

The reminder of the paper is organized as follows. Section 2.2 presents the model. Section 2.3 discusses the impact of government as well as monetary policy uncertainty on the term structure of nominal interest rates, the yield volatility curve and the bond risk premium. Section 2.4 summarizes our empirical results and Section 2.5 concludes.

2.2 The baseline model economy

Our model economy consists of a real and a monetary sector. For the real sector, we consider a production economy with a representative agent producing a single good at a constant return-to-scale production technology. As in Buraschi & Jiltsov (2005), real monetary holdings M_t^d provide a transaction service by reducing the total amount of gross resources required for a given level of consumption C_t.

Assumption 1 (Preferences of Representative Agent)**.** *Let $\mathcal{U}(X_t)$ denote expected utility over the real net consumption holdings X and $\beta > 0$ the subjective discount factor. The agent has constant relative risk aversion (CRRA) preferences given by*

$$\mathcal{U}(X_t) = E_t\left[\int_t^\infty e^{-\beta(u-t)} U(X_u) du\right], \tag{2.1}$$

with

$$U(X_t) = \begin{cases} \frac{1}{\gamma}\left(X_t^\gamma - 1\right), & \text{if } \gamma < 1, \gamma \neq 0, \\ \log(C_t) + \xi \log\left(M_t^d\right) & \text{if } \gamma = 0, \end{cases} \tag{2.2}$$

where γ is equal to one minus the coefficient of risk aversion. In addition, the real net consumption holdings depend on both consumption C_t and real cash balances M_t^d:[9]

$$X_t = C_t (M_t^d)^\xi, \ 0 \leq \xi \leq 1. \tag{2.3}$$

The agent's real output is denoted by Y_t. The drift of Y_t is influenced by a productivity factor A_t that depends on a process g_t, which we refer to as government policy or real uncertainty.

Assumption 2 (Real Sector Dynamics)**.** *Given a filtered probability space $(\Omega, \mathcal{F}, \{\mathcal{F}_t\}_{t\geq 0}, \mathbb{P})$ satisfying the usual conditions, the dynamics of real output Y_t, productivity A_t, and government*

[9] If $\xi = 0$, money does not provide any service and $\xi = 1$ implies that the agent needs to hold exactly one unit of currency for every unit of consumption holdings. Since $0 \leq \xi \leq 1$, a higher level of monetary holdings provides a higher level of transaction services, but at a decreasing return to scale.

policy uncertainty g_t have the following dynamics:

$$\frac{dY_t}{Y_t} = (\mu_Y + q_A A_t)dt + \sigma_Y \sqrt{g_t} dW_t^Y,\ Y_0 \in \mathbb{R}_+, \tag{2.4}$$

$$dA_t = (\kappa_A(\theta_A - A_t) + \lambda g_t)\, dt + \sigma_A \sqrt{g_t} dW_t^A,\ \ A_0 \in \mathbb{R}, \tag{2.5}$$

$$dg_t = \kappa_g\,(\theta_g - g_t)\, dt + \sigma_g \sqrt{g_t} dW_t^g,\ g_0 \in (0, \infty), \tag{2.6}$$

with constants $\mu_Y > 0, q_A, \theta_A, \lambda, \kappa_i > 0, \forall i \in \{A, g\}$, $\sigma_j^2 > 0$, and $\mathbb{P}$-Brownian motions $W_t^j, \forall j \in \{Y, A, g\}$. The processes in (2.4) to (2.6) may have nonzero instantaneous correlation:

$$dW_t^Y dW_t^A = \rho^{AY} dt, \quad dW_t^Y dW_t^g = \rho^{Yg} dt, \quad dW_t^A dW_t^g = \rho^{Ag} dt. \tag{2.7}$$

Productivity A_t in Equation (2.5) is a mean reverting process with a trend and diffusion term that depend on government policy uncertainty g_t. Hence, not only is the productivity's long run mean stochastic, but also its volatility is time-varying. A crucial role is played by the parameter λ. If $\lambda < 0$ ($\lambda > 0$), an increasing g_t will have a negative (positive) effect on long run productivity. If $\lambda = 0$, we obtain a process with constant long run mean θ_A and time-varying volatility.

The government policy uncertainty process g_t in Equation (2.6) describes an unconditionally mean-reverting stationary process. It not only affects productivity A_t, but also the output growth rate dY_t/Y_t through two channels. First, g_t renders output volatility time-varying which, as we will prove in a later section, leads to a stochastic real market risk. Second, it affects the trend output growth rate indirectly as it influences the growth rate of productivity. For example, if $\lambda < 0$, higher government policy uncertainty will reduce the long run level of productivity. Provided that $q_A > 0$, this reduction leads to a decline in expected output growth. To get some further intuition about our model design, we derive the unconditional expectation, variance, and covariance of productivity and government uncertainty below.

Proposition 1 (Stationary moments of productivity and government policy uncertainty process)**.** *The unconditional expectation and variance of productivity A_t and government policy*

uncertainty g_t, and their covariance are given by[10]

$$\mathbb{E}[A_t] = \lim_{T\to\infty} \mathbb{E}_t[A_T] = \theta_A + \frac{\lambda\theta_g}{\kappa_A}, \tag{2.8}$$

$$\mathbb{V}[A_t] = \lim_{T\to\infty} \mathbb{V}_t[A_T] = \theta_g \left(\frac{\sigma_A^2}{2\kappa_A} + \frac{2\kappa_g\lambda\rho^{Ag}\sigma_A\sigma_g + \lambda^2\sigma_g^2}{2\kappa_A\kappa_g(\kappa_A+\kappa_g)} \right), \tag{2.9}$$

$$\mathbb{E}[g_t] = \lim_{T\to\infty} \mathbb{E}_t[g_T] = \theta_g,\ \mathbb{V}[g_t] = \lim_{T\to\infty} \mathbb{V}_t[g_T] = \frac{\theta_g\sigma_g^2}{2\kappa_g}, \tag{2.10}$$

$$\mathbb{C}[A_t, g_t] = \lim_{T\to\infty} \mathbb{C}_t[A_T, g_T] = \frac{\theta_g\sigma_g(2\kappa_g\rho^{Ag}\sigma_A + \lambda\sigma_g)}{2\kappa_g(\kappa_A+\kappa_g)}. \tag{2.11}$$

A first important observation is that the long run level of government policy uncertainty θ_g affects all moments. First it raises (lowers) the unconditional expected productivity growth whenever $\lambda > 0$ ($\lambda < 0$). Second, it not only raises the stationary long run level of g_t proportionally, but also the variance of A_t and g_t. Hence, an increase in θ_g will lead to higher government policy uncertainty and simultaneously also to a higher variance of productivity.

Assuming that the impact of government policy uncertainty on the drift of productivity is negative ($\lambda < 0$) and setting $\rho^{Ag} = 0$ for simplicity, the effect of λ has three important implications. First, it lowers expected growth of productivity proportionally to θ_g/κ_A. Second, it increases volatility of A_t linearly. Lastly, it renders $\mathbb{C}[A_t, g_t]$ negative, which will be of central importance to capture the stylized facts of bond yield volatility within our model.

We can now proceed with the formulation of the agent's capital budget constraint. Without loss of generality, we use capital depreciation as the only cost component.[11]

Assumption 3 (Capital budget constraint)**.** *The real return on capital that can either be allocated to consumption $C_t dt$ or cash balances $M_t^d dt$ or reinvested dK_t is given by*

$$C_t dt + M_t^d dt + dK_t = K_t \frac{dY_t}{Y_t} - \delta K_t dt, \tag{2.12}$$

where $K_t \frac{dY_t}{Y_t}$ is the change in total output and $\delta K_t dt$ is the capital depreciation with deprecation rate $\delta \in [0,1]$.

[10] By $\mathbb{E}[\cdot]$, $\mathbb{V}[\cdot]$, and $\mathbb{C}[\cdot,\cdot]$ ($\mathbb{E}_t[\cdot]$, $\mathbb{V}_t[\cdot]$, $\mathbb{C}_t[\cdot,\cdot]$) we denote the unconditional (conditional on $\mathcal{F}_t$) expectation, variance, and covariance operators.

[11] In our model, we do not include a variable cost component as was done, e.g., in Buraschi & Jiltsov (2005).

Substituting output growth from Equation (2.4), and rearranging we obtain the capital accumulation process as

$$\frac{dK_t}{K_t} = -\left(\frac{C_t}{K_t} + \frac{M_t^d}{K_t}\right) dt + (\mu_y + q_A A_t - \delta)\, dt + \sigma_y \sqrt{g_t} dW_t^Y. \tag{2.13}$$

The capital accumulation process is decreasing in the optimal control variables consumption C_t and money demand M_t^d, which is intuitive as higher C_t and/or M_t^d diminish available resources to be invested in the production technology K_t. Similar to real output, capital is nonstationary whenever $\mu_y \neq \delta$ and time-varying in productivity A_t. Furthermore, Equation (2.13) implies money-neutrality, i.e., monetary shocks do not have an effect on the real side of the economy.[12]

For the monetary sector, we assume that there exists a central bank controlling money supply M_t^S on the basis of a Taylor rule. The monetary authority targets a long term nominal constant money growth rate μ_M, a capital growth rate $\bar{k}$, and an inflation rate equal to $\bar{\pi}$. We assume that transitory deviations from the optimal long run money growth exhibit stochastic volatility. We can interpret this time-variation in money supply, denoted by m_t, as the monetary policy uncertainty factor.

[12]Whether or not real output and capital are money-shock-neutral is debated in macroeconomics for a long time. The neo-classical Keynesian literature argues that any increase in money supply has to be offset by an equivalent proportional rise in prices and wages. A recent paper using a similar setup as ours is Ulrich (2013*a*), who sticks to this neo-classical view. However, there are a number of reasons why inflation may affect the real economy. See, e.g., Fisher & Modigliani (1978), who argue that inflation has a direct influence on purchasing power, because many private contracts are not indexed. A first quantitative study that allows for dependence of the expected return on capital on inflation is Pennacchi (1991), who uses survey data to identify inflationary expectations. Another channel through which inflation can affect the real economy is through taxation of nominal asset returns. This channel was exploited by Buraschi & Jiltsov (2005) to account for the violation of the expectation hypothesis and the determination of the inflation risk premium. Since policy uncertainty affects the real and nominal side of the economy (through the endogenous equilibrium price level), we assume money-neutrality throughout the paper. However, we acknowledge that a feasible extension of our model is to let the capital accumulation process be a function of the price level. We leave this as an interesting theoretical idea which is worthwhile to be considered.

Assumption 4 (Monetary Sector)**.** *The central bank controls money supply growth according to a Taylor rule as follows:*

$$\frac{dM_t^S}{M_t^S} = \mu_M dt + \eta_1 \left(\frac{dK_t}{K_t} - \bar{k} dt \right) + \eta_2 \left(\frac{dp_t}{p_t} - \bar{\pi} dt \right) + \sigma_M \sqrt{m_t} dW_t^M, \tag{2.14}$$

$$dm_t = \kappa_m(\theta_m - m_t)dt + \sigma_m \sqrt{m_t} dW_t^m, \quad dW_t^M dW_t^m = \rho^{Mm} dt, \tag{2.15}$$

where p_t and K_t are the price level and capital accumulation process. We assume that the monetary policy innovation correlates with the money supply by ρ^{Mm}, but is independent of all other sources of risk in the economy.

The crucial parameters in Assumption 4 are η_1 and η_2 in Equation (2.14). Their magnitude determines the sensitivity of money supply growth with respect to deviations of endogenous capital and inflation from their long run target levels. For example, if output growth is above target ($\frac{dK_t^*}{K_t^*} - \bar{k}dt > 0$) and provided that $\eta_1 < 0$, the monetary authority shrinks the money supply, causing interest rates to rise and investment activity to slow down. When inflation is below target ($\frac{dp_t^*}{p_t^*} - \bar{\pi}dt < 0$) and provided that $\eta_2 < 0$, the central bank's response is to increase the money supply. In the case when $\eta_1 = \eta_2 = 0$ money supply is exogenous and therefore does not react to deviations from long run capital nor inflation growth rate. Furthermore, given the money supply rule in Equation (2.14), monetary policy uncertainty renders money supply time-varying in m_t. Having introduced both the real and monetary side of the economy, we next characterize the representative agent's equilibrium.

Definition 2 (Equilibrium Capital Stock and Money Holdings)**.** *Under Assumptions 1 to 4, the representative agent's equilibrium is defined as a vector of optimal consumption, money demand, price and capital processes $[C_t^*, M_t^{d*}, K_t^*, p_t^*]$ that is a solution to the following dynamic Hamilton-Jacobi-Bellmann programming problem*[13]

$$0 = \frac{\partial V(t, K_t, A_t, g_t)}{\partial t} + \max_{\{C_t, M_t^d\}} \left\{ U(C_t, M_t^d) + \mathcal{A}V(t, K_t, A_t, g_t) \right\}, \tag{2.16}$$

[13]By $\mathcal{A}$ we denote the infinitesimal generator. See, e.g., Øksendal (2003) for technical details.

subject to money market-clearing $M_t^S = p_t^* M_t^{d*}$*, the bugdet constraint in* (2.12)*, and the transversality condition* $\lim_{T\to\infty} \mathbb{E}_t \left[e^{-\beta T} V(t, K_t, A_t, g_t)\right] = 0$.

For the problem in Equation (2.16), an explicit solution can only be obtained for the log-utility case. The resulting optimal consumption and money demand holdings are proportional to capital K_t. However, for $\gamma \neq 0$, the asymptotic optimal controls C_t and M_t^d remain linear in the state variables K_t, A_t, and g_t (up to a first-order approximation in γ). This feature allows us to find an explicit affine representation of the term structure of real and nominal interest rates beyond the log-utility case.[14]

Proposition 3 (Perturbed equilibrium of the representative agent's investment and consumption problem)**.** *In equilibrium, the representative agent's value function is*

$$V(t, K_t, A_t, g_t) = \frac{e^{-\beta t}}{\beta\gamma}\left(\left(e^{\phi(A_t, g_t)} K_t^{1+\xi}\right)^{\gamma} - 1\right), \tag{2.17}$$

for some function $\phi(A_t, g_t)$ *of the form*

$$\phi(A_t, g_t) = \phi_0(A_t, g_t) + \gamma\phi_1(A_t, g_t) + O(\gamma^2). \tag{2.18}$$

The agent's first order asymptotic optimal controls are

$$C_t^* = \frac{\beta K_t}{1+\xi}\left[1 + \gamma\left(L - \phi_0(A_t, g_t)\right)\right], \qquad M_t^{d*} = \xi C_t^*, \tag{2.19}$$

and the equilibrium first order asymptotic capital accumulation K_t^* *and price process* p_t^* *satisfy*

$$\frac{dK_t^*}{K_t^*} = \mu_{K^*}(A_t, g_t)\, dt + \sigma_Y \sqrt{g_t} dW_t^Y, \tag{2.20}$$

$$\begin{aligned}\frac{dp_t^*}{p_t^*} = &\left[\frac{\mu_M - \eta_1 \bar{k} - \eta_2 \bar{\pi}}{1-\eta_2} + \frac{\eta_1 - 1}{1-\eta_2}\mu_{K^*}(A_t, g_t) - g_t \frac{(\eta_1 - 1)\sigma_Y^2}{1-\eta_2}\right] dt \\ &+ \frac{\sigma_M \sqrt{m_t}}{1-\eta_2} dW_t^M + \frac{(\eta_1 - 1)\sigma_Y \sqrt{g_t}}{1-\eta_2} dW_t^Y.\end{aligned} \tag{2.21}$$

where

$$\mu_{K^*}(A_t, g_t) := \mu_Y + q_A A_t - \beta - \delta + \gamma\beta\left(\phi_0(A_t, g_t) - L\right) \tag{2.22}$$

[14] Our solution strategy is based on the perturbation method. In particular, we follow the approach of Kogan & Uppal (2001) and approximate our model with respect to the risk aversion parameter around the explicit equilibrium computed under the log-utility assumption. Perturbation methods have been successfully applied in many other studies such as, e.g., Hansen et al. (2008).

denotes the equilibrium drift of the capital accumulation process and $L = \log\left(\frac{\beta^{1+\xi}\xi^{\xi}}{(1+\xi)^{1+\xi}}\right)$ *is a constant. Furthermore,*

$$\phi_0(A_t, g_t) = \phi_{00} + \phi_{0A}A_t + \phi_{0g}g_t \tag{2.23}$$

is an affine function in the state variables (A_t, g_t) *with constants* ϕ_{00}, ϕ_{0A}, ϕ_{0g} *provided in Appendix A.2.*

Since nominal shocks have no real effects, the equilibrium capital accumulation process is only driven by the real sector of the economy, i.e., by productivity A_t and by the government policy uncertainty process g_t. Note that for $\gamma = 0$ the equilibrium capital drift μ_{K^*} becomes independent of g_t. The weighting factor η_2 on inflation-target deviation enters non-linearly into the equilibrium price process.[15]

Proposition 3 also implies that the equilibrium price process is driven by both real and monetary shocks. This result is a consequence of the central bank authority controlling money supply growth based on a Taylor-rule. Hence, by endogenizing money supply growth, we allow for an important link between the real and the nominal sector and government policy uncertainty enters the nominal side of the economy through two different channels, namely though its impact on both the equilibrium capital accumulation process and inflation. This link will prove to be essential to capture key empirical properties of the yield curve and its corresponding term structure of yield volatility.

2.3 The term structure of nominal interest rates

Having obtained the dynamics of the equilibrium price level, we can now solve for the term structure of nominal and real bond prices. Let $B(t, \tau)$ be the nominal pure discount bond paying one unit of currency in $t + \tau$ periods. The price of the nominal bond must satisfy the

[15]Note that for $\eta_2 \approx 1$, small innovations in either A_t, g_t or m_t result in dramatic changes in the equilibrium price process. However, from an economic viewpoint, the parameter η_2 should be negative which, as we will see later, is confirmed by the data.

following Euler equation

$$B(t,\tau) = e^{-\beta\tau}\mathbb{E}_t\left[\frac{U_C(C^*_{t+\tau}, M^{d*}_{t+\tau})}{U_C(C^*_t, M^{d*}_t)}\frac{p^*_t}{p^*_{t+\tau}}\right] = e^{-\beta\tau}\mathbb{E}_t\left[\frac{\exp\{-\log\left(K^*_{t+\tau}\right)\}}{\exp\{-\log\left(K^*_t\right)\}}\frac{p^*_t}{p^*_{t+\tau}}\right], \tag{2.24}$$

which states that in equilibrium the investor should be indifferent between consuming one more unit of currency now or investing one unit of currency in the $t+\tau$ period nominal discount bond.

Proposition 4 (Equilibrium Nominal Term Structure of Interest Rates)**.** *Under time-separable CRRA utility as in Equation* (2.2)*, the nominal discount bond $B(t,\tau)$ with maturity τ is given by*

$$B(t,\tau) = \exp\left\{-b_0(\tau) - b_A(\tau)A_t - b_g(\tau)g_t - b_m(\tau)m_t\right\} \tag{2.25}$$

where

$$b_A(\tau) = C_A\frac{1-e^{-\kappa_A\tau}}{\kappa_A}\,, \tag{2.26}$$

$$-b_g'(\tau) = Z_{0g}(\tau) + Z_{1g}(\tau)b_g(\tau) + Z_{2g}b_g^2(\tau)\,, \tag{2.27}$$

$$b_m(\tau) = \frac{-Z_{1m} + H_m\,Cot\left(\frac{1}{2}\left(-H_m\tau - Tan\left(\frac{2\sqrt{Z_{0m}Z_{2m}}}{H_m}\right)\right)\right)}{2Z_{2m}}\,,\ H_m = 4Z_{0m}Z_{2m} - Z_{1m}^2, \tag{2.28}$$

$$b_0(\tau) = \int_0^\tau C_0(u)du \tag{2.29}$$

and the constant parameters $Z_{0m}, Z_{2i}, i \in \{g,m\}$ and $Z_{0g}(\tau), Z_{1g}(\tau), C_0(\tau)$ are time-to-maturity functions that only depend on the structural model parameters of the economy and are defined in Appendix A.3.

The nominal term structure of interest rates in Proposition 4 belongs to the general affine class of term structure models of discount bond prices introduced by Duffie & Kan (1996). Using Equation (2.25), we obtain the time t yield curve $Y(t,\tau)$ with maturity τ as

$$Y(t,\tau) := -\frac{1}{\tau}\log\left(B(t,\tau)\right) = \frac{b_0(\tau)}{\tau} + \frac{b_A(\tau)}{\tau}A_t + \frac{b_g(\tau)}{\tau}g_t + \frac{b_m(\tau)}{\tau}m_t \tag{2.30}$$

The affine yield model in Equation (2.30) is driven by three factors. As noted, e.g., by Litterman & Scheinkman (1991), such a three factor structure model of the term structure is able to

reproduce most if not all empirically relevant shapes of the yield curve, such as upward sloping, inverted or hump shapes. The affine property in the factor loadings implies linearity of the local variance as in Vasicek (1977), Cox et al. (1985), and others.

Analyzing the expressions for the constant and time-varying parameters $Z_{\cdot,\cdot}$, $Z_{0g}(\tau)$, and $C_0(\tau)$ given in Appendix A.3, we make the following three observations. First, the target growth rates for output $\bar{k}$ and inflation $\bar{\pi}$, the depreciation rate δ, and output μ_Y and money supply growth rate μ_M solely affect the intercept of the yield curve but not its slope. In contrast, their weighting factors η_1 and η_2 affect both the intercept and the slope of the yield curve. Moreover, they do so in a non-linear way.

Second, the parameter λ has a key impact not only on the level of the term structure but also on its slope. The parameter λ affects the level of yields, since both $C_A = C_A(\lambda)$ and $C_g = C_g(\lambda)$ enter the expression for $b_0(\tau)$ and are functions of λ. This dependence in turn implies that λ also affects the slope of the term structure through $b_A(\tau)$ and $b_g(\tau)$. Furthermore, λ also determines the long run level of productivity A_t. To see this, recall that the trend growth rate of the productivity process A_t is not only dependent on the long run level of productivity θ_A but also on the long run level government policy θ_g.[16] Suppose that $\theta_g > 0$ and $\lambda < 0$, and $\theta_A + \frac{\lambda\theta_g}{\kappa_A} < 0$, the term $\frac{b_A(\tau)}{\tau}A_t$, provided that $b_A(\tau) > 0$, will be positive with high probability and therefore will lead to a declining yield curve for any maturity.

Third, the subjective discount factor β and the degree of transaction service money provides ξ also impact the slope of the yield curve through the factor loadings $b_A(\tau)$ and $b_g(\tau)$ whenever $\gamma \neq 0$. Hence, if the representative agent would have log-utility, β and ξ would only exhibit a level effect. In the following section we explore the impact of government and monetary policy uncertainty on the nominal term structure of interest rates in more detail.

[16] In particular, we have $\mathbb{E}[A_t] = \theta_A + \frac{\lambda\theta_g}{\kappa_A}$ (see Equation (2.8) in Proposition 1).

2.3.1 Fitting the model to the data

To fit the model to the term structure data we proceed as follows. We estimate a subset of parameters using maximum likelihood estimation (MLE) and calibrate the remaining parameters to the nominal yield and its corresponding volatility curve simultaneously. We estimate the parameters of the policy uncertainty variables g_t and m_t using (exact) maximum likelihood estimation.[17] Table 2.1 summarizes the results.

	GPU			**MPU**		
	κ_g	θ_g	σ_g	κ_m	θ_m	σ_m
Estimate	0.203	0.931	0.326	0.418	0.935	0.285
Stand. Error	(0.05)	(0.104)	(0.021)	(0.062)	(0.043)	(0.022)

Table 2.1: The label 'GPU' and 'MPU' refer to the government and monetary policy index, respectively. The row 'Estimates' represents the maximum likelihood estimator and the row 'Stand. Error' shows the asymptotic robust standard errors ('Sandwich estimator') of the parameters which is based on the outer product of the Jacobian of the log-likelihood function. Estimation period is January 1990 to June 2014 (295 data points) using monthly data.

The estimated parameters between the GPU index and the MPU index differ mainly in the magnitude of the speed of mean reversion parameter κ. Table 2.1 shows that κ_m is about half the magnitude of κ_m. Hence, a government policy shock will have a more permanent effect than a monetary shock has.[18] Shocks to monetary policy uncertainty are more transitive and mean-reverts faster to its long run mean θ_m.

Next, the parameters related to GDP growth dY_t/Y_t and money supply growth dM_t^S/M_t^S are set equal to their unconditional first and second sample moments. Furthermore, the correlation parameters ρ^{Yg} and ρ^{Mm} are set to their unconditional sample correlation coefficients. The preference parameters (β, γ, ξ), the structural model parameters $(\delta, \eta_1, \eta_2, \bar{k}, \bar{\pi})$, the correlation

[17] Since for the Feller diffusion the transition density is known in closed-form (non-central chi-squared), the transition density does not need to be approximated via quasi maximum likelihood techniques.

[18] The half-life of a shock in g_t when $\kappa_g = 0.203$ is $-\log(0.5)/\kappa_g = 1.48$ months, which implies that it takes a about six weeks for a shock to government policy uncertainty to die out by half. Similarly for the monetary policy shock, we have $-\log(0.5)/\kappa_m = 0.72$ months. It takes about three weeks for a monetary policy shock to die out by half.

parameters (ρ^{Ag}, ρ^{AY}), and the parameters related to the productivity process $(\kappa_A, \theta_A, \sigma_A, q_A, \lambda)$ are calibrated to match key features of the empirical term structure of interest rates and its corresponding volatility curve. The parameters not related to g_t and m_t are summarized in Table 2.2 below.

Model Parameters							
β	0.02	q_A	0.28	σ_M	0.45	κ_A	1.08
ξ	0.85	$\bar{k}$	0.03	ρ^{AY}	0.14	θ_A	4.19
γ	-0.82	$\bar{\pi}$	0.03	ρ^{Ag}	-0.98	σ_A	0.27
δ	0.08	μ_Y	0.38	ρ^{gY}	-0.27	λ	-1.93
η_1	-1.80	σ_Y	0.23	ρ^{Mm}	0.12	A_0	1
η_2	-2.34	μ_M	0.26				

Table 2.2: Summary of parameter values selected for Monte-Carlo Analysis: All parameter values for the process A_t as given in Equation (2.5) and the model parameters β, γ, ξ, q_A, δ, η_1, η_2, $\bar{k}$, $\bar{\pi}$, ρ^{Ag} and ρ^{AY} are calibrated to match simultaneously, the average yield curve and bond volatility curve over the sample period January 1990 to June 2014. A_0 refers to the initial value of A_t.

Given the parameters in Table 2.1 and 2.2, we simulate the economy $M = 1'000$-times on a monthly basis with each time series having length $12 \times N$, where we set $N = 2'500$, using a standard Euler-Maruyama scheme to obtain simulated values for the three Itô diffusions A_t, g_t, and m_t. Having obtained simulated values for those state variables, we then compute the nominal yield curve and its corresponding term structure of bond yield volatility with time to maturity of ten years and then average over the number of Monte-Carlo simulation runs.[19]

[Figure A.3 about here]

From Figure A.3, Panel A, we see that the model is overestimating the yield curve at medium maturities (three to seven years), whereas at the short and at the long end, the model implied yield curve is underestimating the actual the term structure. However, the overall mean error along the entire term structure is 3.07%.[20] As Panel B of Figure A.3 shows, our fitted

[19]We set the starting values of the government and monetary policy uncertainty to one ($m_0 = g_0 = 1$). By using a long time series, we avoid dependence on starting values.

[20]The error is calculated as $\frac{1}{T}\sum_{\tau \in T} |\hat{Y}(t,\tau) - Y(t,\tau)|/\hat{m}$ where $\hat{m} = \frac{1}{T}\sum_{\tau \in T} Y(t,\tau)$, $\hat{Y}(t,\tau)$ is the fitted yield curve and $T = 6$, i.e. the number of maturities.

model is able to reproduce the hump-shape in the term structure of bond yield volatility. This stylized fact of interest rates is very challenging to replicate within the framework of affine term structure models. Indeed, even with their more flexible specification of essentially affine price of risk, Buraschi & Jiltsov (2005) acknowledge that their model cannot fully match the second moments of yields. In contrast, we capture the short end of the yield volatility curve very accurately. We slightly overestimate the actual bond volatility at medium to longer maturities. Nevertheless, the error remains with 4.71% relatively small.

2.3.2 Yield curve and policy uncertainty

We now test a series of implications regarding the effect of policy uncertainty on the yield curve based on our fitted model parameters. Our preliminary empirical analysis between nominal bond yields and policy uncertainty as measured by the EPU index of Baker et al. (2012) shows that there is significant negative correlation between economic policy uncertainty and movements in the yield curve. Splitting the index into government and monetary policy uncertainty shows that the GPU index maintains high negative correlation whereas the MPU index seems to have no correlation with nominal yields at any maturity. Using our affine yield model, we can compute the model-implied correlation in a straightforward way. More specifically, we can show that a higher level in either fiscal or monetary policy uncertainty (g_t or m_t) will lead to a downward shift in yields.

Proposition 5 (Model-implied correlation and impact of policy uncertainty on the yield curve)**.**

1. *Nominal yields are negatively correlated with either fiscal* (g_t) *or monetary* (m_t) *policy uncertainty, i.e.*

$$\varrho\left[Y(t,\tau), g_t\right] \leq 0, \quad \varrho\left[Y(t,\tau), m_t\right] \leq 0, \quad \forall \tau \geq 0$$

and the effect is stronger for fiscal as opposed to monetary policy uncertainty, in other words

$$|\varrho\left[Y(t,\tau), g_t\right]| > |\varrho\left[Y(t,\tau), m_t\right]|$$

2. *Nominal yields yields are decreasing in both fiscal (g_t) and monetary (m_t) policy uncertainty*

$$\frac{\partial Y(t,\tau)}{\partial g_t} = \frac{b_g(\tau)}{\tau} < 0, \qquad \frac{\partial Y(t,\tau)}{\partial m_t} = \frac{b_m(\tau)}{\tau} < 0, \quad \forall \tau \geq 0. \tag{2.31}$$

and this effect is again stronger for fiscal as opposed to monetary policy uncertainty, i.e.,

$$\left|\frac{b_g(\tau)}{\tau}\right| > \left|\frac{b_m(\tau)}{\tau}\right|, \quad \forall \tau \geq 0. \tag{2.32}$$

The results in Proposition 5 above are in line with the empirical observations. The reason why the model implied correlation is negative for any maturity can be directly deduced from the covariance between $Y(t,\tau)$ and g_t which is,

$$\mathbb{C}[Y(t,\tau), g_t] = \frac{b_A(\tau)}{\tau} \frac{\theta_g \sigma_g \left(2\kappa_g \lambda \rho^{Ag} \sigma_A + \lambda \sigma_g\right)}{2\kappa_g(\kappa_A + \kappa_g)} + \frac{b_g(\tau)}{\tau} \frac{\theta_g \sigma_g^2}{2\kappa_g}. \tag{2.33}$$

Given the fitted parameters in Table 2.1 and 2.2, the factor loading $b_A(\tau)$ is always positive whereas $b_g(\tau)$ is negative, which implies that the first and second term in Equation (2.33) will be negative. In this setting, we obtain a model-implied average (along maturity τ) correlation of -0.2934 which is comparable to the empirical sample correlation between nominal yields and the GPU (-0.40). Likewise, since $b_m(\tau) \leq 0$ we obtain $\mathbb{C}(Y(t,\tau), m_t) = \frac{\theta_m \sigma_m^2}{2\kappa_m} \frac{b_m(\tau)}{\tau} \leq 0, \ \forall \tau \geq 0$. Comparing this model correlation coefficient of -0.021 to its empirical counterpart (-0.011), we see that the model is able to match both sample correlation coefficients.

2.3.3 Equilibrium nominal short rate and bond excess returns

We now discuss how the short end of the term structure of interest rates and the bond risk premium are affected by government and monetary policy uncertainty.

Proposition 6 (Equilibrium nominal short rate and bond risk premium)**.** *With time-separable CRRA utility, we have the following first order asymptotic results:*

1. *The nominal short rate R_t is given by*

$$R_t = \frac{(\mu_Y - \beta - \delta - \bar{k})\eta_1 + \beta + \mu_M - \eta_2(\mu_Y + \bar{\pi} - \delta)}{1 - \eta_2} + \gamma \frac{\beta(\eta_1 - \eta_2)(L - \phi_{00})}{1 - \eta_2} - \frac{\sigma_M^2}{(\eta_2 - 1)^2} m_t$$
$$- (q_A + \gamma\beta\phi_{0A}) \left(\frac{\eta_1 - \eta_2}{\eta_2 - 1} \right) A_t - \left(\frac{(\eta_1 - \eta_2)^2 \sigma_Y^2}{(\eta_2 - 1)^2} + \gamma \frac{\beta\phi_{0g}(\eta_1 - \eta_2)}{\eta_2 - 1} \right) g_t \tag{2.34}$$

2. *The nominal price of fiscal risk $\lambda_t^{N,g}$ as well as the market price of monetary risk $\lambda_t^{N,m}$ are*

$$\lambda_t^{N,g} = \frac{\eta_2 - \eta_1}{\eta_2 - 1} \sigma_Y \sqrt{g_t}, \quad \lambda_t^{N,m} = \frac{\sigma_M}{\eta_2 - 1} \sqrt{m_t}. \tag{2.35}$$

3. *The bond risk premia $RP(t, \tau)$ per unit of time is given by*

$$RP(t,\tau) := \frac{1}{dt} \mathbb{E}_t \left[\frac{dB(t,\tau)}{B(t,\tau)} - R_t dt \right]$$
$$= \lambda_t^{N,Y} \left[b_A(\tau) \rho^{AY} \sigma_A + b_g(\tau) \rho^{gY} \sigma_g \right] \sqrt{g_t} + \lambda_t^{N,M} b_m(\tau) \rho^{Mm} \sigma_m \sqrt{m_t} \tag{2.36}$$
$$= \Lambda_t^{N,g} + \Lambda_t^{N,m} \tag{2.37}$$

where $\Lambda_t^{N,g} = \lambda_t^{N,Y} \left[b_A(\tau) \rho^{AY} \sigma_A + b_g(\tau) \rho^{gY} \sigma_g \right] \sqrt{g_t}$ and $\Lambda_t^{N,m} = \lambda_t^{N,M} b_m(\tau) \rho^{Mm} \sigma_m \sqrt{m_t}$ are the factor loadings of government and monetary policy uncertainty, respectively.

The nominal short rate and the nominal market price of risk are all influenced by both the real and nominal sector of the economy, which is a direct consequence of the Taylor rule in Assumption 4. In the special case when money supply is entirely decoupled from the real sector ($\eta_1 = \eta_2 = 0$), the nominal short rate reduces to $R_t = \mu_M + \beta - \sigma_M^2 m_t$ and $\lambda_t^{N,g} = 0$ so that the real side does not affect the nominal short rate and output risk is no longer a nominal risk factor. We get the same result when $\eta_1 = \eta_2 = \eta$, i.e., when the central bank reacts to deviations from its nominal and real targets equally. Then, the nominal short rate is also an affine function of m_t and the risk premium does not depend on g_t. In both cases, the nominal short rate becomes independent of the risk aversion parameter γ.

In the general case, R_t depends on the money supply control variables η_1 and η_2 in a non-linear way. This suggests that relatively small fluctuations in either productivity A_t, monetary or government policy uncertainty may lead to drastic movements in the nominal short rate. Furthermore, risk aversion affects R_t through different channels. First, it affects its level through the second term in Equation (2.34). If risk aversion increases, i.e., if γ decreases, the short rate becomes smaller since $\frac{\beta(\eta_1-\eta_2)(L-\phi_{00})}{\eta_2-1} > 0$. Secondly, the risk aversion coefficient γ loads on both real sector variables A_t and g_t. Therefore, risk aversion also impacts the slope and curvature of the term structure. To what extent risk aversion changes slope and curvature depends on the magnitude of the estimated parameter values.

When $\eta_1 \neq 0$ and $\eta_2 \neq 0$, the nominal price of risk decomposes into two state-dependent market prices of risks $\lambda_t^{N,Y}$ and $\lambda_t^{N,M}$, which are driven by government and monetary policy risk, respectively.[21] Furthermore, the sign of those market prices of risk is determined by η_1 and η_2, the parameters controlling the intensity of adjustments to the long run real output growth target $\bar{k}$ and inflation target $\bar{\pi}$ and therefore can become negative depending on the values of η_1 and η_2.

[Figure A.4 about here]

For the bond risk premium in Equation (2.37), we plot in Figure A.4, Panel A, the loadings of the government policy uncertainty factor g_t and the monetary policy uncertainty factor m_t. Under our estimated parameters, both government and monetary policy uncertainty load positively on the risk premium. Monetary policy uncertainty has a larger impact at the short end of the curve, but flattens out at longer maturities and eventually becomes dominated by government policy uncertainty. Hence, our model predicts that the dominant factor at the short end is monetary policy uncertainty, while the dominant role at the long end of the bond risk premia curve is played by the government policy uncertainty factor.

[21] The results in Proposition 6 reveal that equilibrium relations such as the expected bond excess premium and interest rate volatility as well as the forward term premium, i.e., violation of the expectation hypothesis, will be driven by government and monetary policy uncertainty whenever $\eta_1 \neq 0$ and $\eta_2 \neq 0$.

2.3.4 Bond yield volatility

Many empirical studies find that long run bond yields exhibit higher volatility than implied by the expectation hypothesis. Already Shiller (1979) shows that long term bond yields exhibit excess volatility relative to their model-implied values. From Piazzesi & Schneider (2006) we know that their representative agent-based model explains a smaller fraction of observed volatility of the long-end yields than of the short-end yields. Xiong & Yan (2010) argue that excess bond volatility might be due to differences in beliefs about the long run level of inflation. They show that a higher belief dispersion leads to volatility amplification which allows them to account not only for the empirically observed high bond yield volatility, but also for the hump-shape of the term structure of bond volatility.[22] To explore the key determinants that allow to reproduce the hump-shape in bond volatility, we need to derive the model-implied unconditional variance of nominal yields. It turns out that the variance is a linear combination of the variances of monetary and government policy uncertainty, the variance of productivity, and the covariance of productivity and government policy uncertainty.

Corollary 1 (Term Structure of Nominal Bond Yield Variance)**.** *Let $Y(t,\tau)$ denote the current time t yield with maturity τ. Then the unconditional term structure of bond yield variance is given by*

$$\mathbb{V}[Y(t,\tau)] = \frac{b_A^2(\tau)}{\tau^2}\mathbb{V}[A_t] + \frac{b_g^2(\tau)}{\tau^2}\mathbb{V}[g_t] + \frac{b_m^2(\tau)}{\tau^2}\mathbb{V}[m_t] + 2\frac{b_A(\tau)b_g(\tau)}{\tau^2}\mathbb{C}[A_t, g_t] \tag{2.38}$$

where $\mathbb{V}[m_t] = \frac{\theta_m \sigma_m^2}{2\kappa_m}$ and the expressions for $\mathbb{V}[A_t]$, $\mathbb{C}[A_t, g_t]$, and $\mathbb{V}[g_t]$ are given in Proposition 1.

To explore the key determinants in generating the hump-shape in bond yield variance, Figure A.4 plots the different components contributing to the bond yield variance in Equation (2.38).

[22] Closely related to the 'excess volatility puzzle' phenomenon are also the findings of Gürkaynak et al. (2005*b*). They document that bond yields exhibit excess sensitivity to macroeconomic announcements.

[Figure A.4 about here]

The contribution of both the factor loadings $b_g(\tau)$ and the cross term $b_A(\tau)b_g(\tau)$ are hump shaped, which causes the term structure of yield variance to exhibit a similar pattern. The government policy factor g_t exhibits a hump shape that peaks around the two year maturity. The covariance term $\mathbb{C}(A_t, g_t)$ is also contributing significantly to the hump. Its magnitude is determined by two factors, by the correlation between government policy uncertainty and productivity ($\rho^{Ag} < 0$) and by the impact of government policy uncertainty on productivity ($\lambda < 0$). The impact of the production variance $\mathbb{V}[A_t]$ as well as of monetary policy uncertainty is monotonically decreasing in τ. The latter factor has only little impact. From Corollary 1 and Figure A.4 we can deduce the following:

Proposition 7 (Policy Uncertainty and the term structure of bond yield volatility)**.**

- *Government g_t and monetary m_t policy uncertainty raise the level of bond yield volatility. However, the effect is much stronger for fiscal as opposed to monetary policy uncertainty, i.e.*

$$\frac{b_g^2(\tau)}{\tau^2}\mathbb{V}[g_t] > \frac{b_g^2(\tau)}{\tau^2}\mathbb{V}[m_t] \tag{2.39}$$

- *The function $F^g(\tau) = \frac{b_g^2(\tau)}{\tau^2}\mathbb{V}[g_t]$ is hump-shaped across maturities τ. This implies that the effect of government policy uncertainty is highest for about 2 years maturity according to Figure A.4.*

The first result in Proposition 7 is straight-forward. Since clearly $\frac{b_g^2(\tau)}{\tau^2}\mathbb{V}[g_t] > 0$, $\left(\frac{b_m^2(\tau)}{\tau^2}\mathbb{V}[m_t] > 0\right)$ and $\mathbb{C}(A_t, g_t) > 0$ adding the government (monetary) policy uncertainty factor raises the level of volatility. The second statement above is far less obvious to see, as it crucially depends on the parameter specifications of the model. Therefore, in Panels A through F of Figure A.5, we explore in more detail the parameters responsible for generating the hump shape.

[Figure A.5 about here]

As Panel A illustrates, the term structure of bond yield volatility exhibits a fundamentally different shape whenever λ is negative or when λ is set to zero, in which case government policy uncertainty does not affect the drift of productivity. Not only is the level of the term structure significantly higher whenever $\lambda < 0$ than compared to the case when $\lambda = 0$ but also, bond yield volatility becomes hump-shaped in time to maturity. Panels B and C show that the speed of mean reversion level κ_g and volatility σ_g have a similar effect on bond volatility. A more persistent and a highly volatile uncertainty process generate not only to an upward shift of the bond volatility term structure, but also a hump shape.[23] Similar to Panel B, we observe in Panel D that a more permanent shock in productivity (decrease in κ_A) also accentuates the hump shape. In contrast, increasing production volatility σ_A shifts the volatility term structure upward such that it eventually becomes monotonically decreasing (Panel E). This follows because the factor $\frac{b_A^2(\tau)}{\tau^2}\mathbb{V}(A_t)$ increases proportionally in σ_A^2 and since $\frac{b_A^2(\tau)}{\tau^2}$ is monotonically decreasing. Finally, Panel F shows that bond volatility is highly sensitive to changes in either η_1 or η_2. When the central bank becomes less responsive to deviations of the long term real target $\bar{k}$, the level of bond volatility decreases substantially. In contrast, if the central bank becomes less responsive to deviations of the long term nominal target $\bar{\pi}$, bond volatility increases significantly.[24]

2.4 Empirical analysis

Our theoretical model gives rise to several theoretical predictions. In the subsequent empirical analysis, we examine the following four testable hypotheses.

[23] The long run mean of government policy uncertainty θ_g increases yield dispersion proportionally, since $\frac{\partial \mathbb{V}(Y(t,\tau)}{\partial \theta_g} > 0$. Hence, the long term mean does not contribute to a hump shape.

[24] Without providing the corresponding plots, we remark that whenever both η_1 and η_2 are both reduced, there will be a parallel downward shift in the level of bond yield volatility. Furthermore, the impact of risk aversion on the term structure of bond volatilities is less pronounced and leads to an almost parallel downward shift of the term structure.

Hypothesis 1 (H1): Our first prediction can be deduced directly from Proposition 5, which implies that nominal yields fall when either government or monetary policy uncertainty increases and vice versa. From Proposition 5, this effect is mainly driven by government policy uncertainty (see Equation (2.31)).

Hypothesis 2 (H2): Higher (lower) fiscal or monetary policy uncertainty increases (decreases) nominal yield volatility (see Equation (2.39) in Proposition 7). This effect is again mainly driven by government policy uncertainty.

Hypothesis 3 (H3): From the second result in Proposition 7, the hump shape of the term structure of bond yield volatility is mainly driven by government policy uncertainty and not by monetary policy uncertainty.

Hypothesis 4 (H4): From Equation (2.37) and Panel A in Figure A.4, bond risk premia are increasing in both monetary and government policy uncertainty.

To investigate the joint effect of government and monetary policy uncertainty on the yield curve, its term structure of volatility, and on risk premia, we use as a proxy for both types of policy uncertainties, the economic policy uncertainty (EPU) index developed by Baker et al. (2012). Thus, in our model this index would be approximately equivalent to setting $EPU_t \approx g_t + m_t$. In what follows, we will empirically test the above hypotheses by regressing nominal yields and yield volatility on the EPU index and our time series of government and monetary policy as well as a set of control variables.

2.4.1 Data

We obtain monthly Treasury Bill yields with maturity one, two, three, five, seven, and ten years from the Federal Reserve Board ranging from January 1990 until July 2014, from which we bootstrap the zero-coupon yield curve treating the treasury yields as par yields. From

Datastream, we collect monthly data on a total of 2 macro variables, which we aggregate into a real business cycle activity factor and an inflation factor.[25] As a measure for real activity we use industrial production (IP). As an inflation factor, we use the consumer price index (CPI). We then compute monthly log-growth rates over one year for each of the macro control variables.

As an alternative to the EPU, we proxy for (policy) uncertainty using the VIX index. As a measure for economic condition we include the Chicago Fed National Activity Index (CFNAI), which we obtain from the FRED database (St. Louis Fed).[26] We also use treasury bond implied volatility (TIV) based on weighted average of one-month options on treasury bonds with maturity of two, five, ten, and 30 years as a proxy for bond market volatility.

In addition we collect two time series, which we refer to as Financial Variables' (FV). They include the monthly log growth rate of the S&P composite dividend yield index (DY), which has been shown to have forecasting power by Fama & French (1989), and the term spread measured as the ten-year yield less the federal funds rate (TS).

2.4.2 Construction of government and monetary policy uncertainty index

The economic policy uncertainty (EPU) index developed by Baker et al. (2012) has been recently used by a number of studies.[27] The EPU index is constructed from three main components, namely a news impact part which is based on news paper discussing economic policy uncertainty, a component that summarizes reports by the Congressional Budget Office (CBO) that

[25]Similar control variables have also been used by Ang & Piazzesi (2003), Evans & Marshall (2007), Ludvigson & Ng (2009) or Joslin, Priebisch & Singleton (2014) in their study of the economic determinants of the term structure of nominal interest rates.

[26]The reason why we include the CFNAI regressor is to test whether either monetary or government policy uncertainty has predictive power after controlling for the state the economy is in. This is because it is reasonable to assume that uncertainty about the government's future policy choice is in general larger in weaker economic conditions.

[27]For instance, Pastor & Veronesi (2013) show that government policy uncertainty carries a risk premium, and that stocks are more volatile and more correlated in times of high uncertainty. Brogaard & Detzel (2012) use the same index and find that economic policy uncertainty forecast future market excess returns. Similarly, Gulen & Ion (2012) show that policy-related uncertainty is negatively correlated with firm and industry level investment. When policy uncertainty increases firm's tend to reduce their investment.

compile lists of temporary federal tax code provisions, and a third component called 'economic forecaster disagreement', which draws on the Federal Reserve Bank of Philadelphia's Survey of Professional Forecasters and summarizes data on consumer price forecast dispersion and predictions for purchases of goods and services by state, local and federal government.[28]

For our setting, we need to decompose the EPU index into uncertainty related to government and monetary policy. To disentangle the two types of uncertainties, we use the 'categorical EPU data', which contains time-series on uncertainty related to government and monetary policy as well as further categorical variables.[29] For our measure of government policy uncertainty, we extract the time-series 'fiscal policy', 'taxes', and 'government spending'. Furthermore, we argue that disagreement about temporary federal tax code provisions and forecast variation in local state and federal purchases of goods and services are sources of government policy uncertainty, whereas disagreement about future inflation (CPI disagreement) can be related to monetary uncertainty.

Therefore, in order to construct our index of 'government policy uncertainty' labeled as 'GPU' we include the time series 'fiscal policy', 'Taxes', 'Government', 'FedStateLocal Ex disagreement' and 'Tax expiration'. We place half of the weight to the time series 'fiscal policy' and the other half is equally distributed among the time series 'Taxes', 'Government', 'FedState-Local Ex disagreement' and 'Tax expiration'.[30] Our measure of 'monetary policy' uncertainty, which we abbreviate by 'MPU', consists of the time series 'monetary policy uncertainty' and 'CPI disagreement' of which each obtain weight 1/2.

[28] As Kelly et al. (2013) argue, it is difficult isolate exogenous variation in political uncertainty as it likely depends on various factors such as overall macro uncertainty. Therefore, the EPU index may not only capture government related uncertainty, but can be interpreted as a broader measure of uncertainty about economic fundamentals.

[29] This data is also available from http://www.policyuncertainty.com/.

[30] We divided the time series 'Tax expiration' by a factor of ten, because its impact would otherwise pull the index up substantially at the end of the time series. Furthermore, as tax laws are only altered infrequently, the 'Tax expiration' remains constant over several months up to two years. Its unscaled inclusion would lead to an underestimation in policy uncertainty variation.

2.4.3 Policy uncertainty and the yield curve

To investigate the relationship between the yield curve and the EPU index, we make the following regression,

$$Y(t,\tau) = \beta_0 + \beta_1 PU_t + \epsilon_t, \quad PU_t \in \{EPU_t, GPU_t, MPU_t\}, \tag{2.40}$$

where PU_t denotes either the EPU, GPU, or MPU index at time t, and ϵ_t is the regression error term.[31]

According to hypothesis **H1**, we expect the coefficient in Equation (2.40) to be negative for all the three uncertainty indexes. Additionally, we run the same regression as in Equation (2.40) above, just replacing the PU_t index with the VIX index. Since the VIX index is a generally accepted measure of overall economic uncertainty and positively correlated with the EPU index,[32] we expect the regression coefficient to be negative as well. We also regress $Y(t,\tau)$ on both the VIX and the EPU index, and on the VIX together with the GPU and MPU indices. By doing so, we can identify those variables that exhibit greater predictive power.

In Table 2.3 we summarize the results for the EPU index.[33] The first row labeled 'EPU' shows that higher policy uncertainty EPU reduces yields across all maturities, confirming our model hypothesis **H1**. The effect is highly significant at the 5% level and decreasing in τ, indicating that the short end of the yield curve is more responsive to shocks in policy uncertainty than the long end. Furthermore, the adjusted R^2 indicate that the single factor EPU accounts for 29% of total variability at the short end of the yield curve. This value decreases monotonically to 18% at the long end of the curve.

The row 'VIX' in Table 2.3 shows that, similar to the EPU index, a rise in the VIX index also leads to a statistically significant decline in nominal yields along the entire yield curve. However,

[31] To address potential concerns about robustness of our results, we compute following Newey & West (1994) standard errors with five lags to account for heteroskedasticity and autocorrelation (HAC) in residuals.

[32] For our sample, the correlation coefficient between VIX and EPU is 0.45.

[33] For all the regressions tables that follow the intercept estimate $\hat{\beta}_0$ and corresponding HAC errors are not displayed.

	τ	1Y	2Y	3Y	5Y	7Y	10Y
EPU	EPU	-3.70***	-3.68***	-3.51***	-3.02***	-2.61***	-2.16***
	t_{EPU}	(-7.08)	(-6.95)	(-6.61)	(-5.67)	(-4.95)	(-4.19)
	R^2_{adj}	0.29	0.29	0.28	0.24	0.21	0.17
VIX	VIX	-0.04	-0.05*	-0.05*	-0.05*	-0.04*	-0.04*
	t_{VIX}	(-1.50)	(-1.67)	(-1.76)	(-1.86)	(-1.78)	(-1.91)
	R^2_{adj}	0.02	0.02	0.02	0.02	0.02	0.03
EPU & VIX	EPU	-4.07***	-4.00***	-3.78***	-3.19***	-2.75***	-2.13***
	t_{EPU}	(-8.26)	(-7.77)	(-7.17)	(-5.76)	(-4.80)	(-3.75)
	VIX	0.04	0.03	0.03	0.02	0.01	0.01
	t_{VIX}	(1.62)	(1.37)	(1.17)	(0.75)	(0.58)	(0.15)
	R^2_{adj}	0.30	0.30	0.29	0.24	0.21	0.16

Table 2.3: The table displays slope coefficients of the regression of $Y(t,\tau)$ on EPU_t, $Y(t,\tau)$ on VIX_t, and $Y(t,\tau)$ on EPU_t and VIX_t for τ=1Y, 2Y, 3Y, 5Y, 7Y, and 10Y. Values in brackets below represent HAC-robust $t-$statistics. R^2_{adj} refers to adjusted coefficient of determination. By ***, **, * we denote 1%, 5%, and 10% statistical significance, respectively.

this relationship is statistically significant only at the 10% confidence level and insignificant at the short end of the yield curve. In addition, the impact of the VIX is substantially smaller for any τ as the impact of the EPU and GPU indexes. Moreover, its explanatory power is also considerably lower, with an R^2 between 2% and 3%, compared to R^2 ranging between 18% to 29% for the EPU and 10% to 20% for the GPU.

The row 'EPU & VIX' in Table 2.3 shows that the only significant predictor is the EPU index, as the regression coefficient for the VIX is statistically insignificant across all maturities, once both regressors are added to the regression equation. The same conclusion can be drawn from row 'GPU & VIX' as government policy uncertainty remains the only statistically significant predictor along the entire term structure. Lastly, row 'MPU & VIX' shows that the MPU index has no predictive power for any τ.

To check for the robustness of our results, we add different controls to the regression equation. We add the economic condition (EC) controls 'CFNAI' and 'VIX'. Furthermore, we also include the financial variables (FV) factor and macro controls (MC) as discussed in Section 2.4.1.

	τ	1Y	2Y	3Y	5Y	7Y	10Y
EC	EPU	-4.14***	-4.05***	-3.83***	-3.24***	-2.78***	-2.17***
	t_{EPU}	(-9.51)	(-8.79)	(-7.95)	(-6.15)	(-5.10)	(-4.03)
	R^2_{adj}	0.30	0.30	0.28	0.24	0.21	0.16
EC+FV	EPU	-2.56***	-2.82***	-2.87***	-2.72***	-2.48***	-2.09***
	t_{EPU}	(-4.07)	(-4.27)	(-4.23)	(-3.91)	(-3.62)	(-3.22)
	R^2_{adj}	0.47	0.40	0.35	0.26	0.22	0.17
EC+FV+MC	EPU	-2.75**	-3.02**	-3.07**	-2.91**	-2.66**	-2.28**
	t_{EPU}	(-5.60)	(-5.81)	(-5.75)	(-5.47)	(-5.14)	(-4.73)
	R^2_{adj}	0.62	0.56	0.52	0.47	0.44	0.42

Table 2.4: The table reports slope coefficients of the regression, $Y(t,\tau)$ on EPU_t and EC controls (EC), $Y(t,\tau)$ on EPU_t and EC, FV variables (EC+FV), $Y(t,\tau)$ on EPU_t and $Y(t,\tau)$ on EPU_t, and EC, FV, MC controls (Full Reg.) for τ = 1Y, 2Y, 3Y, 5Y, 7Y and 10Y. Values in brackets below represent HAC-robust $t-$statistics. R^2_{adj} refers to adjusted coefficient of determination. By ***, **, * we denote 1%, 5%, and 10% statistical significance, respectively.

Table 2.4 shows that the EPU regression coefficient remains significant for any maturity and across all regressions. However, compared to Table 2.3, its impact is considerably reduced (primarily at the short end), especially when we include the financial variables (FV). The reason for this decline is because those regressors exhibit strong positive correlation with the EPU index. Not surprisingly, their estimated impact on contemporaneous yield changes is also negative. Their average is -4.62 (DY), and -0.16 (TS). Whereas the R^2_{adj} essentially stays the same after adding the CFNAI control (row 'EC'), it increases considerably, although mainly at the short-end of the yield curve, after adding the financial factors (see row 'EC+FV'). Lastly, as the row labeled 'EC,FV+MC' shows, that whereas adding macro controls to the regression equation does not impact the statistical significance and magnitude of the EPU index, it considerably increases the amount of explained variation as the R^2_{adj} increases substationally across every maturity.[34]

[Figure A.6 about here]

[34]This increase in R^2_{adj} is predominantly driven by inflation as it has a statistically significant, very large and positive impact on the term structure of nominal interest rates.

While Table 2.4 is concerned with the EPU index, we now turn our focus on the individual impact of government and monetary policy uncertainty. In Figure A.6, we plot the estimated regression coefficients of the GPU and MPU index together with their 95% HAC-robust confidence intervals. Panel A and B show that, whereas the impact of fiscal policy uncertainty remains negative and statistically significant after including all control variables (Panel B), the monetary policy uncertainty exhibits a positive and statistically significant effect on contemporaneous yield movements even after including all control variables (Panel B). This somewhat puzzling result indicates that this effect might be do to strong correlation with the GPU index or other control variables. Therefore, in order to separately analyze the impact of fiscal and monetary policy uncertainty, we regress yields on the GPU and MPU individually in Panel C and D (with controls). Whereas the negative and statistically significant effect of the GPU index on contemporaneous yields remains unchanged, the impact of MPU is insignificant for every maturity. These results suggest that, the MPU's strong positive impact on yields is mainly do to its large positive correlation with the GPU index. Overall, we conclude that these results are in line with hypothesis **H1** stated above, i.e. higher fiscal as opposed to monetary policy uncertainty decreases the nominal yields for every maturity.

2.4.4 The term structure of bond yield volatility and policy risk

Our theoretical results from Section 2.3.4 suggest that the inclusion of a time-varying government policy risk factor not only raises the level of the yield curve, but is also a key driver in generating the empirically observed hump shape of the bond volatility term structure. We now test these predictions using both the EPU, and our measures of government and monetary policy uncertainty including all the control variables from above.

Our measure for observed volatility is realized volatility as given in Equation (2.41) aggregated on a monthly level from business day data.

$$\mathcal{V}_t(Y(t,\tau)) = \sqrt{\sum_{d=1}^{D-1}\left(\log\left(\frac{Y(d+1,\tau)}{Y(d,\tau)}\right)\right)^2}, \qquad Y(t,\tau),\ d \in \{1,\dots,D-1\}, \tag{2.41}$$

where D denotes the number of daily observations (about 20 business days per month) and τ=1Y, 2Y, 3Y, 5Y, 7Y and 10Y to construct a time series of monthly realized bond yield volatility. In addition to our control variables from the previous sections, we also include treasury implied volatility (TIV) to proxy for fixed-income implied volatility.[35]

$$\mathcal{V}_t[Y(t,\tau)] = \beta_0 + \beta_1 PU_t + cont_t + \epsilon_t, \tag{2.42}$$

where PU_t denotes either the EPU, GPU, or MPU index at time t, $cont_t$ summarizes all the control variables and ϵ_t is the regression error term. From our hypothesis **H2**, we expect the sign of the regression coefficient in (2.42) of the EPU and the GPU index to be positive for all maturities.[36] Furthermore, from hypothesis **H3** we expect that economic or government policy uncertainty have a hump-shaped effect on the term structure of bond yield volatility. Thus, we should observe that the estimated regression coefficients peaks around the two year maturity as the realized bond volatility curve in Figure A.3 does.

We report the results of the regression in Equation (2.42) in Table 2.5. We find our hypothesis **H2** concerning the EPU confirmed. Higher economic policy uncertainty increases bond volatility for any maturity. Once we include the financial control variables, the impact of the EPU index is reduced for any maturity and the explanatory power increases from an average $\bar{R}^2_{adj} = 0.40$ to $\bar{R}^2_{adj} = 0.47$. This observation suggests, similar to the results in Table 2.4, that financial factors are also important predictors of bond variance. Analyzing in more detail, we

[35]Treasury bond implied volatility is based on weighted average of very liquid one-month options on treasury bonds with maturity 2, 5, 10, and 30 years. To obtain monthly data, we compute the sample mean using daily observations.

[36]From our theoretical analysis from Section A.3 and 2.3.4, the contemporaneous impact of monetary policy uncertainty is marginal and therefore we do not expect to find any significant estimates for the MPU index.

	τ	1	2	3	5	7	10
Simple	EPU	0.192***	0.194***	0.166***	0.121***	0.091***	0.063***
	t_{EPU}	(7.18)	(9.72)	(8.88)	(8.86)	(7.66)	(7.01)
	R^2_{adj}	0.37	0.43	0.44	0.43	0.40	0.37
EC	EPU	0.192***	0.188***	0.156***	0.111***	0.079***	0.051***
	t_{EPU}	(6.39)	(9.37)	(8.73)	(8.60)	(7.46)	(6.67)
	R^2_{adj}	0.39	0.44	0.45	0.45	0.43	0.43
EC +FV & TIV	EPU	0.135***	0.135***	0.118***	0.087***	0.064***	0.042***
	t_{EPU}	(4.08)	(5.41)	(4.99)	(4.91)	(4.18)	(3.70)
	R^2_{adj}	0.44	0.50	0.50	0.48	0.45	0.44
Full Regression	EPU	0.146***	0.145***	0.125***	0.095***	0.071***	0.04***
	t_{EPU}	(4.27)	(6.24)	(5.76)	(6.62)	(5.90)	(5.29)
	R^2_{adj}	0.47	0.56	0.57	0.57	0.57	0.56

Table 2.5: The table displays slope coefficients of the regression of $\mathcal{V}_t[Y(t,\tau)]$ on EPU_t (EPU), $\mathcal{V}_t[Y(t,\tau)]$ on EPU_t and EC controls (EC), $\mathcal{V}_t[Y(t,\tau)]$ on EPU_t EC and FV variables (EC+FV) including the TIV and $\mathcal{V}_t[Y(t,\tau)]$ on EPU_t, EC, FV (including TIV) and MC controls (Full Regression). The yield maturities are 1, 2, 3, 5, 7, and 10 years. Values in brackets below represent HAC-robust $t-$statistics. R^2_{adj} refers to adjusted coefficient of determination. By ***, **, * we denote 1%, 5%, and 10% statistical significance, respectively.

see from row 'Full Regression' that there is only a moderate increase in predictive power once we also include our macro controls.

Concerning hypothesis **H3**, although the impact of economic policy is highly statistically significant, it gradually declines along the entire term structure. Hence, the EPU index is not able to generate a hump in the volatility term structure. Therefore, if we would use the EPU as our proxy for government uncertainty, this result in conflict with our hypothesis **H3**. However, since in the EPU index government and monetary uncertainty factors are intermingled, we need to analyze the impact of the government and monetary policy uncertainty index separately.

[Figure A.7 about here]

Figure A.7 shows that our hypotheses **H2** and **H3** are supported by the data. Not only does realized volatility rise when government policy uncertainty increases, its effect is also hump-shaped with a peak around a maturity of two years. Similar to the yield regressions

from above, once we add all control variables, the estimated impact of the GPU is substantially reduced, yet it remains statistically significant and hump-shaped (Panel B). Moreover, similar to above, we find that the statistical significance of the MPU is misleading. In Panel C we regress realized volatility on the GPU and MPU index individually (Panel D is with controls). Including only the GPU or the MPU shows that, whereas the GPU remains positive, significant and hump-shaped in time to maturity, the MPU index changes signs (compared to Panel A or B) and is no longer significant at the 5% confidence level for all maturities.

2.4.5 Bond risk premia

Hypothesis **H4** states that both government and monetary policy uncertainty should explain bond risk premia. To explore the predictive power of the EPU index as well as our government and monetary policy indexes on future bond excess returns, we denote by

$$r_{t+1}^{E,\tau_i} := \log\left(B(t+1,\tau_i-1)\right) - \log\left(B(t,\tau_i)\right) - Y(t,1)$$

the log-excess return from buying at time t a bond with time-to-maturity τ_i and selling it after one period. Furthermore, the log forward rate a time t for entering contracts between time $t+\tau_i-1$ and $t+\tau_i$ is given by $F(t,\tau_i) = \log(B^N(t,\tau_i-1)/B^N(t,\tau_i))$. The literature on bond risk premia usually compares the predictive power of a new predictor variable against the routinely used Cochrane & Piazzesi (2005) factor (CP), which is constructed based on a tent-shaped linear combination of forward rates.[37] Furthermore, from the covariance matrix of yields we extract the first three principal components which are commonly referred to as 'level', 'slope' and 'curvature' (see Litterman & Scheinkman (1991)) As a further set of control variables, we also include the economic condition, the financial variables (without) and the set of macroeconomic factors as above.

[Figure A.8 about here]

[37] A detailed description of the construction of this factor is given in Cochrane & Piazzesi (2005). To avoid collinearity problems, we only include the current one year yield $Y(t,1)$ and the five- and ten year forward rates and we do not restrict the regression coefficients to sum up to one.

To analyze the forecasting power of the GPU und MPU index for the bond risk premium, we plot in Figure A.8 the corresponding regression coefficients. In Panel A, we jointly regress bond excess bond returns GPU and the MPU in a single regression equation. In line with the factor loadings displayed in Panel A of Figure A.4, both the GPU and the MPU load positively on the risk premium except for the MPU, which loads slightly negatively at the ten-year maturity. However, the loading of the MPU is statistically insignificant at all maturities. In contrast, the regression coefficient of the GPU is statistically significant at medium to longer maturities. Panel B shows that once we control for PCA and CP factors, economic condition, financial variables, and macro factors, the significance of the GPU is still preserved at every maturity, but its magnitude is significantly reduced. On the other hand, the MPU becomes also significant for all maturities and its slope exceeds the one of the GPU factor. The adjusted R^2 after having included all regression controls averages some 89% across all maturities. When we only use the GPU and the MPU, however, the R^2 is just some 3% for the two-year maturity, but rises to 30% at the ten-year maturity. Analyzing the individual impact of the GPU and MPU respectively, we conclude that both are statistically significant and positive predictors of bond risk premia. However, including all our control variables shows that bond excess returns only load statistically significant on the MPU index and not on the GPU index, although its impact remains increasing in time to maturity just as in Panel B above.[38] Hence, overall our hypothesis **H4** is confirmed in that both government and monetary policy uncertainty have a positive significant impact on bond risk premia when added together to the regression equation.

2.5 Conclusion

We present a tractable dynamic equilibrium model of the term structure of interest rates with government (real) and monetary policy uncertainty shocks. Consistent with the data, our model is able to reproduce the flight-to-quality behavior, i.e., the observation that investors tend to

[38] If we exclude the CP factor from the regression, the GPU index becomes a statistically significant predictor of bond risk premia.

increase their bond holdings in times of higher economic or government policy uncertainty and thereby lowering treasury bond yields. We calibrate our model to data and provide a detailed analysis of the dependence of the nominal yield curve and its corresponding term structure of nominal bond yield volatility on the structural model parameters. Even though our model belongs to the class of affine term structure models, it is capable of reproducing the empirically observed hump-shape of the term structure of bond volatility. To achieve this result, two key feature in our model are essential. First, that the long run growth path of productivity is time-varying and negatively dependent on government policy uncertainty. Secondly, that government policy uncertainty affects the nominal side of the economy whenever the central bank responds actively to deviations of output and inflation growth from their respective target rates.

Even though our simple empirical analysis has only illustrative character, it sheds some light on the relationship between contemporaneous movements of the yield and bond yield curve in response to shocks in government and monetary policy uncertainty. Our empirical results support our model-implied predictions that, first, increased policy uncertainty leads to an increased demand in bonds and therefore reducing their yields and, second, that higher economic policy uncertainty not only raises bond volatility but is also a key driver of generating the empirically observed hump-shaped structure of the bond yield volatility curve. Furthermore, by decomposing the EPU index into its components, we identify government policy uncertainty as the main culprit for the negative relationship between policy uncertainty and nominal yields and for the empirically observed high and often hump-shaped term structure of bond yield volatility. The explanatory power of the monetary policy uncertainty index for contemporaneous yields and bond volatility movements is mixed at best and mostly insignificant. However, monetary policy uncertainty is not irrelevant for the term structure of yields. We find it to be a key predictor for bond risk premia at any maturity, while government policy shocks lose some of their statistical significance once all controls are added to the regression equation.

Chapter 3

Robust Portfolio Optimization with Jumps

Yacine Aït-Sahalia and Felix Matthys[1]

I have presented this paper at:

- PhD Defense, September 2014

[1]We gratefully acknowledge the financial support from the Swiss National Science Foundation.

Abstract

We study the consumption-portfolio allocation problem in continuous time when asset prices follow Lévy processes and the investor is concerned about potential model misspecification. We derive optimal portfolio holdings in closed form under model uncertainty, incorporating perturbations to the reference model affecting both the drift and jump intensity. We then present a method for calculating error-detection probabilities by means of Fourier inversion of the conditional characteristic function in the case when the measure change follows a jump-diffusion process.

3.1 Introduction

The study of dynamic intertemporal portfolio choice problems in continuous time has a long history, dating back to Merton (1969) and Merton (1971). In Merton's model, the investor's optimization problem consists of how to optimize his consumption and portfolio allocation in a riskfree and risky assets. The sources of risk in this framework are all diffusive so that sudden large changes in the risky assets are unlikely to occur. Since then, Merton's framework has been extended to allow for asset price discontinuities, driven by jump processes, including Poisson, stable or more general Lévy processes: see, e.g., Aase (1984), Jeanblanc-Picqué & Pontier (1990), Shirakawa (1990), Han & Rachev (2000), Ortobelli et al. (2003), Kallsen (2000), Carr et al. (2001), Choulli & Hurd (2001), Liu et al. (2003), Das & Uppal (2004), Emmer & Klüppelberg (2004), Madan (2004), Cvitanić et al. (2008), Delong & Klüppelberg (2008), Aït-Sahalia et al. (2009) and Aït-Sahalia & Hurd (2016), with the latter two providing an explicit solution to the investor's optimization problem.

However, the literature on portfolio optimization with jumps has so far treated the parameters of the returns distribution, such as the expected return, jump intensity and jump size distribution as if they were known to the investor. In practice, these parameters are in fact unknown and therefore the investor faces a considerable amount of model uncertainty. And in some cases, a precise, control theory-derived optimal solution derived under a misspecified model that is assumed to be exact can be worse than a naive, perhaps approximate, solution that is not so closely tied to the incorrect model; for instance, in the case of portfolio optimization, there is a substantial evidence that "$1/n$" (equally weighted) portfolios can dominate portfolios that are mean-variance optimized, owing in part to the large uncertainty surrounding expected returns (see, e.g., DeMiguel et al. (2009)). If anything, the presence of jumps makes this problem worse: jumps are rare events, which makes pinning down their distributional characteristics, or even simply their arrival rate, difficult on the basis of historical returns data.

One possible approach for the investor to account for this model uncertainty consists in employing robust control, keeping his reference model in mind but also considering a set of alternative models when optimizing his decisions. In this setting, among the class of alternative models for asset returns, the investor recognizes that he is unable to know exactly the true underlying model and instead seeks portfolio policies that should perform reasonably well across the set of alternative models. We employ the penalty-based framework of robust decision making pioneered by Hansen and Sargent (see, e.g., Hansen & Sargent (2008).[2]) It introduces a set of alternative models which are statistically close to the reference model in the sense of entropy minimization. There are alternative, related, ways to approach this problem. In Bayesian decision analysis, the investor forms a prior over models and maximizes his expected utility; model uncertainty adds averaging over models to integrating over shocks. Owing to its origins in engineering, robust control by contrast typically focuses on minimizing the worst case loss over the set of possible models, rather than averaging over models.

Knightian, ambiguity, and uncertainty aversion are closely related concepts. One way of introducing ambiguity aversion is through the formulation of multiple priors preferences as presented by Gilbao & Schmeidler (1989). Given such preferences, optimal decisions are taken under the premise that state variables are governed by the worst-case probability model among a set of candidate models.[3] Chen & Epstein (2002) formulate an inter-temporal recursive multiple-priors utility problem that incorporates Knightian ambiguity aversion. An extension of this formulation of ambiguity aversion in continuous time is given in Leippold et al. (2007) which combines learning based on optimal Bayesian updating and ambiguity aversion. Uncertainty aversion has been employed to study consumption and asset allocation problems in the purely diffusive setting. For instance, Uppal & Wang (2003) derive a model of inter-temporal portfolio choice of an investor who takes model misspecification into account. Trojani & Vanini (2004)

[2]See also Anderson et al. (2003), Hansen et al. (2006), Cogley et al. (2008), Hansen & Sargent (2010) and Hansen & Sargent (2011).

[3]For a discussion and comparison of the max-min expected utility of Gilbao & Schmeidler (1989) and robust control theory, see Hansen & Sargent (2001) and Hansen et al. (2006).

solve two versions of a robust control problem and examine its impact on the resulting asset allocation. Trojani & Vanini (2000) derive robust consumption and investment rules that can be compared to those of a non-robust decision-maker in Merton's model. Maenhout (2004) studies an inter-temporal portfolio problem of an investor who worries about model misspecification and shows that, if the investor seeks robust decision rules, then the demand for equities is significantly reduced. Maenhout (2006) extents the robust portfolio allocation analysis by a allowing for a time-varying mean-reverting risk premium and shows that while the desire for robustness lowers the total equity share, the proportion of the inter-temporal hedging demand is increased.

Robustness with respect to model misspecification has also been applied to models of the term structure of nominal interest rates. Ulrich (2013*b*) employs a robust decision making framework to analyze how model uncertainty with respect to monetary policy affects the term premium on nominal bond yields. Kleshchelski & Vincent (2007) present an equilibrium model of the term structure in a robust control setting where consumption growth exhibits stochastic volatility. They show that, if the representative agent demands optimal policies that are robust to model misspecification substantially amplifies the effect of conditional heteroskedasticity in consumption growth.

As of this writing, the literature on robust asset allocation and consumption problems when assets follow jump-diffusive or Lévy processes remains sparse. Lui et al. (2005) employ a pure-exchange economy framework with a representative agent who faces model uncertainty with respect to jumps in the underlying aggregate endowment (rare events) in order to study the equilibrium equity price. However the focus of that paper is not on portfolio policies; in the setting of that paper, the representative agent sets his share of wealth allocated to the risky asset to always be one. Drechsler (2013) uses a similar robust decision making framework in an equilibrium model in order to capture salient features of equity and options markets when the risky assets follow a jump-diffusion process. However, since the framework is also an aggregate endowment economy populated by a representative agent, the optimal portfolio

allocation consists again for the investor in putting all his wealth in the consumption claim. Branger et al. (2014) study a model where the state of the economy is driven by a hidden Markov chain and filtering the unknown jump intensities lead to the filtered intensities having self-exciting properties.

The novelty in the present paper is to introduce robustness concerns of the investor when making his consumption and portfolio choice decisions, when the underlying risky asset follows a Lévy process, and studying the change in optimal portfolio (and consumption) policies necessary to make them robust. We include model misspecification with respect to both the drift and jump intensity parameters and solve for the investors' optimal consumption and portfolio allocation in closed form. Additionally, we derive a semi-closed form formula for detection-error probabilities, i.e. for the likelihood that the investor selects the wrong model based on a sample time series asset returns. This gives a quantitative upper bound on the set of alternative models which seem reasonably close to his reference model.

The remainder of the paper is organized as follows. Section 3.2 introduces the general robust portfolio allocation problem. Section 3.3 derives optimal robust portfolio weights under both drift and jump intensity perturbation. Section **??** derives a semi-explicit expression for computing a formula for error-detection probability when the underlying measure change follows a Lévy jump-diffusive process. Section 3.5 conducts Monte-Carlo simulations to assess expected utility under various different portfolio holding strategies, comparing in particular robust to non-robust optimal policies. Section 3.6 concludes. The Appendix contains further derivations and technical details.

3.2 The Robust Portfolio Allocation Problem with Jumps

We consider an infinite horizon expected utility maximization problem where the investor chooses his consumption level and allocates his funds between a riskless and a risky asset subject to both diffusive and jump risks. For this purpose, the investor employs a particular model which presumably represents his best estimate of the risky asset dynamics under a benchmark or reference probability measure. However, the investor fears that the model he uses is potentially misspecified: he believes that the true model could lie in a larger set of alternative models that are statistically difficult to distinguish from his reference model. In order to mitigate the effect of potential model misspecification on his utility, the investor wants to choose optimal consumption and portfolio holdings that are robust with respect to small perturbations of his reference model. Ultimately, he seeks to make wise decisions although he knows enough to distrust his model.

The first issue is to specify the set of alternative models for asset returns which the investor considers as plausible alternatives. Following the Hansen-Sargent approach, the set of alternative models considered by the investor consists of those models whose relative entropy (or Kullback-Leibler) distance from the reference model is bounded. The idea is that models in this set should be difficult to distinguish statistically by the investor from his reference model. The Lagrange approach then converts the entropy constraint into a penalty on perturbations from the reference model. We obtain the optimal robust solution in closed form.

3.2.1 Asset Price Dynamics under the Reference and Robust Measures

We assume a complete, filtered probability space $(\Omega, \mathcal{F}, \mathbb{F} = (\mathcal{F}_t)_{t\geq 0}, \mathbb{P})$ satisfying the usual assumption. $\mathbb{P}$ denotes the reference (or physical) probability measure. The investment set

available to the investor at time $t \geq 0$ consists of a riskless (locally deterministic) asset with price $S_{0,t}$ and a risky asset with price $S_{1,t}$ following a compensated exponential Lévy process. More specifically, the dynamics of the two assets are given by

$$\frac{dS_{0,t}}{S_{0,t}} = rdt,\ S_{0,0} > 0 \tag{3.1}$$

$$\frac{dS_{1,t}}{S_{1,t_-}} = (r+R)dt + \sigma dB_t + Jd\widetilde{Y}_t,\ S_{1,0} > 0,\ \mathbb{P}-a.s. \tag{3.2}$$

where $r \geq 0$ is the riskless return, $R \in \mathbb{R}$ denotes the excess return of the risky asset over the riskfree asset, $\sigma > 0$ is the volatility parameter, $B_t = (B_t)_{t\geq 0}$ is a Brownian motion under $\mathbb{P}$ and $J \in (-1,1)$ is a jump scaling factor. $\widetilde{Y}_t = Y_t - \Lambda_t$ is a compensated pure jump process with Lévy measure $\lambda\nu(dz)$, where $\lambda \geq 0$ is a fixed jump intensity parameter. The Lévy measure ν satisfies $\int_{\mathbb{R}} \min(1,|z|)\nu(dz) < \infty$, so that jumps have finite variation. We write $\Lambda_t = \lambda\kappa t$ where $\kappa = \mathbb{E}[Z_t] < \infty$ denotes the predictable compensator of the jump process Y_t.

In the sequel, we assume that Y_t is a compensated compound Poisson process, i. e. $\widetilde{Y}_t = \sum_{n=1}^{N_t} Z_n - \Lambda_t$, where N_t is a scalar Poisson process with jump intensity, or arrival rate, λ. The jump sizes Z_n are independent of N_t and are assumed to be i.i.d. with Lévy measure $\nu(dz)$. Given these assumptions, the dynamics of the risky asset under the reference measure can be expressed as

$$\begin{aligned}
\frac{dS_{1,t}}{S_{1,t_-}} &= (r+R)dt + \sigma dB_t + Jd\widetilde{Y}_t \\
&= (r+R)dt + \sigma dB_t + J\left(dY_t - \mathbb{E}[Z_t dN_t]\right) \\
&= (r+R)dt + \sigma dB_t + J\left(dY_t - \int_{\mathbb{R}} z\nu(dz)\mathbb{E}[dN_t]\right) \\
&= \left(r + R - \lambda J\int_{\mathbb{R}} z\nu(dz)\right)dt + \sigma dB_t + JdY_t,\ S_{1,0} > 0,\ \mathbb{P}-\text{a.s.}
\end{aligned} \tag{3.3}$$

In order to introduce the notion of model misspecification we need to specify a set of alternative or worst-case robust dynamics which are statistically close to the reference dynamics in (3.3). For this purpose, consider an equivalent probability measure which we denote by $\mathbb{P}^\vartheta$ and in the sequel refer to it as the robust measure. The investor considers alternative models

under the robust measure $\mathbb{P}^{\vartheta}$ which take the general form

$$\frac{dS_{1,t}}{S_{1,t_-}} = \left(r + R + \sigma h_t - \lambda^{\vartheta} J \int_{\mathbb{R}} z\nu(dz)\right) dt + \sigma dB_t^{\vartheta} + JdY_t^{\vartheta},\ S_{1,0} > 0,\ \mathbb{P}^{\vartheta} - \text{a.s.} \tag{3.4}$$

First, (3.4) shows that the drift has changed from $(r+R)$ under the measure $\mathbb{P}$ to $(r+R+\sigma h_t - \lambda^{\vartheta} J \int_{\mathbb{R}} z\nu^{\vartheta}(dz))$ under the measure $\mathbb{P}^{\vartheta}$ where $(h_t)_{t\geq 0}$ is a continuous $\mathcal{F}_t$ -measurable function of the Markovian state $S_{1,t}$ with the same dimensionality as the one-dimensional Brownian motion. In what follows, we refer to h_t as a drift perturbation function, since it perturbs the drift dynamics of the risky asset under $\mathbb{P}$ and does not affect the jump component $\widetilde{Y}_t$. Second, the stochastic process $B_t^{\vartheta} = (B_t^{\vartheta})_{t\leq 0}$ is a Brownian motion but now under the perturbed or robust measure $\mathbb{P}^{\vartheta}$. Third, the other set of perturbations affect the jump component $\widetilde{Y}_t^{\vartheta}$ in (3.4), namely the jump intensity and the jump size distribution under $\mathbb{P}^{\vartheta}$. The jump intensity λ is transformed into λ^{ϑ} under the robust probability measure as follows

$$\lambda^{\vartheta} = e^a \lambda,\ a \in \mathbb{R} \tag{3.5}$$

where a is a scalar jump intensity perturbation parameter that amplifies or diminishes the jump intensity. Therefore, under the robust measure, the investor is worried about model misspecification with respect to the jump arrival intensity, meaning how frequently jumps occur.

From (3.4) we observe that perturbating the intensity has two effects on the risky assets dynamics. It both alters the drift and changes the frequency of jumps occurring in the Poisson process N_t. Consider the case when there are only negative jumps in the stock price dynamics of (3.4), for example by assuming that the jump size z has positive support and $J \in (-1, 0)$. Under this assumption, increasing the jump intensity leads on the one hand to more frequent negative jumps but also on the other hand, due to compensation, raises the expected return on the risky asset, which is consistent with the empirical risk and return trade-off observed in financial markets. In other words, compensating the jump process leads to the stock price S_t carrying a risk premium for intensity misspecification. As we later show, this modeling

assumption has fundamental implications as to how jump risk will affect optimal portfolio holdings. For instance, in a diffusive setting, i.e. if we set $\lambda = 0$ in (3.4), where the investor is only concerned about potential drift misspecification, the optimal portfolio weight in the risky asset is then simply reduced as model misspecification concerns lead to a decrease in the expected return while leaving volatility unchanged. However, in the robust setting here, there exists a trade-off between higher frequency of jumps occurring and simultaneously higher jump risk compensation.

The jump size distribution under $\mathbb{P}^\vartheta$ has Lévy measure

$$\nu^\vartheta(dz) = \nu(dz; b),\ b \in \mathbb{R}^L, : L \geq 1 \tag{3.6}$$

where b is a set of possibly vector valued perturbation parameters. For instance, if the jump size distribution is normal, $Z_n \overset{i.i.d}{\sim} \mathcal{N}(\mu, \sigma^2)$, a jump size perturbed model may read $Z_n \overset{i.i.d}{\sim} \mathcal{N}(\mu + \delta_\mu, \sigma^2 v_\sigma)$, where $\delta_\mu \in \mathbb{R}$ shifts the mean from μ under $\mathbb{P}$ to $\mu + \delta_\mu$ under $\mathbb{P}^\vartheta$ and likewise the variance is scaled by $v_\sigma > 0$. So for $a = \delta_\mu = 0$ and $v_\sigma = 1$ we get back the jump distributions of the reference model under the measure $\mathbb{P}$.

3.2.2 Measure Change for Itô Semimartingales

The dynamics of the compensated exponential Lévy process under the reference as well as under the robust measure are linked through a specific likelihood ratio or Radon-Nikodym density process ϑ_t. This density process not only allows to change the dynamics of the risky asset but also, as it will be shown in the next section, restricts the size of alternative models that are statistically difficult to distinguish from the reference model. To be more precise, let $\mathbb{P}^\vartheta$ be the robust or perturbed measure which is absolutely continuous with respect to the reference measure $\mathbb{P}$. Fix $T > 0$ and define

$$\vartheta_t = (\vartheta_t)_{t\in[0,T]} = \left.\frac{d\mathbb{P}^\vartheta}{d\mathbb{P}}\right|_{\mathcal{F}_t} = \vartheta_t = \vartheta_t^D \vartheta_t^J \tag{3.7}$$

where ϑ_t^D is a $(\mathcal{F}_t, \mathbb{P})$- martingale that defines the measure change of the continuous part of the stochastic process and ϑ_t^J, also a $(\mathcal{F}_t, \mathbb{P})$- martingale, that defines the measure change of the discontinuous or jump part. The change of measures of the diffusive and jump part factor only when the continuous and the jump part of the stochastic process are independent, which is the case in the setting we employ above, since $[N, W]_t = 0$.

In a jump diffusive setting, where the jumps follow a compound Poisson process, there are three ways to change the measure, i. e. from $\mathbb{P}$, the reference measure to $\mathbb{P}^\vartheta$, the robust measure:

1. Measure change of the diffusive part through ϑ_t^D affecting the drift and the Brownian motion.

2. Measure change of the jump part through ϑ_t^J by changing the jump intensity of the process under $\mathbb{P}^\vartheta$.

3. Measure change of the jump part through ϑ_t^J by changing the jump size of the process under $\mathbb{P}^\vartheta$.[4]

From Girsanovs' theorem for Itô semimartingales, for the diffusive drift measure change ϑ_t^D, with $(h_t)_{t\geq 0}$ being a progressively measurable process, we have that

$$B_t^\vartheta = B_t - \int_0^t h_s ds \tag{3.8}$$

is a Brownian motion with respect to the measure $\mathbb{P}^\vartheta$. Then it follows that, an absolutely continuous change of measure can be represented by an exponential $(\mathbb{P}, \mathcal{F}_t)$- martingale ϑ_t satisfying

$$\vartheta_t^D = \exp\left\{\int_0^t h_s dB_s - \int_0^t \frac{h_s^2}{2} ds\right\},\ \mathbb{E}_0\left[\vartheta_t\right] = \vartheta_0 = 1,\ \mathbb{P} - a.s. \tag{3.9}$$

[4]One distinguishes between a finite number of jump sizes and the case where the jump sizes can take on a continuum of values.

where $\mathbb{E}_t[\cdot] = \mathbb{E}[\cdot|\mathcal{F}_t]$ denotes the conditional expectation up to time t with respect to the measure $\mathbb{P}$ and likewise we define by $\mathbb{E}_t^{\vartheta}[\cdot]$ the conditional expectation up to time t with respect to the robust measure $\mathbb{P}^{\vartheta}$.

Concerning the jump part of the risky asset, we let $N = (N_t)_{t\in[0,T]}$ be a Poisson process with jump intensity $\lambda > 0$ on the probability space $(\Omega, \mathcal{F}_t, \mathbb{P})$ and $T > 0$ again fixed. We want to change the intensity λ of the Poisson process $(N_t)_{t\in[0,T]}$ on $\mathbb{P}$ to a jump intensity λ^{ϑ} under the robust measure $\mathbb{P}^{\vartheta}$. Likewise, we want to perturb the Lévy measure such that the jumps have distribution $\nu^{\vartheta}(dz) = \nu(dz; b)$ under the robust measure. The appropriate measure change $\vartheta^J = (\vartheta_t^J)_{t\in[0,T]}$ is

$$\left.\frac{d\mathbb{P}^{\vartheta}}{d\mathbb{P}}\right|_{\mathcal{F}_t} = \vartheta_t^J = e^{(\lambda-\lambda^{\vartheta})t}\prod_{n=1}^{N_t}\frac{\lambda^{\vartheta}}{\lambda}\frac{\nu^{\vartheta}(Z_n)}{\nu(Z_n)},\ \mathbb{E}\left[\vartheta_t^J\right] = \vartheta_0^J = 1,\ \mathbb{P}-a.s. \tag{3.10}$$

which is a $(\mathcal{F}_t, \mathbb{P}^{\vartheta})$- martingale and satisfies

$$d\vartheta_t^J = \vartheta_{t-}^J\, d\left(H_t - \lambda^{\vartheta}\right) - \vartheta_t^J d\left(N_t - \lambda t\right),\ H_t = \sum_{n=1}^{N_t}\frac{\lambda^{\vartheta}}{\lambda}\frac{\nu^{\vartheta}(Z_n)}{\nu(Z_n)}. \tag{3.11}$$

where H_t is a compound Poisson process and $H_t - \lambda^{\vartheta}t$ is a $(\mathcal{F}_t, \mathbb{P}^{\vartheta})$-martingale. Therefore, the density process in (3.10) is a right-continuous, adapted process with left limits (càdlàg).

3.2.3 Relative Entropy Growth Bounds and Error-Detection Probabilities

By changing the perturbation parameters a, b and h_t in (3.5), (3.6) and (3.8) we control the discrepancy between the dynamics of the risky asset under the reference measure with respect to its dynamics under the robust measure. Therefore, the more h_t, a and b deviate from their no-perturbation values, the more different the dynamics of the risky asset become under the reference with respect to the robust measure, i.e. the set of alternative models expands. However, the possible set of models under consideration has to be restricted to a subset of models which are statistically difficult to distinguish from the reference model. A

natural statistical tool to measure distances between two probability distributions is relative entropy, and it is well suited for the purpose of defining alternative models in robust control (see Anderson et al. (2003)).

The alternative set of possible models that are similar in a statistical sense are linked to the measure change ϑ_t. Given two probability measures $\mathbb{P}$ and $\mathbb{P}^{\vartheta}$, growth in entropy of $\mathbb{P}^{\vartheta}$ relative to $\mathbb{P}$ over the time interval $[t, t+\Delta t]$ is defined as

$$G(t, t+\Delta t) \equiv \mathbb{E}_t^{\vartheta}\left[\log\left(\frac{\vartheta_{t+\Delta t}}{\vartheta_t}\right)\right], \quad \mathcal{R}(\vartheta_t) \equiv \lim_{\Delta t \to 0} \frac{G(t, t+\Delta t)}{\Delta t} \qquad \forall t \geq 0 \tag{3.12}$$

Thus the set of admissible model misspecification can be characterized as

$$\{\vartheta_t : \mathcal{R}(\vartheta_t) \leq \eta, \ \forall t \geq, \ \eta \geq 0\} \tag{3.13}$$

where η is a constant that defines an upper bound on the set of alternative models.As $\eta \to 0$, the investor becomes fully confident about his reference model, while increasing η expands the set of alternative models that are statistically further away from the reference model,so overall model uncertainty increases. Due to the independence of the diffusive and the jump component, the measure change is given by $\vartheta_t = \vartheta_t^D \vartheta_t^J$, which implies that relative entropy growth is simply the sum of the two components 'drift' and 'jump', namely $\mathcal{R}(\vartheta_t) = \mathcal{R}(\vartheta_t^D) + \mathcal{R}(\vartheta_t^J)$. Therefore, by varying the perturbation function h_t and perturbation parameters a and b we regulate the space of admissible models within the set $[0, \eta], \ \forall t \geq 0$.

An immediate question that arises in this context is: What is a reasonable value for η? Anderson et al. (2003) provide a statistical tool for model detection based on the log of the measure change ϑ_t in the form of detection-error probabilities in order to quantify the amount of model uncertainty that seems plausible to the investor. The basic intuition behind this test statistic is, given the right model is $\mathbb{P}$ and a finite time series sample of the state variable (in our case the risky asset) of length $T - t$, how likely will the investor mistakenly assume the data have been generated by model $\mathbb{P}^{\vartheta}$ instead of the true model $\mathbb{P}$. The detection-error probability is precisely quantifying the likelihood that the investor is going to select the wrong

model. Thus if the true model is $\mathbb{P}$, the investor will falsely reject it for model $\mathbb{P}^{\vartheta}$ based on a time series sample of length $T-t$ whenever $\log(\vartheta_T) > 0$. Conversely, if the true model is $\mathbb{P}^{\vartheta}$ he will erroneously reject it for model $\mathbb{P}$ whenever $\log(\vartheta_T) < 0$.

3.2.4 Wealth Dynamics and Utility Specification under Robustness

We denote by $X_t = (X)_{t\geq 0}$ the investor's wealth at time t. Let $\omega_{0,t} = w_{0,t}/X_t$ be the percentage of wealth (or portfolio weight) invested in the risk free asset and $\omega_{1,t} = w_{1,t}/X_t$, an adapted predictable càdlàg process, be the percentage of wealth invested in the risky asset; $w_{i,t},\ i \in \{0,1\}$ is the absolute amount of money invested into asset i. The portfolio weights satisfy $\omega_{0,t} + \omega_{1,t} = 1$. The investor consumes at an instantaneous rate C_t at time t. Under the robust dynamics given in (3.4) his wealth evolves according to

$$\begin{aligned} dX_t &= \omega_{0,t}X_t\frac{dS_{0,t}}{S_{0,t}} + \omega_{1,t}X_t\frac{dS_{1,t}}{S_{1,t_-}} - C_t dt \\ dX_t &= \left[X_t\left(r + \omega_t R + \sigma h_t\omega_t - \omega_t\lambda^{\vartheta}J\int_{\mathbb{R}} z\nu^{\vartheta}(dz)\right) - C_t\right]dt + \omega_t X_t\sigma dW_t^{\vartheta} + \omega_t X_t J d\widetilde{Y}_t^{\vartheta}, \end{aligned} \tag{3.14}$$

with $X_0 > 0,\ \mathbb{P}^{\vartheta} - a.s.$ and we have set $\omega_t = \omega_{1,t}$.

As a first step, the investor's robust consumption and portfolio allocation problem is to choose, a set of worst-case drift perturbation functions $\{h_s\}_{t\leq s<\infty}$ and worst-case jump intensity and jump size parameters a, b. As a second step, the investor has to select admissible consumption and portfolio holdings $\{C_s, \omega_s\}_{t\leq s<\infty}$ that maximize his expected utility of consumption under the worst-case scenario. More formally, with $\beta \in (0,\infty)$ denoting his subjective discount or "impatience" rate, the optimal robust consumption and portfolio problem is given by

$$\max_{\{C_s,\omega_s\}_{t\leq s<\infty}}\ \min_{\{h_s\}_{t\leq s<\infty},a,b}\ \mathbb{E}_t^{\vartheta}\left[\int_t^{\infty} e^{-\beta s}U(C_s)ds\right] \tag{3.15}$$

subject to the wealth dynamics in (3.14) and the entropy growth constraint

$$\mathcal{R}(\vartheta_t) \leq \eta, \qquad \forall t \geq 0. \tag{3.16}$$

We define as

$$V = V(X_t, t) = \max_{\{C_s,\omega_s\}_{t\leq s<\infty}} \min_{\{h_s\}_{t\leq s<\infty},a,b} \mathbb{E}_t^{\vartheta}\left[\int_t^{\infty} e^{-\beta s} U(C_s)ds\right] \tag{3.17}$$

the value function associated with the optimal stochastic robust control problem in (3.15). Since we work in incomplete markets and thus the martingale measure is not unique, we have to rely on standard stochastic dynamic programming techniques. Using Itô's formula for semimartingales, the perturbed Hamilton-Jacobi-Bellman (HJB) equation characterizing the optimal robust consumption and portfolio allocation problem is given by

$$\begin{aligned} 0 = \max_{\{C_t,\omega_t\}} \min_{\{h_t\},a,b} & e^{-\beta t}U(C_t) + \frac{\partial V(X_t,t)}{\partial t} + \frac{\partial V(X_t,t)}{\partial X}\left[X_t\left(r + \omega_t\left(R + \sigma h_t - \lambda^{\vartheta} J\int_{\mathbb{R}} z\nu(dz)\right)\right) - C_t\right] \\ & + \frac{1}{2}\frac{\partial^2 V}{\partial X^2}\omega_t^2 X_t^2\sigma^2 + \lambda e^a \int_{\mathbb{R}}\left[V(X_{t_-} + X_{t_-}\omega_t Jz, t) - V(X_{t_-}, t)\right]\nu(dz, b) \end{aligned} \tag{3.18}$$

subject to

$$\mathcal{R}(\vartheta_t) \leq \eta \tag{3.19}$$

and the transversality condition

$$\lim_{t\to\infty} \mathbb{E}_t^{\vartheta}\left[V(X_t, t)\right] = 0. \tag{3.20}$$

Then, usual time-homogeneity arguments for infinite horizon problems imply that

$$\begin{aligned} e^{\beta t}V(X_t,t) &= \max_{\{C_s,\omega_s\}_{t\leq s<\infty}} \min_{\{h_s\}_{t\leq s<\infty},a,b} \mathbb{E}_t^{\vartheta}\left[\int_t^{\infty} e^{-\beta(s-t)}U(C_s)ds\right] \\ &= \max_{\{C_{t+u},\omega_{t+u}\}_{t\leq u<\infty}} \min_{\{h_{t+u}\}_{t\leq u<\infty},a,b} \mathbb{E}_t^{\vartheta}\left[\int_t^{\infty} e^{-\beta u}U(C_{t+u})du\right] \\ &= \max_{\{C_u,\omega_u\}_{0\leq u<\infty}} \min_{\{h_u\}_{0\leq u<\infty},a,b} \mathbb{E}_0^{\vartheta}\left[\int_0^{\infty} e^{-\beta u}U(C_u)du\right] \\ &\equiv L(X_t) \end{aligned} \tag{3.21}$$

where the third equality follows because the optimal robust control is Markov and $L(X_t)$ is independent of time. Thus $V(X_t, t) = e^{-\beta t}L(X_t)$.

Next, we scale the entropy penalty term

$$\theta_t = \theta(X_t) = \widetilde{\theta}(1-\gamma)V(t, X_t) > 0, \quad \widetilde{\theta} \in \mathbb{R}_+. \tag{3.22}$$

This specification renders the Lagrange multiplier state-dependent in wealth which will allow us to find a closed form solution to the consumers' consumption and investment problem.

The optimal robust control problem in (3.18) reduces to a time-homogeneous problem in $L(X_t)$

$$0 = \max_{\{C_t,\omega_t\}} \min_{\{h_t\},a,b} U(C_t) - \beta L(X_t) + \frac{\partial L(X_t)}{\partial X}\left[X_t\left(r + \omega_t R + \sigma h_t \omega_t - \omega_t \lambda^{\vartheta} J \int_{\mathbb{R}} z\nu(dz)\right) - C_t\right] + \frac{1}{2}\frac{\partial^2 L(X_t)}{\partial X^2}\omega_t^2 X_t^2 \sigma^2 + \lambda e^a \int_{\mathbb{R}} \left[L(X_{t_-} + X_{t_-}\omega_t J z) - L(X_{t_-})\right]\nu(dz;b) \tag{3.23}$$

subject to

$$\mathcal{R}(\vartheta_t) \leq \eta \tag{3.24}$$

and the transversality condition

$$\lim_{t\to\infty} \mathbb{E}_t^{\vartheta}\left[L(X_t)\right] = 0. \tag{3.25}$$

To find a solution of the problem in (3.23) subject to the entropy growth constraint in (3.24), we formulate it as a Lagrange optimization problem with inequality constraints. We first determine the optimal robust control policies h_t^*, a^* and b^*, by solving a constraint optimization problem. We denote by $\mathcal{L} = \mathcal{L}(C_t, \omega_t, h_t, a, b, \theta_t)$ the Lagrangian associated to the problem given in (3.23) and by θ_t the corresponding state-dependent Lagrange-multiplier of the entropy growth constraint in (3.24). Then the first order optimality conditions for the minimization part of (3.23) are given by

$$\frac{\partial \mathcal{L}}{\partial h_t} = \sigma\omega_t - \frac{\partial}{\partial h_t}\theta_t\left(\mathcal{R}(\vartheta_t) - \eta\right) = 0, \tag{3.26}$$

$$\frac{\partial \mathcal{L}}{\partial a} = \frac{\partial}{\partial a}\lambda e^a \int_{\mathbb{R}} \left[L(X_{t_-} + X_{t_-}\omega_t J z) - L(X_{t_-})\right]\nu(dz,b) - \frac{\partial}{\partial a}\theta_t\left(\mathcal{R}(\vartheta_t) - \eta\right) = 0, \tag{3.27}$$

$$\frac{\partial \mathcal{L}}{\partial b_l} = \frac{\partial}{\partial b_l}\lambda e^a \int_{\mathbb{R}} \left[L(X_{t_-} + X_{t_-}\omega_t J z) - L(X_{t_-})\right]\nu(dz;b_l) - \frac{\partial}{\partial b_l}\theta_t\left(\mathcal{R}(\vartheta_t) - \eta\right) = 0,\ l = 1,\ldots,L, \tag{3.28}$$

$$\frac{\partial \mathcal{L}}{\partial \widetilde{\theta}} = \mathcal{R}(\vartheta_t) - \eta = 0, \qquad \theta_t \geq 0, \qquad \theta_t\left(\mathcal{R}(\vartheta_t) - \eta\right) = 0. \tag{3.29}$$

Each equation in (3.26) to (3.29) summarizes two opposing effects. For instance, from (3.26), the left term $\partial \mathbb{E}^{\vartheta}\left[V(X_t)\right]/\partial h_t = \sigma\omega_t$ characterizes the marginal impact on the investor's

utility that results from increasing perturbation. The right term in (3.26) $(\partial/\partial h_t)\,\theta\,(\mathcal{R}(\vartheta_t) - \eta)$ captures the associated increase in detectability of the robust model. Thus under the robust measure, the perturbation of the reference model is such that its effect is most harmful to the investor's utility and simultaneously remaining difficult to detect statistically.

To solve the problem, from the first order conditions in (3.26) to (3.29) we obtain the optimal amount of perturbation of the drift component h_t^*, jump intensity a^* and size perturbation $b^* \in \mathbb{R}^L$, that satisfy the entropy growth constraint, the complementary slackness condition and non-negativity constraint of θ^* in (3.29). Having obtained a set of optimal robust control parameters $\{h_t^*, a^*, b^*\}$, we then plug them back into the Lagrangian and solve the corresponding perturbed HJB equation for the optimal consumption policy C_t^* and portfolio weights ω^*. Thus given $\{h_t^*, a^*, b^*\}$, the first order condition for the investor's optimal consumption and portfolio policies are given by,

$$\frac{\partial \mathcal{L}(h_t^*, a^*, b^*, \theta^*)}{\partial C_t} = \frac{\partial U(C_t)}{\partial C_t} = \frac{\partial L(X_t)}{\partial X} \rightarrow C_t^* = \left[\frac{\partial U}{\partial X}\right]^{-1} \frac{\partial L(X_t)}{\partial X} \tag{3.30}$$

$$\begin{aligned}\frac{\partial \mathcal{L}(h_t^*, a^*, b^*, \theta^*)}{\partial \omega_t} = \frac{\partial}{\partial \omega_t}\Bigg[\frac{\partial L(X_t)}{\partial X}\Bigg[X_t\left(r + \omega_t R + \sigma h_t \omega_t - \omega_t \lambda^{\vartheta} J \int_{\mathbb{R}} z\nu(dz)\right) - C_t\Bigg] \\ + \frac{1}{2}\frac{\partial^2 L(X_t)}{\partial X^2}\omega_t^2 X_t^2 \sigma^2 + \lambda e^{a^*} \int_{\mathbb{R}} \left[L(X_{t_-} + X_{t_-}\omega_t J z) - L(X_{t_-})\right] \nu(dz; b^*)\Bigg]\end{aligned} \tag{3.31}$$

The first order condition for optimal consumption is standard and says that at the optimum, marginal utility of consumption must be equal to the marginal utility of wealth. Since U is concave, the investor wants to smooth consumption. From (3.31) we obtain the optimal portfolio allocations as a function of the perturbation parameters $\{h_t^*, a^*, b^*\}$. We are now going to discuss the case when both drift and jump intensity are being distorted.

3.3 Explicit Robust Portfolio Weights: Drift and Jump Intensity Perturbations

In order to derive more explicit results, we need to make some further assumptions about the investor's utility, the Lévy measure characterizing the jump sizes and the amount of perturbation of the reference model we allow for. We consider an investor with power utility,

$$U(c) = c^{1-\gamma}/\left(1-\gamma\right) \tag{3.32}$$

and CRRA coefficient $\gamma \in (0,1) \bigcup (1,\infty)$; $U(c) = -\infty$ whenever $c \leq 0$. Furthermore, in order to obtain fully explicit portfolio weights, we do not perturb the Lévy measure, in other words, the jump size distribution is the same under both measures, i.e. $\nu(dz;b) = \nu(dz)$. We only perturb the arrival rate of the jumps.

We conjecture a solution of the form

$$L(x) = \frac{K^{-\gamma}x^{1-\gamma}}{(1-\gamma)}, \quad \text{with} \quad \frac{\partial L(x)}{\partial x} = (1-\gamma)L(x)/x, \quad \frac{\partial^2 L(x)}{\partial x^2} = -\gamma(1-\gamma)L(x)/x^2 \tag{3.33}$$

for some constant K. Then, after division by $(1-\gamma)L(X_t)$ the HJB equation is given by

$$\begin{aligned} 0 = \max_{C_t,\omega_t}\min_{h_t,a} \frac{U(C_t)}{(1-\gamma)L(X_t)} - \frac{\beta}{(1-\gamma)} + \left[r + \omega_t R + \sigma h_t \omega_t - \omega_t \lambda^{\vartheta} J \int_{\mathbb{R}} z\nu(dz) - \frac{C_t}{X_t}\right] \\ - \frac{1}{2}\gamma\omega_t^2\sigma^2 + \frac{\lambda^{\vartheta}}{(1-\gamma)}\int_{\mathbb{R}}\left[(1+\omega_t J z)^{1-\gamma} - 1\right]\nu(dz), \quad \text{subject to } \mathcal{R}(\vartheta_t) \leq \eta. \end{aligned} \tag{3.34}$$

Given $\{h_t^*, a^*\}$ and θ_t^*, $[R + \sigma h_t]\,\omega_t - (1/2)\gamma\omega_t^2\sigma^2$ and $\left(\lambda^{\vartheta}/(1-\gamma)\right)\int_{\mathbb{R}}\left[(1+\omega_t J z)^{1-\gamma} - 1\right]\nu(dz)$ are both concave in ω_t, thus any solution to (3.34) will always have a unique maximizer. Note that if we were to allow for a jump size perturbation, the investor would additionally need to decide upon the optimal jump size perturbation b^*. This type of perturbation leads to highly-nonlinear first order conditions of both the jump size perturbation parameter b as well as for the optimal portfolio holdings which can only be resolved numerically.

The objective function is time independent. This follows because γ, R, σ, J and λ are constant which implies that the optimal drift perturbation parameter h_t will also be independent of time, $h_t = h,\ \forall t \geq 0$. Furthermore, since $\left[R + \sigma h_t - \lambda^{\vartheta} J \int_{\mathbb{R}} z\nu(dz)\right] \omega_t - (1/2)\gamma\omega_t^2\sigma^2 + \left(\lambda^{\vartheta}/(1-\gamma)\right) \int_{\mathbb{R}} \left[(1+\omega_t Jz)^{1-\gamma} - 1\right] \nu(dz)$ does not depend on the investor's time t wealth X_t, the optimal portfolio share will not only be time- but also be state-independent, i. e. $\omega^*(X_t, t) = \omega^*,\ \forall t \geq 0$. On the other hand, the optimal portfolio allocation will of course be a function of the perturbation parameters $\{h^*, a^*\}$, in other words, $\omega^* = \omega^*(h^*, a^*)$.

Lastly, we derive the measure change, in order to fully characterize the set of alternative models. When there is no jump size perturbation, the Radon-Nikodym derivative in (3.11) reduces to

$$d\vartheta_t^I = (e^a - 1)\vartheta_{t\_}^J \, d\hat{N}_t, \qquad \vartheta_0^J = 1 \text{ with } \widehat{N}_t = N_t - \lambda t \tag{3.35}$$

whose solution is given by

$$\vartheta_t^J = \exp\left\{aN_t - \lambda\left(e^a - 1\right)t\right\},\ \vartheta_0^J = 1. \tag{3.36}$$

Therefore, together with (3.9) characterizing the measure change of the diffusive part we arrive at

$$\mathcal{R}(\vartheta_t) = \mathcal{R}(\vartheta_t^D) + \mathcal{R}(\vartheta_t^J) = \frac{1}{2}h_t^2 + e^a\lambda\left(a - 1\right) + \lambda. \tag{3.37}$$

The investor's consumption and portfolio choice problem is summarized by (3.34) and (3.37), which limits the set of alternative models. The solution to this problem is given by a two step-procedure. In a first step, which corresponds to the min-part in (3.34), the investor has to decide how rich the alternative set of models is that he considers reasonably close to his reference model. In doing so, he specifies his preference for robustness with respect to small perturbations of his reference model by optimally choosing $\{h^*, a^*\}$. In a second step, he has to decide on his optimal consumption and portfolio policies. With CRRA preferences, from the first order condition of consumption in (3.30) we obtain

$$C_t^* = C_t^*(h^*, a^*) = K(h^*, a^*)X_t \tag{3.38}$$

where we require that $X_t > 0$ such that consumption remains non-negative. Then given $\{h^*, a^*\}$ evaluating (3.34) at optimal consumption C_t^* and portfolio holdings ω_t^* the constant K is given by

$$K^* = K(h^*, a^*) = \frac{\beta}{\gamma} - \frac{(1-\gamma)}{\gamma}\left[r + \omega^*\left(R + \sigma h^* - J\lambda e^{a^*}\int_{\mathbb{R}} z\nu(dz)\right)\right] + \frac{(1-\gamma)}{2}\omega^{*2}\sigma^2$$
$$- \frac{\lambda e^{a^*}}{\gamma}\int_{\mathbb{R}}\left[(1+\omega^* Jz)^{1-\gamma} - 1\right]\nu(dz) > 0 \tag{3.39}$$

which will be fully determined once we have first solved for the optimal perturbation parameters $\{h^*, a^*\}$ and secondly obtained the optimal portfolio holdings ω^*. Furthermore, from (3.38) and (3.39) it follows that the investor's optimal consumption is affected by robustness concerns.

Finally, given optimal consumption in (3.38) and the constant in (3.39) we can now check that the transversality condition is satisfied. Evaluating (3.15) and taking conditional time t expectations with respect to the robust measure we have that

$$\mathbb{E}^{\vartheta}\left[V(t, X_t^*)\right] = \mathbb{E}^{\vartheta}\left[\int_t^{\infty} e^{-\beta u} U(C_u^*)du\right] = \mathbb{E}^{\vartheta}\left[\int_t^{\infty} KV(u, X_u^*)du\right] \tag{3.40}$$

Since the optimal robust control parameters h^* and a^* as well as the model parameters R, σ, J and λ are constant, applying Leibniz rule for differentiating integrals, we obtain that

$$\mathbb{E}^{\vartheta}\left[V(t, X_t^*)\right] =: \psi(t) \tag{3.41}$$

solves the following ordinary differential equation

$$\psi^{'}(t) = \frac{d\mathbb{E}^{\vartheta}\left[V(t, X_t^*)\right]}{dt} = -K^*\psi(t), \quad \psi(0) = K^* X_0 \tag{3.42}$$

from which it follows that $\mathbb{E}^{\vartheta}\left[V(t, X_t^*)\right] = K^* X_0 e^{-K^* t}$ converges to zero exponentially fast as $t \to \infty$, which establishes that the transversalilty condition is satisfied.

3.3.1 Closed Form Robust Portfolio Weights

In order to obtain fully explicit portfolio weights, we further specify the level of risk aversion, the Lévy measure and the treatment of the entropy growth constraints. In the sequel, we focus

on a Lévy measure $\nu(dz)$ defined on $(0,1]$ and restrict the deterministic jump scaling factor J to the open interval $(-1,0)$. This implies that we only consider negative jumps in the asset price dynamics. However, those are the ones the investor is more concerned about as they are more harmful to his utility. We set $\nu(dz)$ to follow a power law under both measures, i. e.

$$\nu^{\vartheta}(dz) = \nu(dz) = dz/z, \text{ if } z \in (0,1]. \tag{3.43}$$

Concerning the treatment of the entropy growth constraints, since total relative entropy separates into a diffusive and a jump part, i.e. $\mathcal{R}(\vartheta_t) = \mathcal{R}(\vartheta_t^D) + \mathcal{R}(\vartheta_t^J)$, we can treat entropy growth with respect to the drift and jump parts independently.[5] However, this implies that the total maximal amount of robustness η is the sum of the maximal amount of robustness with respect to drift misspecification, denoted by η^D and the maximal amount of robustness with respect to jump intensity misspecification, denoted by η^J. Therefore $\eta = \eta^D + \eta^J$ which implies that we can write $\eta^D = \zeta^D \eta$ and thus $\eta^J = \left(1 - \zeta^D\right)\eta$, where $\zeta^D \in [0,1]$ denotes the share of total amount of robustness that is allocated to drift perturbation. Therefore, when $\zeta^D = 0$ the investor has full confidence in his drift specification and all the robustness concerns relate to the jump intensity. Likewise, when $\zeta^D = 1$, the investor beliefs that there is no jump intensity miss specification and thus is only concerned that the drift might be miss specified. With this decomposition, the entropy growth constraints are given by

$$\mathcal{R}(\vartheta_t^D) \leq \eta^D, \qquad \mathcal{R}(\vartheta_t^J) \leq \eta^J, \ \forall t \geq 0. \tag{3.44}$$

[5] A similar idea has also been used by Chen & Epstein (2002), Sbuelz & Trojani (2008), Ulrich (2010), Ulrich (2012), Drechsler (2013) to solve a model ambiguity problem when the risks are only diffusive. In our case, a joint entropy growth constraint gives rise to first order conditions of the drift and the jump intensity perturbation parameter which cannot be solved analytically and one needs to rely on numerical techniques to solve the system.

Define as $\mathcal{L}(\omega_t, h_t, \widetilde{\theta}^D, \widetilde{\theta}^J)$ the Lagrangian associated to the constraint HJB problem in (3.34) with constant Lagrange multipliers $\widetilde{\theta}^D$ and $\widetilde{\theta}^J$. Then taking $\gamma = 2$ we obtain

$$\begin{aligned}\mathcal{L}(\omega, h, a, \widetilde{\theta}^D, \widetilde{\theta}^J) = \omega R + \sigma h\omega - \omega\lambda J e^a - \omega^2\sigma^2 + \lambda e^a \log(1 + \omega_t J) \\ + \widetilde{\theta}^D\left(\frac{1}{2}h^2 - \eta^D\right) + \widetilde{\theta}^I\left(\lambda e^a(a-1) + \lambda - \eta^J\right). \end{aligned} \tag{3.45}$$

The necessary first order optimality conditions for the robustness parameters h and a are

$$\frac{\partial\mathcal{L}(\omega, h, a, \widetilde{\theta}^D, \widetilde{\theta}^J)}{\partial h} = \sigma\omega_t + \widetilde{\theta}^D h = 0, \ \rightarrow h^* = -\frac{\sigma\omega_t}{\widetilde{\theta}^D}, \qquad \widetilde{\theta}^D \geq 0 \tag{3.46}$$

$$\frac{\partial\mathcal{L}(\omega, h, a, \widetilde{\theta}^D, \widetilde{\theta}^J)}{\partial a} = \lambda e^a\left(a\widetilde{\theta}^I + \log(1 + J\omega) - wJ)\right) = 0, \tag{3.47}$$

$$\rightarrow a = \frac{\omega J - \log(1 + J\omega)}{\widetilde{\theta}^J}, \ \theta^J \geq 0 \tag{3.48}$$

$$\frac{\partial\mathcal{L}(\omega, h, a, \widetilde{\theta}^D, \widetilde{\theta}^J)}{\partial\widetilde{\theta}^D} = \eta^D - \frac{1}{2}h^2 = 0, \ \rightarrow \widetilde{\theta}^{D*} = \pm\sqrt{\frac{\sigma^2\omega^2}{2\eta^D}} \tag{3.49}$$

$$\frac{\partial\mathcal{L}(\omega, h, a, \widetilde{\theta}^D, \widetilde{\theta}^J)}{\partial\widetilde{\theta}^J} = \eta^J - \lambda e^a(a-1) - \lambda = 0. \ \rightarrow \widetilde{\theta}^{J*} = \frac{\omega J - \log(1 + J\omega)}{1 + W\left(\frac{\eta^J - \lambda}{e\lambda}\right)} \geq 0. \tag{3.50}$$

From the system of equations (3.46) to (3.50) we find that the optimal drift h^* and jump intensity (a^*) perturbation parameters are given by

$$h_t^* = h^* = -\sqrt{2\eta^D}, \ \forall\eta^D \geq 0, \qquad a^* = 1 + W\left(\frac{\eta^J - \lambda}{e\lambda}\right) \geq 0, \ \forall\eta^J \geq 0, \lambda \in (0, \infty) \tag{3.51}$$

where $W\left(\left(\eta^J - \lambda\right)/(e\lambda)\right) = W(\cdot; \lambda)$ denotes Lambert's W function and e is Euler's constant. The function $W(\cdot, \lambda)$ is plotted in Figure B.1.[6]

[Figure B.1 about here]

Note that $\lim_{\eta\to 0} W(\eta; \lambda) = W(-1/e; \lambda) = -1$ so that $\lambda^\vartheta = \lambda$, in other words we are back to the case where there are no robustness concerns of the investor with respect to the jump intensity parameter.

[6]Since η is real, the function W is not injective on the interval $-1/e \leq \eta < 0$. However, we set $W(\cdot, \lambda) \geq -1$ such that $W(\cdot, \lambda)$ is single valued and therefore represents a well defined function. Furthermore, on the domain $[-1/e, \infty]$ the function $W(\cdot, \lambda)$ is real for any $\lambda > 0$ and $\eta \in [0, \infty)$. Furthermore, note that for $\eta^J < \lambda$ we have $W\left(\frac{\eta^J - \lambda}{e\lambda}\right) < 0$ and for $\eta^J > \lambda$ we obtain $W\left(\frac{\eta^J - \lambda}{e\lambda}\right) > 0$.

Furthermore, $\lambda^{\vartheta} > \lambda,\ \forall \eta, \lambda > 0$. Thus, the robust jump intensity under the robust measure $\mathbb{P}^{\vartheta}$ is always higher than the jump intensity under the reference measure $\mathbb{P}$. Since $\lambda > 0$, λ^{ϑ} is increasing in η^J as

$$\frac{\partial W}{\partial \eta} = \frac{W\left(\frac{\eta^J - \lambda}{e\lambda}\right)}{(\eta^J - \lambda)(1 + W\left(\frac{\eta^J - \lambda}{e\lambda}\right)} > 0 \ \ \forall \eta^J, \lambda > 0.$$

This implies that the larger the set of potential models ($\eta^J \uparrow$) is we allow for, the higher the jump frequency under the robust measure becomes.

In order to make sure that the optimal robust control variables h^* and a^* are indeed (global) minimizers we need to check the second order optimality conditions. For the optimal drift perturbation parameter h^* we have

$$\frac{\partial^2 \mathcal{L}(\omega, h, a, \widetilde{\theta}^D, \widetilde{\theta}^I)}{\partial h^2} = \widetilde{\theta}^D$$

and thus we need $\widetilde{\theta}^D \geq 0$ such that $\mathcal{L}(\omega, h, a, \widetilde{\theta}^D, \widetilde{\theta}^I)$ is convex in h and therefore the solution in (3.51) is indeed a (global) minimum. This implies $\widetilde{\theta}^D = \sqrt{\frac{\sigma^2\omega^2}{2\eta}} \geq 0$ and therefore the second order Lagrange-conditions are satisfied for h^* and $\widetilde{\theta}^{D*}$. Along the same line of argument, we have

$$\widetilde{\theta}^{J*} = \frac{\omega J - \log\left(1 - J^2 w^2\right)}{1 + W\left(\frac{\eta^J - \lambda}{e\lambda}\right)} \geq 0$$

for any ω satisfying the solvency constraint $|\omega J| < 1$ and $1 + W\left(\left(\eta^J - \lambda\right)/\left(e\lambda\right)\right) \in (0, \infty),\ \forall \lambda, \eta^J > 0$, and

$$\frac{\partial \mathcal{L}^2(\omega, h^*, a^*, \widetilde{\theta}^{D*}, \widetilde{\theta}^{J*})}{\partial a^2} = e^a \lambda \widetilde{\theta}^{J*} \geq 0$$

which shows that a^* is the global minimizer.

Next, using the optimal perturbation parameters h^* and a^* we can now solve for the optimal robust portfolio weights in closed form. Given $\mathcal{L} = \mathcal{L}(\omega, h^*, a^*, \widetilde{\theta}^{D*}, \widetilde{\theta}^{J*})$ in (3.45) the first order condition for ω is given by

$$\frac{\partial \mathcal{L}}{\partial \omega} = R - \sqrt{2\eta^D}\sigma - \lambda J e^{1 + W\left(\frac{\eta^J - \lambda}{e\lambda}\right)} - 2\omega\sigma^2 + J\lambda e^{1 + W\left(\frac{\eta^J - \lambda}{e\lambda}\right)} / (1 + \omega J) = 0$$

which is a quadratic polynomial in the portfolio weights ω whose solution can be expressed as

$$\omega^*(h^*, a^*) = \frac{J\left(R - \sqrt{2\eta^D}\sigma\right) - J^2\lambda e^{1+W\left(\frac{\eta^J-\lambda}{e\lambda}\right)} - 2\sigma^2 + H(\eta)}{4J\sigma^2} \tag{3.52}$$

$$H(\eta) = \sqrt{h_1(\eta) + h_2^2(\eta)}$$

$$h_1(\eta) := 8\sigma^2\lambda J^2 e^{1+W\left(\frac{\eta^J-\lambda}{e\lambda}\right)}$$

$$h_2(\eta) := J\left(R - \sqrt{2\eta^D}\sigma\right) + 2\sigma^2 - J^2\lambda e^{1+W\left(\frac{\eta^J-\lambda}{e\lambda}\right)}$$

and we require that the solvency constraint $|\omega^* J| < 1$ holds at the optimal portfolio allocation ω^*. In Figure B.2 we plot the optimal robust portfolio weights as a function of the share of total robustness assigned to drift perturbation ζ^D.

[Figure B.2 about here]

As expected, the robust portfolio allocation is such that the amount invested into the risky asset is lower compared to the case when the investor has full confidence in his reference model ($\eta = 0$). Further, regardless of the share of η allocated to drift or jump intensity robustness, the optimal portfolio weights are more sensitive when η is low compared to the case when η is large. This implies that the marginal effect of increasing the total amount of robustness on $\omega^*(h^*, a^*)$ is declining. Next, comparing the case of only drift $\zeta^D = 1$ to only jump intensity $\zeta^D = 0$ perturbation shows that ω^* is reduced more in the case when there are solely concerns about potential drift as opposed to only jump intensity misspecification. However, this is a direct consequence of compensating the Lévy process as the expected return on the risky asset is higher due to adding the compensator. Lastly, the asymptotic behavior of the portfolio weights when the total amount of robustness tends to infinity, shows that

$$\lim_{\eta\to\infty} \omega^*(h^*, a^*) = -\infty$$

which implies that regardless of whether the drift or the jump intensity is misspecified or both, the investor optimally chooses to short the risky asset (up until the solvency constraint $|\omega^* J| < 1$ holds) when model uncertainty approaches infinity.

3.3.2 Further Closed Form Solutions

Other special cases which lead to fully explicit portfolio weights arise when $\gamma = 3$ or 4. The first order conditions for optimal portfolio holdings lead to a cubic (resp. quartic) equation, which given that $|wJ| < 1$, is solvable in closed form using standard methods.

There are also other settings where one can derive fully explicit portfolio weights. Using the same dynamics of the stock price process as in (3.4), we can derive fully explicit portfolio weights if we assume that the jump sizes are uniformly distributed on $(0, 1)$ and the coefficient of risk aversion is equal to either 3 or 4. An interesting example is when the Poisson process is not compensated, meaning $Y_t = \sum_{n=1}^{N_t} Z_n$ and the i.i.d. jumps Z_n have symmetric Lévy measure about zero, i. e.

$$\lambda\nu(dz) = \begin{cases} \lambda dz/z & \text{if } z \in (0, 1], \\ -\lambda dz/z & \text{if } z \in [-1, 0) \end{cases} \tag{3.53}$$

so that the underlying asset exhibits both positive and negative jumps (see Section B.1 for a discussion). The quantitative behavior of the optimal portfolio weights is very similar to the compensated Lévy case. An other interesting example is given when the jumps are negative (no positive jumps) and we do not compensate the Lévy - process S_t. In this case, the portfolio weights are more sensitive to jump intensity perturbation, meaning the fraction of wealth invested into the risky asset is not only lower, but also decreases in η^J substantially faster compared to the compensated Lévy case. Lastly, in Section B.2 we solve the consumption and investment problem where the investor has exponential utility and the risky asset follows a compensated exponential Lévy process.

3.3.3 Sensitivity Analysis of Optimal Portfolio Weights

Given the explicit portfolio weights we can now analyze their sensitivity with respect to both the asset price parameters R, σ, J, λ of the model and the entropy growth parameters η^D and η^J. We start our analysis by comparing ω^* in (3.52) to the classical Merton solution with and without robustness concerns, which can be obtained by letting $\lambda \to 0$. In this case the risks are only diffusive, and since we have set $\gamma = 2$ the optimal portfolio holding ω^* reduces to

$$\omega^*_{\mathrm{RM}} = \frac{R - \sqrt{2\eta^D}\sigma}{2\sigma^2} \tag{3.54}$$

where the subscript RM refers to the robust Merton portfolio allocation. The standard (non-Merton) policy is

$$\omega^*_{\mathrm{M}} = \frac{R}{2\sigma} \tag{3.55}$$

obtained by setting $\eta^D = 0$ in (3.54).

From (3.54) one can immediately see that an investor who is concerned about potential model misspecification will always invest less into the risky asset. Next, going back to the robust jump diffusive weights in (3.52), for any $\lambda > 0$, we have that $\omega^* = 0$ whenever $R = \sqrt{2\eta^D}\sigma$. This is intuitive as when the expected return under the robust measure is zero and since $\mathbb{E}^{\vartheta}_t[\widetilde{Y}_t] = 0$, the investor has no benefit in allocating funds into the risky asset. Note that

$$\frac{\partial \omega^*}{\partial R} = \frac{1}{4J\sigma^2}\left(1 + \frac{\left(R - \sqrt{2\eta^D}\sigma\right) - e^{1+W\left(\frac{\eta^J-\lambda}{e\lambda}\right)}J^2\lambda + 2\sigma^2}{2H}\right) > 0 \leftrightarrow 0 < J^2\lambda e^{1+W\left(\frac{\eta^J-\lambda}{e\lambda}\right)}, \tag{3.56}$$

from which we see that the inequality in (3.56) will always be satisfied under both measures. Thus increasing the expected return will lead to an increase of investment into the risky asset. Next, the limit of the optimal robust jump diffusive weights when volatility tends to infinity is 0, i.e.

$$\lim_{\sigma \to \infty} \omega^*(h^*, a^*) = 0 \tag{3.57}$$

The rate at which the portfolio weights approach zero is affected by the amount of drift perturbation η^D in the following way,

$$\omega^*|_{\sigma\to\infty} \sim -\sqrt{\frac{\eta^D}{2}}\sigma + O\left(\frac{1}{\sigma^2}\right) \tag{3.58}$$

suggesting that the rate at which the portfolio weights approach zero is lower whenever there is doubt about the drift specification of the model. Furthermore, the partial derivative of ω^* with respect to the jump intensity λ is

$$\frac{\partial\omega^*}{\partial\lambda} = \frac{J\left(e^{W\left(\frac{\eta^J-\lambda}{e\lambda}\right)}-1\right)\left(2\sigma^2 - J\left(R-\sqrt{2\eta^D}\sigma\right) + e^{1+W\left(\frac{\eta^J-\lambda}{e\lambda}\right)}J^2\lambda - H\right)}{4\sigma^2 H\left(1+W\left(\frac{\eta^J-\lambda}{e\lambda}\right)\right)}$$

The interesting observation from inspection of $\frac{\partial\omega^*}{\partial\lambda}$ is that an increase in the jump intensity does not necessarily lead to a decline in the share of wealth allocated to the risky asset. This is even true if there is no concern about jump intensity misspecification, i. e. $\eta^J = 0$. This somewhat counterintuitive result is due to compensating the jump process.[7] Increasing (decreasing) the jump intensity leads to negative jumps occurring more (less) frequently but simultaneously leads to an increase (decrease) in the compensator and thus in the expected return. This explains why the sign of $\frac{\partial\omega^*}{\partial\lambda}$ can be positive or negative depending on the parameter values of the model. Note that when $R = \sqrt{2\eta^D}\sigma$ we have that $\partial\omega^*/\partial\lambda = 0$ for any $\eta^J > 0$. Furthermore, for $\lambda \to \infty$ the optimal portfolio weight approach zero at the following rate

$$\omega^*|_{\lambda\to\infty} \sim \frac{1}{\lambda}\frac{R-\sqrt{2\eta^D}\sigma}{J^2 e^{1+W\left(\frac{\eta^J-\lambda}{e\lambda}\right)}} + O\left(\frac{1}{\lambda^2}\right) \tag{3.59}$$

Thus, whenever $R - \sqrt{2\eta^D}\sigma > 0$, $\omega^* > 0$ the optimal portfolio weight approaches zero from positive territory and vice versa when $R - \sqrt{2\eta^D}\sigma < 0$. Further, under the robust measure the rate is lower due to both drift (downward level shift) and jump intensity perturbation (downward scaling). Next, analyzing the sensitivity of the optimal robust portfolio weights

[7] In Aït-Sahalia et al. (2009), an increase in the likelihood of jumps occurring always leads to a reduction in the amount invested into the risky asset. This result is due to the fact, that in their model, the jump component is not compensated which implies that the risky asset does not carry a jump risk premium.

with respect to η shows that

$$\frac{\partial \omega^*}{\partial \eta} = -\left(\frac{\sqrt{\zeta^D}}{4\sqrt{2\eta}\sigma} + \frac{J\left(1-\zeta^D\right)}{4\sigma^2\left(1+W\left(\frac{\eta^J-\lambda}{e\lambda}\right)\right)}\right)(1+F(\eta)) + \frac{J\left(1-\zeta^D\right)}{\left(1+W\left(\frac{\eta^J-\lambda}{e\lambda}\right)\right)H(\eta)} \tag{3.60}$$

where $F(\cdot) = \frac{h_2(\cdot)}{H(\cdot)} : \eta \to (-1, 1)$. Evaluating Equation (3.60) above for $\eta = 0$, we can infer using l'hôpitals rule that

$$\left.\frac{\partial \omega^*}{\partial \eta}\right|_{\eta=0} = -\infty \tag{3.61}$$

which implies that optimal portfolio weights are highly sensitive when robustness concerns are introduced into the reference model.[8] Furthermore, we show in Section B.4 that the optimal portfolio weights are monotonically declining in uncertainty η, which indicates that the investor optimally reduces his position in the risky asset when parameter uncertainty increases. Lastly, we plot the robust jump diffusive and the jump diffusive portfolio weights for a wide range of parameter values for a fixed total amount of robustness η and vary the parameters R, σ, J and λ.

[Figure B.3 about here]

Figure B.3 shows that, under robustness concerns, the amount invested into the risky asset is always lower than when the investor has full confidence in his reference model. From Panel A we see that increasing volatility of the risky asset leads the investor to optimally decrease $\omega^*(h^*, a^*)$ and even short the asset whenever R is sufficiently low. Panel B shows that when both J and λ are high, then the investor simply allocates all his funds into the risk free asset. Thus, the model can capture the well-documented empirical flight-to-quality behavior when jump risk λ is high and J approaches -1. However, contrarily to the case when jumps are only negative and the process is not compensated which leads the investor to optimally short the risky asset, i. e. $\omega^* \to -\infty$ as $\lambda \to \infty$ (see Aït-Sahalia et al. (2009)), in this setting, our robust

[8] Furthermore, one can show that

$$\left.\frac{\partial \omega^*}{\partial \eta}\right|_{\eta=\infty} = 0 \tag{3.62}$$

which implies that the marginal impact of increasing model uncertainty diminishes as η increases.

investor does not short the risky asset whenever J and λ are sufficiently high, but instead optimally chooses $\omega^* = 0$.

Further, if either the jump scaling parameter or the intensity approach zero, i. e. the risky assets dynamics converges to a purely diffusive process, $\omega^*(h^*, a^*)$ increases non-linearly and the gap between the robust and non-robust portfolio weights widens. This suggests that for low jump risks $\lambda \downarrow$ and simultaneously low jump size scaling $J \to 0$, perturbations of the reference model have a higher impact on $\omega^*(h^*, a^*)$, meaning that there is a significant drop in the amount invested into the risky asset, compared to the case when both J and λ are high.

3.4 Error-Detection Probability for Lévy Jump-Diffusive Processes

The robust portfolio weights derived in the previous sections crucially depend on the amount of model uncertainty we allow for. In order to quantify how much uncertainty seems reasonable to the investor, we make use of detection-error probabilities as suggested by Anderson et al. (2003). More formally, let $\xi_t = \log(\vartheta_t)$ and $\mathcal{F}_t$ be the filtration with respect to which the probabilities and expectations are conditioned, the error-detection probability $\pi(t, T; \eta)$ is defined as the conditional probability at time t of making a detection-error given a sample of length $T > 0$,

$$\pi(t, T; \eta) = \frac{1}{2}\left(\mathbb{P}\left[\xi_T > 0 | \mathcal{F}_t\right] + \mathbb{P}^{\vartheta}\left[\xi_T < 0 | \mathcal{F}_t\right]\right), \qquad 0 \leq t \leq T. \tag{3.63}$$

Therefore, as η increases, so does the set of admissible models for the risky asset under $\mathbb{P}$ and $\mathbb{P}^{\vartheta}$, thereby causing the detection-error probability to decrease towards zero. Thus the larger η, the easier statistical discrimination between the model dynamics under $\mathbb{P}$ and $\mathbb{P}^{\vartheta}$ becomes. Anderson et al. (2003) suggest to choose η such that the error-detection probability is at least 10%. Note that when $\pi(t, T; \eta) = 0.5$ the models are statistically indistinguishable.

We now derive an expression for the conditional probabilities in (3.63) by means of Fourier transformation of the conditional probability measures. The conditional characteristic functions

of ξ_T, under the reference measure $\mathbb{P}$, denoted by $\phi_{\mathbb{P}}(k,t,T)$ and $\phi_{\mathbb{P}^\vartheta}(k,t,T)$ under the robust measure $\mathbb{P}^\vartheta$ are given by

$$\phi_{\mathbb{P}}(k,t,T) = \mathbb{E}^{\mathbb{P}}\left[e^{ik\xi_T}|\mathcal{F}_t\right] = \mathbb{E}^{\mathbb{P}}\left[\vartheta_T^{ik}|\mathcal{F}_t\right] \tag{3.64}$$

$$\phi_{\mathbb{P}^\vartheta}(k,t,T) = \mathbb{E}^{\mathbb{P}^\vartheta}\left[e^{ik\xi_T}|\mathcal{F}_t\right] = \mathbb{E}^{\mathbb{P}^\vartheta}\left[\vartheta_T^{ik}|\mathcal{F}_t\right] \tag{3.65}$$

where $i = \sqrt{-1}$ and $k \in \mathbb{R}$ is the transform variable. Using a simple measure change of the form

$$\phi_{\mathbb{P}^\vartheta}(k,t,T) = \int_{\omega\in\Omega} \vartheta_T^{ik}\vartheta_T d\mathbb{P}(\omega) = \mathbb{E}^{\mathbb{P}}\left[\vartheta_T^{1+ik}|\mathcal{F}_t\right] \tag{3.66}$$

the Fourier transform under the robust measure can be obtained by integrating with respect to the reference measure. By an application of Feynman-Kac's theorem, we can compute the conditional expectations (3.64) and (3.66) by solving a partial differential difference equation (PDDE) with appropriate boundary conditions. If we were to also perturb the jump sizes, the measure change would satisfy a partial integral-differential equation.

In order to derive this PDDE for both conditional Fourier transforms we need the dynamics of the measure change under $\mathbb{P}$ given the optimal perturbation policies h_t^* and a^*. An application of Itô's product formula for semi martingales to the optimally perturbed ϑ_t^* shows that

$$\begin{aligned}\vartheta_t^* = \vartheta_t^{*,D}\vartheta_t^{*,J} &= \vartheta_0^{*,D}\vartheta_0^{*,J} + \int_0^t \vartheta_{s_-}^{*,J} d\vartheta_s^{*,D} + \int_0^t \vartheta_s^{*,D} d\vartheta_s^{*,J} + \left[\vartheta^{*,D}, \vartheta^{*,J}\right]_t \\ &= \vartheta_0^{*,D}\vartheta_0^{*,J} + \int_0^t \vartheta_{s_-}^{*,J} d\vartheta_s^{*,D} + \int_0^t \vartheta_s^{*,D} d\vartheta_s^{*,J}\end{aligned}$$

Then applying Itô's formula to (3.9) and using (3.35) we obtain

$$d\vartheta_t^* = \vartheta_t h_t^* dB_t + \vartheta_{t_-}\left(e^{a^*} - 1\right) d\hat{N}_t \tag{3.67}$$

From (3.67), the dynamics of the log measure change are

$$\begin{aligned}\xi_t &= \xi_0 + \int_0^t h_s^* dB_s - \int_0^t \left(\frac{1}{2}h_s^{*2} + \lambda\left(e^{a^*} - 1\right)\right) ds + \sum_{0<s\le t}\left(\xi_s - \xi_{s_-}\right) \\ &= \xi_0 + \int_0^t h_s^* dB_s - \int_0^t \left(\frac{1}{2}h_s^{*2} + \lambda\left(e^{a^*} - 1\right)\right) ds + a^* N_t\end{aligned} \tag{3.68}$$

and therefore the PDDE for $\phi_{\mathbb{P}}(t) = \phi_{\mathbb{P}}(k,t,T)$ is given by

$$\begin{aligned} 0 &= \mathcal{A}\phi_{\mathbb{P}}(k,t,T) \\ &= \frac{\partial \phi_{\mathbb{P}}}{\partial t} - \frac{\partial \phi_{\mathbb{P}}}{\partial \xi}\left(\frac{1}{2}h_t^{*2} + \lambda\left(e^{a^*}-1\right)\right) + \frac{1}{2}\frac{\partial^2 \phi_{\mathbb{P}}}{\partial \xi^2}h_t^{*2} + \lambda\left(\phi_{\mathbb{P}}(k,t,T) - \phi_{\mathbb{P}}(k,t_-,T)\right) \end{aligned} \tag{3.69}$$

subject to the following boundary condition

$$\phi_{\mathbb{P}}(k,T,T) = \vartheta_T^{ik} \tag{3.70}$$

Likewise the PDDE for $\phi_{\mathbb{P}^\vartheta}(t) = \phi_{\mathbb{P}^\vartheta}(k,t,T)$ is equivalent and given by

$$\begin{aligned} 0 &= \mathcal{A}\phi_{\mathbb{P}^\vartheta}(k,t,T) \\ &= \frac{\partial \phi_{\mathbb{P}^\vartheta}}{\partial t} - \frac{\partial \phi_{\mathbb{P}^\vartheta}}{\partial \xi}\left(\frac{1}{2}h_t^{*2} + \lambda\left(e^{a^*}-1\right)\right) + \frac{1}{2}\frac{\partial^2 \phi_{\mathbb{P}^\vartheta}}{\partial \xi^2}h_t^{*2} + \lambda\left(\phi_{\mathbb{P}^\vartheta}(k,t,T) - \phi_{\mathbb{P}^\vartheta}(k,t_-,T)\right) \end{aligned} \tag{3.71}$$

subject to a different boundary condition given by

$$\phi_{\mathbb{P}^\vartheta}(k,T,T) = \vartheta_T^{1+ik}.$$

The PDDE in (3.71) admits a unique affine solution of the form

$$\phi_{\mathbb{P}}(k,t,T) = e^{\alpha(T-t)+\beta(T-t)\xi_t} \tag{3.72}$$

where $\alpha(\cdot)$ and $\beta(\cdot)$ are both deterministic functions of time to maturity $\tau = T-t$. Inserting the conjecture of (3.72) into (3.69) gives

$$0 = -\alpha' - \beta'\xi_t - \beta\left(\frac{1}{2}h_t^{*2} + \lambda\left(e^{a^*}-1\right)\right) + \frac{1}{2}h_t^{*2}\beta^2 + \lambda\left(e^{\beta a^*}-1\right).$$

Using the fact that this equation has to hold for all ξ_t and the constant terms we get two equations, namely

$$\beta(T-t) = \beta = \int_t^T \beta' = K \rightarrow K = ik = \beta \tag{3.73}$$

$$\alpha(T-t) = \int_t^T \alpha' = \left[-\beta\left(\frac{1}{2}h_t^{*2} + \lambda\left(e^{a^*}-1\right)\right) + \frac{1}{2}h_t^{*2}\beta^2 + \lambda\left(e^{\beta a^*}-1\right)\right](T-t) \tag{3.74}$$

where the expression for β in (3.73) follows from the boundary condition in (3.70) and $\alpha(0) = 0$. The solution for (3.71) is identical except that $\beta = 1+ik$. Given these conditional characteristic

functions $\phi_{\mathbb{P}^\vartheta}(k,t,T)$ and $\phi_{\mathbb{P}}(k,t,T)$, the error-detection probability in (3.63) based on a sample of length $T-t$ is given by

$$\pi(t,T;\eta) = \frac{1}{2} - \frac{1}{2\pi}\int_0^\infty \left(\mathrm{Re}\left[\frac{\phi_{\mathbb{P}^\vartheta}(k,0,T)}{ik}\right] - \mathrm{Re}\left[\frac{\phi_{\mathbb{P}}(k,0,T)}{ik}\right]\right) dk$$

where $\mathrm{Re}(\cdot)$ denotes the real part of a complex number. In Figure B.4, we plot the error-detection probability as a function of the robustness parameter η using monthly and weekly sampled data points over a time period of one year $T = 1$.

[Figure B.4 about here]

As expected, $\pi(t,T;\eta)$ is monotonously decreasing in η, which is intuitive as the set of alternative models increases, which implies that the dynamics of the process under $\mathbb{P}$ becomes more distinct from the dynamics of the process under $\mathbb{P}^\vartheta$. Furthermore, the two graphs in Figure B.4 imply that making an error in classifying, whether a given time series was generated under the reference or the robust measure, is smaller in the case when we have weekly data available as opposed to only monthly data. This is due to the fact that it becomes increasingly easier to distinguishing between two stochastic processes (one under the reference and the other under the robust measure), the longer the available time series is. Lastly, the same conclusion can be drawn when increasing the jump intensity parameter λ.

3.5 Expected Utility Comparison: Monte-Carlo Simulations

In this section, we conduct simulations to compare the utility resulting from following four different portfolio policies: standard Merton diffusive policy, robust Merton diffusive policy, standard optimal jump-diffusive policy and robut optimal jump-diffusive policy.

Given the optimal drift h^* and jump intensity a^* perturbation parameter, we evaluate expected utility

$$F_t^{\mathbb{J}}(X_t^*;\omega^{*,i},h^*,a^*) := \mathbb{E}_t^{\mathbb{J}}\left[V(t,X_t^*)\right] = \mathbb{E}_t^{\mathbb{J}}\left[\int_t^\infty e^{-\beta u}U(C_u^*)du\right] = \int_t^\infty \mathbb{E}_t^{\mathbb{J}}\left[K(a^*,h^*)V\left(u,X_u^*\right)\right]du \tag{3.75}$$

under both the reference and robust measure $\mathbb{J} = \{\mathbb{P}, \mathbb{P}^\vartheta\}$ for the four different portfolio holdings $\omega^{*,i}(h^*,a^*),\ i \in \{\mathrm{M}, \mathrm{rM}, \mathrm{JD}, \mathrm{rJD}\}$ which are, the Merton (i.e. (3.54) with $\eta^D = 0$), the robust Merton (3.54) where $\eta^D = \eta$), jump-diffusive (i.e. (3.52) with $\eta^D = \eta^J = 0$) and robust jump diffusive weights, i.e. (3.52), respectively. Under the correct measure, the optimal portfolio holdings will maximize (3.75), meaning that if the stock price follows the compensated exponential Lévy process under the robust measure, the robust jump diffusive portfolio weights will give highest expected utility.[9]

The aim of this Monte Carlo simulation exercise is not only to verify this under a variety of different parameter specifications, but also to quantify the utility loss that results from using the wrong portfolio strategy. Of course, since the notion of expected utility is ordinal, a numerical comparison, we can only rank expected utility for the various portfolio strategies. The benchmark parameters for the Monte Carlo simulations as well as the alternative parameters, which we use for conducting a comparative static analysis, are given in Table B.1.

[Table B.1 about here]

In order to fully specify the dynamics under the robust measure $\mathbb{P}^\vartheta$ we have to quantify the maximal amount of robustness $\eta = \eta^D + \eta^J$. We numerically choose η such that the target error-detection probability is $\bar{\pi} = 10\%$ which is the value suggested by Anderson et al. (2003), i.e.

$$\arg\min_{\eta\in[0,\infty)} ||\pi(t,T_d;\eta) - \bar{\pi}||, \qquad 0 \le t \le T_d.$$

where $\pi(t,T_d;\eta) = \frac{1}{2}\left(\mathbb{P}\left[\xi_T > 0|\mathcal{F}_t\right] + \mathbb{P}^\vartheta\left[\xi_T < 0|\mathcal{F}_t\right]\right)$ and T_d is the time series length.

[9] Likewise, if the stock price follows the compensated exponential Lévy process under the reference measure, the jump diffusive portfolio weights will give highest expected utility.

We also vary η^D as well as η^J in order to quantify the effect of changing the absolute level of drift against jump intensity perturbation. In the extreme case when $\eta^D = 0$ ($\eta^J = 0$), the investor has full confidence in the drift (jump intensity) estimate of the stock price process.

The reason we consider differential time series lengths for quantifying the amount of maximal robustness and the investment horizon, is due to the fact we mentioned in Section 3.4 (see Figure B.4), namely that statistical discrimination between two processes becomes easier the longer the available time series is. For instance, if we consider a sample path of the risky asset for two different time series lengths $T_d^1 = 1$ and $T_d^2 = 3$ and evaluate (3.76) such that the error-detection probability is 10%, we find that $\eta(T_d^1) = 0.0132$ and $\eta(T_d^d) = 0.0044$, which corresponds to a threefold increase in the amount of model uncertainty. Furthermore, comparing the optimal drift h^* and jump intensity a^* perturbation parameters for the two time series lengths we find that $h^*(T_d^1) = 0.051$ and $a^*(T_d^1) = 0.067$ as opposed to $h^*(T_d^2) = 0.030$ and $a^*(T_d^2) = 0.039$. Hence, if the investor has fewer data points available, the estimated maximal amount of robustness is considerably higher, as it is more difficult two distinguish between two realized sample paths obtained over a shorter time period.

We consider two different frequencies, daily (assuming 252 trading days per year) and intra-daily (60min sampling) assuming 6h 30 min. hours per day which are the official trading hours of the New York Stock Exchange (NYSE). This gives us a total number of observations of $N = T_d \times 252 \times 6.5 \times 60/m = 1,512$, where m is the sampling frequency. Lastly, we specify two jump size distributions, namely the power law in (3.53) and uniform jumps on $(0, 1)$ for which fully closed form solutions of the portfolio weights are obtainable as we showed above. The simulation of jump sizes in the case when they follow a power law is detailed in Appendix B.3. In the case when jumps are uniformly distributed on (0,1), fully closed form portfolio weights can be obtained for risk aversion $\gamma = 3, 4$.

In order to facilitate expected utility comparison, for each measure, we compute

$$REU^{\mathbb{P}} := \frac{F_t^{\mathbb{J}}(X_t^*; \omega^{*,i}, h^*, a^*)}{F_t^{\mathbb{P}}(X_t^*; \omega^{*,i}, h^* = 0, a^* = 0)} \tag{3.76}$$

$$REU^{\mathbb{P}^\vartheta} := \frac{F_t^{\mathbb{J}}(X_t^*; \omega^{*,i}, h^*, a^*)}{F_t^{\mathbb{P}^\vartheta}(X_t^*; \omega^{*,i}, h^*, a^*)} \tag{3.77}$$

where $REU^{\mathbb{P}}$ denotes the ratio of expected utility deviation for each portfolio allocation, relative to the expected utility derived using the correct jump - diffusive portfolio weights under the reference measure. Similarly, $REU^{\mathbb{P}^\vartheta}$ denotes the ratio of expected utility deviation for each portfolio allocation, relative to the expected utility derived using the correct robust jump - diffusive portfolio weights under the robust measure. Clearly, we would expect that $|REU^{\mathbb{J}}| > 1$, $\mathbb{J} = \{\mathbb{P}, \mathbb{P}^\vartheta\}$ whenever we do not use the optimal portfolio weights.

In Table B.2, we summarize the simulation results for the benchmark parameters.

[Table B.2 about here]

Using daily data, the first column labeled 'Weights' shows that the standard optimal Merton weight ω_{M}^* is the highest holding of the risky asset, whereas its robust counterpart ω_{RM}^* has the lowest holding in the risky asset. This is mainly a consequence of setting $\eta^D = \eta$ in which case the maximum amount of model uncertainty concerns only the drift part and therefore lowers to excess considerably (see column 'Drift'). The optimal jump diffusive and robust jump diffusive weights lie in between the two Merton weights. Since we are compensating the negative jumps, a higher jump intensity not only increases the likelihood of jumps occurring, but also raises the expected return as the compensator adds a jump risk premium to the drift of the stock price. Following this line of argumentation, this also implies that under the robust measure, the jump intensity as well as the jump risk premium are higher, compared to the jump intensity and jump risk premium under the reference measure. Furthermore, the next four columns essentially verify our claim from above that under the correct measure with the optimal portfolio allocation, expected utility is highest. For instance, under the robust measure,

expected utility of the investor is highest, whereas using the wrong portfolio weights leads to a utility loss.

Lastly, the remaining four columns compare the drift and jump intensities under the two different measures. Comparing the drift in a purely diffusive setting, the stock price drift is 5%, whereas in a jump diffusive setting the drift is increased to 6.09% which is a direct consequence of compensating the jump part. Furthermore, under the robust measure, the jump intensity is increased by a little less than 16% indicating that jumps are 16% more likely to occur compared the jump process under the reference measure. The last two columns quantify the robust control parameters for optimal drift and jump intensity perturbation. In the robust Merton case, the expected drift is reduced by $h^*(\zeta^D = 1)\sigma = 3.23\%$, whereas for the robust jump diffusive case, the reduction in expected return due to drift robustness is only $h^*(\zeta^D = 0.1)\sigma = 1.03\%$. This is due the fact that we only allocate 10% of total robustness η to drift perturbation and the remaining 90% to jump intensity perturbation. The second part of Table B.2 summarized the results for case when the stock price data are sampled intra daily. Since model misspecification does not affect the classical Merton and jump diffusive weights, those holdings do not change compared to the case when the stock price data are collected on a daily basis. However, the robust Merton and robust jump - diffusive holdings are now larger compared to the their counterpart portfolio holdings based on daily data. The reason why those weights are higher when we use intra day data, is because we have more data available which makes it easier to distinguish between the reference and robust dynamics of the risky asset and therefore reduces the maximal amount of robustness η (Compare the two graphs in Figure B.4). This also explains why the optimal drift perturbation h^*, for both the robust Merton and the robust jump-intensity weights (also true for a^*), is considerably reduced in the case we use intra day data.

Next, we now conduct a comparative static analysis in order to assess the utility loss under various different market scenarios. To be more precise, we vary each parameter of the model

individually and compute expected utility for each portfolio strategy.[10] Table B.3 summarizes the results.

[Table B.3 about here]

A first conclusion we can draw from Table B.3, is that regardless of the market scenario, the robust jump - diffusive weights give highest expected utility whenever the stock price follows the compensated exponential Lévy dynamics under the robust measure $\mathbb{P}^{\vartheta}$ (see 3.4 above).[11] Secondly, the ordering of the investors' utility loss crucially depends on the market scenario we analyze. For instance, comparing utility loss when the risk free rate increases to 2%, to utility loss when the jump intensity increases fivefold, we see that the Merton portfolio weight yields second highest expected utility in the former scenario but gives lowest expected utility in the latter scenario.

3.6 Conclusion

In this paper, we study a robust optimal consumption and portfolio choice problem where the underlying risky asset follows a Lévy process. We introduce model misspecification with respect to drift and jump intensity parameters and derive explicit expressions for optimal consumption and portfolio rules. Even though our setting is only slightly different from the standard jump diffusive robust control frameworks used so far in the literature (see for instance Drechsler (2013) or Lui et al. (2005)), it introduces an intensity misspecification premium which has important implications for robust portfolio allocations. This is achieved by simply compensating the jump component of the exponential Lévy model we employ in this paper. This implies, that under the robust measure, the drift of the risky asset is also reduced under the robust measure which is a standard result when doing asset pricing with the robust control, however, the reduction is

[10] The alternative parameter values are given in row 'Alternative' in Table B.1.

[11] The same is true for the jump diffusive weights, as expected utility under the reference measure is highest for those weights no matter the market scenario.

smaller as through compensating the jump component, we add a jump intensity misspecification premium that increases the drift of the risky asset. A direct consequence of this assumption is that the optimal allocation in the risky asset is higher under the assumption that the stock price follows a compensated exponential jump diffusive process, compared to the case when the risky asset follows a non compensated jump diffusive process which is the standard assumption on the robust dynamics of the process. This modeling specification helps to address the commonly stated critic that robust portfolio allocations are too conservative, meaning the weight in the risky asset is too low, and therefore the investor forgoes much of the upside potential. Lastly, the introduction of a jump compensator adds more realism to the model as in times of higher uncertainty, stocks become more risky and therefore have to offer a higher risk compensation in order for the investor to hold them. Furthermore, analyzing various different specifications of the risky assets price process, we find that perturbations of the drift are relatively more important than perturbation of the jump intensity in the case when jumps are symmetric about zero, i. e. the occurrence of positive and negative jumps is equally likely. However, assuming only negative jumps and without compensating the jump part in the underlying asset shows that optimal portfolio weights become not only more sensitive to perturbations of the jump intensity but also, that misspecification with respect to the jump intensity becomes more important than misspecification of the drift. Additionally, we derive a semi-closed form solution for detection-error probabilities by means of Fourier inversion techniques. Our analysis shows that the detection-error probability is very sensitive to the length of data we have available, which implies that for two processes, one generated under the reference and another one generated under the robust measure, it becomes easier to statistically discriminate one from another the long the available time series of observations is. Finally, in our Monte - Carlo analysis, where we quantify utility loss under various portfolio strategies shows that the utility loss largely depends on the specific market scenario we are investigating. However, as expected, highest utility is always achieved when using the appropriate portfolio allocation strategy under the correct measure.

Chapter 4

Endogenous Markov Switching Regression Models for High-Frequency Data under Microstructure Noise

Markus Leippold and Felix Matthys[1]

I have presented this paper at:

- 7th Bachelier Finance Society World Congress 2012 in Sydney
- 1. Econometrics Workshop in Zurich 2012
- 7th International Conference on Computational and Financial Econometrics (CFE 2013), London, United Kingdom, December 2013

[1]For helpful comments we thank Tim Bollerslev, Hansruedi Künsch, Marc Paolella, Fabio Trojani, Eric Jandeau, Loriano Mancini, Olivier Scaillet, Antonio Mele, Michael Wolf and the participants of the 7th Bachelier Finance Society World Congress 2012 in Sydney, and the 1. Econometrics Workshop in Zurich 2012. Financial support from the Swiss Finance Institute (SFI), Bank Vontobel, and the National Centre of Competence in Research Financial Valuation and Risk Management (FINRISK) is gratefully acknowledged.

Abstract We present a novel method in analyzing microstructure noise of high-frequency data as a measurement error problem. In particular, we study the estimation of endogenous Markov-switching regression models, in which the regression disturbance and the latent state variable controlling the regime are correlated. We show infill asymptotic results and prove that under endogeneity the popular realized variance estimator is biased and no longer converges to the integrated regime dependent volatility. Exploring high-frequency intraday return data on foreign exchange rates, we find that the state variable is indeed endogenous. Similar to the popular volatility signature plot suggested by Andersen et al. (2000b), we propose an endogeneity plot which indicates as to which sampling frequency the assumption of exogeneity of the state variable controlling the regime remains valid.

4.1 Introduction

Markov switching regression models have gained much popularity in recent years not only in applied macroeconomics but more increasingly also in empirical finance. Ever since Hamilton (1989) suggested to describe the business life cycle as a Markov switching autoregressive process the model was used in numerous empirical studies both in finance and economics.[2] The increasing availability of high frequency data opens up another natural application of Markov switching regression models (see Chen et al. (2013) for a recent application of these models). For example, many empirical studies have documented (see for instance Andersen et al. (2012)) that intraday volatility is U-shaped across trading days. Thus one can easily imagine that intraday volatility is subject to different regimes depending on the intensity of trading in the market. In practice however, the estimation of such Markov switching regression models based on high frequency return data is a delicate issue due to microstructure contaminations. The assumption that the continuous log-price process is observable and free of any measurement error does not hold in the real data. The log-price process in continuous time is latent and one can observe the process at discrete time intervals only. More recently, for single regime switching diffusions, the study of the stochastic properties of returns and realized volatility has surged. One of the first paper to rigorously discuss the econometric properties of realized volatility, defined as the sum of squared intra-day log-returns, is due to Barndorff-Nielsen & Shephard (2001) and Barndorff-Nielsen & Shephard (2002). Under the assumption of a very general class of volatility models they were able to characterize the asymptotic distribution of the realized volatility error - the difference between realized and the "actual" volatility which is the discretized integrated volatility. They show that from the theory of quadratic variation (see Protter (2004)), the realized volatility estimator converges uniformly in probability to the

[2]For instance the volatility feedback model of Turner et al. (1989), regime switching interest rate models as in Ang & Bekaert (1998) and regime switching VARs as in Sims & Zha (2006). There exists an extensive literature on Markov switching (G)ARCH processes, see for instance Cai (1994), Hamilton & Susmel (1994), and Mun (1998) or Haas et al. (2004), Gray (1996) and Klaassen (2002).

integrated volatility as the sampling frequency tends to infinity.[3] However, with increasing intra-day return sampling frequency, various empirical studies have shown that market microstructure noise distort the efficient and unbiased estimation of volatility considerably (see Fang (1996), Andreou & Ghysels (2002) and X. Bai (2004)). Hence any econometric measure of integrated volatility will be subject to finite-sample measurement error,[4] since the computation of the realized variance is contaminated by market microstructure noise. Since the publication of an article by Zhou (1996), numerous papers have studied the impact of market microstructure frictions on the estimation of integrated volatility (see Aït-Sahalia et al. (2005), Hansen & Lunde (2003), Hansen & Lunde (2006), Zhang (2004) and Zhang et al. (2003)).[5] A simple form of market microstructure noise arises because stock price time series are only observed discretely. Harris (1990) and Harris (1991) show that discretization of the stock price process introduces noise to the price series which in turn induces increased return variances and adds negative serial correlation to return series. Additionally, bid-ask bounces and price reporting errors tend to amplify serial correlation at higher sampling frequencies. Other sources of market microstructure noise are due to properties of the trading mechanism. Amihud & Mendelson (1987) argue that the mechanism by which securities are traded significantly effects stock price behavior. They find that opening returns tend to exhibit greater dispersion, larger deviations from normality and a more pronounced negative autocorrelation pattern relative to closing returns.[6] Furthermore, the construction of intraday returns requires the use of different sampling schemes such as the previous tick (Wasserfallen & Zimmermann (1985)) or the linear interpolation method (see Andersen & Bollerslev (1997)) which constitutes another form of market microstructure noise. So far, the academic literature has come up with various econometric measures of realized variance, such as kernel-based estimators (see Zhou (1996), Hansen &

[3] See also Andersen, Bollerslev, Diebold & Labys (2001).

[4] We use the term measurement error or endogenity interchangeably.

[5] High-frequency based quantities of realized volatility have proven to be useful in obtaining accurate measures of daily volatility, see e.g. Maheu & McCurdy (2002), Barndorff-Nielsen et al. (2002), Frijns & Lehnert (2004) and Owens & Steigerwald (2009). High-frequency based estimators are also extensively used in the context of forecasting of volatility, see e.g. Engle & Sun (2007), Koopman et al. (2005), Andersen et al. (2011) and Ghysels et al. (2006).

[6] For more references on this literature see O'Hara (1995) and Hasbrouck (2004).

Lunde (2003) and Barndorff-Nielsen et al. (2004)) or the closely related subsample based estimators as in Zhou (1996), Zhang et al. (2003) and Zhang (2004) and filtering techniques as in Ebens (1999), Andersen, Bollerslev, Diebold & Ebens (2001) and Maheu & McCurdy (2002).[7] Standard Markov regime-switching models which are used in empirical studies treat the latent variable controlling the regime as exogenous. However, many applications of the model are in macroeconomics or in finance in situations where it is natural to assume the state to be endogenous.[8] For example, to motivate the usage of endogenous switching, it is often the case that the state variable has a strong correlation with the business cycle. In recent applied work on identifying exogenous and endogenous component in monetary policy, regime-switching VARs have been estimated (see for instance Oomen (2002)). It seems plausible that the shocks to the regression, such as macroeconomic shocks to the VAR, would be correlated with the business cycle. A further example is the application of models where the parameters depend on the reactions of agents to realization of a state (See for instance the volatility feedback model by Turner et al. (1989)). However, it seems reasonable to assume that agents do not directly observe the state but instead draw their conclusions based on a specific information set available to them at a given time, which does not necessarily coincide with the information set of the econometrician. The use of the actual state as a proxy for this inference leads to a measurement error in the explanatory variables of the regression and thus to endogeneity.

Our paper has two main contributions. On the theoretical side, we show that when the state variable is endogenous the popular realized variance estimator will be biased. The reason why the state variable may emerge endogenously is, because the estimation of the efficient price process subject to microstructure noise can be interpreted as a measurement error problem which in turn in a Gaussian regime-switching context leads to endogenous switching. We argue that by allowing the state variable to switch endogenously, the effect of noise induced by market

[7] More recent papers by Jacod et al. (2009) present a pre-average approach or range-based estimators (see Christensen & Podolskij (2007)) that allows for consistent estimation of realized volatility.

[8] Several ideas have been proposed in the literature on how to deal with the problem of endogeneity in Markov-switching regression models, for instance Kim (2004), Kim et al. (2008), Kim (2009), Otranto et al. (2005), Kimhi (1999) , for a survey see Dutoit (2007) and for an analysis of the problem of endogeneity in an extented state space representation see Kang (2010).

microstructure frictions on the estimation of the regime dependent integrated variance can be quantitatively measured. We also discuss the econometric techniques employed to measure the degree of microstructure noise and therefore of endogeneity in the data. From the empirical side, we make use of the econometric model developed in Kim et al. (2008) and show, using FX intraday data, for various standard Markov switching models that microstructure noise indeed renders the state endogenous and therefore leading to biased parameter estimates. We also introduce an "endogeneity plot" which essentially, similar to the popular "Volatility Signature plot" as proposed by Andersen et al. (2000b), indicates as to which maximal sampling frequency one can safely assume exogeneity of the state variable controlling the regime.

The paper is organized as follows. Section 2 introduces the basic setup of endogenous regime switching. Section 3 discusses the estimation of endogenous Markov switching regression models under microstructure noise. Section 4 presents the Monte-Carlo analysis. Section 5 discusses the sampling scheme used to construct the high-frequency data. Section 6 presents empirical stylized facts about microstructure noise. Section 7 presents the empirical results and Section 6 concludes. All proofs, tables and additional figures are given in the Appendix.

4.2 Endogenous regime switching

In this section, we introduce first the basic setup of endogenous regime switching. We then derive some limit results and discuss the estimation of integrated variance. Throughout this section, we assume that the Markov Chain and the Brownian Motion are defined on the same complete filtered probability space $(\Omega, \mathcal{F}, \{\mathcal{F}_t\}, \mathbb{P})$.

4.2.1 Basic setup and notation

We denote the latent continuous-time log-price process by p_t^*. We consider a price process, which follows a local martingale with regime-dependent volatility.

Assumption 5. *The latent price process p_t^* follows*

$$p^*(t) = \int_0^t \sigma_{r_u} dW_u, \tag{4.1}$$

where $\{W_t\}_{t\geq 0}$ is a standard Brownian motion independent of the regime-dependent cádlág volatility process σ_{r_t} and regimes r_t. We assume that the price process is measurable with respect to $\mathcal{F}_t = \mathcal{F}_{r_t} \cup \mathcal{F}_t^W = \sigma\{r_s,\ W_s; s \leq t\}$, where $\mathcal{F}_{r_t} = \sigma\{r_s, s \leq t\}$ and $\mathcal{F}_t^W = \sigma\{W_u, u \leq t\}$.

The true underlying price process $p^*(t)$ is not observable. We denote the observable price process by $p(t)$. The wedge between $p^*(t)$ and $p(t)$ is caused by microstructure noise such as bid-ask bounces, but it may also arise due to the technique used to construct p_t out of transaction data.

Assumption 6. *The discrepancy between the latent and observable price process $p(t)$ is caused by some microstructure contamination ξ_t,*

$$\xi(t) = p(t) - p^*(t), \tag{4.2}$$

which is independent and identically distributed (i.i.d.) with mean zero.

Finally, we need to make some assumptions about the regime switches.

Assumption 7. *The finite-state and unobservable regime $r_t \in \{1, \ldots, N\}$ with generator $\mathcal{Q}$,*

$$\mathcal{Q} = \{q_{ij}\}_{N\times N}, \quad q_{ij} \geq 0,\ \forall j \neq i, \quad q_{ii} = -\sum_{i=1, j\neq i}^{N} q_{ij}, \tag{4.3}$$

evolves according to a continuous-time first-order Markov chain with transition probabilites:

$$\mathbb{P}\left[r(t+s) = i | r(s) = j, \mathcal{F}_{r_s}\right] = \mathbb{P}_{ij}(t), \quad s, t \geq 0,\ i, j = 1, \ldots, N.$$

Our object of interest is the integrated variance over a fixed time interval, say $[t_0, T]$, which is defined as

$$IV_{t_0,T} \equiv \int_{t_0}^{T} \sigma_{r_u}^2 du. \tag{4.4}$$

Since the integrated variance in (4.4) is not directly observable, we need to search for a consistent estimator. Although the formulation of the price dynamics in terms of a stochastic differential equation as in Assumption 5 is very convenient from a theoretical viewpoint, the prices we need to calculate a variance estimator are invariably observable only at discrete time intervals. Therefore, we partition a given time interval $[t_0, T]$ into m subintervals. For a fixed m, the k-th subinterval is given by $[t_{k-1,m}, t_{k,m}]$ with $t_0 = t_{0,m} < t_{1,m} < \ldots < t_{m,m} = T$ and we assume that $\sup_{k=1,\ldots,m} \Delta_m = O(1/m)$ with $\Delta_m \equiv t_{k,m} - t_{k-1,m}$. Furthermore, we define the returns taken at the discrete points in time as

$$y^*_{k,m} \equiv p^*_{t_{k,m}} - p^*_{t_{k-1,m}},$$

and

$$y_{k,m} \equiv p_{t_{k,m}} - p_{t_{k-1,m}},$$

respectively. To find an estimator of integrated variance, we focus on a discrete approximation of the efficient log return process. Analogously to Assumption 5, we make the following assumption for the return process in discrete time.

Assumption 8. *In discrete time, the state-dependent return process evolves as*

$$y^*_{k,m} = \sigma_{r_{k,m}} u_{k,m}, \tag{4.5}$$

where $u_{k,m} \overset{iid}{\sim} \mathcal{N}(0,1)$ *and we assume that* $\sigma_{r_{k,m}}$ *is bounded.*

Hence, given the specification in Assumption 8, we are looking for a variance estimate such that in absence of any measurement error and exogeneity of the state variable, we have

$$\lim_{m\to\infty} \Delta_m^{1/2} \sum_{i=1}^{\lfloor mt \rfloor} \sigma_{r_{k,m}} u_{k,m} \overset{D}{=} \int_{t_0}^{T} \sigma_{r_u} dW_u, \tag{4.6}$$

where $\overset{D}{=}$ denotes equivalence in distribution and $r_{k,m}$ is the continuous-time regime r_t at time k. Under the specification of the price process in (4.1), we have $\mathbb{V}(y^*_{k,m}|r_{k,m}) = \mathbb{E}[y^{*2}_{k,m}|r_{k,m}] = \sigma^2_{r_{k,m}}$, where $\mathbb{V}(\cdot)$ denotes the standard variance operator. Hence, we can estimate the integrated

variance over the interval $[t_0, T]$ using the realized variance defined by the sum of squared intraday latent log returns,

$$RV^*_{t_0,T;m} \equiv \sum_{k=1}^{m} y^{*2}_{k,m}, \tag{4.7}$$

given the partition with m subintervals.

For the single regime case, the asymptotic properties of realized variance is discussed in Barndorff-Nielsen & Shephard (2002), Meddahi (2002) and Mykland & Zhang (2006). Furthermore, as shown in Protter (2004), $RV^*_{t_0,T}$ is a consistent estimator of $IV_{t_0,T}$ as $m \to \infty$. However, RV^*_m is an estimator based on the latent process p^*_t and thus infeasible to compute. A feasible IV estimator would be the realized variance of the observable log-price,

$$RV_{t_0,T;m} \equiv \sum_{k=1}^{m} y^2_{k,m}. \tag{4.8}$$

However, the estimator in (4.8) is biased and inconsistent (see, e.g., Bandi & Russell (2008) and Zhang et al. (2003)).

In contrast to the previous literature, we work in a multiple regime setting. Since we can only observe returns and prices at discrete times, we also need a discrete-time version of the continuous-time Markov chain r_t given in Assumption 7. To this end, we introduce the following notation. By $\mathbb{P}\left[r_{k,m}|r_{k-1,m}, \mathcal{F}_{k-1,m}\right]$ we denote the probability of moving to regime $r_{k,m}$ at time k conditional on the information set $\mathcal{F}_{k-1,m}$ and the previous regime $r_{k-1,m}$. The information set $\mathcal{F}_{k-1,m}$ is generated by the observed realized path of the dependent variable $y_{k,m}$ given by $\tilde{y}_{k-1,m} = \{y_{k-1,m}, y_{k-2,m}, \ldots\}$ and the unobserved regime path $\tilde{r}_{k-1,m} = \{r_{k-1,m}, r_{k-2,m}, \ldots\}$. For the specification of the regime switching process, we rely on a probit model as in Kim et al. (2008).

Assumption 9. *The regime $r_{k,m}$ evolves according to a discrete-time first-order Markov chain with transition probabilities,*

$$\mathbb{P}\left[r_{k,m} = i|r_{k-1,m} = j, \mathcal{F}_{k-1,m}\right] = \mathbb{P}_{ij}, \quad i, j = 1, \ldots, N,$$

and stationary unconditional probabilities $\mathbb{P}[r_{k,m} = i] = \mathbb{P}[r = i]$. *The regime switching process is specified as follows:*

$$r_{k,m} = \begin{cases} 1 & \text{if} \quad -\infty & \leq \eta_{k,m} < & a_{1,j}(\Delta_m) \\ 2 & \text{if} \quad a_{1,j}(\Delta_m) & \leq \eta_{k,m} < & a_{2,j}(\Delta_m) \\ \vdots & \vdots & & \vdots \\ N-1 & \text{if} \quad a_{N-2,j}(\Delta_m) & \leq \eta_{k,m} < & a_{N-1,j}(\Delta_m) \\ N & \text{if} \quad a_{N-1,j}(\Delta_m) & \leq \eta_{k,m} < & \infty \end{cases}, \tag{4.9}$$

where $\eta_{k,m} \overset{i.i.d}{\sim} \mathcal{N}(0,1)$.

Under Assumption 9, the transition probabilities are then given by

$$\mathbb{P}_{ij}(\Delta_m) \equiv \mathbb{P}(r_{k,m} = j | r_{k-1,m} = i) = \Phi\left(a_{i,j}(\Delta_m)\right) - \Phi\left(a_{i-1,j}(\Delta_m)\right), \tag{4.10}$$

with $a_{0,j}(\Delta_m) = -\infty$, $a_{N,j}(\Delta_m) = \infty$, and $\Phi(\cdot)$ the standard normal cumulative distribution function. To model endogenous switching, the regression disturbance $u_{k,m}$ has to be linked with the state variable $\eta_{k,m}$ controlling the regime. Given the Gaussian regime setting, we can model endogeneity by letting the error terms through their bivariate normal joint density function be correlated. In other words, we make the following assumption.

Assumption 10. *The joint density function of* $u_{k,m}$ *and* $\eta_{k,m}$ *is bivariate normal, i.e.,*

$$\begin{bmatrix} u_{k,m} \\ \eta_{k,m} \end{bmatrix} \sim \mathcal{N}(0, \Sigma), \quad \textit{with} \quad \Sigma = \begin{bmatrix} 1 & \rho \\ \rho & 1 \end{bmatrix}, \tag{4.11}$$

where $u_{k,m}$ *and* $\eta_{h,m}$ *are uncorrelated for* $h \neq k$. *Furthermore,* $u_{k,m}$ *is independent of* $r_{h,m}$, $h \neq k$.

4.2.2 Limit results for regime switching under endogeneity

The following theorem, based on the three-series Theorem by Kolmogorov, summarizes the infill asymptotic results in the case where the state variable controlling the regime is exogenous. We relegate all proofs to Appendix A.

Proposition 8. (Infill asymptotics: Exogenous switching) *Given Assumptions 8 to 10 under exogenous switching with $\rho = 0$ we have for some $p > 2$ with $p \in \mathbb{N}$:*

$$\Delta_m^{1/2} \sum_{k=1}^{\lfloor mt \rfloor} y_{k,m} \xrightarrow{D} \int_{t_0}^{T} \sigma_{r_u} dW_u \tag{4.12}$$

$$\Delta_m^{1/2} \sum_{k=1}^{\lfloor mt \rfloor} \mathbb{E}\left[y_{k,m} \middle| \mathcal{F}_{k-1,m}, r_{k,m} \right] \xrightarrow{D} 0 \tag{4.13}$$

$$\Delta_m \sum_{k=1}^{\lfloor mt \rfloor} \mathbb{E}\left[y_{k,m}^2 | \mathcal{F}_{k-1,m}, r_{k,m} \right] \xrightarrow{D} \int_{t_0}^{T} \sigma_{r_u}^2 du \tag{4.14}$$

$$\Delta_m^{p/2} \sum_{k=1}^{\lfloor mt \rfloor} \mathbb{E}\left[|y_{k,m}|^p | \mathcal{F}_{k-1,m}, r_{k,m} \right] \xrightarrow{D} 0. \tag{4.15}$$

Proposition 8 shows that under exogenous regime switching, the discrete-time approximation of the return process converges in distribution to a regime dependent martingale. As a next step, we examine the case when the state is switching endogenously.

Proposition 9. (Infill asymptotics: Endogenous switching) *Given Assumptions 8 to 10 under endogenous switching with $\rho \neq 0$ we have for some $p > 2$ with $p \in \mathbb{N}$:*

$$\Delta_m^{1/2} \sum_{k=1}^{\lfloor mt \rfloor} \mathbb{E}\left[y_{k,m} \middle| \mathcal{F}_{k-1,m}, r_{k,m} \right] \xrightarrow{D} -\rho \int_{t_0}^{T} \frac{\phi(a_{i,j}(u)) - \phi(a_{i-1,j}(u))}{\mathbb{P}_{i,j}(u) - \mathbb{P}_{i-1,j}(u)} \sigma_{r_u} du \tag{4.16}$$

$$\Delta_m \sum_{k=1}^{\lfloor mt \rfloor} \mathbb{E}\left[y_{k,m}^2 | \mathcal{F}_{k-1,m}, r_{k,m} \right] \xrightarrow{D} \int_{t_0}^{T} \left(1 + \rho^2 \frac{\phi(a_{i,j}(u)) - \phi(a_{i-1,j}(u))}{\mathbb{P}_{i,j}(u) - \mathbb{P}_{i-1,j}(u)} \right) \sigma_{r_u}^2 du \tag{4.17}$$

$$\Delta_m^{p/2} \sum_{k=1}^{\lfloor mt \rfloor} \mathbb{E}\left[|y_{k,m}|^p | \mathcal{F}_{k-1,m}, r_{k,m} \right] \xrightarrow{D} 0, \tag{4.18}$$

where $\phi(\cdot)$ denotes the probability density function of a standard normally distributed random variable.

Proposition 9 suggests that under endogenous switching the expectation of the discrete approximation is biased whenever $\rho \neq 0$. Moreover, the discrete approximation does not converge in distribution to the integrated regime dependent variance. We also note that the scaled sum is not divergent when $m \to \infty$, which differs from the findings of Hansen & Lunde (2006) or Bandi & Russell (2008). The reason for this result is that the noise in our setting is of the same order as the efficient price process, whereas in the setting of Hansen & Lunde (2006) or Bandi & Russell (2008) the noise is $O(1)$ and the efficient price process is $O(1/m)$. As Aït-Sahalia et al. (2005) have shown, under the assumption of serially correlated diffusive noise the realized variance estimator is no longer divergent as $m \to \infty$, since both noise and efficient price process are of order $O(1/m)$.

4.2.3 Two-states Gaussian regime switching model

To illustrate the effect of endogeneity on the realized variance estimator, we assume that the efficient price processes follows a two-states regime switching diffusion with constant variance within each state. Hence, the model is conditionally Gaussian. For the regimes switching process, Assumption 9 reduces to:

$$r_{k,m} = \begin{cases} 1 & \text{if} \quad \eta_{k,m} < a_j(\Delta_m) \\ 2 & \text{if} \quad \eta_{k,m} \geq a_j(\Delta_m) \end{cases}. \tag{4.19}$$

From Proposition 8, it follows directly that if $\rho = 0$, the squared log-returns are an unbiased estimator of the latent variance process. However, under endogeneity we do not obtain convergence of the realized variance estimator to the integrated regime dependent variance process.

To see this, we can explicitly calculate the expectation of the realized variance as

$$\begin{aligned}
\mathbb{E}\left[RV_m\right] &= \mathbb{E}\left[\sum_{k=1}^{m} \sigma^2_{r_{k,m}} u^2_{k,m}\right] \\
&= \mathbb{E}\left[\mathbb{E}\left[\sum_{k=1}^{m} \sigma^2_{r_{k,m}} u^2_{k,m} | \mathcal{F}_{k-1,m}, r_{k,m} = i, r_{k-1,m} = j\right]\right] \\
&= \mathbb{E}\left[\sum_{k=1}^{m}\left[\sigma_{r_{k,m}}\left(1 + \rho^2 \frac{\phi(a_{i-1,j}(\Delta_m))a_{i-1,j}(\Delta_m) - \phi(a_{i,j}(\Delta_m))a_{i,j}(\Delta_m)}{\mathbb{P}_{i,j}(\Delta_m) - \mathbb{P}_{i-1,j}(\Delta_m)}\right)\right]\right], \quad (4.20)
\end{aligned}$$

where for $r_{k,m} = i$ the formula in equation (4.20) reduces to

$$\mathbb{E}\left[RV_m\right] = \mathbb{E}\left[\sum_{k=1}^{m} \sigma^2_{r_{k,m}}\left(1 + \rho^2 \zeta_l(a_j(\Delta_m))\right)\right] \quad (4.21)$$

with

$$\begin{aligned}
\zeta_1(a_j(\Delta_m)) &= -\frac{\phi(a_j(\Delta_m))a_j(\Delta_m)}{\Phi(a_j(\Delta_m))}, \\
\zeta_2(a_j(\Delta_m)) &= \frac{\phi(a_j(\Delta_m))a_j(\Delta_m)}{1 - \Phi(a_j(\Delta_m)}.
\end{aligned}$$

Hence, by dominated convergence and since $\sigma^2_{r_{k,m}}$ is bounded, the regime dependent variance process converges in distribution to the regime dependent integrated variance if and only if $\rho = 0$, i.e.,

$$\begin{aligned}
\lim_{m\to\infty} \mathbb{E}\left[\sum_{k=1}^{m} \tilde{y}_{k,m} - \int_{t_0}^{T} \sigma^2_{r_u} du\right] = 0 \\
\mathbb{E}\left[\lim_{m\to\infty} \sum_{i=1}^{m} \sigma^2_{r_{k,m}} - \int_{t_0}^{T} \sigma^2_{r_u} du\right] = 0.
\end{aligned}$$

For $\rho \neq 0$ the realized variance estimator is biased. However, by Proposition 9, the bias remains finite as the sampling frequency m approaches infinity.

Proposition 10. (Asymptotic Convergence) *Given Assumptions 8 to 10denoting by* $\mathbb{V}(\cdot|\mathcal{F}_{k,m}, r_{k,m})$ *the conditional variance given the information set, the current and previous regime at a given sampling frequency* m*. Then using the bias results from Equation* (4.20)*,*

respectively, the conditional variance of the realized variance estimator for $r_{k,m} = i$ *is given by*

$$\mathbb{V}\left[RV_m|\mathcal{F}_{k-1,m}, r_{k,m} = i, r_{k-1,m} = j\right] = \sum_{k=1}^{m} \sigma^4_{r_{k,m}} \Gamma_{\rho,i}(a_j(\Delta_m)) \tag{4.22}$$

where

$$\Gamma_{\rho,i}(a_j(\Delta_m)) \equiv 2 - sign(i)\rho^2\zeta_i(a_j(\Delta_m))\left(4 + sign(i)\rho^2\left(\zeta_i(a_j(\Delta_m)) + 3sign(i)\left(a_j(\Delta_m)^2 - 1\right)\right)\right) \tag{4.23}$$

with

$$sign(l) \equiv \begin{cases} 1 & \text{if } i = 1, \\ -1 & \text{if } i = 2. \end{cases} \tag{4.24}$$

Then conditional on $r_{k,m} = i$ *we have*

$$\frac{RV_m - \sum_{k=1}^{m} \sigma^2_{r_{k,m}} \left(1 - sign(i)\rho^2\zeta_i(a_j(\Delta_m))\right)}{\sqrt{\sum_{k=1}^{m} \sigma_i^4 \Gamma_{\rho,i}(a_j(\Delta_m))}} \xrightarrow{D} \mathcal{N}(0,1) \tag{4.25}$$

as $m \to \infty$.

Proposition 10 shows that the conditional variance of the realized variance estimator is biased whenever $\rho \neq 0$. If $\rho = 0$, we obtain

$$\mathbb{V}\left[RV_m|\mathcal{F}_{k-1,m}, r_{k,m}\right] = 2\sum_{k=1}^{m} \sigma^4_{r_{k,m}} = 2\frac{T - t_0}{m} \int_{t_0}^{T} \sigma^4_{r_u} du + o(1/m), \tag{4.26}$$

where $\int_{t_0}^{T} \sigma^4_{r_u} du$ is the regime dependent analog of the integrated quarticity as introduced by Barndorff-Nielsen & Shephard (2002) when there is no microstructure noise.

4.3 Endogenous Markov Switching Regression Models and Microstructure Noise

In this section, we discuss the econometric techniques to account for microstructure noise in the data and the latency of the efficient price process $y^*_{k,m}$. We consider a Gaussian regime-switching model where the return process $\{y_{k,m}\}$ can switch between two states $r_{k,m} \in \{1, 2\}$.

In particular, we assume the following structure:

$$\begin{aligned} y_{k,m} &= x_{k,m}^{'}\beta_{r_{k,m}} + \epsilon_{k,m}, \\ &= x_{k,m}^{'}\beta_{r_{k,m}} + \sigma_{r_{k,m}} u_{k,m} \quad \text{where } u_{k,m} \overset{i.i.d}{\sim} \mathcal{N}(0,1), \end{aligned} \tag{4.27}$$

where $x \in \mathbb{R}^P$ is a vector of observed explanatory variables. These variables are exogenous, regime dependent, and may also include lagged values of $y_{k,m}$. By $\beta_{r_{k,m}}$ we denote the set of possibly regime dependent parameters, which need to be estimated. The variance $\sigma^2_{r_{k,m}}$ is regime dependent. To relate endogenous switching with microstructure noise, we can decompose the intraday return as

$$y_{k,m} = y^*_{k,m} + e_{k,m}, \quad \mathbb{E}\left[e_{k,m}|r_{k,m}\right] = 0, \tag{4.28}$$

with $e_{k,m} = \xi_{t_{k,m}} - \xi_{t_{k-1,m}}$. Hence, the intraday return consists of the efficient latent return process plus an unobservable noise component. However, one can not directly estimate (4.28) as both the efficient price process as well as the microstructure noise is not directly observable. From an econometric point of view, the microstructure noise can be interpreted as any other noise. In this Gaussian regime-switching context we may take $\epsilon_{k,m}\,|\mathcal{F}_{k-1,m}, r_{k,m} \overset{i.i.d}{\sim} \mathcal{N}(0, \sigma^2_{r_{k,m}})$ as a measure for the microstructure noise. However, the econometrician does not observe the efficient price but has to rely on the contaminated observable price process and therefore has to approximate the efficient price process by a parametric regime-switching model as in (4.27), in other words replace $y_{k,m}$ by $x_{k,m}^{'}\beta_{r_{k,m}}$. Using this substitution gives directly an estimateable equation for the observable log return process but introduces measurement error, i.e., correlation between the state variable controlling the regime and the regression disturbance as given in (4.19). To see this, we start with (4.28) rewrite the equation as follows

$$y_{k,m} = y^*_{k,m} + e_{k,m} = x_{k,m}^{'}\beta_{r_{k,m}} + \nu_{k,m}, \tag{4.29}$$

where

$$\nu_{k,m} = y^*_{k,m} + e_{k,m} - x_{k,m}^{'}\beta_{r_{k,m}}. \tag{4.30}$$

Thus if we assume a regime dependent parametric model of the form $y_{k,m} = x_{k,m}^{'}\beta_{r_{k,m}} + \nu_{k,m}$ then $\mathbb{E}\left[y_{k,m}\right] = \mathbb{E}\left[y_{k,m}^{*}\right] = \mathbb{E}\left[x_{k,m}^{'}\beta_{r_{k,m}}\right]$ holds true of course only if there is no measurement error. Note that with the model specification given in (4.29) and (4.30) we have transformed the original equation (4.28) involving only unobservable quantities into a Markov Switching regression framework based on observable exogenous regressors. However, in doing so we also introduced a measurement error, namely that the regressors in $\beta_{r_{k,m}}$ are now correlated with the error term. To see this, applying repeatedly the law of iterated expectations and using (4.30) we obtain

$$\mathbb{C}\left(x_{k,m}^{'}\beta_{r_{k,m}}, \nu_{k,m}\right) = \mathbb{C}\left(y_{k,m}^{*}, x_{k,m}^{'}\beta_{r_{k,m}}\right) - \mathbb{V}\left(x_{k,m}^{'}\beta_{r_{k,m}}\right), \tag{4.31}$$

where $\mathbb{C}(\cdot)$ denotes the standard covariance operator. Thus (4.31) shows that the regressor $\beta_{r_{k,m}}$ is correlated with the disturbance term $\nu_{k,m}$ due to the errors-in-variable problem. Note, if $\nu_{k,m} = w_{k,m}$, where $w_{k,m}, |r_{k,m}, \mathcal{F}_{k-1,m}$ is an exogenous $i.i.d.$ mean zero and unit variance error term, would imply exogeneity of the regression disturbance and therefore no measurement error. Therefore, it follows directly that $\mathbb{C}\left(w_{k,m}, x_{k,m}^{'}\beta_{r_{k,m}}\right) = 0$. Hence any Markov switching regression model that is based on the assumption of independence of the state variable controlling the regime $\eta_{k,m}$ and the regressors $\beta_{r_{k,m}}$ will result in biased parameter estimates. To account for this possible measurement error problem an empirical model may read

$$\begin{aligned}
y_{k,m} &= x_{k,m}\beta_{r_{k,m}} + \sigma_{r_{k,m}}u_{k,m}, \quad u_{k,m} \overset{i.i.d}{\sim} \mathcal{N}(0,1) \\
r_{k,m} &= a_{r_{k-1,m}}, \quad \eta_{k,m} \overset{i.i.d}{\sim} \mathcal{N}(0,1) \\
r_{k,m} &= \begin{cases} 0 & \text{if } \eta_{k,m} < a_{r_{k-1,m}} \\ 1 & \text{if } \eta_{k,m} \geq a_{r_{k-1,m}} \end{cases}
\end{aligned} \tag{4.32}$$

and

$$\begin{bmatrix} u_{k,m} \\ \eta_{k,m} \end{bmatrix} \sim \mathcal{N}\left(0, \Sigma\right), \text{ with } \quad \Sigma = \begin{bmatrix} 1 & \rho \\ \rho & 1 \end{bmatrix} \tag{4.33}$$

with $\mathbb{E}\left[u_{k,m}\eta_{k-l,m}\right] = 0$ for all $l \neq 0$. Hence, we account for this endogeneity problem by allowing the regression disturbance and the state variable to be correlated. This allows us to

estimate the model by quasi maximum likelihood (QML) and controlling for microstructure noise by the correlation parameter ρ. The more severe the measurement problem, the larger (in absolute value) ρ will be.

4.4 Monte Carlo Analysis

In this section we investigate the finite sample properties of the quasi-maximum likelihood (QML) estimator for the endogenous Markov switching model. We focus on several regime models which will be latter on applied to real intra day FX data. The goal of this analysis is on the one hand side to study the performance of the endogenous maximum likelihood estimator on the other hand to numerically quantify the bias when endogeneity is neglected.[9] The models we consider are the following

INSERT TABLE D.1 ABOUT HERE

The models with regime dependent drift aim at capturing different dynamics depending on the prevailing regime. As shown in Timmermann (2000) such a specification is able to introduce autocorrelation in the return series depending on the persistence of the Markov chain. To be more precise, if $\sum_{i=1}^{N} \mathbb{P}_{ii} > 1$ where $\mathbb{P}_{ii}$ denotes the probability of staying in a given regime, the model will produce positive serial correlation and if $\sum_{i=1}^{N} \mathbb{P}_{ii} < 1$ it will produce negative serial correlation. Thus, to some limited extend, the models with regime dependent conditional mean may be able to capture excessive first order dynamics of the return series induced by microstructure noise. Additionally, different intercepts across regimes is necessary to capture the significant sample skewness for higher frequently sampled return series.[10] The

[9] One important point to be mentioned is that the conditional density is non-Gaussian when $\rho \neq 0$ and thus rendering the maximum likelihood estimator a QML estimator which is inconsistent for Markov-switching models in general (see Kim et al. (2008) and Campbell (2002)). This study provides some limited evidence to which extent the QML estimator does not exhibit the theoretical asymptotic normality assumption.

[10] We estimated sample skewness and kurtosis of the return series and found that for higher frequent data the return series is heavily negatively skewed and excess kurtosis is very large compared to lower frequent return series such as for instance return series sampled every hour.

models incorporating an AR(1) structure, possibly regime dependent, aim directly at correcting the bias introduced microstructure noise which manifests itself empirically by significant (first order) serial correlation in the intraday return series (see section 17).[11] Additionally, including unequal lagged autoregressive components across regimes also allows to disentangle the different first or higher order dynamics of the return series in each regime. While both, regime dependent conditional means and first order autoregressive models with possibly regime dependent parameters may capture some of the microstructure noise contamination and the return dynamics, the residual noise effect should manifest itself in an significant nonzero endogeneity estimate $\hat{\rho}$.

We consider two time series length $T = 800$ and $T = 8'000$ and simulate each time $M = 1'000$ Monte Carlo runs. For each simulation run we generate data from a given model as in D.1 with parameter values as given in table D.2 below.

INSERT TABLE D.2 ABOUT HERE

We start our Monte Carlo analysis by investigating the finite sample properties of the endogenous quasi-maximum likelihood estimator, i.e. $\rho \neq 0$ for all the models as described above. We take $\rho = (0.1, 0.5, 0.9)$ for both time series lengths $T = 800$ and $T = 8'000$. Table D.3 to D.8 summarize the results for both time series length.[12]

INSERT TABLE D.3 ABOUT HERE

[11] This has also been suggested by Dacorogna et al. (2001).

[12] We also considered endogeneity levels of $|\rho| < 0.1$. However, our Monte Carlo analysis shows that for such low levels of measurement error, the endogenous and exogenous estimators delivers practically identical results, meaning that the finite sample bias is of about the same magnitude even for the longer time series. To separate estimation error from bias induced by endogeneity, we also tested the estimators for time series of length $T = 16'000$ or $24'000$ where the exogenous estimator is slightly yet only marginally more biased than the endogenous estimator.

INSERT TABLE D.4 ABOUT HERE

INSERT TABLE D.5 ABOUT HERE

INSERT TABLE D.6 ABOUT HERE

INSERT TABLE D.7 ABOUT HERE

INSERT TABLE D.8 ABOUT HERE

For longer time series lengths, the endogenous estimator produces point estimates that are very close to the true simulated values, which indicates that the joint normality assumption of the regression disturbance term and the state variable is a reasonable approximation. For shorter time series the QML estimates show signs of biasedness, as the average Monte Carlo QML estimates are further away from their true value compared to the estimates based on the longer time series. However, this deviation is mainly due to estimation error which is more pronounced for shorter than for longer time series. Next, we analyze the efficiency of the endogenous estimator when in fact the state is exogenous, i. e. $\rho = 0$. Tables D.10 and D.9 report QML estimates for the endogenous and exogenous estimator, respectively.

INSERT TABLE D.10 ABOUT HERE

INSERT TABLE D.9 ABOUT HERE

The endogenous estimator is inefficient when $\rho = 0$, i. e. exhibits higher standard errors. This can be seen in both Tables D.10 and D.9 for $T = 800$ and $T = 8'000$, respectively. Lastly, we investigate the finite sample properties of the exogenous ML estimator when the state is in fact endogenous. We take again $\rho \in \{0.1, 0.5, 0.9\}$ and simulate data from the data generating processes with endogenous switching as given in Table D.1 with values as reported in Table D.2 and analyze the biased incurred when neglecting endogeneity. Tables D.11 and D.12 summarize the results when $T = 800$ and $T = 8'000$, respectively.

INSERT TABLE D.11 ABOUT HERE

INSERT TABLE D.12 ABOUT HERE

Table D.11 and Table D.12 demonstrate that the ML estimates are in general biased when endogeneity is erroneously omitted. As expected, the deviations of the Monte Carlo averages for shorter time series is larger for shorter time series than longer time series due to the presence of estimation error. However, not all the parameters are affected by neglecting endogenous switching in the same manner and the bias strongly depends on the time series length. For shorter time series, similar as to the results before, the observed deviation from the true parameter is not only due to endogeneity in the data but also due to estimation error. Furthermore, whereas the bias is increasing in the endogeneity level ρ for some parameters, for other parameters the opposite or no particular pattern can be found. To put this somewhat surprising result into perspective, we calculate the Monte Carlo average relative bias for a given parameter and then sum them up over all parameters for a given model, i.e. $SrB_k = \sum_{p=1}^{P} \hat{\theta}_p$, where $\hat{\theta}_p = \sum_{i=1}^{M} |\hat{\theta}_{p,i} - \theta_p|/|\theta_p|$ where $\theta_{p,i}$ and $\hat{\theta}_{p,i}$ are the true and estimated QML values for

parameter p for a given model k and Monte Carlo simulation i as summarized in Table D.1. This test statistic, the sum of the relative bias (SrB_k), gives an indication of the total bias for a given model. Therefore, the longer the time series, the less is the QML estimator prone to estimation error and therefore the observed deviation of the Monte Carlo ML estimates from the true values, can be attributed to the effect of neglecting endogeneity in the data generating process. Furthermore, whereas SrB_k exhibits no particular pattern for $T = 800$, it is strictly increasing for all the models considered when $T = 8'000$ showing that endogenous switching renders the parameter estimates indeed biased.

4.5 Sampling Scheme

Before we turn to the empirical section, we briefly discuss the sampling scheme we use for constructing equispaced intra day returns. The literature mainly focuses on two sampling schemes, namely the previous tick method (see Wasserfallen & Zimmermann (1985)) or a linear interpolation method as employed for instance in Andersen & Bollerslev (1997). A price series can then either be constructed using the former method where simply for each $\tau \in [t_{k-1,m}, t_{k,m})$ the first quoted price will be recorded, i.e.

$$p(\tau) \equiv p_{t_{k-1,m}}$$

or using the latter method we obtain the equidistant price series as follows

$$p^l(\tau) \equiv p_{t_{k-1,m}} + \frac{\tau - t_{k-1,m}}{t_{k,m} - t_{k-1,m}}(p_{t_{k,m}} - p_{t_{k-1,m}})$$

As Hansen & Lunde (2006) have shown, linear interpolation cases the realized variance estimator to converge in probability to zero as the sampling frequency is increased. This a direct consequence of the piecewise (Lipschitz) continuity and linearity of $p^l(\tau)$ on the interval $[t_0, T]$. On the other hand, constructing the price series by the previous tick method leads to a piecewise constant and discontinuous price series.

Lemma 1. *Let the equidistant price series be constructed using the previous tick method, i. e.* $\tau \in [t_{k-1,m}, t_{k,m})$, $p(\tau) \equiv p_{t_j}$ *and let the efficient log price series follow a regime dependent diffusion process as in* (4.1). *Then assuming no microstuctural noise in the data, i.e.* $\rho = 0$ *the quadratic variation is bounded away from zero for every* $t > 0$ *if the regime dependent diffusion process is not degenerate, i.e.* $\sigma_{r_\tau} = 0$ *and finite* $\mathbb{P}$ *a.s.*

Moreover, since the differences between two instantaneous prices constitute a stochastic integral we may also bound it from above. If there exists a K such that $\sigma_{r_\tau} < K < \infty \; \forall \; \tau \geq 0$, then we have $\mathbb{P}$ a.s.

$$\mathbb{P}\left[\sup_{a \leq u \leq b} | \int_{t_{k-1,m}}^{t_{k,m}} \sigma_{r_u} dW_u| > \delta\right] \leq \exp\left(\frac{\delta^2}{2K^2(t_{k,m} - t_{k-1,m})}\right) \quad \forall \; \delta > 0. \tag{4.34}$$

Therefore, the regime switching diffusion is well defined over the interval $[t_{k-1,m}, t_{k,m})$.

4.6 Measuring microstructure Effects: Empirical Evidence

In this section, we analyze our data set using two standard statistical measures for detecting microstructure noise in intra day return series (see Zhou (1996), Andersen et al. (1999) or Andersen, Bollerslev, Diebold & Ebens (2001)). As a first measure we computed the empirical sample autocorrelation function. As an other measure we plot the realized variance estimator as a function of the sampling frequency, which is commonly referred to as a "volatility signature plot". It is a well known fact (see Zhou (1996) or Hansen & Lunde (2006)) that the former is a measure for microstructure effects, as intra day return series tend to be more autocorrelated at higher sampling frequencies. Complementary to the former, the latter measure provides information as to which sampling frequency the realized variance estimator is not (upward) biased. To start the empirical analysis, in Figure 4.1 below, we show the average first order autocorrelation estimates for varying degrees of frequency levels.

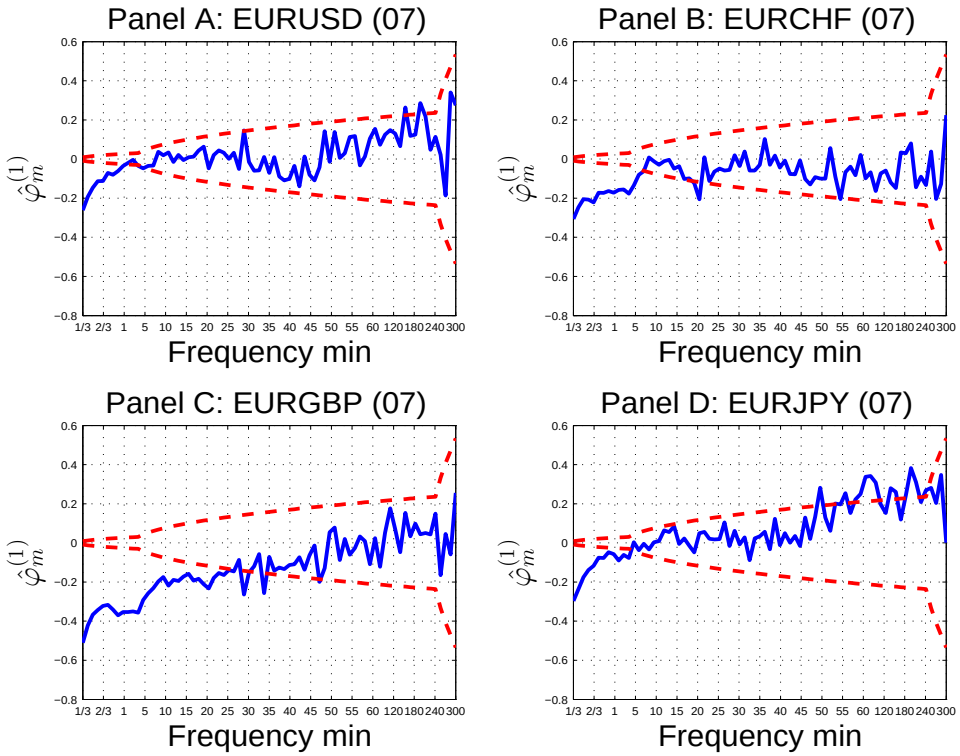

Figure 4.1: The figure shows the estimated first order autocorrelation coefficient $\hat{\varphi}_m^{(1)}$ as a function of the sampling frequency m. Red lines represent approximate $\alpha = 5\%$ confidence intervals as given in Box et al. (1994) for a given sampling frequency m. Log-return series were constructed using Mid-quotes of the currency pairs EUR/USD, EUR/CHF, EUR/GBP and EUR/JPY of the year 2007 using previous tick price recording, starting on January 2nd 5pm.

What is common to all return series is the highly negative and statistically significant first order autocorrelation coefficient at the highest sampling $m = 5$ *sec.* until roughly $5 - 20$ *min.* sampling frequency. This particular pattern is mainly due to bid-ask bounds which is a well-known empirical stylized fact. Decreasing m the coefficients tend to be less negative or even reach positive territory but eventually stabilize around zero and become statistically insignificant at the 5% confidence level.[13] Interestingly, the autocorrelation coefficients for the EUR/JPY exchange rate and to a lesser extent also for the EUR/USD show large significant positive first order serial correlation at around 50 min. to 3h sampling for the former currency pair and simliarly for the latter pair this can be observed at around 2h sampling frequency. We

[13]Note that the grid in 4.1 is not equidistant. This explains the kink in the confidence bands at $m = 1min.$ and $m = 1hr.$

also estimated higher order autoregressive terms for all currency pairs for various frequencies. Figure E.3 below displays the estimates for the first five lags of the EUR/USD currency pair.[14]

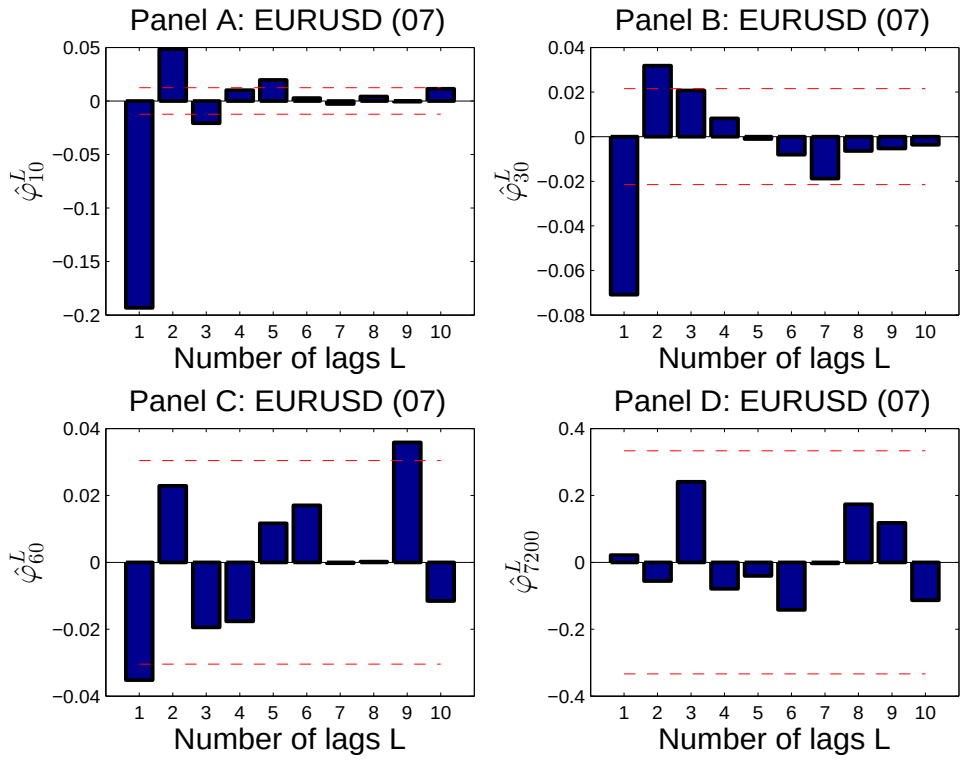

Figure 4.2: The figure shows the estimated autocorrelation coefficient $\hat{\varphi}_m^{(L)}$ for lag values $L = 1, \ldots, 10$ for the spot EUR/USD exchange rate. The selected sampling frequencies are $m = 10sec.$, $30sec.$ $1min.$ and $2hr.$, respectively. Red lines represent approximate $\alpha = 5\%$ confidence intervals as given in Box et al. (1994). Log-return series were constructed using Mid-quotes of the currency pairs EUR/USD, EUR/CHF, EUR/GBP and EUR/JPY of the year 2007 using previous tick price recording, starting on January 2nd 5pm.

A first observation is the decreasing number of significant autocorrelation coefficients as the sampling frequency decreases. Also, the magnitude of the first order autocorrelation coefficient is decreasing in m. This observation is line with many empirical findings such as for instance the well-known article by Cont (2001) or a more recent study by Goncalves & Meddahi (2008*a*) showing that log-return series at roughly daily sampling frequency do not exhibit any significant first order serial correlation. As a second measure for analyzing microstructure noise we

[14]The remaining higher order serial correlation plots are given in appendix E.

compute the realized variance estimator $\widehat{RV}_t^m$ and plot it against the sampling frequency m, shown in Figure 4.3 below

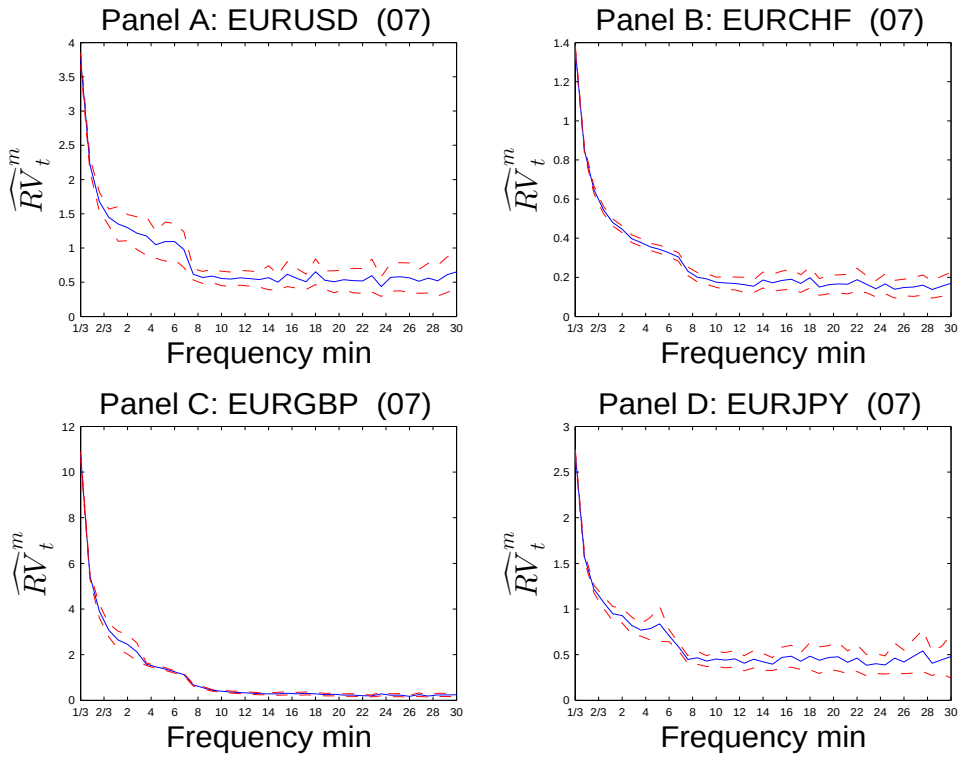

Figure 4.3: Volatility signature plot of RV_t^m based on mid quote data for the currency pairs EUR/USD, EUR/CHF, EUR/GBP and EUR/JPY on the 1st of January 2007 at 8.00 pm. until 2nd of January 2007 using previous tick price recording. Redlines represent approximated edgeworth corrections for realized volatility using the approximation given in Goncalves & Meddahi (2008*b*).

In absence of microstructure noise, the realized variance estimator as a function of the sampling frequency should lie on a straight horizontal line. As Figure 4.3 clearly indicates, at higher sampling frequencies the return series, tends to be upward biased, which is a standard empirical observation documented in many studies (see for instance Andersen et al. (2000b)). Furthermore, the bias seems to increase over proportionally in m, which an indication that the impact of the noise is larger at higher sampling frequencies. To sum up this section, standard empirical measures presented in this section demonstrate that microstructure noise is indeed present in the data. Furthermore, lagged serial correlation coefficients, and among

them most prominently the first order autoregressive coefficient, tend to be only significant at higher sampling frequencies.

4.7 Empirical Analysis

In this section we demonstrate empirically the presence of endogeneity in the return series at higher sampling frequencies and that parameter estimates for the endogenous and exogenous model differ substantially. To be more precise, we investigate the QML estimates for the models 1-8 when the state variable is assumed to be endogenous and compare these estimates to the ones where we restrict $\rho = 0$. We consider a time series length of $T = 8'000$ and fit for each frequency $m = \{5sec, \ldots, 55sec, 1min, 2min, \ldots, 59min, 1hr, 2hr, \ldots, 24hr\}$ a model as specified in Table D.1. In Table D.13 we present the estimation results based on the log-return series sampled every ten seconds.

INSERT TABLE D.13 ABOUT HERE

Overall the model estimates differ substantially between the endogenous and exogenous estimator for all models. The difference in magnitude appears to be related to the degree of endogeneity in the data. For instance, for the most basic model M_5 where only the volatility parameter is different across regime, the estimated coefficient for ρ indicates very high level of endogeneity. As a result of this, the regime persistence parameters a_1 as well as a_2 and the high volatility parameter σ_2 differ sizable in comparison to the exogenous QML estimates. Furthermore, standard model selection criteria such as $AIC_{Endo} = 2p - 2\log\hat{\mathcal{L}} = -3'355.2$ ($AIC_{Exo} = -52'440.4$) and $BIC_{Endo} = -2\log\hat{\mathcal{L}} + p\log(T) = -3'320.3$ ($BIC_{Exo} = -52'405.1$), where p denotes the number of parameters for a given model, indicate that the endogenous is superior to the exogenous estimator.[15] The same conclusion can be drawn when a constant mean is added to the

[15]Furthermore, the likelihood ratio test statistic is 5.4928 which is significant at the 5% confidence level ($\mathbb{P}$-value=0.0191), however not at the 1% level (critical value 6.635).

regression equation (M_6). Adding instead a regime dependent drift (M_1) shows that the estimated endogeneity level decreases considerably. This might be partially due to the introduced first order autocorrelation which can be easily obtained when the drift differs across regime.[16] As Dacorogna et al. (2001) propose and section 17 demonstrated, at higher sampling frequencies, it is necessary to include lagged autoregressive terms to capture the statistically significant negative (first-order) autocorrelation. Its interesting to see that for both regime independent (M_7) and regime dependent λ (M_2) the coefficient is large, negative and statistically significant for all the models considered. Adding a regime dependent autoregressive coefficient ($\lambda_{r_{k-1,m}}$) shows that for the calm volatility regime 1, the autoregressive term is of the same magnitude as for the single regime parameter λ. However, the coefficient λ_2 has opposite sign and is of lower magnitude indicating positive autocorrelation in the high volatility regime. Additionally, the estimated endogeneity level decreases with the inclusion of autoregressive terms, either regime dependent or not. Furthermore, this indicates that these autoregressive terms capture some of the first order dynamics of the contaminated return series which are driven primarily by microstructure noise.[17] To analyze the endogeneity level across frequencies we reestimate all the models at 20 min. sampling. As section 17 on serial correlation and the volatility signature plots has shown, returns sampled every 20 min. contain very little or no microstructure noise

[16]Note that the autocorrelation function for model M_1 assuming that the state variable is exogenous is given by

$$\begin{aligned}\gamma^1_{M_1} &= \frac{(\mu_1-\mu_2)^2\pi_1(1-\pi)(\mathbb{P}_{11}+\mathbb{P}_{22}-1)}{\mathbb{V}[y_{k,m}]}\\ \mathbb{V}[y_{k,m}] &= \pi_1\mu_2^4+(1-\pi_1)\mu_2^4+6\left(\pi_1\mu_1^2\sigma_1^2+(1-\pi_1)\mu_2^2\sigma_2^2\right)+3\left(\pi_1\sigma_1^4+(1-\pi_1)\sigma_2^2\right)\\ &\quad-\left(\pi_1\sigma_1^2+(1-\pi_1)\sigma_2^2+(1-\pi_1)\pi_1(\mu_2-\mu_1)^2+\left(\pi_1\mu_1+(1-\pi_1)\mu_2\right)^2\right)\end{aligned}$$

where $\pi_1=\frac{1-\mathbb{P}_{22}}{1-\mathbb{P}_{11}-\mathbb{P}_{22}}$ and $\pi_2=\frac{1-\mathbb{P}_{11}}{1-\mathbb{P}_{11}-\mathbb{P}_{22}}$. Thus with the given parameter estimates as in D.13 this implies a first order autocorrelation of the exogenous model of 0.0648. Since the presence of the process in the two state is persistent,i.e. $\mathbb{P}_{11}+\mathbb{P}_{22}-1>0$ the model will produce positive first order correlation.

[17]Including higher order autoregressive terms is not straight forward as one would need to calculate the joint density of $y_{k,m}, y_{k-1,m}, \ldots, y_{k-l,m}$ where $l<k$ is the number of lags. In the case of endogenous switching, it is not clear if it is possible to derive the joint density for an arbitrary lag $l>1$. However, as the empirical analysis in section has shown, the first order serial correlations seem to capture most of the spurious first order effects which are due to microstructure noise.

and thus we expect the QML estimate for ρ to be of smaller magnitude. Table D.14 summarizes the results.

INSERT TABLE D.14 ABOUT HERE

A striking difference in comparison to Table D.13 is that the estimated endogeneity level for all models is significantly reduced. This gives an indication that to some extent the endogeneity coefficient ρ captures microstructure noise. The autoregressive terms, possibly regime dependent, are of considerably smaller magnitude compared to the autoregressive terms in Table D.13 indicating that the return series is no longer contaminated by microstructure noise. Interestingly, the regime determining parameters a_1 and a_2 are in both regimes of lower magnitude as compared to the estimates in Table D.13 for both the endogenous and exogenous estimator. This implies also that regime persistence is lower at lower frequencies for both regimes.[18] Furthermore, the parameter estimates do not differ considerably anymore for most models, except for model M_4 where the autoregressive term and both regime dependent drift parameters have opposite sign. However, as the Monte Carlo analysis has shown, this observation might be due to the fact that the endogenous estimator is inefficient. Therefore, this difference in the estimates can be attributed to estimation error. Next as a robustness exercise we examine the endogeneity parameter for each sampling frequency $m = \{5sec, \ldots, 55sec, 1min, 2min, \ldots, 59min, 1hr, 2hr, \ldots, 24hr\}$ in more detail. To be precise, for each model we estimate ρ for a given sampling frequency m and time series length $T = 8'000$. Then we shift the estimation window by W periods and reestimate ρ again for each model.[19] We repeat this procedure S-times and compute the average absolute endogeneity level

[18]Note the average regime persistence across models in Table D.13 is $\mathbb{P}_{11} = 0.9989$ (0.9970) and $\mathbb{P}_{22} = 0.9106$ (0.9137) for the endogenous (exogenous) estimator and in Table D.14it is $\mathbb{P}_{11} = 0.9354$ (0.9343) and $\mathbb{P}_{22} = 0.8348$ (0.8298) for the endogenous (exogenous) estimator, respectively.

[19]The reason why we use a rather long time series of length $T = 8'000$ is because shorter time are more prone to estimation error. As the Monte Carlo analysis demonstrated, the QML estimates are less precise, i.e. having higher bias in absolute value and also higher dispersion, meaning larger standard errors on average for $T = 800$ as the QML based on the longer time series $T = 8'000$. It is for this reason that we fix the time series length

$\bar{\hat{\rho}}^W_{m,T} = \frac{1}{S}\sum_{s=1}^{S} |\hat{\rho}^W_{m,T,s}|$. In Figure G.7 and Figure G.8 we show the average absolute endogeneity level for a given sampling frequency.

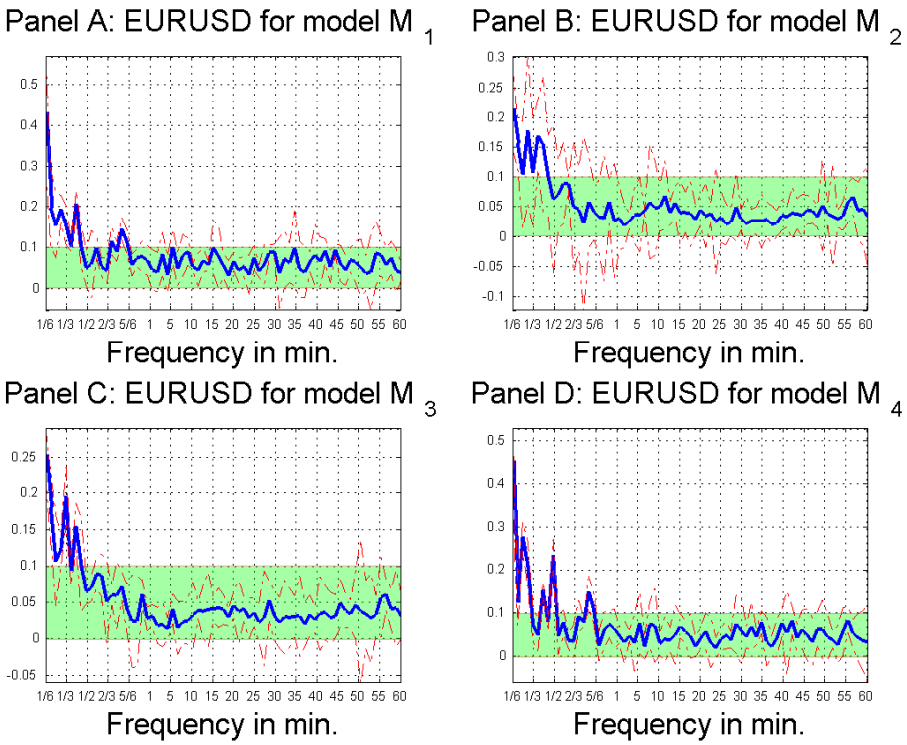

Figure 4.4: EUR/USD spot exchange rate: Average absolute endogeneity level $\bar{\hat{\rho}}^W_{m,T} = \frac{1}{S}\sum_{s=1}^{S} |\hat{\rho}^W_{m,T,s}|$ for models $M_1 - M_4$ with corresponding 95% confidence intervals. The estimation period starts on January 2nd 5 pm and contains for each model 8'000 observations with rolling window of W=200 for a given sampling frequency $m = \{5sec, \ldots, 55sec, 1min, 2min, \ldots, 1hr\}$.

For all the models considered, the endogeneity plot exhibits a similar shape, i. e. as the sampling frequency increases so does the average estimated absolute endogeneity level. Furthermore, the magnitude of the measurement error is only substantial when sampling at 60 sec. or higher. At the highest sampling frequency $5 - 15sec.$ we see that $\bar{\hat{\rho}}^W_{m,T}$ however differs substantially across models. For instance in figure G.7, for model M_1 where we only included a regime dependent drift, the estimated average absolute endogeneity level is about double of the endogeneity level of model M_2 where we included lagged regime dependent regressors. Also, as

used for estimating the models regardless of the frequency we consider. Of course, this procedure implies that for a given model, the data used is not that same for two different frequencies and thus the data sets for a given model are overlapping.

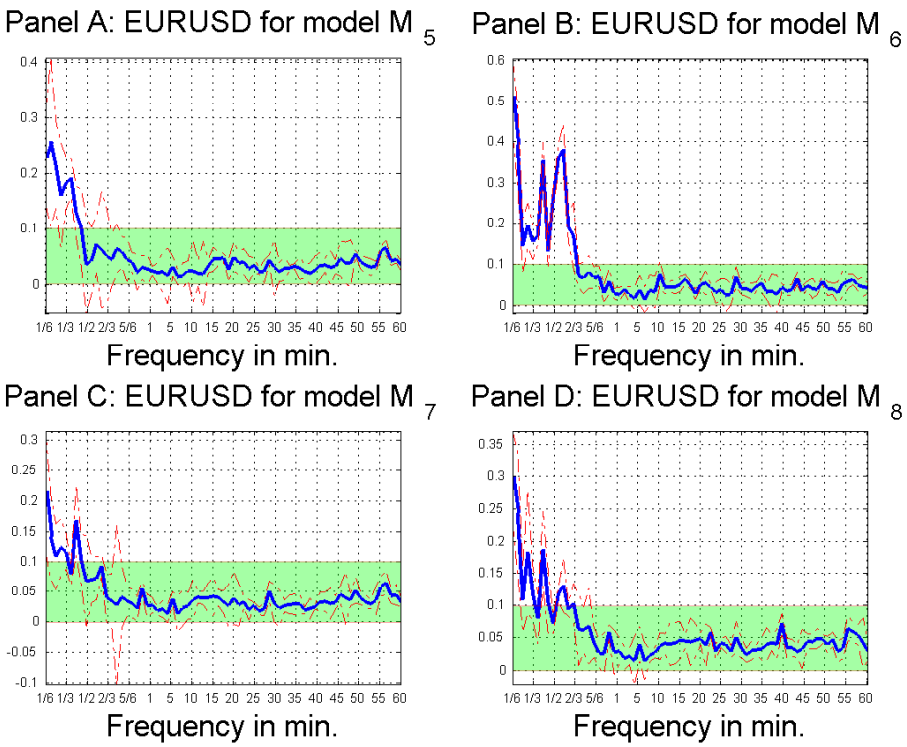

Figure 4.5: EUR/USD spot exchange rate: Average absolute endogeneity level $\bar{\hat{\rho}}_{m,T} = \frac{1}{S}\sum_{s=1}^{S}|\hat{\rho}^{W}_{m,T,s}|$ for models $M_5 - M_8$ with corresponding 95% confidence intervals. The estimation period starts on January 2nd 5 pm and contains for each model 8'000 observations with rolling window of W=200 for a given sampling frequency $m = \{5sec, \ldots, 55sec, 1min, 2min, \ldots, 1hr\}$.

Figure G.8 shows, including autoregressive terms (see model M_7) helps to reduce the estimated endogeneity level relative to a model with a constant drift (see M_6). This implies that on average, models with lagged coefficients tend to capture the spurious first order serial correlation introduced by measurement error such as microstructure noise better than for instance models with constant drift, possibly regime dependent. Concerning the former models, their estimated level of endogeneity is not only significantly reduced in magnitude but also appears to be present only at higher frequencies as compared to the other models. However, at the highest sampling frequencies, all endogeneity plots show that there is still residual endogeneity present which is not captured in any of the model coefficients. As a robustnes check for our results, we repeated the analysis also for the remaining currency pairs where we find similar results, i. e. higher (lower) estimated endogeneity when the sampling frequency increases (decreases).

When reducing the time series length to $T = 800$ (see section G), the estimated endogeneity level is substantially larger as compared to the case when $T = 8'000$. However, as section 4.4 shows, this observation is mainly due to higher estimation error as opposed to higher levels of endogeneity in the data. A final observation to conclude is that as the sampling frequency is reduced, the estimated average endogeneity level appears to vanish, i. e. becomes insignificant indicating that exogeneity of the state variable can be safely assumed.

4.8 Conclusion

In this paper we establish a link between microstructure noise and endogenous switching and discussed its effect on the estimation of the integrated regime dependent variance. We quantify the bias induced by this endogeneity problem on the realized variance estimator, when the state variable controlling the regime is indeed endogenous. The empirical application of the model shows due to the presence of microstructure noise, that at higher sampling frequency there is indeed significant evidence for endogenous switching of the regime. However, the degree of endogeneity varies across models and also the highest sampling frequency as to which the state variable can be assumed to be exogenous is dependent on the particular model employed.

Part II

Appendices

Appendix A

Economic Policy Uncertainty and the Yield Curve

A.1 Proof of Proposition 1

Proof. We start by deriving an n-th order recursive moment formula for the expectation of the government policy uncertainty process g_t with dynamics

$$dg_t = \kappa_g \left(\theta_g - g_t\right) dt + \sigma_g \sqrt{g_t} dW_t^g \tag{A.1}$$

To compute its moments, let $f(g) = g^n$ where $n \in \mathbb{N}$, then an application of Itô's lemma and using Equation (A.1) gives

$$\begin{aligned} dg_t^n &= n g_t^{n-1} dg_t + \frac{1}{2} n(n-1) g_t^{n-2} \sigma_g^2 g_t dt \\ &= \left(-n\kappa_g g_t^n + g_t^{n-1}(n\kappa_g \theta_g + \frac{n}{2}(n-1)\sigma_g^2)\right) dt + n g_t^{n-1} \sigma_g \sqrt{g_t} dW_t^g \end{aligned} \tag{A.2}$$

Integrating from t to T, taking expectations on both sides, using Fubini's theorem and the law of iterated expectation, differentiating with respect to T gives

$$\psi_t^{'}(T) = \Upsilon_0(T) + \Upsilon_1(T)\psi_t(T) \tag{A.3}$$

$$\Upsilon_0(T) = \mathbb{E}_t\left[g_{t+\tau}^{n-1}\right]\left(n\kappa_g\theta_g + \frac{n}{2}(n-1)\sigma_g^2\right) \tag{A.4}$$

$$\Upsilon_1(T) = -n\kappa_g \tag{A.5}$$

Conditional on $\kappa_g > 0$, the solution to Equation (A.3) is

$$\psi_t(t+\tau) = e^{\psi_1\tau}g_t^n + \int_t^{t+\tau}\Upsilon_0(t+\tau-u)e^{\Upsilon_1(t+\tau-u)}du \tag{A.6}$$

Then the first moment satisfies

$$\psi_g^{'}(t,T) := \frac{\mathbb{E}_t[g_T]}{dT} = \kappa_g(\theta_g - \mathbb{E}_t[g_T]) \tag{A.7}$$

$$\psi_g(t,t) := g_t > 0 \tag{A.8}$$

where Equation (A.8) represents the initial condition. The solution this fist order linear differential equation in (A.7) can be represented as

$$\psi_g(t,T) := \mathbb{E}_t[g_T] = \theta_g + (g_t - \theta_g)e^{-\kappa_g\tau} \tag{A.9}$$

and similarly, using Equation (A.9) one obtains that the second moment is given by

$$\psi_{g^2}(t,T) := \mathbb{E}_t[g_T^2] = g_t^2e^{-2\kappa_g\tau} + \frac{\left(e^{-\kappa_g\tau} - e^{-2\kappa_g\tau}\right)\left(2\theta_g\kappa_g + \sigma_g^2\right)}{2\kappa_g}g_t + \frac{\theta_g(2\theta_g\kappa_g + \sigma_g^2)\left(1 - e^{-\kappa_g\tau}\right)^2}{2\kappa_g}$$

$$\psi_{g^2}(t,t) := g_t^2 > 0$$

from which one can immediately deduce that the variance of g_t is

$$\mathbb{V}_t[g_T] = \mathbb{E}[g_T^2] - \mathbb{E}[g_T]^2 = \frac{\left(2g_t\left(e^{-\kappa_g\tau} - e^{-2\kappa_g\tau}\right) + \theta_g\left(1 - e^{-\kappa_g\tau}\right)^2\right)\sigma_g^2}{2\kappa_g} \tag{A.10}$$

and its unconditional variance is

$$\mathbb{V}[g_t] = \frac{\theta_g\sigma_g^2}{2\kappa_g} \tag{A.11}$$

Along the same line of argumentation, integrating Equation (2.5), applying Fubini's theorem and the law of iterated expectations we obtain that the conditional expected value of A_t satisfies

$$\begin{aligned}\psi_A^{'}(t,T) &:= \frac{\mathbb{E}_t[A_T]}{dT} = \kappa_A\left(\theta_A - \psi_A(t,T)\right) + \lambda\psi_g(t,T) \\ \psi_A(t,t) &= A_t \ \in \ \mathbb{R}\end{aligned} \tag{A.12}$$

where Equation (A.12) represents the initial condition for the process A_t. Using the expression for $\psi_g(t,T)$ in Equation (A.9), the solution can be obtained using standard methods. Passing to the limit, i.e., $T \to \infty$, gives the stationary expectation of A_t in Proposition 1. Next, in order to derive the second moment of the productivity process A_t, we have to first derive the an expression for the product expectation $\psi_{Ag}(t,T) := \mathbb{E}_t\left[A_{t+\tau}g_{t+\tau}\right]$. An application of Itô's formula to $A_t g_t$ results in the following dynamics

$$d\left(A_t g_t\right) = \left[\left(\kappa_A\theta_A + \rho^{Ag}\sigma_A\sigma_g\right)g_t + \kappa_A\theta_A A_t - (\kappa_A+\kappa_g)A_t g_t + \lambda g_t^2\right]dt + \sigma_A g_t^{3/2}dW_t^A + \sigma_g g_t^{3/2}dW_t^g$$

Then, as above, integrating from t to $T = t+\tau$, applying Fubini's theorem and taking time t conditional expectation shows that $\psi_{Ag}(t,T)$ satisfies

$$\begin{aligned}\psi_{Ag}^{'}(t,T) &:= \frac{\mathbb{E}_t[A_T g_T]}{dT} = \left(\kappa_A\theta_A + \rho^{Ag}\sigma_A\sigma_g\right)\psi_g(t,T) + \kappa_A\theta_A\psi_A(t,T) - (\kappa_A+\kappa_g)\psi_{Ag}(t,T) + \lambda\psi_{g^2}(t,T) \\ \psi_{Ag}(t,t) &= A_t g_t\end{aligned} \tag{A.13}$$

where Equation (A.13) represents the initial condition. Solving this first order differential equation with time-dependent functions $\psi_g(t,T)$, $\psi_{g^2}(t,T)$ and $\psi_A(t,T)$ gives the conditional covariance expression. Having obtained explicit conditional moments for A_t, g_t and $A_t g_t$, the stationary covariance expression immediately follows from letting $T \to \infty$, i.e. $\lim_{T\to\infty} = \mathbb{C}_t(A_{t+\tau}, g_{t+\tau}) = \mathbb{E}_t[A_{t+\tau}, g_{t+\tau}] - \mathbb{E}_t[A_{t+\tau}]\mathbb{E}_t[g_{t+\tau}]$. Finally, by similar arguments as above and an application of Itô's formula to A_t^2 we obtain that the second moment of A_t satisfies

$$\begin{aligned}\psi_{A^2}^{'}(t,T) &:= \frac{\mathbb{E}_t[A_T^2]}{dT} = 2\kappa_A\left(\theta_A - \psi_A(t,T)\right) + 2\lambda\psi_{Ag}(t,T) + \sigma_A^2\psi_g(t,T)\psi_{g^2}(t,T) \\ \psi_{A^2}(t,t) &= A_t^2\end{aligned} \tag{A.14}$$

Solving this ordinary first order differential equation with time-dependent coefficients gives the expression for the conditional expectation of A_t. From $\mathbb{V}_t(A_{t+\tau}) = \mathbb{E}[A_{t+\tau}^2] - \mathbb{E}[A_{t+\tau}]^2$ and letting $T \to \infty$ we immediately obtain the stationary variance expression for A_t. □

A.2 Proof of Proposition 3

The optimal consumption and investment problem is

$$\max_{C_s, M_s^d} \mathbb{E}_t \left[\int_t^\infty e^{-\beta s} U(C_s, M_s^d) dt \right], \tag{A.15}$$

where $U(C_t, M_t^d) = \frac{1}{\gamma} \left(\left(C_t (M_t^d)^\xi \right)^\gamma - 1 \right)$ subject to the capital constraint in Equation (2.12). To simplify notation, let $X_t = (A_t, g_t)$ such that the value function is given by

$$V = V(t, K_t, X_t) = \max_{\{C_s, M_s^d\}_{t \le s < \infty}} \mathbb{E}_t \left[\int_t^\infty e^{-\beta s} U(C_s, M_s^d) ds \right]. \tag{A.16}$$

In equilibrium, there exists a value function $V(t, K_t, X_t)$ and control variables $\{C_t, M_t^d\}$ satisfying the HJB equation

$$-\frac{\partial V(t, K_t, X_t)}{\partial t} = \max_{\{C_t, M_t^d\}} \left\{ U(C_t, M_t^d) + \mathcal{A} V(t, K_t, X_t) \right\}. \tag{A.17}$$

By standard time-homogeneity arguments for infinite horizon problems we have that

$$\begin{aligned} e^{\beta t} V(t, K_t, X_t) &= \max_{\{C_s, M_s^d\}_{t \le s < \infty}} \mathbb{E}_t \left[\int_t^\infty e^{-\beta (s-t)} U(C_s, M_s^d) ds \right] \\ &= \max_{\{C_{t+u}, M_{t+u}^d\}_{t \le u < \infty}} \mathbb{E}_t \left[\int_t^\infty e^{-\beta u} U(C_{t+u}, M_{t+u}^d) du \right] \\ &= \max_{\{C_u, M_u^d\}_{0 \le u < \infty}} \mathbb{E}_0 \left[\int_0^\infty e^{-\beta u} U(C_u, M_u^d) du \right] \\ &\equiv H(K_t, X_t), \end{aligned} \tag{A.18}$$

where the third equality follows because the optimal robust control is Markov and $H(K_t, X_t)$ is independent of time. Therefore, we conjecture that the value function has the following form

$$V(t, K_t, X_t) = a(t) H(K_t, X_t) = \frac{e^{-\beta t}}{\beta} H(K_t, X_t) = \frac{e^{-\beta t}}{\beta \gamma} \left(\left(e^{\phi(X_t)} K_t^\xi \right)^\gamma - 1 \right), \tag{A.19}$$

where $\phi : \mathbb{R}^2 \to \mathbb{R}$ is $\mathcal{C}^N$-differentiable function of the state vector X_t that needs to be determined in equilibrium. Inserting (A.19) into the HJB equation in (A.17), the first order conditions are given by

$$C_t^* = \frac{K_t \left(K_t^Q e^{\phi(X_t)}\right)^{-\gamma}}{\beta Q} \left(\frac{\beta Q \left(K_t^Q e^{\phi(X_t)}\right)^{\gamma} \left(\left(-\frac{(\gamma-1)\beta^{\frac{1}{1-\gamma}} Q^{\frac{1}{1-\gamma}} K_t^{\frac{1-\gamma Q}{\gamma-1}} e^{\frac{\gamma\phi(X_t)}{1-\gamma}}}{\xi} \right)^{\frac{1-\gamma}{\gamma\xi+\gamma-1}} \right)^{-\xi}}{K_t} \right)^{\frac{\gamma}{\gamma-1}} \tag{A.20}$$

$$M_t^{d*} = \left(\frac{(1-\gamma)\beta^{\frac{1}{1-\gamma}} Q^{\frac{1}{1-\gamma}} K_t^{\frac{1-\gamma Q}{\gamma-1}} e^{\frac{\gamma\phi(X_t)}{1-\gamma}}}{\xi} \right)^{\frac{1-\gamma}{\gamma\xi+\gamma-1}}, \tag{A.21}$$

with $Q = 1 + \xi$. In general, the function $\phi(X_t)$ cannot be obtained in closed form. However, we can obtain an asymptotic expansion to $g(X_t)$ with respect to the risk aversion parameter γ. Assuming a power series expression for $\phi(X_t)$ in γ as follows

$$\phi(X_t) = \phi_0(X_t) + \gamma\phi_1(X_t) + O(\gamma^2),$$

where $\phi_0(X, t)$ is obtained from the logarithmic utility case, we can then solve the HJB problem in Equation (A.17) for $\gamma \neq 0$ in closed form. To do so, we solve first the HJB problem in the case where utility of the representative agent is logarithmic.

Log-utility case

Note that for $\gamma \to 0$ the utility reduces to

$$\lim_{\gamma \to 0} U(C_t, M_t^d) = \log(C_t) + \xi \log\left(M_t^d\right). \tag{A.22}$$

The optimal consumption and investment problem is[1]

$$\max_{C_t, M_t^d} \mathbb{E}_0 \left[\int_0^\infty e^{-\beta t} \left[\log(C_t) + \xi \log\left(M_t^d\right) \right] dt \right], \tag{A.23}$$

[1]The proof of this proposition is similar to the one presented in Buraschi & Jiltsov (2005).

subject to the capital constraint in Equation (2.12). In equilibrium, there exists a value function $V^{log}(t, K_t, X_t) = a(t)H^{log}(K_t, X_t)$ and control variables $\{C_t, M_t^d\}$ satisfying the HJB equation

$$-\frac{\partial\left(a(t)H^{log}(K_t, X_t)\right)}{\partial t} = a(t)\left(\max_{\{C_t, M_t^d\}}\left\{U^{log}(C_t, M_t^d) + \mathcal{A}H^{log}(K_t, X_t)\right\}\right). \tag{A.24}$$

We consider the following linear conjecture for the value function $V^{log}(\cdot)$

$$a(t)H^{log}(K_t, X_t) = \frac{e^{-\beta t}}{\beta}\left[Q\log(K_t) + g_0(X_t)\right], \tag{A.25}$$

and where the function $g(X_t)$ is affine in the state variables, i.e.,

$$\phi(X_t) = \phi_{00} + \phi_{0A}A_t + \phi_{0g}g_t. \tag{A.26}$$

Applying the generator to Equation (A.25), using the productivity, the government policy, and equilibrium capital accumulation dynamics in Equation (2.5), (2.6) and (2.20), we obtain

$$\begin{aligned}\mathcal{A}V^{log} &= \frac{\partial V^{log}}{\partial t} + \frac{\partial V^{log}}{\partial K}\mu_K + \frac{\partial V^{log}}{\partial A}\mu_A + \frac{\partial V^{log}}{\partial g}\mu_g + \frac{1}{2}\frac{\partial^2 V^{log}}{\partial K^2}\sigma_K^2 \\ &= Q\left[\mu_Y + q_A A_t - \left(\frac{C_t}{K_t} + \frac{M_t^d}{K_t}\right) - \frac{1}{2}\sigma_Y^2 g_t\right] \qquad \text{(A.27)} \\ &\quad + \left(\kappa_A\left(\theta_A - A_t\right) + \lambda g_t\right)\phi_{0A} + \kappa_g\left(\theta_g - g_t\right)\phi_{0g}. \qquad \text{(A.28)}\end{aligned}$$

The first order optimality conditions for consumption and money holdings are

$$\frac{e^{-\beta t}}{C_t} - \frac{Q}{\beta}\frac{e^{-\beta t}}{K_t} = 0 \Longleftrightarrow C_t^* = \frac{\beta K_t}{Q}, \tag{A.29}$$

$$\frac{e^{-\beta t}\xi}{M_t^d} - \frac{Q}{\beta}\frac{e^{-\beta t}}{K_t} = 0 \Longleftrightarrow M_t^{d*} = \frac{\beta\xi K_t}{Q}. \tag{A.30}$$

Substituting the optimal controls C_t^* and M_t^{d*} into Equation (A.24) and matching coefficients of $\log(K_t)$, A_t, g_t and the constant terms, we obtain

$$Q = 1 + \xi \tag{A.31}$$

and

$$\phi_{00} = \frac{(1+\xi)\left(-\theta_g\kappa_g\sigma_Y^2(\beta+\kappa_A)+2\mu_Y(\beta+\kappa_A)(\beta+\kappa_g)+2\theta_g\kappa_g\lambda q_A\right)}{2\beta(\beta+\kappa_A)(\beta+\kappa_g)} \tag{A.32}$$
$$- \frac{(1+\xi)(\beta(\beta+\delta)+\kappa_A(\beta+\delta-\theta_A q_A))}{\beta(\beta+\kappa_A)} + L,$$

$$\phi_{0A} = \frac{(1+\xi)q_A}{(\kappa_A+\beta)}, \qquad \phi_{0g} = \frac{(1+\xi)\left(\frac{2\lambda q_A}{\beta+\kappa_A}-\sigma_Y^2\right)}{2(\kappa_g+\beta)}, \tag{A.33}$$

where L is defined as

$$L = \log\left(\frac{\beta^{1+\xi}\xi^{\xi}}{(1+\xi)^{1+\xi}}\right). \tag{A.34}$$

The coefficients are all uniquely determined, state-independent and also independent of K_t. Substituting the expressions back into the HJB equations verifies that the guess was correct.

Perturbed solution

To derive an asymptotic approximation to the function $\phi(X_t)$, where the expansion taken with respect to the risk aversion parameter γ, let $V = V(t, K_t, X_t)$ denote the value function as given in Equation (A.16). Utility is now given by the following non-separable preferences

$$U(C_t, M_t^d) = \frac{1}{\gamma}\left(\left(C_t(M_t^d)^{\xi}\right)^{\gamma} - 1\right). \tag{A.35}$$

From the HJB equation in (A.17), the optimal consumption C_t^* and money demand M_t^{d*} policy holdings are given by[2]

$$C_t^* = \left(M_t^d\right)^{-\xi}\left(\frac{Q\left(M_t^d\right)^{-\xi}\left(K_t^Q e^{\phi(X_t)}\right)^{\gamma}}{\beta K_t}\right)^{\frac{1}{\gamma-1}}, \tag{A.36}$$

$$M_t^{d*} = \left(\frac{QC_t^{-\gamma}K_t^{\gamma Q-1}e^{\gamma\phi(X_t)}}{\beta\xi}\right)^{\frac{1}{\gamma\xi-1}}. \tag{A.37}$$

Inserting optimal money demand (A.37) into the first order condition of consumption (A.36), using the power series representation of $g(X_t)$ as given in Equation (2.18) and perturbing the

[2]Inserting Equation (A.36) into (A.37) gives the optimal money demand in Equation (A.21) from which the optimal consumption in Equation (A.20) can easily be deduced.

resulting expression around the log-utility case (and analogously for optimal money demand), substituting $Q = 1 + \xi$ from Equation (A.31), the perturbed optimal consumption and money holdings are given by

$$C_t^{*,P} = \frac{\beta K_t}{(1+\xi)} \left[1 + \gamma \left(\log \left(\frac{\beta^{1+\xi} \xi^{\xi}}{(1+\xi)^{1+\xi}} \right) - \phi_0(X_t) \right) \right] + O(\gamma^2), \tag{A.38}$$

$$M_t^{d*,P} = \frac{\beta \xi K_t}{(1+\xi)} \left[1 + \gamma \left(\log \left(\frac{\beta^{1+\xi} \xi^{\xi}}{(1+\xi)^{1+\xi}} \right) - \phi_0(X_t) \right) \right] + O(\gamma^2). \tag{A.39}$$

There are a number of important conclusions that can be drawn from the optimal perturbed solutions in Equations (A.38) and (A.39). First, both equations only depend on $\phi_0(X_t)$ and do not depend on $\phi_1(X_t)$ which implies that solving the consumption-investment problem with log-utility is sufficient to fully characterize the optimal perturbed consumption and money holdings up to first order. Secondly, $C_t^{*,P}$ and $M_t^{d*,P}$ are affine functions not only of capital K_t but also of the state vector X_t. This property of the solution will not only render the equilibrium path process of K_t affine, but also implies that optimal inflation dp_t^*/p_t^* remain affine in the state variables. Next, substituting $C_t^{*,P}$ and $M_t^{d*,P}$ into Equation (2.13) immediately gives the equilibrium capital process K_t^* in Equation (2.20). To show the equilibrium price dynamics in (2.21), we apply Itô's lemma to the money market clearing condition $M_t^S = p_t^* M_t^{d*}$ and obtain[3]

$$dM_t^S = M_t^{*d} dp_t^* + p_t^* dM_t^{d*} + \mathbb{C}_t \left(dp_t^*, dM_t^{*d} \right). \tag{A.40}$$

Then using the optimal controls C_t^* and M_t^{d*} and inserting the money market clearing condition from Equation (A.40) yields

$$\frac{dp_t^*}{p_t^*} = \frac{dM_t^S}{M_t^S} - \frac{dK_t^*}{K_t^*} - \mathbb{C}_t \left(\frac{dp_t^*}{p_t^*} \frac{dK_t^*}{K_t^*} \right). \tag{A.41}$$

Inserting the money supply rule of Equation (2.14) and the equilibrium capital accumulation process into (A.41) gives the equilibrium price process as in Equation (2.21). To verify that the guess for the value function $V(\cdot)$ was correct, we substitute the equilibrium values back into the HJB problem in Equation (A.17).

[3] Assuming that at $t = 0$ markets are cleared. Hence, $p_0^* M_0^{d*} = M_0^S$.

A.3 Proof of Proposition 4

To simplify notation, let $\kappa_t^* = \log(K_t^*) + \beta t$. The using the equilibrium capital accumulation process implies that κ_t^* satisfies

$$d\kappa_t^* = \left(\mu_y + q_A A_t - \delta - \frac{1}{2}\sigma_Y^2 g_t + \beta\gamma\left(g_0(X_t) - L\right)\right)dt + \sigma_Y\sqrt{g_t}dW_t^Y. \tag{A.42}$$

The Euler condition in Equation (2.24) can then be expressed as

$$\begin{aligned} B(t,\tau) &= e^{-\beta\tau}\mathbb{E}_t\left[\frac{U_C(C_{t+\tau}^*, M_{t+\tau}^{d*})}{U_C(C_t^*, M_t^{d*})}\frac{p_t^*}{p_{t+\tau}^*}\right] = e^{-\beta\tau}\mathbb{E}_t\left[\frac{K_t^*}{K_{t+\tau}^*}\frac{p_t^*}{p_{t+\tau}^*}\right] = e^{-\beta\tau}\mathbb{E}_t\left[\frac{\exp\{-\log\left(K_{t+\tau}^*\right)\}}{\exp\{-\log\left(K_t^*\right)\}}\frac{p_t^*}{p_{t+\tau}^*}\right] \\ &= \mathbb{E}_t\left[\frac{\exp\{-\left(\log\left(K_{t+\tau}^*\right) + \beta(t+\tau)\right)\}}{\exp\{-\left(\log\left(K_t^*\right) + \beta t\right)\}}\frac{p_t^*}{p_{t+\tau}^*}\right] = \mathbb{E}_t\left[\frac{\exp\{-\kappa_{t+\tau}^*\}}{\exp\{-\kappa_t^*\}}\frac{p_t^*}{p_{t+\tau}^*}\right]. \end{aligned} \tag{A.43}$$

To solve the problem in Equation (A.43) we follow Ulrich (2013*a*) and Buraschi & Jiltsov (2005) and define

$$f = f(\kappa_t^*, p_t^*, A_t, g_t, m_t, \tau) = \mathbb{E}_t\left[\frac{e^{-\kappa_{t+\tau}^*}}{p_{t+\tau}^*}\right]. \tag{A.44}$$

Then, conjecturing a log-linear guess for $f(\cdot)$ of the form

$$f(\kappa_t^*, p_t^*, A_t, g_t, m_t, \tau) = \frac{e^{-\kappa_t^*}}{p_t^*}\exp\left\{-b_0(\tau) - b_A(\tau)A_t - b_g(\tau)g_t - b_m(\tau)m_t\right\}. \tag{A.45}$$

If our log-linear guess in Equation (A.45) solves the stochastic problem in (A.44) then it is also the solution to the following PDE

$$-\frac{\partial f(\cdot,\tau)}{\partial\tau} = \mathcal{A}f(\cdot,\tau),\ f(\cdot,0) = \frac{e^{-\kappa_t^*}}{p_t^*}. \tag{A.46}$$

The left-hand side of Equation (A.46) is given by

$$\frac{\partial f(\cdot,\tau)}{\partial\tau} = \left[-b_0'(\tau) - b_A'(\tau)A_t - b_g'(\tau)g_t - b_m'(\tau)m_t\right]f(\cdot,\tau). \tag{A.47}$$

Setting $\Theta = \{\kappa_t^*, p_t^*, A_t, g_t, m_t\}$, an application of Itô's lemma to the right-hand side of (A.46) gives

$$\mathcal{A}f(\kappa_t^*, p_t^*, A_t, g_t, m_t, \tau) = \sum_{i\in\Theta}\frac{\partial f}{\partial\Theta^i}\mu_{\Theta^i}dt + \frac{1}{2}\sum_{i\in\Theta}\frac{\partial^2 f}{\partial\widetilde{\Theta}^{i2}}d\langle\Theta^i,\Theta^i\rangle_t + \sum_{\substack{i,j\in\Theta\\ i\neq j}}\frac{\partial^2 f}{\partial\Theta^i\Theta^j}d\langle\Theta^i,\Theta^j\rangle_t. \tag{A.48}$$

Writing out the expression above, recalling that $\rho^{gm} = \rho^{Ag} = \rho^{MA} = \rho^{Mg} = 0$ and substituting the dynamics of $\kappa_t^*,\ p_t^*,\ A_t,\ g_t$, and m_t, we get

$$\begin{aligned}
\mathcal{A}f = & \frac{\partial f}{\partial \kappa^*}\left(\mu_{K^*}\left(A_t, g_t\right) - \frac{1}{2}\sigma_Y^2 g_t\right) \\
& + \frac{\partial f}{\partial p_t^*} p_t^* \left[\frac{\mu_M - \eta_1 \bar{k} - \eta_2 \bar{\pi}}{1-\eta_2} + \frac{\eta_1 - 1}{1-\eta_2}\mu_{K^*}\left(A_t, g_t\right) - g_t \frac{(\eta_1 - 1)\sigma_Y^2}{1-\eta_2}\right] \\
& + \frac{\partial f}{\partial A}\left(\kappa_A(\theta_A - A_t) + \lambda g_t\right) + \frac{\partial f}{\partial g}\kappa_g(\theta_g - g_t) + \frac{\partial f}{\partial m}\kappa_m(\theta_m - m_t) \\
& + \frac{1}{2}\left[\frac{\partial^2 f}{\partial \kappa^{*2}}\sigma_Y^2 g_t + \frac{\partial^2 f}{\partial p^{*2}} p_t^{*2}\left[g_t\left(\frac{\eta_1 - 1}{1-\eta_2}\right)^2 \sigma_Y^2 + m_t \frac{\sigma_M^2}{(1-\eta_2)^2}\right]\right. \\
& \left. + \frac{\partial^2 f}{\partial A^2}\sigma_A^2 g_t + \frac{\partial^2 f}{\partial g^2}\sigma_g^2 g_t + \frac{\partial^2 f}{\partial m^2}\sigma_m^2 m_t\right] \\
& + \frac{\partial^2 f}{\partial \kappa^* \partial p^*} p_t^* \sigma_Y^2 g_t \frac{\eta_2 - 1}{1-\eta_2} + \frac{\partial^2 f}{\partial \kappa^* \partial A}\sigma_A \sigma_Y \rho^{AY} g_t + \frac{\partial^2 f}{\partial \kappa^* \partial g}\sigma_g \sigma_Y \rho^{gY} g_t \\
& + \frac{\partial^2 f}{\partial p^* \partial A} p_t^* \frac{\eta_1 - 1}{1-\eta_2}\sigma_A \sigma_Y g_t \rho^{AY} + \frac{\partial^2 f}{\partial p^* \partial g} p_t^* \frac{\eta_1 - 1}{1-\eta_2}\sigma_g \sigma_Y g_t \rho^{gY}.
\end{aligned}$$

Computing the derivatives and separating variables one obtains the following system of first order asymptotic (Riccati) ODE's:

$$0 = -C_A + \kappa_A b_A(\tau) + b_A'(\tau), \tag{A.49}$$

$$0 = Z_{0g}(\tau) + b_g(\tau) Z_{1g}(\tau) + Z_{2g} b_g^2(\tau) + b_g'(\tau), \tag{A.50}$$

$$0 = Z_{0m} + b_m(\tau) Z_{1m} + Z_{2m} b_m^2(\tau) + b_m'(\tau), \tag{A.51}$$

$$0 = -b_0'(\tau) + C_0(\tau) \tag{A.52}$$

subject to $b_A(0) = b_g(0) = b_m(0) = b_0(0) = 0$ and where

$$C_A = (q_A + \gamma\beta\phi_{0A}) \left(\frac{\eta_1 - \eta_2}{1 - \eta_2} \right), \tag{A.53}$$

$$Z_{0g}(\tau) = \left(q_A^2 + 2\gamma\beta\phi_{0A}\right) \left(\frac{\eta_1 - \eta_2}{1 - \eta_2} \right)^2 \frac{(1 - e^{-\kappa_A \tau})^2 \sigma_A^2}{2\kappa_A^2} + \frac{(\eta_1 - \eta_2)^2 \sigma_Y^2}{(\eta_2 - 1)^2} + \gamma \frac{\beta\phi_{0g}(\eta_1 - \eta_2)}{\eta_2 - 1}$$
$$- b_A(\tau) \left(\frac{(\eta_2 - 1)\lambda + (\eta_1 - \eta_2)\rho^{AY}\sigma_A\sigma_Y}{\eta_2 - 1} \right), \tag{A.54}$$

$$Z_{1g}(\tau) = \kappa_g + b_A(\tau)\rho^{Ag}\sigma_A\sigma_g + \frac{(\eta_2 - \eta_1)\rho^{gY}\sigma_g\sigma_Y}{\eta_2 - 1}, \tag{A.55}$$

$$Z_{2g} = \sigma_g^2/2,\ H_g(\tau) = \sqrt{4Z_{0g}(\tau)Z_{2g} - Z_{1g}^2}, \tag{A.56}$$

$$Z_{0m} = \frac{\sigma_M^2}{(\eta_2 - 1)^2},\ Z_{1m} = \kappa_m + \frac{\rho^{Mm}\sigma_m\sigma_M}{1 - \eta_2},\ Z_{2m} = \frac{\sigma_m^2}{2},\ H_m = \sqrt{4Z_{0m}Z_{2m} - Z_{1m}^2}, \tag{A.57}$$

$$C_0(\tau) = \frac{(\mu_Y - \beta - \delta - \bar{k})\eta_1 + \beta + \mu_M - \eta_2(\mu_Y + \bar{\pi} - \delta)}{1 - \eta_2}$$
$$+ \sum_{i \in \{A,g,m\}} b_i(\tau)\theta_i\kappa_i + \gamma \frac{\beta(\eta_1 - \eta_2)(L - \phi_{00})}{\eta_2 - 1}. \tag{A.58}$$

For the existence of a solution to the bond pricing PDE that excludes arbitrage opportunities, requires that the Riccati equations in (A.50) and (A.51) above, satisfy the following periodicity condition

$$4Z_{0g}(\tau)Z_{2g} - Z_{1g}^2(\tau) < 0,\ 4Z_{0m}Z_{2m} - Z_{1m}^2 < 0,\ \forall\, \tau \geq 0. \tag{A.59}$$

This condition essentially rules out singularities of the solution of the Riccati equation above, i.e., for $\tau \geq 0$, the function $b_i(\tau), i \in \{g, m\}$ is continuous in τ.

A.4 Proof of Proposition 5

The unconditional correlation coefficient of the nominal yield curve $Y(t,\tau)$ and g_t is given by

$$\varrho\left[Y(t,\tau), g_t\right] = \frac{\mathbb{C}\left[Y(t,\tau), g_t\right]}{\sqrt{\mathbb{V}[Y(t,\tau)]\mathbb{V}[g_t]}}$$

Using the affine expression in Equation (2.30) and the results from Proposition 1, the unconditional covariance is

$$\mathbb{C}[Y(t,\tau),g_t]=\frac{b_A(\tau)}{\tau}\mathbb{C}[A_t,g_t]+\frac{b_g(\tau)}{\tau}\mathbb{V}[g_t]=\frac{b_A(\tau)}{\tau}\frac{\theta_g\sigma_g\left(2\kappa_g\lambda\rho^{Ag}\sigma_A+\lambda\sigma_g\right)}{2\kappa_g(\kappa_A+\kappa_g)}+\frac{b_g(\tau)}{\tau}\frac{\theta_g\sigma_g^2}{2\kappa_g},$$

where the unconditional variance of term structure is $\mathbb{V}[Y(t,\tau)]=\frac{b_A^2(\tau)}{\tau^2}\mathbb{V}[A_t]+\frac{b_g^2(\tau)}{\tau^2}\mathbb{V}[g_t]+\frac{b_m^2(\tau)}{\tau^2}\mathbb{V}[m_t]+2\frac{b_A(\tau)}{\tau}\frac{b_g(\tau)}{\tau}\mathbb{C}\left[A_t,g_t\right]$. Along the same line of argumentation, we have that

$$\mathbb{C}(Y(t,\tau),m_t)=\frac{\theta_m\sigma_m^2}{2\kappa_m}\frac{b_m(\tau)}{\tau} \tag{A.60}$$

and since $b_m(\tau)\leq 0,\ \tau\geq 0$ the result follows immediately.

A.5 Proof of Proposition 6

In this section we derive the first order asymptotic nominal short rate and the market prices of real and nominal risks when the investor has CRRA utility. The nominal short rate is defined as the following limit

$$R_t:=\lim_{\tau\to 0}Y(t,\tau)=\lim_{\tau\to 0}-\frac{1}{\tau}\left(\log(B(t,\tau))\right). \tag{A.61}$$

To prove Equation (2.34) we make repeated use of Bernoulli's rule. For instance, to compute $\lim_{\tau\to 0}\frac{b_0(\tau)}{\tau}$ we set $f(\tau):=\int_0^\tau C_0(u)du$ and $g(\tau)=\tau$. Then, using Leibniz' integral rule we obtain

$$\begin{aligned}\lim_{\tau\to 0}\frac{f(\tau)}{g(\tau)}&=\lim_{\tau\to 0}\frac{f'(\tau)}{g'(\tau)}\\&=\lim_{\tau\to 0}C_0(\tau)=\frac{(\mu_Y-\beta-\delta-\bar{k})\eta_1+\beta+\mu_M-\eta_2(\mu_Y+\bar{\pi}-\delta)}{1-\eta_2}+\gamma\frac{\beta(\eta_1-\eta_2)(L-\phi_{00})}{\eta_2-1},\end{aligned}$$

Similarly we have

$$\begin{aligned}\lim_{\tau\to 0}\frac{b_A(\tau)}{\tau}&=C_A,\\\lim_{\tau\to 0}\frac{b_g(\tau)}{\tau}&=-Z_{0g}(0)=-\left(\frac{(\eta_1-\eta_2)^2\sigma_Y^2}{(\eta_2-1)^2}+\gamma\frac{\beta\phi_{0g}(\eta_1-\eta_2)}{\eta_2-1}\right),\\\lim_{\tau\to 0}\frac{b_m(\tau)}{\tau}&=-Z_{0m}=-\frac{\sigma_M^2}{(\eta_2-1)^2},\end{aligned} \tag{A.62}$$

which gives the expression for the short rate in Equation (2.34). Next, in order to derive the bond excess return, we apply Itô's rule to the closed-form bond price formula in Equation (2.25) and obtain the following dynamics

$$\frac{dB(t,\tau)}{B(t,\tau)} = \frac{\partial B(t,\tau)}{\partial t}dt + \sum_{i\in\Theta}\frac{\partial B(t,\tau)}{\partial \Theta^i}d\Theta_t^i + \frac{1}{2}\sum_{i\in\Theta}\frac{\partial^2 B(t,\tau)}{\partial \Theta^{i2}}d\langle\Theta^i,\Theta^i\rangle_t, \tag{A.63}$$

where $\Theta = \{A, g, m\}$. Taking time t conditional expectation on both sides and using Equation (A.50) and (A.51) from above, we obtain that the expected infinitesimal bond risk premia is given by

$$RP(t,\tau) := \frac{1}{dt}\mathbb{E}_t\left[\frac{dB(t,\tau)}{B(t,\tau)} - R_t dt\right] = \frac{\eta_2-\eta_1}{\eta_2-1}\sigma_Y\left[b_A(\tau)\rho^{AY}\sigma_A + \sigma_g b_g(\tau)\rho^{gY}\right]g_t + b_m(\tau)\frac{\sigma_M\sigma_m\rho^{Mm}}{\eta_2-1}m_t, \tag{A.64}$$

which is after defining the nominal market price of risks the expression in Equation (2.37). The results for the log-utility agent can be easily derived by simply setting $\gamma = 0$ in Proposition (6). However, for verifying our results and to explain why we defined the market prices of government $\lambda_t^{N,Y}$ and monetary policy risk $\lambda_t^{N,M}$ as above, we derive both the nominal short rate, the market prices of risk and the term premium from a different angle using the stochastic discount factor approach. Recall that the real short rate can be obtained directly from the real stochastic discount factor which we denote by ζ_t^R. Its dynamics take the general form

$$d\zeta_t^R = \mu(\zeta^R, t)dt + \boldsymbol{\sigma}(\boldsymbol{\zeta^R, t})' d\boldsymbol{W}_t, \tag{A.65}$$

where $\mu(\cdot,\cdot)$ and $\boldsymbol{\sigma(\cdot,\cdot)}$ are $\mathcal{F}_t$-measurable bounded scalar drift and vector diffusion processes and $\boldsymbol{W}_t = (W_t^Y, W_t^M)$. In our setup, $\zeta_t^R = e^{-\rho t}U_C(X_t^*)$ from which, after an application of Itô's lemma we find

$$\frac{d\zeta_t^R}{\zeta_t^R} = -\left(\mu_Y + q_A A_t - \delta - \sigma_Y^2 g_t\right)dt - \sigma_y\sqrt{g_t}dW_t^Y, \tag{A.66}$$

from which we can read off the real short rate as $r_t = -\mu(\zeta^R, t)$ and the market price of the real productivity innovation risk by $\lambda_t^{R,\cdot} = \sigma_Y\sqrt{g}_t$. Following Veronesi & Jared (2000) or Piazzesi

& Schneider (2006), the dynamics of the nominal stochastic discount factor ζ_t^N are given by

$$-\frac{d\zeta_t^N}{\zeta_t^N} = \left\{ \frac{\mu_M + \beta(1-\eta_1) - \eta_1\bar{k} - \eta_2\bar{\pi} - (\eta_1-\eta_2)(\delta-\mu_Y)}{\eta_2 - 1} + \frac{q_A(\eta_1-\eta_2)}{1-\eta_2} A_t \right.$$
$$\left. -\frac{(\eta_1-\eta_2)^2\sigma_Y^2}{(\eta_2-1)^2} g_t - \frac{\sigma_M^2}{(\eta_2-1)^2} m_t \right\} dt + \frac{(\eta_1-\eta_2)\sigma_Y}{1-\eta_2}\sqrt{g_t} dW_t^Y + \frac{\sigma_M}{1-\eta_2}\sqrt{m_t} dW_t^M, \tag{A.67}$$

from which we deduce that $R_t = -\mu(\zeta^N, t)$. Similarly we have that the nominal market prices of risk is given by $\lambda_t^{N,\cdot} = -\boldsymbol{\sigma(\zeta^N, t)}$. Next, in order to determine the term premium on nominal bond yields under log-utility, we make use of the closed-form solution of the nominal bond price as given in Proposition 4, and the nominal short rate together with the associated market prices $\lambda_t^{N,Y}$ and $\lambda_t^{N,M}$ as in Proposition 6. An application of Itô's lemma to Equation (2.25) shows that the risk-neutral dynamics of the bond price equals to

$$\frac{dB(t,\tau)}{B(t,\tau)} = R_t dt - b_A(\tau)\sigma_A\sqrt{g_t}d\widetilde{W}_t^A - b_g(\tau)\sigma_g\sqrt{g_t}d\widetilde{W}_t^g - b_m(\tau)\sigma_m\sqrt{m_t}d\widetilde{W}_t^m, \tag{A.68}$$

where $\widetilde{W}_t^i,\ i \in \{A, g, m\}$ are $\mathcal{F}_t$-measurable Brownian innovation processes under the risk neutral measure $\mathbb{Q}$. According to Proposition 4, only government and nominal monetary policy risk are priced. We can decompose the Brownian innovations $\widetilde{W}_t^A$, $\widetilde{W}_t^g$ and $\widetilde{W}_t^m$ into two orthogonal complements as follows

$$\begin{aligned}
d\widetilde{W}_t^A &= \rho^{AY} d\widetilde{W}_t^Y + \sqrt{1-\rho^{AY\,2}} d\widehat{W}_t^A, \qquad d\widetilde{W}_t^Y d\widehat{W}_t^A = 0, \\
d\widetilde{W}_t^g &= \rho^{Yg} d\widetilde{W}_t^Y + \sqrt{1-\rho^{Yg\,2}} d\widehat{W}_t^g, \qquad d\widetilde{W}_t^Y d\widehat{W}_t^g = 0 \\
d\widetilde{W}_t^m &= \rho^{Mm} d\widetilde{W}_t^M + \sqrt{1-\rho^{Mm\,2}} d\widehat{W}_t^m, \qquad d\widehat{W}_t^M d\widehat{W}_t^Y = 0.
\end{aligned} \tag{A.69}$$

Hence, substituting the decomposed Brownian motions into Equation (A.68), the bond price dynamics are then given by

$$\begin{aligned}\frac{dB(t,\tau)}{B(t,\tau)} = R_t dt &- b_A(\tau)\sigma_A\sqrt{g_t}\left(\rho^{AY}d\widetilde{W}_t^Y + \sqrt{1-\rho^{AY\,2}}d\widehat{W}_t^A\right)\\ &- b_g(\tau)\sigma_g\sqrt{g_t}\left(\rho^{Yg}d\widetilde{W}_t^Y + \sqrt{1-\rho^{Yg\,2}}d\widehat{W}_t^g\right)\\ &- b_m(\tau)\sigma_m\sqrt{m_t}\left(\rho^{Mm}d\widetilde{W}_t^M + \sqrt{1-\rho^{Mm\,2}}d\widehat{W}_t^m\right).\end{aligned}$$

Next, in order to express the bond under the physical measure $\mathbb{P}$ we apply Girsanov's theorem to perform a measure change from $\mathbb{Q}$ to $\mathbb{P}$ as follows. We set the change of the drift equal to the market price of risk, in other words we have $d\widetilde{W}_t^Y = \lambda_t^{N,Y}dt + dW_t^Y$ and $d\widetilde{W}_t^M = \lambda_t^{N,M}dt + dW_t^M$. Then, given the correlation structure of the factors we obtain that the equilibrium term premium under the physical measure $\mathbb{P}$ is given by

$$\frac{1}{dt}\mathbb{E}_t\left[\frac{dB(t,\tau)}{B(t,\tau)} - R_t dt\right] = \lambda_t^{N,Y}\left[b_A(\tau)\rho^{AY}\sigma_A + \sigma_g b_g(\tau)\rho^{gY}\right]\sqrt{g_t} - b_m(\tau)\lambda_t^{N,M}\sqrt{m_t}. \quad \text{(A.70)}$$

A.6 Supplementary Tables

	EPU	GPU	MPU	1Y	2Y	3Y	5Y	7Y	10Y
EPU	1	0.857	0.657	-0.544	-0.542	-0.533	-0.500	-0.468	-0.425
GPU		1	0.572	-0.450	-0.444	-0.435	-0.401	-0.369	-0.324
MPU			1	-0.036	-0.037	-0.026	0.006	0.029	0.056
1Y				1	0.993	0.982	0.952	0.927	0.896
2Y					1	0.997	0.979	0.961	0.936
3Y						1	0.991	0.979	0.958
5Y							1	0.997	0.987
7Y								1	0.996
10Y									1.000

Table A.1: Sample correlation matrix of EPU, GPU and MPU index with nominal yields with $\tau=$ 1Y, 2Y, 3Y, 5Y, 7Y and 10Y using data from January 1990 until June 2014.

	EPU	GPU	MPU	1Y	2Y	3Y	5Y	7Y	10Y
EPU	1	0.8573	0.6573	0.6272	0.6611	0.664	0.6533	0.6254	0.6048
GPU		1	0.5724	0.4898	0.527	0.5211	0.5218	0.495	0.462
MPU			1	0.1081	0.1236	0.1451	0.1309	0.1175	0.1243
1Y				1	0.9406	0.9214	0.8784	0.8497	0.8261
2Y					1	0.9887	0.9644	0.9381	0.9067
3Y						1	0.9815	0.9595	0.9335
5Y							1	0.9935	0.9728
7Y								1	0.9877
10Y									1

Table A.2: Sample correlation matrix of EPU, GPU and MPU index with realized volatility as in Equation (2.41) with $\tau=$ 1Y, 2Y, 3Y, 5Y, 7Y and 10Y using data from January 1990 until June 2014.

	τ	1Y	2Y	3Y	5Y	7Y	10Y
Full regression	GPU	0.051	0.0558	0.05*	0.042**	0.032*	0.022**
	t_{GPU}	(2.89)	(5.36)	(5.37)	(8.22)	(8.03)	(7.46)
	R^2_{adj}	0.69	0.81	0.80	0.83	0.83	0.83
Full Regression	MPU	0.011	-0.012	0.011*	0.01**	0.007*	0.05**
	t_{MPU}	(1.11)	(1.49)	(1.67)	(1.961)	(1.91)	(1.961)
	R^2_{adj}	0.65	0.76	0.75	0.76	0.76	0.77

Table A.3: Summary of regression results: Table displays the slope coefficients of the regression of $\mathcal{V}_t[Y(t,\tau)]$ on MPU_t and GPU_t individually, plus the economic condition controls (EC), the financial variables (FV) plus macro factors (RA and IF) for τ=1Y, 2Y, 3Y, 5Y, 7Y, and 10Y. Values in brackets below represent HAC-robust $t-$statistics. R^2_{adj} refers to adjusted coefficient of determination. By ***, **, * we denote 1%, 5%, and 10% statistical significance, respectively.

A.7 Figures

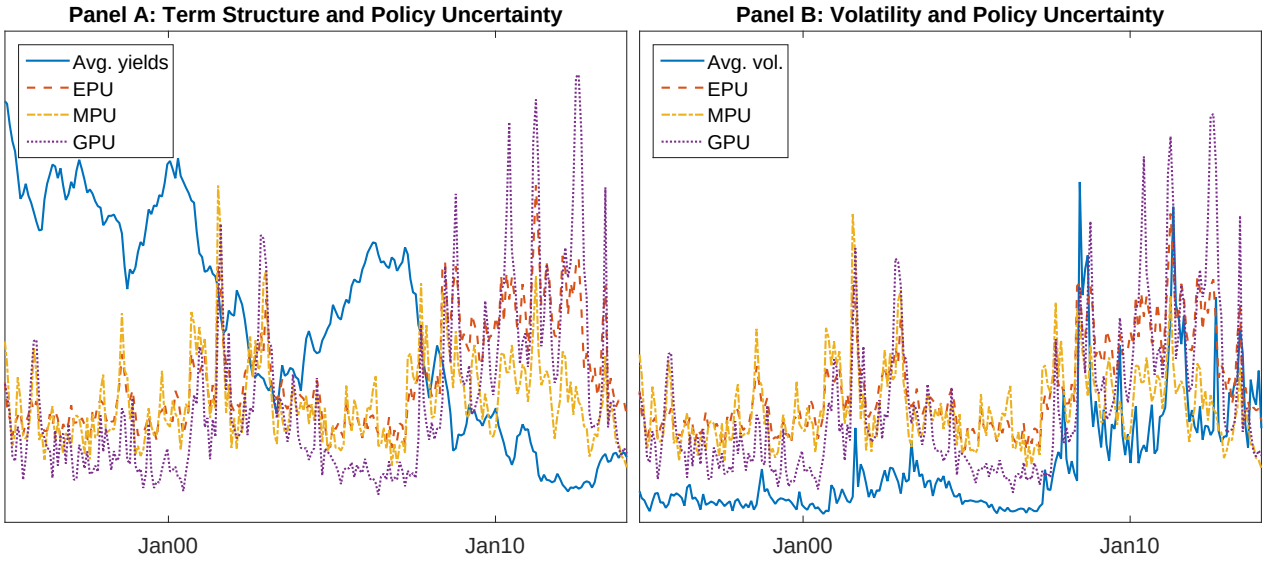

Figure A.1: US Treasury bond yields (Panel A) and realized yield volatility (Panel B) with maturity τ = 1Y, 2Y, 3Y, 5Y, 7Y and 10Y and the economic policy uncertainty (EPU) index as constructed by Baker et al. (2012) plus the government (GPU) and monetary policy (MPU) index. Sample period ranges from January 1990 until June 2014. All indexes are scaled to match the scale of the Treasury bond yields and volatilities.

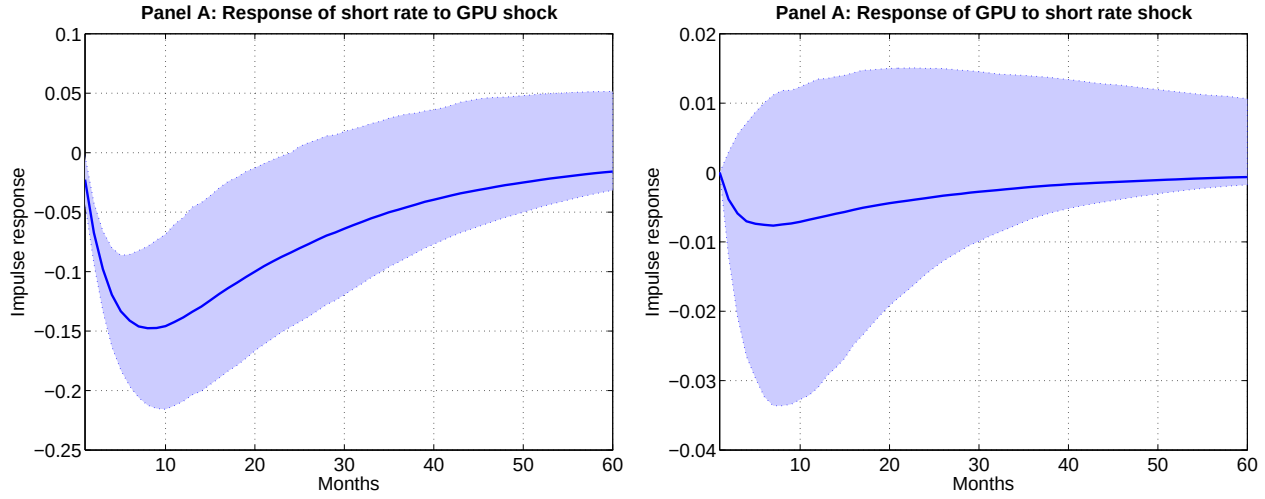

Figure A.2: The figure plots the impulse response functions of a shock to the GPU on the short rate (Panel A) and a shock to the short rate on the GPU (Panel B). The short rate is approximated by the three-month T-bill rate. The impulse response functions are based on a VAR model including the GPU, MPU, and the three-month T-bill rate. The data sample spans the period from January 1990 to June 2014. The shaded are corresponds to the 95% confidence interval.,

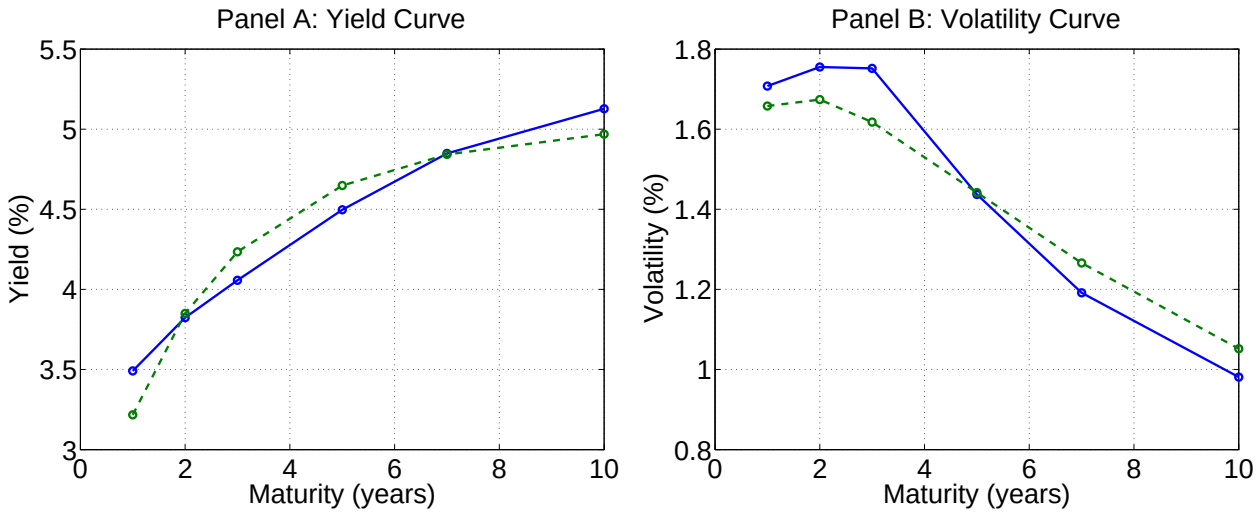

Figure A.3: Empirical and fitted affine yield curve model. In Panel A we plot the empirical unconditional nominal yield curve based on monthly zero-coupon bonds (solid line) with the model implied yield curve (dashed line). Panel B compares the model-implied bond volatility term-structure (dashed line) to the empirical unconditional realized volatility term structure (solid line). Unconditional realized volatility is computed using monthly log-yield changes as described in Equation (2.41) with maturities of one, two, three, five, seven and ten years. Parameter values are given in Table 2.1 and 2.2, respectively.

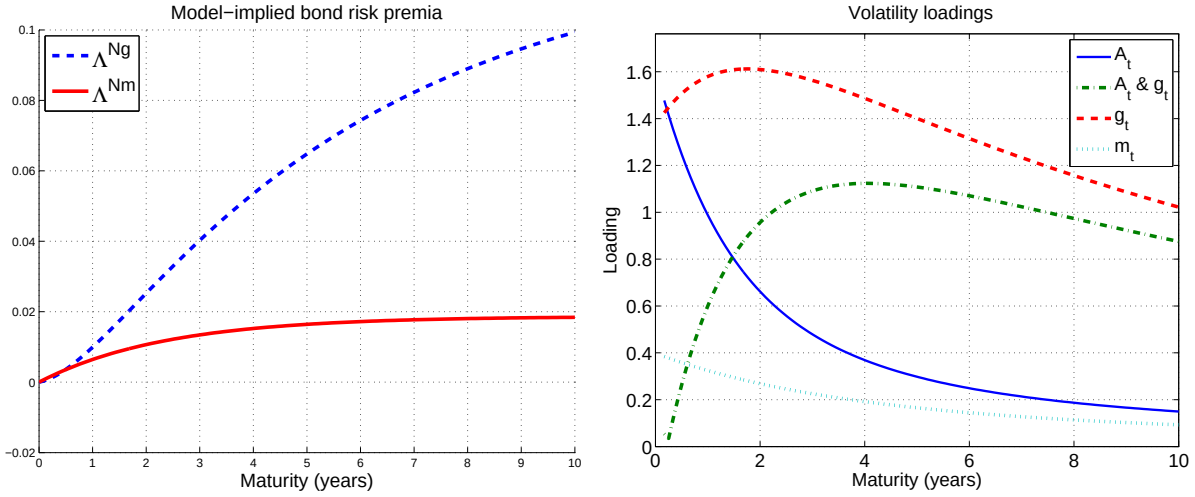

Figure A.4: Loadings for bond risk premia and bond volatility. Panel A shows the different loadings of the government (dashed line) and monetary (solid line) policy uncertainty factors in the bond risk premium in Equation (2.37). Panel B shows the different loadings to total yield variance $\mathbb{V}[Y(t,\tau)]$ in Equation (2.38) of the productivity factor variance $\mathbb{V}[A_t]$ (solid line), government policy uncertainty factor variance $\mathbb{V}[g_t]$ (dashed line), the cross term $\mathbb{C}[A_t, g_t]$ (dash-dotted line) and the monetary policy uncertainty factor variance $\mathbb{V}[m_t]$ (dotted line).

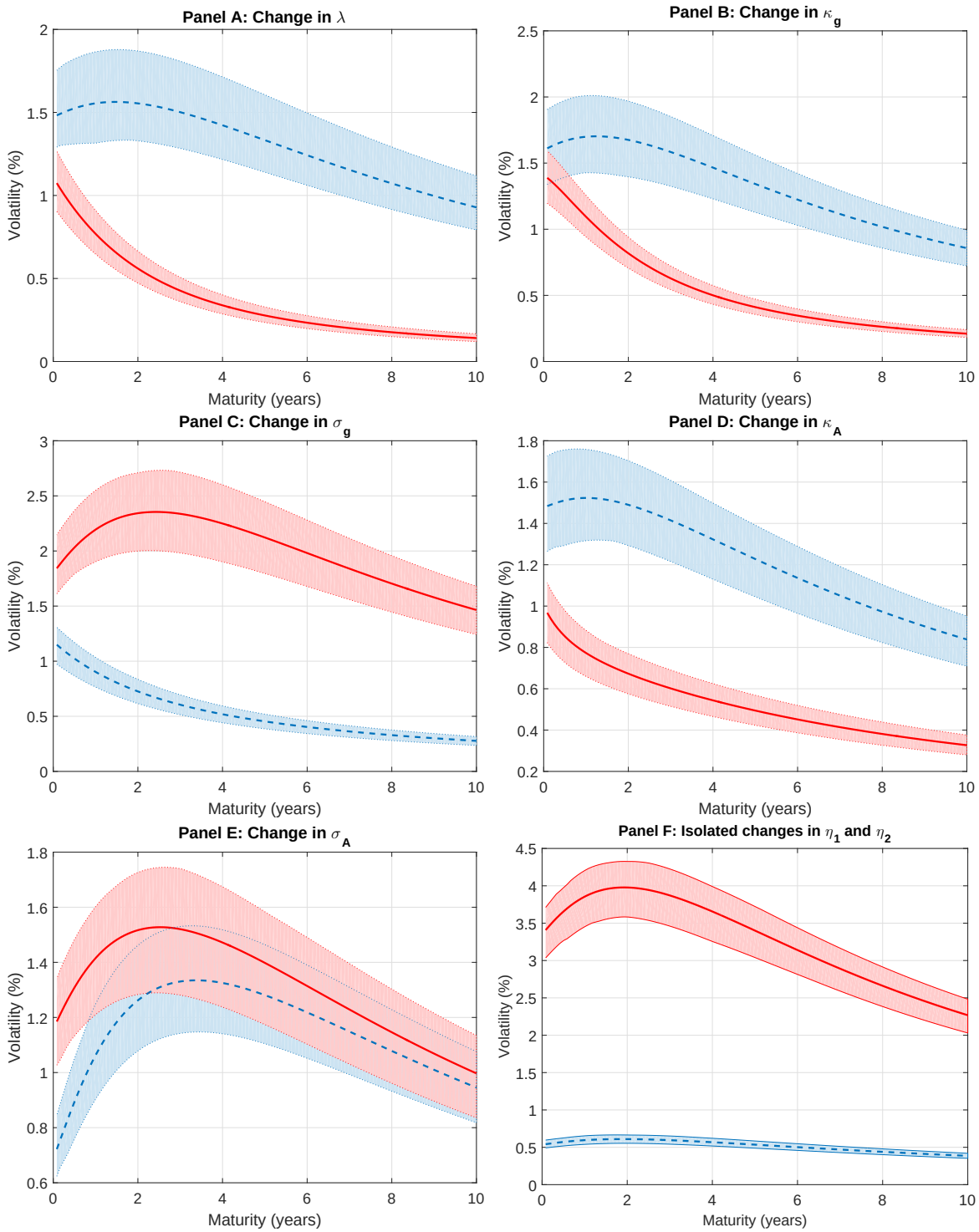

Figure A.5: Volatility curve sensitivities. In Panel A, we plot the volatility term structure for $\lambda = 0$ (solid line) and $\lambda = -1$ (dashed line). In Panel B, we increase κ_g from 0.3 (dashed line) to 3 (solid line) and in Panel C we increase σ_g from 0.05 (dashed line) to 0.5 (solid line). In Panel D, we plot the volatility curve for $\kappa_A = 0.75$ (dashed line) and $\kappa_A = 2.5$ (solid line) and Panel E shows the volatility curve for $\sigma_A = 0.15$ (dashed line) and $\sigma_A = 0.5$ (solid line). In Panel F, we analyze the impact of changing η_1 and η_2. The dashed (solid) line represents the case when we leave η_2 (η_1) unchanged while reducing η_1 (η_2) by 20%. All other parameters are as in Table 2.2. Shaded areas correspond to 95%-confidence bound of the estimated yield curves.

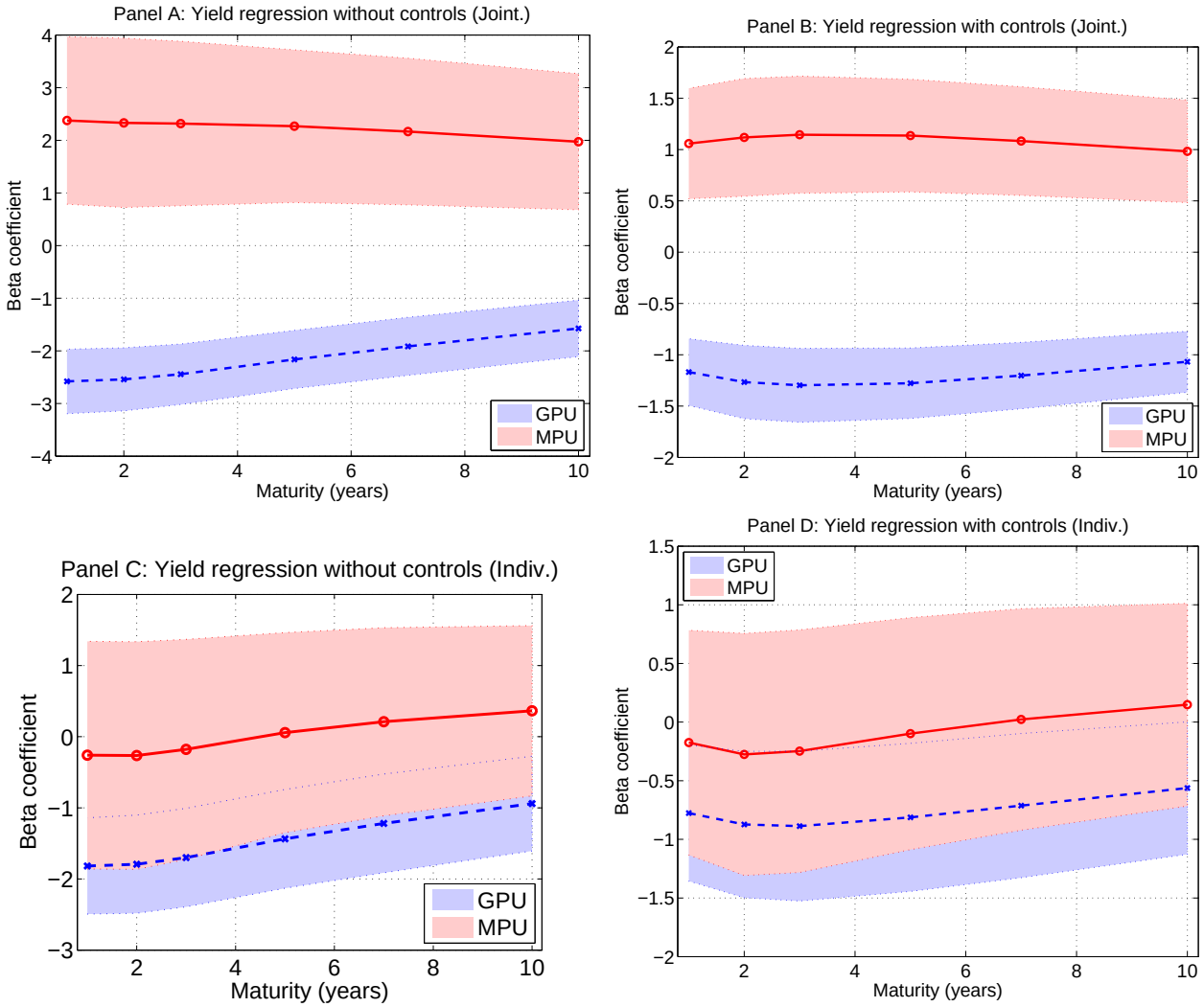

Figure A.6: Yield curve regressions. Panel A displays the slope coefficients of the *joint* regression of yields $Y(t,\tau)$ on both the GPU (dashed line) and MPU (full line). In Panel B, we regress *jointly* $Y(t,\tau)$ on the GPU (dashed line) and on the MPU (full line) including the controls EC, FV and MC. Similarly in Panel C we display the slope coefficients of the *individual* regression of $Y(t,\tau)$ on only the GPU (dashed line) and $Y(t,\tau)$ on only the MPU (full line). In Panel D, we regress *individually* $Y(t,\tau)$ on the GPU (dashed line) and $Y(t,\tau)$ on the MPU (full line) including the controls EC, FV and MC for each regression. The yield maturities are 1, 2, 3, 5, 7, and 10 years. Shaded areas represent HAC-robust 95% confidence bounds.

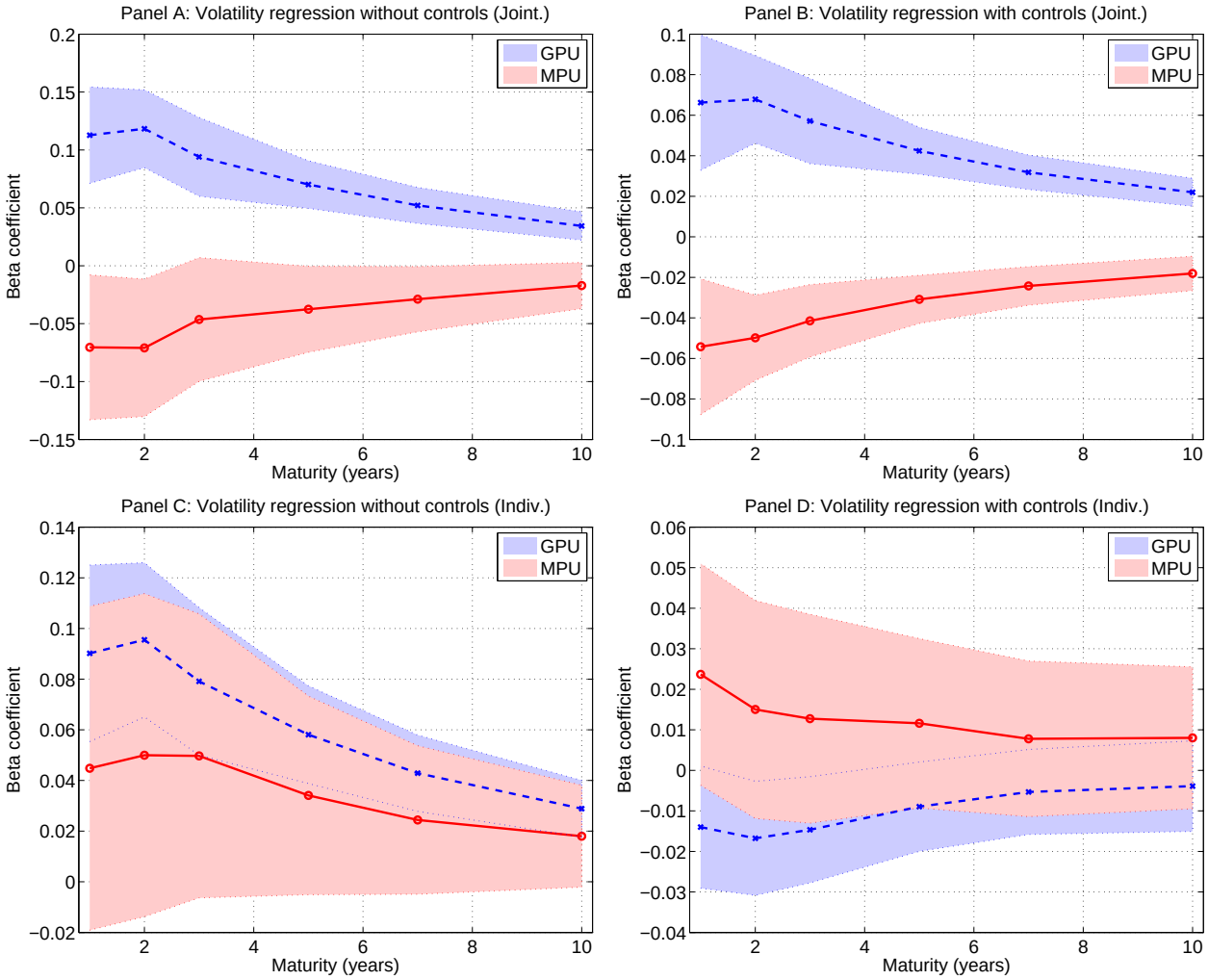

Figure A.7: Yield volatility curve regressions. Panel A displays the slope coefficients of the *joint* regression of yield volatility $\mathcal{V}_t[Y(t,\tau)]$ on both the GPU (dashed line) and MPU (full line). In Panel B, we regress *jointly* $\mathcal{V}_t[Y(t,\tau)]$ on both the GPU (dashed line) and on the MPU (full line) including the controls EC, FV (with TIV) and MC. Similarly in Panel C we display the slope coefficients of the *individual* regression of $\mathcal{V}_t[Y(t,\tau)]$ on only the GPU (dashed line) and $\mathcal{V}_t[Y(t,\tau)]$ on only the MPU (full line). In Panel D, we regress *individually* $\mathcal{V}_t[Y(t,\tau)]$ on the GPU (dashed line) and $\mathcal{V}_t[Y(t,\tau)]$ on the MPU (full line) including the controls EC, FV (with TIV) and MC for each regression. The yield maturities are 1, 2, 3, 5, 7, and 10 years. Shaded areas represent HAC-robust 95% confidence bounds.

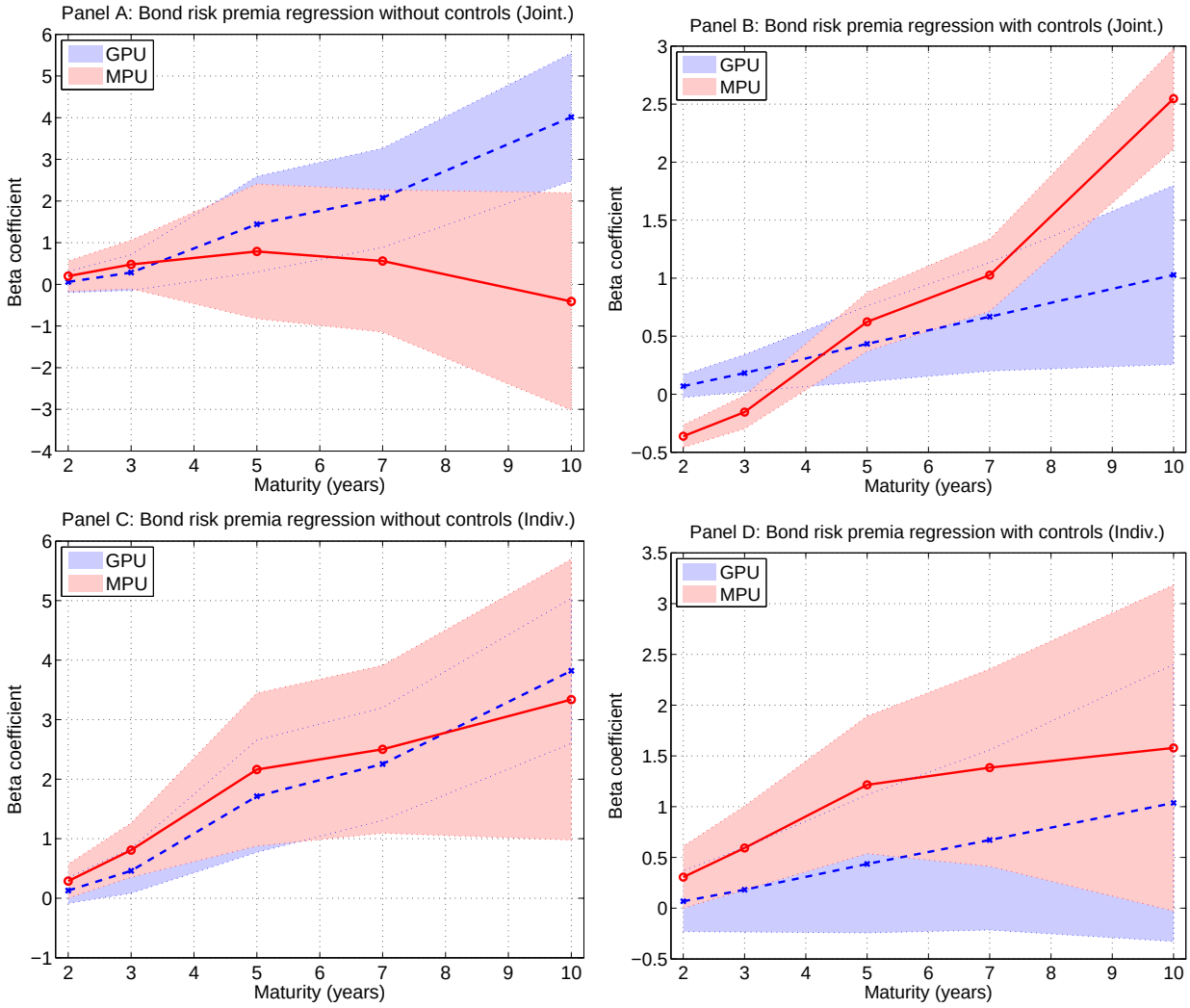

Figure A.8: Bond risk premium regressions. Panel A displays the slope coefficients of the *joint* regression of the monthly excess returns r_{t+1}^{E,τ_i} on both the GPU (dashed line) and MPU (full line). In Panel B, we regress *jointly* r_{t+1}^{E,τ_i} on both the GPU (dashed line) and on the MPU (full line) including the controls CP, PCA, EC, FV and MC for each regression. Similarly in Panel C we display the slope coefficients of the *individual* regression of the monthly excess returns r_{t+1}^{E,τ_i} on the GPU (dashed line) and the monthly excess returns r_{t+1}^{E,τ_i} on the MPU (full line). In Panel D, we regress *individually* the monthly excess returns r_{t+1}^{E,τ_i} on the GPU (dashed line) and the monthly excess returns r_{t+1}^{E,τ_i} on the MPU (full line) including the controls CP, PCA, EC, FV and MC for each regression. The yield maturities are 1, 2, 3, 5, 7, and 10 years. Shaded areas represent HAC-robust 95% confidence bounds.

Appendix B

Robust Portfolio Optimization with Jumps

B.1 Joint Drift and Jump Intensity Perturbation with CRRA Utility and Symmetric Jumps

In this section, we derive explicit portfolio weights when the risky asset follows an exponential Lévy process (no jump compensation) under the robust measure $\mathbb{P}^{\vartheta}$ of the form

$$\frac{dS_{1,t}}{S_{1,t_-}} = (r + R + \sigma h_t)dt + \sigma dB_t^{\vartheta} + JdY_t^{\vartheta},\ S_{1,0} > 0,\ \mathbb{P}^{\vartheta} - a.s.$$

and jumps follow a symmetric power law distribution as in (3.53). Then the corresponding Lagrangian reads

$$\begin{aligned}\mathcal{L}(\omega, h, a, \widetilde{\theta}^D, \widetilde{\theta}^I) = \omega R + \sigma h\omega - \omega\lambda J e^a - \omega^2\sigma^2 + \lambda e^a \log\left(1 + \omega_t J\right) \\ + \widetilde{\theta}^D\left(\frac{1}{2}h^2 - \eta^D\right) + \widetilde{\theta}^I\left(\lambda e^a(a-1) + \lambda - \eta^J\right).\end{aligned} \tag{B.1}$$

from which we obtain the following first order conditions

$$\widetilde{\theta}^{D*} = \pm\sqrt{\frac{\sigma^2\omega^2}{2\eta^D}} \rightarrow h_t^* = -\sqrt{2\eta^D} \tag{B.2}$$

$$\widetilde{\theta}^{J*} = \frac{-\log\left(1-J^2\omega^2\right)}{1+W\left(\frac{\eta^J-\lambda}{e\lambda}\right)} \rightarrow a^* = 1+W\left(\frac{\eta^J-\lambda}{e\lambda}\right) \tag{B.3}$$

Note that $\widetilde{\theta}^{J*}(\omega) \geq 0$ for any ω satisfying the solvency constraint $|\omega^* J| < 1$. Given the optimal perturbation parameters in (B.2) and (B.3), the objective function is

$$\begin{aligned}\mathcal{L}(\omega, h^*, a^*, \widetilde{\theta}^{D*}, \widetilde{\theta}^{J*}) = \omega R - \sigma\omega\sqrt{2\eta^D} - \omega^2\sigma^2 + \lambda e^{1+W\left(\frac{\eta^J-\lambda}{e\lambda}\right)}\log\left(1+\omega J\right) \\ + \lambda e^{1+W\left(\frac{\eta^J-\lambda}{e\lambda}\right)}\log\left(1-\omega J\right)\end{aligned} \tag{B.4}$$

and the first order condition for the optimal portfolio weight is

$$\begin{aligned}\frac{\mathcal{L}(\omega, h^*, a^*, \widetilde{\theta}^{D*}, \widetilde{\theta}^{J*})}{\partial\omega} = R - \sigma\sqrt{2\eta^D} - 2\omega\sigma^2 + \lambda e^{1+W\left(\frac{\eta^J-\lambda}{e\lambda}\right)} J/(1+\omega J) \\ - \lambda e^{1+W\left(\frac{\eta^J-\lambda}{e\lambda}\right)} J/(1-\omega J) = 0.\end{aligned} \tag{B.5}$$

So (B.5) is a cubic polynomial in the portfolio weights ω. Let

$$\begin{aligned} A = 2J^2\sigma^2, \qquad & B^{DJ} = J^2(\sqrt{2\eta^D}\sigma - R) \\ C^{DJ} = -2\left(\sigma^2 + J^2\lambda e^{1+W\left(\frac{\eta^J-\lambda}{e\lambda}\right)}\right), \qquad & D^{DJ} = R - \sqrt{2\eta^D}\sigma \end{aligned}$$

Then (B.5 can be written as $Ax^3 + Bx^2 + Cx + D$. Defining $a^{DJ} = B^{DJ}/A$, $b^{DI} = C^{DJ}/A$, $c^{DJ} = D^{DJ}/A$ and $G^{DJ} = ({a^{DJ}}^2 - 3b^{DJ})/9$, $H^{DJ} = (2{a^{DJ}}^2 - 9a^{DJ}b^{DJ} + 27c^{DJ})/54$ the solution to (B.5 subject to the solvency condition $|J\omega| < 1$ is given by

$$\omega^* = -2\sqrt{G^{DJ}}\cos\left(\text{acos}\left(\frac{1}{3}H^{DJ}/\sqrt{G^{DJ}} - \frac{2\pi}{3}\right)\right) - a^{DJ}/3 \tag{B.6}$$

B.2 Exponential Utility: Closed - form portfolio weights with compensated exponential Lévy dynamics

In this section we consider an investor with exponential utility of the form

$$U(C) = -\frac{1}{q}e^{-qC}, \text{ with CARA coefficient } q > 0$$

where his wealth dynamics under the robust measure evolves as in (3.14), that is no jump size perturbation. We analyze robust optimal portfolio holdings where the jumps sizes follow an exponential distribution, i. e. $Z_n \overset{i.i.d}{\sim} \text{Exp}(\xi)$, with $\nu(dz) = f_Z(z;\xi) = \xi e^{-z\xi},\ z \geq 0$. Then conjecturing a solution to (3.23) of the form $L(x) = -K/qe^{-rqx}$ where are $r > 0$ is the risk free rate in (3.1) and K some constant to be determined, we have

$$\frac{\partial L(x)}{\partial x} = -rqL(x),\ \frac{\partial^2 L(x)}{\partial x^2} = r^2q^2L(x) \tag{B.7}$$

The robust control problem in (3.23) is then given by

$$\begin{aligned} 0 = \max_{\{C_t,\omega_t\}} \min_{\{h_t\},a} & U(C_t) - \beta L(X_t) - rqL(X_t)\left[X_t\left(r + \omega_t\left(R + \sigma h_t - \lambda e^a J\int z\nu(dz)\right)\right) - C_t\right] \\ & + \frac{1}{2}r^2q^2L(X_t)\omega_t^2X_t^2\sigma^2 + \lambda e^a\int\left[e^{-rqX_{t_-}\omega_{t_-}Jz}L(X_{t_-}) - L(X_{t_-})\right]\nu(dz) \end{aligned} \tag{B.8}$$

subject to

$$\frac{1}{2}h_t^2 \leq \eta^D,\ \lambda e^a(a-1) + \lambda \leq \eta^D,\ \eta^D \geq 0,\ \eta^J \geq 0 \tag{B.9}$$

We fix $J = (-1, 0)$, so that jumps are negative. Dividing (B.8) above by $-rqL(X_t) > 0$ we obtain

$$\begin{aligned} 0 = \max_{\{C_t,\omega_t\}} \min_{\{h_t\},a} & -\frac{U(C_t)}{rqL(X_t)} + \frac{\beta}{qr} + X_t\left(r + \omega_t\left(R + \sigma h_t + \lambda e^a\int z\nu(dz)\right)\right) - C_t \\ & - \frac{1}{2}rq\omega_t^2X_t^2\sigma^2 - \frac{\lambda e^a}{rq}\int\left[e^{-rqwz} - 1\right]\nu(dz) \end{aligned} \tag{B.10}$$

subject to

$$\frac{1}{2}h_t^2 \leq \eta^D,\ \lambda e^a(a-1) + \lambda \leq \eta^J,\ \eta^D \geq 0,\ \eta^J \geq 0 \tag{B.11}$$

We define as $\mathcal{L} = \mathcal{L}(C_t, h_t, a, \widetilde{\theta}^D, \widetilde{\theta}^J)$ the Lagrangian corresponding to the perturbed HJB problem in (B.8) with Lagrange multiplier $\widetilde{\theta}^D$ and $\widetilde{\theta}^J$ for the diffusive and jump intensity part of the entropy constraint respectively. Then we have[1]

$$\begin{aligned}\mathcal{L}(C_t, w, h_t, a, \widetilde{\theta}^D, \widetilde{\theta}^J) = &-\frac{U(C_t)}{rqL(X_t)} + w\left(R + \sigma h_t + \lambda e^a \int z\nu(dz)\right) - C_t - \frac{1}{2}rqw^2\sigma^2 \\ &- \frac{\lambda e^a}{rq}\int \left[e^{-rqwz} - 1\right]\nu(dz) + \theta^D\left(\frac{1}{2}h_t^2 - \eta^D\right) + \theta^J\left(\lambda e^a(a-1) + \lambda - \eta^J\right)\end{aligned} \tag{B.12}$$

where $w = \omega_t X_t$ is the (absolute) amount of money invested into the risky asset. Given the optimal perturbation parameters, the objective function is

$$\begin{aligned}\mathcal{L}(C_t, w, h^*, a^*, \widetilde{\theta}^{D*}, \widetilde{\theta}^{I*}) = &-\frac{U(C_t)}{rqL(X_t)} + \frac{\beta}{qr} + X_t\left(r + \omega_t\left(R + h^*\sigma + \lambda e^{a^*}\int z\nu(dz)\right)\right) - C_t \\ &- \frac{1}{2}qr\sigma^2w^2 - \frac{\lambda e^a}{rq}\int \left[e^{-rqwz} - 1\right]\nu(dz)\end{aligned} \tag{B.13}$$

Then optimal consumption given (B.13) is

$$C_t^* = rX_t - \frac{1}{q}\ln(rK) \tag{B.14}$$

Furthermore, in order to determine the constant we evaluate (B.13) and use optimal consumption C_t^* from above and the optimal robust portfolio holdings $w(h^*, a^*)$. Then the constant satisfies,

$$K = \frac{1}{r}\exp\left\{1 - \frac{\beta}{r} - w\left(R + h^*\sigma + J\lambda e^{a^*}\int z\nu(dz)\right) + \frac{1}{2}rq^2w^2\sigma^2 + \frac{\lambda e^{a^*}}{rq}\int \left[e^{-rqwz} - 1\right]\nu(dz)\right\}$$

Then, assuming that the jump sizes are exponentially distributed with parameter ξ, we obtain that the Lagrangian satisfies

$$\begin{aligned}\mathcal{L}(C_t, w, h^*, a^*, \widetilde{\theta}^{D*}, \widetilde{\theta}^{I*}) = &-\frac{U(C_t)}{rqL(X_t)} + \frac{\beta}{qr} + X_t\left(r + \omega_t\left(R + h^*\sigma + \frac{\lambda e^a}{\xi}\right)\right) - C_t \\ &- \frac{1}{2}qr\sigma^2w^2 - \frac{\lambda e^a w}{\xi - qrw}\end{aligned} \tag{B.15}$$

[1]The integral with respect to the jump measure in B.10 is only convergent if $\xi - qrw > 0$ which is very likely to be satisfied given standard parameter values for risk aversion $q \in \{1, \ldots, 10\}$, $r \in [0, 0.05]$ and $\xi > 10$ which would correspond to a jump size of 10% or less.

As before, it follows that $h_t^* = h^* = -\sqrt{2\eta^D}$, $\widetilde{\theta}^D = \sqrt{\frac{\sigma^2\omega^2}{2\eta^D}}$ and $a^* = 1 + W\left(\frac{\eta^J-\lambda}{e\lambda}\right)$, $\widetilde{\theta}^J = \frac{qrw^2}{\xi\left(1+W\left(\frac{\eta^J-\lambda}{e\lambda}\right)\right)(\xi-qrw)} \geq 0, \forall w \in \mathbb{R}$. Then, the first order condition for the optimal portfolio weight w is

$$-\lambda\frac{e^{1+W\left(\frac{\eta^J-\lambda}{e\lambda}\right)}qrw}{(\xi-qrw)^2} + \frac{\lambda e^{1+W\left(\frac{\eta^J-\lambda}{e\lambda}\right)}}{\xi} - \frac{\lambda e^{1+W\left(\frac{\eta^J-\lambda}{e\lambda}\right)}}{\xi-qrw} - \sqrt{2\eta^D}\sigma - qr\sigma^2 w + R = 0 \qquad \text{(B.16)}$$

which is a cubic polynomial in the amount invested in the risky asset. Let

$$A(\xi) = -\xi q^3 r^3 \sigma^2, \qquad B^{DJ}(\xi) = q^2 r^2\left(\lambda e^{1+W\left(\frac{\eta^J-\lambda}{e\lambda}\right)} + \xi\left(R - \sqrt{2\eta^D}J\sigma + 2\xi\sigma^2\right)\right),$$

$$C^{DJ}(\xi) = -\xi qr\left(2e^{1+W\left(\frac{\eta^J-\lambda}{e\lambda}\right)}\lambda + \xi\left(2(R-\sqrt{2\eta^D}\sigma) + \xi\sigma^2\right)\right), \qquad D^{DJ}(\xi) = \xi^3\left(\sqrt{2\eta^D}\sigma - R\right)$$

Then (B.16) can be written as $A(\xi)x^3 + B^{DI}(\xi)x^2 + C^{DI}(\xi)x + D^{DI}(\xi)$. Next, we define $a^{DI}(\xi) = B^{DI}(\xi)/A(\xi)$, $b^{DI}(\xi) = C^{DI(\xi)}/A(\xi)$, $c^{DI}(\xi) = D^{DI}(\xi)/A(\xi)$ and $G^{DI}(\xi) = \left(a^{DI}(\xi)^2 - 3b^{DI}(\xi)\right)/9$, $H^{DI}(\xi) = \left(2a^{DI}(\xi)^2 - 9a^{DI}(\xi)b^{DI}(\xi) + 27c^{DI}(\xi)\right)/54$ such that the solution to (B.16) subject to the integral convergence condition $\xi - qrw > 0$ is given by

$$w_E^* = -2\sqrt{G^{DJ}(\xi)}\cos\left(\text{acos}\left(\frac{1}{3}H^{DJ}(\xi)/\sqrt{G^{DJ}(\xi)} - \frac{2\pi}{3}\right)\right) - a^{DJ}(\xi)/3$$

where w_E^* refers to both drift and jump intensity compensated portfolio weights when the investor is assumed to have exponential utility. In Figure (B.5) we plot the portfolio weights for different levels of jump sizes ξ. [Figure B.5 about here]

A first important observation from Panel A to D is that increasing the size of the jumps ($\xi \downarrow$) reduces the absolute amount invested into the risky asset w_E^* as $\mathbb{E}^{\vartheta}[z] = \mathbb{E}[z] = 1/\xi$. A tenfold increase in the coefficient of risk aversion (q) leads to a proportional decrease in w_E^*. On the other hand, increasing the frequency of jumps (λ) by a factor of ten, shows that the optimal investment into the risky asset decreases over-proportionally.

B.3 Simulating Power Law Distributed Jump Sizes

The power law measure defined in (3.53) is not a proper probability density function as it does not integrate to one. Moreover, for simulating the jump sizes we have to truncate the support of the power law to the closed interval $[\epsilon, 1]$, where $\epsilon > 0$ but close to zero.[2] To see why, let the Lévy measure be defined as $\nu^\epsilon(z) = \frac{1}{z}\mathbb{I}_{\epsilon \leq x \leq 1}$ with normalizing constant

$$\lambda^\epsilon = \int_\epsilon^1 \nu^\epsilon(z)dz = \log\left(\frac{1}{\epsilon}\right)$$

from which it immediately follows that $\lambda^\epsilon \to \infty$ as $\epsilon \to 0$. Then the jump size density is

$$f_Z^\epsilon(z) = \frac{\nu^\epsilon(z)}{\lambda^\epsilon}, \quad z \in [\epsilon, 1] \tag{B.17}$$

which by construction satisfies $\int_\epsilon^1 f_Z^\epsilon(z)dz = 1$. In order to simulate random power law distributed draws from (B.17) we apply the inverse transform method. The truncated cumulative distribution function is

$$F_Z^\epsilon(z) = \int_\epsilon^z f_Z^\epsilon(u)du = \frac{\log\left(\frac{z}{\epsilon}\right)}{\log\left(\frac{1}{\epsilon}\right)} \tag{B.18}$$

Then, let U be uniformly distributed, i.e. $U \sim U[0, 1]$, we invert (B.18) by solving

$$u = F_Z^\epsilon(z) \leftrightarrow z = \epsilon e^{u\log\left(\frac{1}{\epsilon}\right)} = F_Z^{\epsilon\,-1}(z) \tag{B.19}$$

Therefore, we obtain random samples of Z by generating uniformly distributed random variables U on (0,1) and apply (B.19) above.

B.4 Proof Monotonicity of optimal portfolio weights with respect to uncertainty

In this section, we show that the derivative of the optimal portfolio weights with respect to η is strictly negative for any $\eta \in (0, \infty)$. Let $f'(\eta) := \frac{\partial \omega^*}{\partial \eta}$ denote the partial derivative of

[2] For our simulation, we set $\epsilon = 10^{-4}$.

the optimal portfolio weights with respect to uncertainty where $\eta \in (0, \widetilde{\eta})$ and $\widetilde{\eta}$ is some finite positive constant. Applying the mean value theorem, we have

$$f^{'}(\eta) = \frac{f^{'}(\widetilde{\eta}) - f^{'}(0)}{\widetilde{\eta}} = \frac{-1}{4J\sigma^2\widetilde{\eta}} \left[J^2\lambda \left(e^{1+W\left(\frac{\widetilde{\eta}^J - \lambda}{e\lambda}\right)} - 1 \right) + J\sqrt{2\widetilde{\eta}^D}\sigma - H(\widetilde{\eta}) + H(0) \right] \quad \text{(B.20)}$$

In order to proof that the optimal portfolio weights are monotonically declining in uncertainty, we need to show that $f^{'}(\eta) < 0, \ \forall \ \eta \in (0, \widetilde{\eta})$. In other words, using (B.20) we have to verify the following inequality

$$H(\widetilde{\eta}) - J\sqrt{2\widetilde{\eta}^D}\sigma > J^2\lambda \left(e^{1+W\left(\frac{\widetilde{\eta}^J - \lambda}{e\lambda}\right)} - 1 \right) + H(0) \quad \text{(B.21)}$$

Since both sides of (B.21) are strictly positive we can square them and obtain

$$\begin{aligned} 0 < H(0)J^2\lambda \left(e^{1+W\left(\frac{\widetilde{\eta}^J - \lambda}{e\lambda}\right)} - 1 \right) - J\sqrt{2\widetilde{\eta}^D}\sigma H(\widetilde{\eta}) - \lambda^2 J^2 \left(e^{1+W\left(\frac{\widetilde{\eta}^J - \lambda}{e\lambda}\right)} - 1 \right)^2 \\ + 2J^2\widetilde{\eta}^D\sigma + 8\lambda J^2\sigma^2 \left(1 + e^{1+W\left(\frac{\widetilde{\eta}^J - \lambda}{e\lambda}\right)} \right) + h_2^2(\widetilde{\eta}) \end{aligned} \quad \text{(B.22)}$$

The only negative term in (B.22) is

$$-\left(e^{1+W\left(\frac{\widetilde{\eta}^J - \lambda}{e\lambda}\right)} - 1 \right)^2 = -e^{2\left(1+W\left(\frac{\widetilde{\eta}^J - \lambda}{e\lambda}\right)\right)} + 2e^{1+W\left(\frac{\widetilde{\eta}^J - \lambda}{e\lambda}\right)} - 1 \quad \text{(B.23)}$$

Because $e^{1+W\left(\frac{\widetilde{\eta}^J - \lambda}{e\lambda}\right)} > 1, \ \forall \widetilde{\eta} > 0$, only the first term in (B.23) is negative. Recalling that $h_2^2(\widetilde{\eta})$ contains the same term, i.e. $e^{2\left(1+W\left(\frac{\widetilde{\eta}^J - \lambda}{e\lambda}\right)\right)}$ but with positive sign immediately implies that the inequality in (B.22) has to hold and therefore shows that the partial derivative of the optimal portfolio weights with respect to uncertainty is indeed negative, i.e. is monotonically declining in η.

	r	R	σ	J	λ	β	γ	ζ^D	Jump Dist.	Freq.	T_d	T_h	$\bar{\pi}$
Benchmark	0.01	0.05	0.2	-0.10	1	0.01	2	10%	Power Law	Daily	1	1	10%
Alternative	0.02	0.07	0.3	-0.15	5	0.03	3	50%	Uniform	ID	3	10	20%

Table B.1: Benchmark parameter values for Monte Carlo simulations

Notes: ζ^D refers to the percentage of total maximal amount of robustness η which is allocated to drift perturbation. T_d refers to the time series length in years used to quantify the maximal amount of robustness η, whereas T_h refers to the investment horizon (in years). ID stands for intra day returns where we sample the data every $m = 60$ min. Number of simulation runs is $M = 10'000$ and initial wealth X_0 as well as stock price S_0 are equal to 100.

Daily Data									
	Weights	Ref. M.	Rank Ref.	Rob. M.	Rank Rob.	Drift	Jump Int.	h^*	a^*
w_M^*	0.625	1.012	2	1.077	4	5.00	-	-	-
w_{rM}^*	0.217	1.168	4	1.075	3	1.77	-	16.2	-
w_{JD}^*	0.552	1.000	1	1.031	2	6.09	1	-	-
w_{rJD}^*	0.431	1.015	3	1.000	1	5.23	1.159	5.16	14.74
Intra Day Data									
	Weights	Ref. M.	Rank Ref.	Rob. M.	Rank Rob.	Drift	Jump Int.	h^*	a^*
w_M^*	0.625	1.012	4	1.030	4	5.00	-	-	-
w_{rM}^*	0.459	1.008	3	1.001	2	3.68	-	6.59	-
w_{JD}^*	0.552	1.000	1	1.006	3	6.09	1	-	-
w_{rJD}^*	0.502	1.001	2	1.000	1	5.74	1.063	2.09	6.16

Table B.2: Monte Carlo simulation results

Notes: The time series length for daily sampled data is $T_d \times 252 = 252$, whereas for intra daily sampled data, the time series length is $= T_d \times 252 \times 6,5 \times 60/m = 1'512$ where $m = 60$ min denotes hourly sampling frequency. The column 'Weights' refers to the optimal portfolio holdings, where w_M^* denote the Merton, w_{rM}^* the robust Merton, w_{JD}^* the jump diffusive and w_{rJD}^* robust jump diffusive weights, respectively. Columns 'Ref. M.' and 'Rob. M.' show the expected utility ratio as defined in (3.76) and (3.77), respectively. The columns 'Rank Ref.' and 'Rank Rob.' rank expected utility using the four portfolio allocations. The column 'Drift' represents the expected return in percent where the Merton drift is R, the robust Merton drift is $R-h^*\sigma$ where $h^* = \sqrt{2\eta^D}$ with $\eta^D = \eta$, the jump diffusive drift is $R+((1-\epsilon)/\log(1/\epsilon))\, J\lambda$ and the robust jump diffusive drift is $R - h^*\sigma + ((1-\epsilon)/\log(1/\epsilon))\, J\lambda e^{a^*}$. The column 'Jump Int.' compares the jump intensities λ (reference measure) and λ^ϑ (robust measure). The column 'h^*' shows the optimal drift perturbation in percent for the robust Merton solution with $h^* = \sqrt{2\eta^D}$ where $\eta^D = \eta$ and for the robust jump diffusive solution with $h^* = \sqrt{2\eta^D}$. The last column 'a^*' shows the optimal jump intensity perturbation $a^* = 1 + W\left(\left(\eta^J - \lambda\right)/(e\lambda)\right)$ in percent for the robust jump diffusive solution.

	Risk Free Rate $r = 0.02$			Excess Return $R = 0.07$			Volatility $\sigma = 0.3$		
	Weights	Ref. M.	Rob. M.	Weights	Ref. M.	Rob. M.	Weights	Ref. M.	Rob. M.
w^*_M	0.5	1.006	1.051	0.875	1.027	1.099	0.278	1.002	1.043
w^*_{rM}	0.092	1.162	1.073	0.467	1.078	1.030	0.006	1.312	1.145
w^*_{JD}	0.442	1.000	1.023	0.771	1.000	1.031	0.263	1.000	1.031
w^*_{rJD}	0.323	1.014	1.000	0.646	1.004	1.000	0.18	1.025	1.000
	Jump Scaling $J = 0.05$			Jump Intensity $\lambda = 5$			Impatience Rate $\beta = 0.03$		
	Weights	Ref. M.	Rob. M.	Weights	Ref. M.	Rob. M.	Weights	Ref. M.	Rob. M.
w^*_M	0.625	1.002	1.033	0.625	1.220	1.510	0.625	1.009	1.048
w^*_{rM}	0.217	1.215	1.106	0.219	1.048	1.010	0.217	1.096	1.041
w^*_{JD}	0.605	1.000	1.025	0.379	1.000	1.029	0.552	1.000	1.020
w^*_{rJD}	0.478	1.019	1.000	0.294	1.008	1.000	0.431	1.008	1.000
	Risk Aversion $\gamma = 3$			$\zeta^D = 50\%$			Jump Size Dist. $U(0,1)$		
	Weights	Ref. M.	Rob. M.	Weights	Ref. M.	Rob. M.	Weights	Ref. M.	Rob. M.
w^*_M	0.417	1.018	1.136	0.625	1.012	1.284	0.625	1.003	1.05
w^*_{rM}	0.144	1.341	1.145	0.219	1.166	1.010	0.217	1.195	0.139
w^*_{JD}	0.368	1.000	1.052	0.552	1.000	1.157	0.574	1.000	1.024
w^*_{rJD}	0.287	1.032	1.000	0.295	1.089	1.000	0.45	1.020	1.000
	Sampling Length $T_d = 3$			Invest. Horizon T_h			Error Detect. Prob. $\bar{\pi} = 20\%$		
	Weights	Ref. M.	Rob. M.	Weights	Ref. M.	Rob. M.	Weights	Ref. M.	Rob. M.
w^*_M	0.625	1.012	1.040	0.625	1.011	1.046	0.625	1.011	1.046
w^*_{rM}	0.39	1.030	1.010	0.375	1.047	1.017	0.374	1.047	1.017
w^*_{JD}	0.552	1.000	1.011	0.552	1.000	1.014	0.552	1.000	1.014
w^*_{rJD}	0.482	1.003	1.000	0.475	1.005	1.000	0.472	1.005	1.000

Table B.3: Comparative statics

Notes: Unless stated otherwise, the parameter values are those from Table B.1. The column 'Weights' refers to the optimal portfolio holdings, where w^*_M denote the Merton, w^*_{rM} the robust Merton, w^*_{JD} the jump diffusive and w^*_{rJD} robust jump diffusive weights, respectively. Columns 'Ref. M.' and 'Rob. M.' show the expected utility ratio as defined in (3.76) and (3.77), respectively. Number of simulation runs is $M = 10'000$ and initial wealth X_0 as well as stock price S_0 are equal to 100. For all the simulation runs, we generate daily sample paths of the stock price.

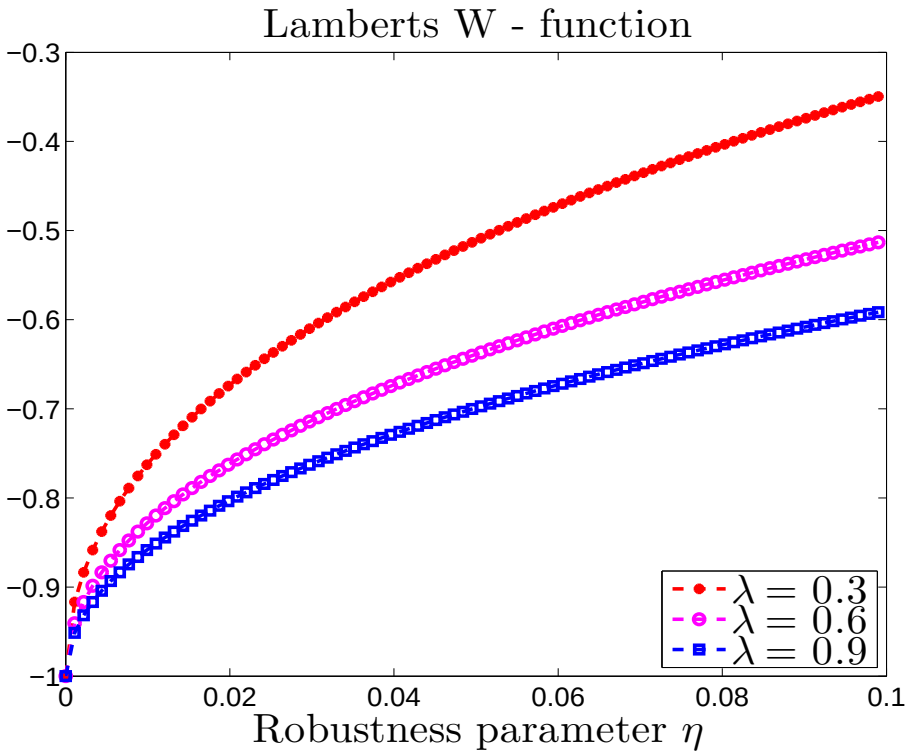

Figure B.1: Lambert's W-Function for various levels of jump intensities λ.

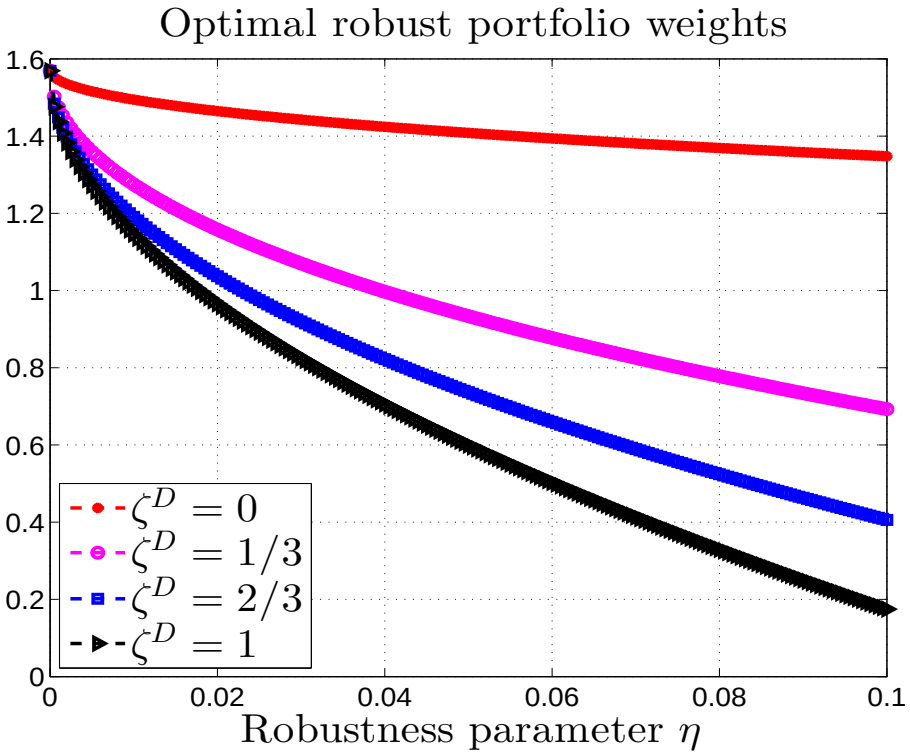

Figure B.2: Comparison of optimal robust portfolio weights

Notes: The optimal robust portfolio weights aere as given in (3.52) for $\zeta^D \in \{0, 1/3, 2/3, 1\}$. The selected parameters values are: $R = 0.1$, $\sigma = 0.1$, $J = -0.3$, $\lambda = 1$, $\gamma = 2$, jump size distribution is given in (3.43) and $\eta \in [0, 0.05]$.

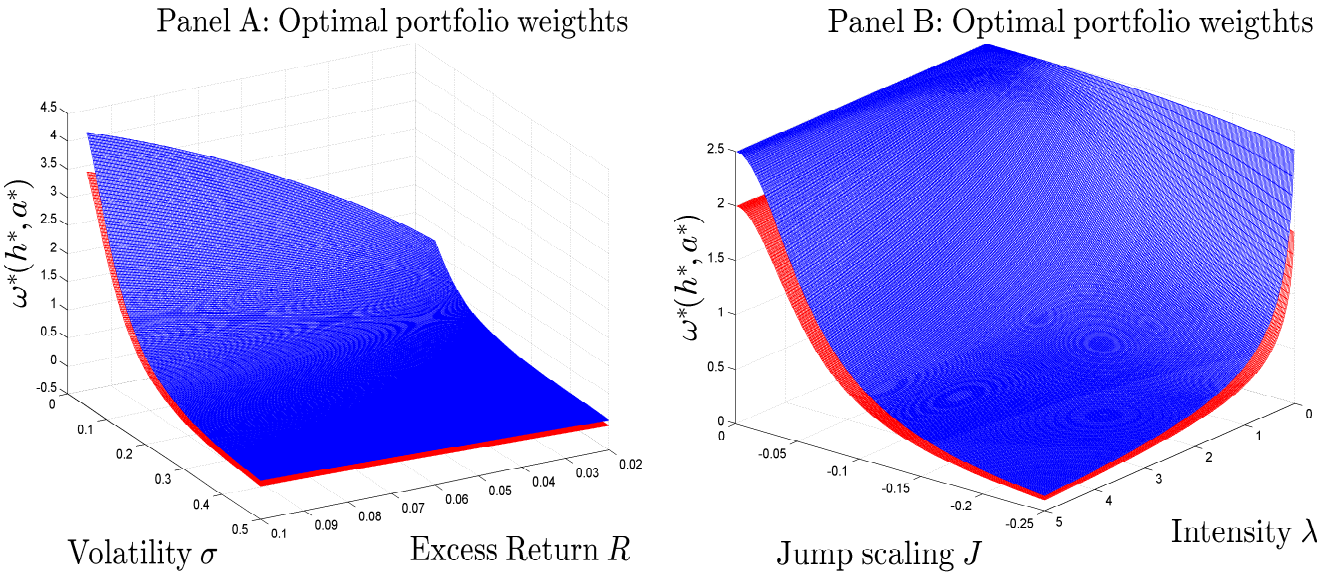

Figure B.3: Comparison of robust and non-robust portfolio allocations when both drift and jump intensity are perturbed

Notes: Panel A displays the optimal robust jump - diffusive weights $\omega^*(h^*, a^*)$ (in red) and the optimal jump diffusive weights $\omega^*(h^* = 0, a^* = 0)$ (in blue) when both the expected return R and the volatility σ vary. Panel B displays optimal robust jump - diffusive weights $\omega^*(h^*, a^*)$ (in red) and optimal jump diffusive weights $\omega^*(h^* = 0, a^* = 0)$ (in blue) when both the jump scaling parameter J and the intensity λ vary. Unless stated otherwise, the selected parameters values are: $R = 0.05$, $\sigma = 0.1$, $J = -0.1$, $\lambda = 1$, $\gamma = 2$, $\zeta^D = 0.1$, jump size distribution is given in (3.43) and $\eta = 0.05$.

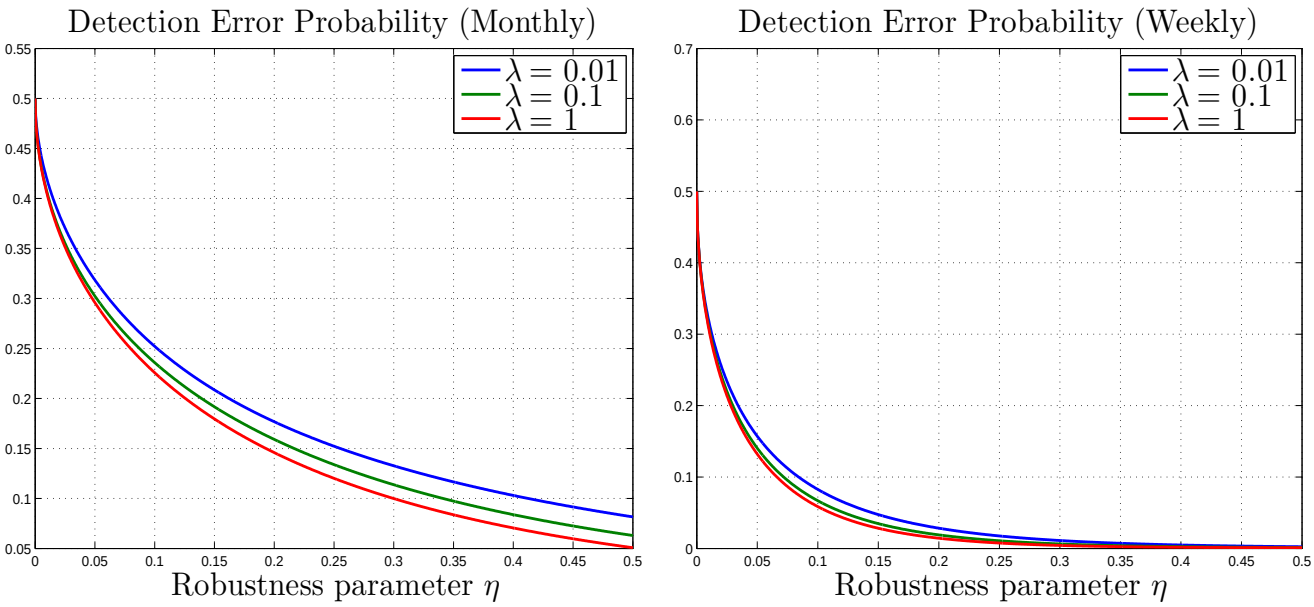

Figure B.4: Error-detection probability $\pi(t, T; \eta)$ computed from a time series length of 1 year

Notes: The left figure plots $\pi(t, T; \eta)$ using weekly data (52 observations) and the right figure plots $\pi(t, T; \eta)$ using monthly data (12 observations). The selected parameters values are: $\sigma = 0.2$ and $\widehat{\eta}^D = 10\%$.

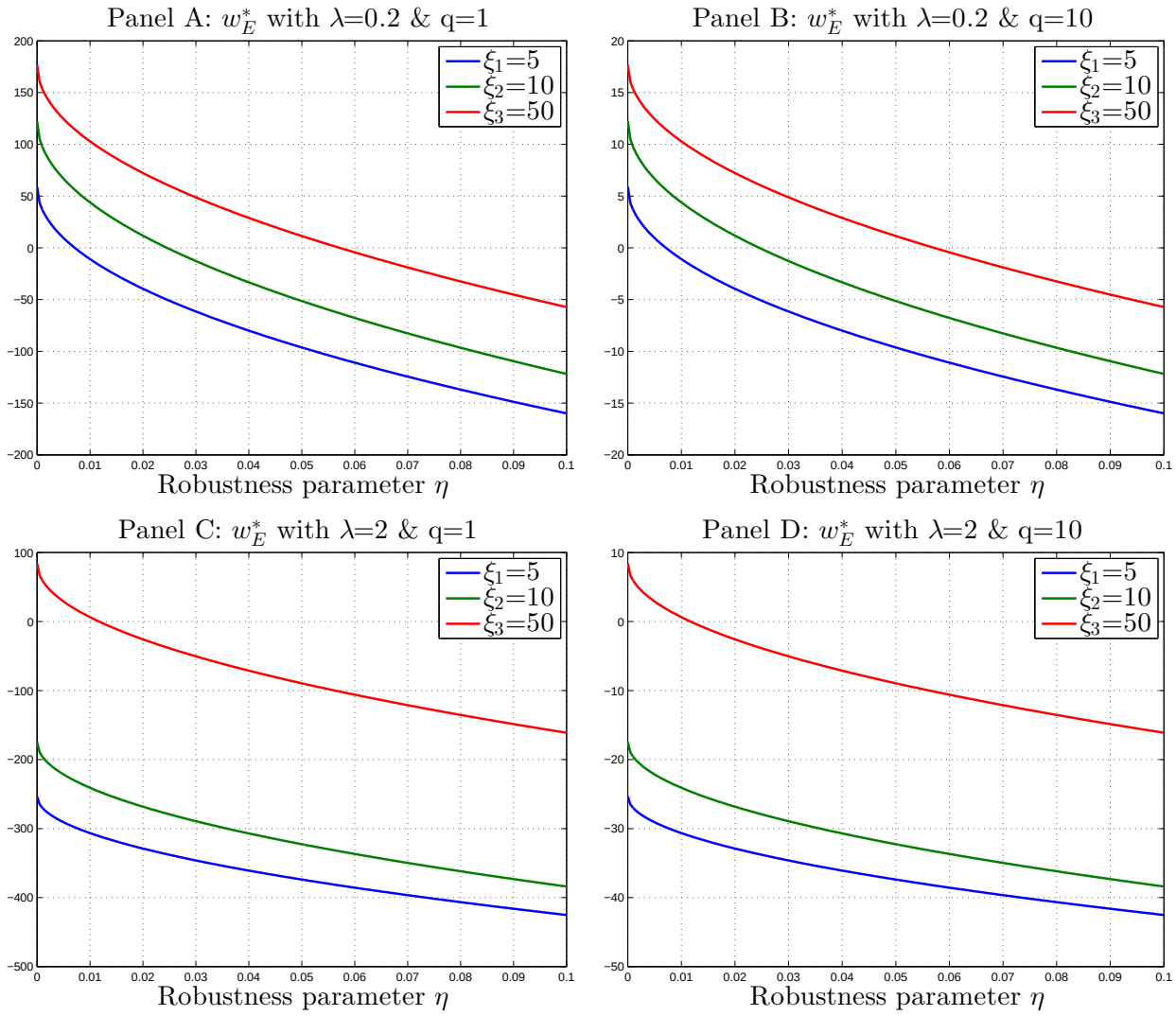

Figure B.5: Optimal portfolio holdings in the case of exponential utility when the underlying risky asset exhibits compensated Lévy dynamics and both drift and jump intensity are perturbed

Notes: The compensated Lévy dynamics are as given in (3.3). The benchmark parameters values are: $R = 0.1$, $\sigma = 0.2$, $J = 0.2$, $\lambda = 0.2, 2$, $q = 1, 10$ and $\eta \in [0, 0.1]$.

Appendix C

Proof of results

C.1 Proof of Proposition 8

The proof relies on Theorem 2.28 in Jacod & Shiryaev (2003) and Theorem 2.2.14 and Theorem 2.2.15 in Jacod & Protter (2012). However, we first need the following lemma on the decomposition of discrete-time Markov chains.

Lemma 2. *Given the continuous time Markov chain $r(t)$ with generator $\mathcal{Q}$ given in equation* (4.3)*, the transition probability matrix $\mathbb{P}_{ij}(\Delta_m)$ of the discrete Markov chain r_{Δ_m} can be constructed as follows*

$$\mathbb{P}(\Delta_m) = \mathbb{I} + \Delta_m \mathcal{Q} + o(\Delta_m), \tag{C.1}$$

where $\mathbb{I}$ is the N dimensional identity matrix.

Proof. By the Chapman-Kolmogorov equation (see, e.g., Lawler (1995), Karlin & Taylor (1981), and Norris (1998)), the transition probability matrix is differentiable. A Taylor expansion at $t_{k,m} = 0$ gives

$$\mathbb{P}(\Delta_m) = \mathbb{P}(0) + \mathbb{P}^{'}(0)\Delta_m + o(\Delta_m) \tag{C.2}$$

For the first term note that

$$\mathbb{P}_{ij}(0) = \delta_{ij} = \begin{cases} 1, & \text{for } i = j \\ 0, & \text{for } i \neq j, \end{cases} \tag{C.3}$$

and for the second term we have

$$\mathbb{P}^{'}(0) = \lim_{\Delta_m \to 0} \frac{\mathbb{P}(\Delta_m) - \mathbb{I}}{\Delta_m}. \tag{C.4}$$

A closer look at the off-diagonal elements shows that

$$\mathbb{P}^{'}_{ij}(0) = \lim_{\Delta_m \to 0} \frac{\mathbb{P}_{ij}(\Delta_m)}{\Delta_m} = \lim_{\Delta_m \to 0} \frac{\mathbb{P}_{ij}(r_{t+\Delta_m} = i | r_t = j)}{\Delta_m}. \tag{C.5}$$

These probabilities describe the transitional dynamics, the rate at which a transition is made from state j to state i. For the diagonal elements we obtain

$$\begin{aligned}
\mathbb{P}^{'}_{jj}(0) &= \lim_{\Delta_m \to 0} \frac{\mathbb{P}(\Delta_m) - 1}{\Delta_m} = \lim_{\Delta_m \to 0} \frac{\mathbb{P}(r(t+\Delta_m) = i | r(t) = i)}{\Delta_m} \\
&= - \lim_{\Delta_m \to 0} \frac{\mathbb{P}(r(t+\Delta_m) \neq i | r(t) = i)}{\Delta_m} \\
&= - \lim_{\Delta_m \to 0} \sum_{i,j \, \in \, \mathcal{M}} \frac{\mathbb{P}(r(t+\Delta_m) = j | r(t) = i)}{\Delta_m} \\
&= - \sum_{i,j \, \in \, \mathcal{M}} q_{ij},
\end{aligned}$$

where the last equality, i.e., the interchange of summation and the limit, follows from the finiteness of the state space $\mathcal{M}$ and the limit follows from the Chapman-Kolmogorov equation.

□

To proceed we define the piecewise constant interpolated processes via

$$\left.\begin{aligned}
&p_{\Delta_m}(t) = p_k \\
&r_{\Delta_m}(t) = r_k \\
&W_{\Delta_m}(t) = \textstyle\sum_{k=1}^{\lfloor t/\Delta_m \rfloor} \Delta u_{k,m}
\end{aligned}\right\} t \in [t_k, t_k + \Delta_m). \tag{C.6}$$

Then, we have the following result on the weak convergence of the Markov chain and the Brownian motion.

Lemma 3. *Given the interpolated processes in* (C.6) *we have*

1. $r_{\Delta_m}(\cdot) \xrightarrow{D} r(\cdot)$, *i.e. the discrete time Markov Chain* $r_{k,m}$ *converges weakly (in distribution D) to* $r(\cdot)$ *the Markov Chain with generator* $\mathcal{Q}$.

2. $W_{\Delta_m}(\cdot) \xrightarrow{D} W(\cdot)$, *i.e. the discrete time Brownian Motion* $W_{\Delta_m}(t)$ *converges weakly to a standard Brownian Motion.*

Proof. The proof of the first assertion follows directly by an application of Lemma 3.1 in Yin & Zhou (2004). The second assertion follows by Donsker's Theorem (see, e.g., Billingsley (2008)). □

Now, the first statement of Proposition 8 follows from an application of Lemma 3, since

$$\lim_{m\to\infty} \Delta_m^{1/2} \sum_{k=1}^{\lfloor mt \rfloor} \sigma_{r_{k,m}} u_{k,m} \overset{D}{=} \int_a^b \sigma_{r_u} dW_u. \tag{C.7}$$

Hence, both the discrete-time Markov chain and the sum of i.i.d. normally distributed random variables converge weakly to the continuous-time Markov chain and Brownian motion, respectively. Next, statement (4.16) follows immediately from the law of iterated expectations:

$$\Delta_m^{1/2}\mathbb{E}\left[\sum_{k=1}^{\lfloor mt \rfloor} \sigma_{r_{k,m}} u_{k,m}\right] = \Delta_m^{1/2}\mathbb{E}\left[\sum_{k=1}^{\lfloor mt \rfloor} \sigma_{r_{k,m}} \mathbb{E}\left[u_{k,m} | \mathcal{F}_{k-1,m}, \mathcal{F}_{r_{k,m}}\right]\right] = 0.$$

Note that unconditionally, $y_{k,m}$ are independent but not identically distributed since their variance can take N different regimes. Therefore, to show that the series converges we need a slight generalization of the central limit theorem, the Lindeberg-Feller Theorem (see, e.g., Jacod & Shiryaev (2003)). Then, the third statement can be shown if the Lindeberg condition is satisfied, which states for every $\epsilon > 0$, if

$$\forall \epsilon > 0, \ \lim_{m\to\infty} \Delta_m^{1/2}\mathbb{E} \sum_{k=1}^{\lfloor mt \rfloor} \left[y_{k,m}^2 \mathbb{I}_{\{y_{k,m} > \epsilon\}}\right] = 0. \tag{C.8}$$

Applying the tower property of conditional expectations and since $\sigma_{r_{k,m}}$ is a constant given $r_{k,m}$, then by integration by parts and using the conditional symmetry of the Gaussian distribution

we obtain

$$0 = \lim_{m\to\infty} \Delta_m \mathbb{E}\left[\sum_{k=1}^{\lfloor mt\rfloor} \sigma^2_{r_{k,m}} \mathbb{E}\left[u^2_{k,m}\mathbb{I}_{\left\{u_{k,m}>\epsilon/\Delta_m^{1/2}\sigma_{r_{k,m}}\right\}}|\mathcal{F}_{k-1,m},\mathcal{F}_{r_{k,m}}\right]\right]$$
$$= \lim_{m\to\infty} \Delta_m \sum_{k=1}^{\lfloor mt\rfloor} \sigma^2_{r_{k,m}}\left(1-\Phi\left(\frac{\epsilon}{\sigma^2_{r_{k,m}}\Delta_m^{1/2}}\right)+\phi\left(\frac{\epsilon}{\Delta_m^{1/2}\sigma^2_{r_{k,m}}}\right)\frac{\epsilon}{\sigma^2_{r_{k,m}}\Delta_m^{1/2}}\right), \tag{C.9}$$

where the second term in (C.9) can be shown to converge to zero by an application of l'hÃ´pitals rule and $\Phi(\cdot)$ and $\phi(\cdot)$ denote the standard normal cumulative and density function respectively. Therefore, we can conclude that $\sum_{k=1}^{\lfloor mt\rfloor}\mathbb{E}\left[\tilde{y}^2_{k,m}\middle|\,\mathcal{F}_{k-1,m},\mathcal{F}_{r_{k,m}}\right]<\infty$. Next, by the law of iterated expectations, we obtain

$$\mathbb{E}\left[\mathbb{E}\left[\Delta_m\sum_{k=1}^{\lfloor mt\rfloor}\sigma^2_{r_{k,m}}\,u^2_{k,m}\middle|\,\mathcal{F}_{k-1,m},\mathcal{F}_{r_{k,m}}\right]\right] = \mathbb{E}\left[\Delta_m\sum_{k=1}^{\lfloor mt\rfloor}\sigma^2_{r_{k,m}}\right]. \tag{C.10}$$

Applying dominated convergence, we have

$$\lim_{m\to\infty}\Delta_m\mathbb{E}\left[\sum_{k=1}^{\lfloor mt\rfloor}\sigma^2_{r_{k,m}}\right] = \mathbb{E}\left[\lim_{m\to\infty}\Delta_m\sum_{k=1}^{\lfloor mt\rfloor}\sigma^2_{r_{k,m}}\right] = \mathbb{E}\left[\int_a^b \sigma^2_{r_u}du\right]. \tag{C.11}$$

Concerning the last statement, using that the random variables are normally distributed we have

$$\Delta_m^{p/2}\mathbb{E}\left[\sum_{k=1}^{\lfloor mt\rfloor}|\sigma_{r_{k,m}}u_{k,m}|^p\right] = \frac{1}{m^{p/2}}\sum_{k=1}^{\lfloor mt\rfloor}\mathbb{E}\left[\sigma^p_{r_{k,m}}\mathbb{E}\left[|u_{k,m}|^p|\mathcal{F}_{k-1,m},\mathcal{F}_{r_{k,m}}\right]\right]$$
$$= \frac{2^{p/2}\Gamma\left(\frac{1+p}{2}\right)}{\sqrt{\pi}}\left(\frac{(T-t_0)}{m}\right)^{p/2}\mathbb{E}\left[\sum_{k=1}^{\lfloor mt\rfloor}\sigma^p_{r_{k,m}}\right]. \tag{C.12}$$

Therefore, for $p>2$,

$$\left(\frac{(T-t_0)}{m}\right)^{p/2}\mathbb{E}\left[\sum_{k=1}^{\lfloor mt\rfloor}|\sigma_{r_{k,m}}u_{k,m}|^p\right]\xrightarrow{D}0, \tag{C.13}$$

when $m\to\infty$. ■

C.2 Proof of Proposition 9

Since the state variable controlling the regime and the regression disturbance are correlated we may write the variance-covariance matrix as follows

$$\begin{bmatrix} \eta_{k,m} \\ u_{k,m} \end{bmatrix} = A \begin{bmatrix} \eta_{k,m} \\ \omega_{k,m} \end{bmatrix} \tag{C.14}$$

where $\omega_{k,m} \overset{i.i.d}{\sim} \mathcal{N}(0,1)$, $u_{k,m} \sim \mathcal{N}(0,1)$ $\omega_{k,m} \perp \eta_{k,m}$ where the symbol $\perp$ stochastic independence between random variables and A is the Cholesky decomposition of Σ so that $AA' = \Sigma$. Therefore, we can write

$$u_{k,m} = \rho\eta_{k,m} + \sqrt{1-\rho^2}\omega_{k,m}. \tag{C.15}$$

Applying Bayes' rule yields

$$\begin{aligned} \mathbb{E}\left[u_{k,m} | a_{i-1,j}(\Delta_m) \leq \eta_{k,m} \leq a_{i,j}(\Delta_m)\right] &= \frac{\mathbb{E}\left[u_{k,m}; a_{i-1,j}(\Delta_m) \leq \eta_{k,m} \leq a_{i,j}(\Delta_m)\right]}{\mathbb{E}\left[\mathbb{I}_{\{a_{i-1,j}(\Delta_m) \leq \eta_{k,m} \leq a_{i,j}(\Delta_m)\}}\right]} \\ &= \frac{\mathbb{E}\left[u_{k,m}; a_{i-1,j}(\Delta_m) \leq \eta_{k,m} \leq a_{i,j}(\Delta_m)\right]}{\mathbb{P}_{i,j}(\Delta_m) - \mathbb{P}_{i-1,j}(\Delta_m)}, \end{aligned} \tag{C.16}$$

where $\mathbb{P}_{i,j} = \Phi(a_{i-1,j}(\Delta_m))$. Using (C.15) and the independence of $u_{k,m}$ and $\omega_{k,m}$, the numerator in (C.16) is

$$\mathbb{E}\left[u_{k,m}; a_{i-1,j}(\Delta_m) \leq \eta_{k,m} \leq a_{i,j}(\Delta_m)\right] = \mathbb{E}\left[\rho\eta_{k,m} + \sqrt{1-\rho^2}\omega_{k,m}; a_{i-1,j}(\Delta_m) \leq \eta_{k,m} \leq a_{i,j}(\Delta_m)\right]$$

$$\begin{aligned} &= \int_{a_{i-1,j}(\Delta_m)}^{a_{i,j}(\Delta_m)} \int_{\mathbb{R}} \left(\eta_{k,m} + \sqrt{1-\rho^2}\omega_{k,m}\right) f_{\eta_{k,m},\Omega_{k,m}}(\eta_{k,m}, \omega_{k,m}) d\omega_{k,m} d\eta_{k,m} \\ &= \rho \int_{a_{i-1,j}(\Delta_m)}^{a_{i,j}(\Delta_m)} \eta_{k,m}\phi(\eta_{k,m}) d\eta_{k,m} \int_{\mathbb{R}} \phi(\omega_{k,m}) d\omega_{k,m} \\ &+ \sqrt{1-\rho^2} \int_{a_{i-1,j}(\Delta_m)}^{a_{i,j}(\Delta_m)} \phi(\eta_{k,m}) d\eta_{k,m} \int_{\mathbb{R}} \phi(\omega_{k,m})\omega_{k,m} d\omega_{k,m} \\ &= -\rho \frac{\phi(a_{i,j}(\Delta_m)) - \phi(a_{i-1,j}(\Delta_m))}{\mathbb{P}_{i,j}(\Delta_m) - \mathbb{P}_{i-1,j}(\Delta_m)}. \end{aligned}$$

Therefore we obtain for the first statement

$$-\Delta_m^{1/2}\sum_{k=1}^{\lfloor mt\rfloor}\left[\sigma_{r_{k,m}}\rho\frac{\phi(a_{i,j}(\Delta_m))-\phi(a_{i-1,j}(\Delta_m))}{\mathbb{P}_{i,j}(\Delta_m)-\mathbb{P}_{i-1,j}(\Delta_m)}\right], \tag{C.17}$$

which is a standard Riemann sum and thus we have

$$-\Delta_m^{1/2}\sum_{k=1}^{\lfloor mt\rfloor}\left[\sigma_{r_{k,m}}\rho\frac{\phi(a_{i,j}(\Delta_m))-\phi(a_{i-1,j}(\Delta_m))}{\mathbb{P}_{i,j}(\Delta_m)-\mathbb{P}_{i-1,j}(\Delta_m)}\right]\xrightarrow{D}-\rho\int_{t_0}^{T}\frac{\phi(a_{i,j}(u))-\phi(a_{i-1,j}(u))}{\mathbb{P}_{i,j}(u)-\mathbb{P}_{i-1,j}(u)}\sigma_{r_u}du. \tag{C.18}$$

By a similar argument using $u_{k,m}^2=(\rho\eta_{k,m}+\sqrt{1-\rho^2}\omega_{k,m})^2$ we obtain

$$\begin{aligned}&\Delta_m\sum_{k=1}^{\lfloor mt\rfloor}\left[\sigma_{r_{k,m}}\left(1+\rho^2\frac{\phi(a_{i-1,j}(\Delta_m))a_{i-1,j}(\Delta_m)-\phi(a_{i,j}(\Delta_m))a_{i,j}(\Delta_m)}{\mathbb{P}_{i,j}(\Delta_m)-\mathbb{P}_{i-1,j}(\Delta_m)}\right)\right]\\&\xrightarrow{D}\int_{t_0}^{T}\left(1+\rho^2\frac{\phi(a_{i-1,j}(u))a_{i-1,j}(u)-\phi(a_{i,j}(u))a_{i,j}(u)}{\mathbb{P}_{i,j}(u)-\mathbb{P}_{i-1,j}(u)}\right)\sigma_{r_u}du,\end{aligned} \tag{C.19}$$

which proofs the second claim. For the last statement, note that the distribution of the error is now skewed normal, i.e. $u_{k,m}\overset{i.i.d}{\sim}\mathcal{SN}(0,1,\rho)$ where $\mathcal{SN}(\mu,\sigma,\cdot)$ is the location-scale skew-normal with centrality parameter μ, scale parameter σ and skewness parameter ρ. For p a positive integer the even moments of $u_{k,m}$ are equivalent to $\omega_{k,m}^2$ for which the statement follows directly from the previous theorem. For $p=2l+1$ where $l\geq 0$ the odd incomplete moments can be explicitly derived as shown in Chiogna (1998) and are given by

$$\mathbb{E}\left[|u_{k,m}|^{2l+1}|\mathcal{F}_{k-1,m},\mathcal{F}_{r_{k,m}}\right]=C(\phi,\mathbb{P}_{ij},\rho)\left\{\sqrt{\frac{2}{\pi}}l!2^{l+1}-2\sqrt{\frac{2}{\pi}}l!\left[\frac{\frac{\rho}{\sqrt{1+\rho^2}}(2l+1)!!}{(1+\rho^2)^l}\sum_{h=0}^{l}\frac{2^{h-1}\rho^{2h}}{(2h+1)!!(l-h)!}\right]\right\}, \tag{C.20}$$

where $(2l+1)!!=1\times 3\times 5\cdots\times(2l+1)$ and $C(\phi,\mathbb{P},\rho)$ is some constant depending on the distribution function ϕ, the transition probability $\mathbb{P}_{ij}$, and the endogeneity parameter ρ. Thus

$$\frac{C(\phi,\mathbb{P}_{ij},\rho)}{m^{p/2}}\sum_{k=1}^{m}|\sigma_{r_{k,m}}|^p\left\{\sqrt{\frac{2}{\pi}}l!2^{l+1}-2\sqrt{\frac{2}{\pi}}l!\left[\frac{\frac{\rho}{\sqrt{1+\rho^2}}(2l+1)!!}{(1+\rho^2)^l}\sum_{h=0}^{l}\frac{2^{h-1}\rho^{2h}}{(2h+1)!!(l-h)!}\right]\right\}\xrightarrow{D}0. \tag{C.21}$$

■

C.3 Proof of Proposition 10

Since the $\tilde{y}_{k,m}^2$ are uncorrelated for $r_{k,m} = i$, we can write

$$\begin{aligned}\mathbb{V}\left[RV_m|\mathcal{F}_{k-1,m}, r_{k,m} = i, r_{k-1,m} = j\right] &= \sum_{k=1}^{m} \mathbb{V}\left[\tilde{y}_{k,m}^2|\mathcal{F}_{k-1,m}, r_{k,m} = i, r_{k-1,m} = j\right] \\ &= \sum_{k=1}^{m} \left\{\mathbb{E}\left[\sigma_{k,m}^4 u_{k,m}^4|\mathcal{F}_{k-1,m}, r_{k,m} = i, r_{k-1,m} = j\right]\right. \\ &\quad \left. - \left(\mathbb{E}\left[\sigma_{r_{k,m}}^2 u_{k,m}^2|\mathcal{F}_{k-1,m}, r_{k,m} = i, r_{k-1,m} = j\right]\right)^2\right\} \quad \text{(C.22)}\end{aligned}$$

Using similar arguments as in the proof of Proposition 9, the first term can be obtained by setting $u_{k,m}^4 = (\rho\eta_{k,m} + \sqrt{1-\rho^2}\omega_{k,m})^4$ and the second term in (C.22) is given in equation (4.20) from which the variance expression for $r_{k,m} = i$ for $i = 1, 2$ follows directly.

C.4 Proof of Lemma 1

Define $p(\tau) = \mathbb{I}_{\{\tau \geq t_{k-1,m}\}}$ and $p_m(\tau) = \mathbb{I}_{\{\tau \geq t_{k-1,m} - \frac{1}{m}\}}$ with $m \in \mathbb{N}$ for some $\tau \in [t_{k,m}, t_{k+1,m}]$ with $\mathbb{I}_{\{\cdot\}}$ denoting the indicator function. Thus we have

$$\lim_{m\to\infty} \sup |p_m(\tau) - p(\tau)| = 1, \quad \text{(C.23)}$$

if $p_{t_{k-1,m}} \neq p_{t_{k,m}}$. Therefore if there exists at least one $i, j = 1, \ldots, N$ such that $p_{t_{i,m}} \neq p_{t_{j,m}}$ it immediately follows that $\tilde{y}_t \equiv \tilde{y}_{\infty,t} = dp_t \neq 0$ as $m \to \infty$, since

$$\int_a^b \sigma_{r_u}^2 du = \lim_{m\to\infty} \sum_{k=1}^{m} \sigma_{r_{k,m}}^2 = \lim_{m\to\infty} \sum_{k=1}^{m} (p_{t_{k,m}} - p_{t_{k-1,m}})^2 > 0. \quad \text{(C.24)}$$

As the sum in (C.24) contains at least one none zero element. If not then the price process is not only locally constant, but globally in other words price process is not changing over the entire interval $[a, b]$.

To proof equation 4.34, we rely on the Doobs martingale inequality and the law of iterated expectations. For any nonnegative constant λ we can write

$$\begin{aligned}
\mathbb{P}\left[\sup_{t_{k-1,m}\leq u\leq t_{k},m} |\int_{t_{k-1,m}}^{t_{k,m}} \sigma_{r_u} dW_u| > \delta\right] &= \mathbb{P}\left[\sup_{t_{k-1,m}\leq u\leq t_{k,m}} |\exp\left(\lambda \int_{t_{k-1,m}}^{t_{k,m}} \sigma_{r_u} dW_u\right)| > \exp\left(\lambda\delta\right)\right] \\
&\leq \frac{\mathbb{E}\exp\left(\left[\lambda \int_{t_{k-1,m}}^{t_{k,m}} \sigma_{r_u} dW_u\right]\right)}{e^{\lambda\delta}} \\
&= \frac{\mathbb{E}\left[\mathbb{E}\left[\exp\left(\lambda \int_{t_{k-1,m}}^{t_{k,m}} \sigma_{r_u} dW_u\right)|\mathcal{F}_{r_u}\right]\right]}{e^{\lambda\delta}} \\
&= \mathbb{E}\left[\exp\left(\frac{1}{2}\lambda^2 \int_{t_{k-1,m}}^{t_{k,m}} \sigma_{r_u}^2 du - \lambda\delta\right)\right] \\
&\leq \exp\left(\frac{1}{2}\lambda^2 K^2 (t_{k,m} - t_{k-1,m}) - \lambda\delta\right).
\end{aligned}$$

Since the initial statement does not depend on λ we can minimize $\exp\left(\frac{1}{2}\lambda^2 K^2 (t_{k,m} - t_{k-1,m}) - \lambda\delta\right)$ with respect to λ and obtain for the optimal value $\lambda^* = \frac{\delta^2}{K^2(t_{k,m} - t_{k-1,m})}$ from which the claim follows immediately.

Appendix D

Tables

D.1 Model and Parameter Specification

M_1 :	$y_{k,m} = \mu_{r_{k,m}} + \sigma_{r_{k,m}} u_{k,m}$	M_5:	$y_{k,m} = \sigma_{r_{k,m}} u_{k,m}$
M_2 :	$y_{k,m} = \lambda_{r_{k-1,m}} y_{k-1,m} + \sigma_{r_{k,m}} u_{k,m}$	M_6:	$y_{k,m} = \mu + \sigma_{r_{k,m}} u_{k,m}$
M_3 :	$y_{k,m} = \mu + \lambda_{r_{k-1,m}} (y_{k-1,m} - \mu) + \sigma_{r_{k,m}} u_{k,m}$	M_7:	$y_{k,m} = \lambda y_{k-1,m} + \sigma_{r_{k,m}} u_{k,m}$
M_4 :	$y_{k,m} = \mu_{r_{k,m}} + \lambda \left(y_{k-1,m} - \mu_{r_{k-1,m}}\right) + \sigma_{r_{k,m}} u_{k,m}$	M_8:	$y_{k,m} = \mu + \lambda y_{k-1,m} + \sigma_{r_{k,m}} u_{k,m}$

Table D.1: Model Selection for Monte Carlo Study.

Monte Carlo Study: True model parameters specification

	a_1	a_2	μ	λ	μ_1	μ_2	λ_1	λ_2	σ_1	σ_2		ρ		
M_1	2.5	-2.2	-	-	0.1	-0.15	-	-	0.2	1	0.1	0.5	0.9	
M_2	2.5	-2.2	-	-	-	-	0.05	-0.2	0.2	1		0.1	0.5	0.9
M_3	2.5	-2.2	0.1	-	-	-	0.05	-0.2	0.2	1	0.1	0.5	0.9	
M_4	2.5	-2.2	-	0.05	0.1	-0.15	-	-	0.2	1	0.1	0.5	0.9	
M_5	2.5	-2.2	-	-	-	-	-	-	0.2	1		0.1	0.5	0.9
M_6	2.5	-2.2	0.1	-	-	-	-	-	0.2	1		0.1	0.5	0.9
M_7	2.5	-2.2	-	0.05	-	-	-	-	0.2	1		0.1	0.5	0.9
M_8	2.5	-2.2	0.1	0.05	-	-	-	-	0.2	1		0.1	0.5	0.9

Table D.2: Monte Carlo Study: True model parameters specification. The selected true parameter value a_1 and a_2 correspond to regime persistence probabilities of $\mathbb{P}_{11} = 0.9938$ and $\mathbb{P}_{22} = 0.9861$, respectively.

D.1.1 Performance Endogenous Estimator: $T = 800$

	M_1		M_2		M_3		M_4	
	Estimate	True value	Estimate	True value	Estimate	True value	Estimate	True value
a_1	**2.543**	**2.500**	**2.535**	**2.500**	**2.531**	**2.500**	**2.529**	**2.500**
	(0.103)	-	(0.063)	-	(0.090)	-	(0.074)	-
a_2	**-2.118**	**-2.200**	**-2.100**	**-2.200**	**-2.100**	**-2.200**	**-2.085**	**-2.200**
	(0.168)	-	(0.080)	-	(0.107)	-	(0.104)	-
μ	**-**	**-**	**-**	**-**	**0.100**	**0.100**	**-**	**-**
	-	-	-	-	(0.001)	-	-	-
λ	**-**	**-**	**-**	**-**	**-**	**-**	**0.046**	**0.050**
	-	-	-	-	-	-	0.007	-
μ_1	**0.100**	**0.100**	**-**	**-**	**-**	**-**	**0.098**	**0.100**
	(0.001)	-	-	-	-	-	(0.009)	-
μ_2	**-0.145**	**-0.150**	**-**	**-**	**-**	**-**	**-0.150**	**-0.150**
	(0.051)	-	-	-	-	-	(0.020)	-
λ_1	**-**	**-**	**0.049**	**0.050**	**0.046**	**0.050**	**-**	-
	-	-	(0.005)	-	(0.008)	-	-	-
λ_2	**-**	**-**	**-0.197**	**-0.200**	**-0.193**	**-0.200**	**-**	-
	-	-	(0.013)	-	(0.021)	-	-	-
σ_1	**0.200**	**0.200**	**0.201**	**0.200**	**0.210**	**0.200**	**0.206**	**0.200**
	(0.002)	-	(0.001)	-	(0.001)	-	(0.005)	-
σ_2	**0.991**	**1.000**	**0.989**	**1.000**	**0.975**	**1.000**	**0.984**	**1.000**
	(0.021)	-	(0.007)	-	(0.010)	-	(0.011)	-
ρ	**0.103**	**0.100**	**0.085**	**0.100**	**0.081**	**0.100**	**0.081**	**0.100**
	(0.135)	-	(0.080)	-	(0.039)	-	(0.038)	-

	M_5		M_6		M_7		M_8	
	Estimate	True value	Estimate	True value	Estimate	True value	Estimate	True value
a_1	**2.522**	**2.500**	**2.525**	**2.500**	**2.522**	**2.500**	**2.527**	**2.500**
	(0.093)	-	(0.071)	-	(0.147)	-	(0.067)	-
a_2	**-2.129**	**-2.200**	**-2.127**	**-2.200**	**-2.126**	**-2.200**	**-2.124**	**-2.200**
	(0.134)	-	(0.087)	-	(0.174)	-	(0.076)	-
μ	**-**	**-**	**0.100**	**0.100**	**-**	**-**	**0.100**	**0.100**
	-	-	(0.001)	-	-	-	(0.001)	-
λ	**-**	**-**	**-**	**-**	**0.051**	**0.050**	**0.049**	**0.050**
	-	-	-	-	(0.020)	-	(0.004)	-
μ_1	**-**	**-**	**-**	**-**	**-**	**-**	**-**	**-**
	-	-	-	-	-	-	-	-
μ_2	**-**	**-**	**-**	**-**	**-**	**-**	**-**	**-**
	-	-	-	-	-	-	-	-
λ_1	**-**	**-**	**-**	**-**	**-**	**-**	**-**	**-**
	-	-	-	-	-	-	-	-
λ_2	**-**	**-**	**-**	**-**	**-**	**-**	**-**	**-**
	-	-	-	-	-	-	-	-
σ_1	**0.212**	**0.200**	**0.206**	**0.200**	**0.215**	**0.200**	**0.211**	**0.200**
	(0.004)	-	(0.001)	-	(0.002)	-	(0.001)	-
σ_2	**0.985**	**1.000**	**0.990**	**1.000**	**0.975**	**1.000**	**0.984**	**1.000**
	(0.011)	-	(0.008)	-	(0.011)	-	(0.008)	-
ρ	**0.101**	**0.100**	**0.100**	**0.100**	**0.076**	**0.100**	**0.088**	**0.100**
	(0.041)	-	(0.033)	-	(0.049)	-	(0.027)	-

Table D.3: Monte Carlo Simulation: The table reports QML estimates averaged over $M = 1'000$ simulation runs for the endogenous estimator. Time series length is $T = 800$ and $\rho = 0.1$. Averaged standard errors are given in parentheses and are based on numerically evaluating second order derivatives of the log-likelihood function.

	M_1		M_2		M_3		M_4	
	Estimate	True value	Estimate	True value	Estimate	True value	Estimate	True value
a_1	**2.533**	**2.500**	**2.538**	**2.500**	**2.541**	**2.500**	**2.544**	**2.500**
	(0.063)	-	(0.067)	-	(0.072)	-	(0.053)	-
a_2	**-2.125**	**-2.200**	**-2.115**	**-2.200**	**-2.116**	**-2.200**	**-2.108**	**-2.200**
	(0.070)	-	(0.098)	-	(0.079)	-	(0.073)	-
μ	**-**	**-**	**-**	**-**	**0.100**	**0.100**	**-**	**-**
	-	-	-	-	(0.001)	-	-	-
λ	**-**	**-**	**-**	**-**	**-**	**-**	**0.045**	**0.050**
	-	-	-	-	-	-	(0.003)	-
μ_1	**0.100**	**0.100**	**-**	**-**	**-**	**-**	**0.099**	**0.100**
	(0.001)	-	-	-	-	-	(0.001)	-
μ_2	**-0.152**	**-0.150**	**-**	**-**	**-**	**-**	**-0.158**	**-0.150**
	(0.014)	-	-	-	-	-	(0.016)	-
λ_1	**-**	**-**	**0.048**	**0.050**	**0.046**	**0.050**	**-**	-
	-	-	(0.005)	-	(0.006)	-	-	-
λ_2	**-**	**-**	**-0.196**	**-0.200**	**-0.195**	**-0.200**	**-**	-
	-	-	(0.013)	-	(0.014)	-	-	-
σ_1	**0.200**	**0.200**	**0.202**	**0.200**	**0.210**	**0.200**	**0.202**	**0.200**
	(0.000)	-	(0.001)	-	(0.000)	-	(0.001)	-
σ_2	**0.994**	**1.000**	**0.988**	**1.000**	**0.981**	**1.000**	**0.984**	**1.000**
	(0.007)	-	(0.008)	-	(0.012)	-	(0.006)	-
ρ	**0.488**	**0.500**	**0.490**	**0.500**	**0.470**	**0.500**	**0.493**	**0.500**
	(0.044)	-	(0.061)	-	(0.061)	-	(0.054)	-

	M_5		M_6		M_7		M_8	
	Estimate	True value	Estimate	True value	Estimate	True value	Estimate	True value
a_1	**2.529**	**2.500**	**2.523**	**2.500**	**2.523**	**2.500**	**2.523**	**2.500**
	(0.102)	-	(0.063)	-	(0.066)	-	(0.080)	-
a_2	**-2.137**	**-2.200**	**-2.131**	**-2.200**	**-2.142**	**-2.200**	**-2.157**	**-2.200**
	(0.127)	-	(0.080)	-	(0.083)	-	(0.077)	-
μ	**-**	**-**	**0.100**	**0.100**	**-**	**-**	**0.101**	**0.100**
	-	-	(0.001)	-	-	-	(0.001)	-
λ	**-**	**-**	**-**	**-**	**0.048**	**0.050**	**0.048**	**0.050**
	-	-	-	-	(0.004)	-	(0.004)	-
μ_1	**-**	**-**	**-**	**-**	**-**	**-**	**-**	**-**
	-	-	-	-	-	-	-	-
μ_2	**-**	**-**	**-**	**-**	**-**	**-**	**-**	**-**
	-	-	-	-	-	-	-	-
λ_1	**-**	**-**	**-**	**-**	**-**	**-**	**-**	**-**
	-	-	-	-	-	-	-	-
λ_2	**-**	**-**	**-**	**-**	**-**	**-**	**-**	**-**
	-	-	-	-	-	-	-	-
σ_1	**0.216**	**0.200**	**0.206**	**0.200**	**0.229**	**0.200**	**0.208**	**0.200**
	(0.001)	-	(0.000)	-	(0.001)	-	(0.001)	-
σ_2	**0.974**	**1.000**	**0.986**	**1.000**	**0.964**	**1.000**	**0.989**	**1.000**
	(0.009)	-	(0.008)	-	(0.009)	-	(0.008)	-
ρ	**0.462**	**0.500**	**0.487**	**0.500**	**0.455**	**0.500**	**0.477**	**0.500**
	(0.081)	-	(0.048)	-	(0.057)	-	(0.059)	-

Table D.4: Monte Carlo Simulation: The table reports QML estimates averaged over $M = 1'000$ simulation runs for the endogenous estimator. Time series length is $T = 800$ and $\rho = 0.5$. Averaged standard errors are given in parentheses and are based on numerically evaluating second order derivatives of the log-likelihood function.

	M_1		M_2		M_3		M_4	
	Estimate	True value	Estimate	True value	Estimate	True value	Estimate	True value
a_1	**2.531**	**2.500**	**2.535**	**2.500**	**2.539**	**2.500**	**2.533**	**2.500**
	(0.475)	-	(0.439)	-	(0.512)	-	(0.667)	-
a_2	**-2.140**	**-2.200**	**-2.136**	**-2.200**	**-2.145**	**-2.200**	**-2.132**	**-2.200**
	(0.633)	-	(0.645)	-	(0.437)	-	(0.495)	-
μ	**-**	**-**	**-**	**-**	**0.100**	**0.100**	**-**	**-**
	-	-	-	-	(0.011)	-	-	-
λ	**-**	**-**	**-**	**-**	**-**	**-**	**0.047**	**0.050**
	-	-	-	-	-	-	(0.096)	-
μ_1	**0.100**	**0.100**	**-**	**-**	**-**	**-**	**0.100**	**0.100**
	(0.015)	-	-	-	-	-	(0.017)	-
μ_2	**-0.159**	**-0.150**	**-**	**-**	**-**	**-**	**-0.161**	**-0.150**
	(0.148)	-	-	-	-	-	(0.222)	-
λ_1	**-**	**-**	**0.050**	**0.050**	**0.044**	**0.050**	**-**	**-**
	-	-	(0.086)	-	(0.146)	-	-	-
λ_2	**-**	**-**	**-0.192**	**-0.200**	**-0.194**	**-0.200**	**-**	-
	-	-	(0.114)	-	(0.134)	-	-	-
σ_1	**0.200**	**0.200**	**0.205**	**0.200**	**0.207**	**0.200**	**0.203**	**0.200**
	(0.012)	-	(0.011)	-	(0.008)	-	(0.018)	-
σ_2	**0.989**	**1.000**	**0.985**	**1.000**	**0.985**	**1.000**	**0.987**	**1.000**
	(0.155)	-	(0.094)	-	(0.142)	-	(0.143)	-
ρ	**0.897**	**0.900**	**0.889**	**0.900**	**0.888**	**0.900**	**0.901**	**0.900**
	(0.614)	-	(0.644)	-	(0.505)	-	(0.711)	-

	M_5		M_6		M_7		M_8	
	Estimate	True value	Estimate	True value	Estimate	True value	Estimate	True value
a_1	**2.517**	**2.500**	**2.545**	**2.500**	**2.503**	**2.500**	**2.517**	**2.500**
	(0.352)	-	(0.340)	-	(0.456)	-	(0.354)	-
a_2	**-2.164**	**-2.200**	**-2.142**	**-2.200**	**-2.165**	**-2.200**	**-2.153**	**-2.200**
	(0.285)	-	(0.342)	-	(0.524)	-	(0.423)	-
μ	**-**	**-**	**0.100**	**0.100**	**-**	**-**	**0.100**	**0.100**
	-	-	(0.005)	-	-	-	(0.014)	-
λ	**-**	**-**	**-**	**-**	**0.049**	**0.050**	**0.049**	**0.050**
	-	-	-	-	(0.049)	-	(0.080)	-
μ_1	**-**	**-**	**-**	**-**	**-**	**-**	**-**	**-**
	-	-	-	-	-	-	-	-
μ_2	**-**	**-**	**-**	**-**	**-**	**-**	**-**	**-**
	-	**-**	-	**-**	-	**-**	-	**-**
λ_1	**-**	**-**	**-**	**-**	**-**	**-**	**-**	**-**
	-	-	-	-	-	-	-	-
λ_2	**-**	**-**	**-**	**-**	**-**	**-**	**-**	**-**
	-	-	-	-	-	-	-	-
σ_1	**0.224**	**0.200**	**0.207**	**0.200**	**0.247**	**0.200**	**0.213**	**0.200**
	(0.012)	-	(0.006)	-	(0.008)	-	(0.012)	-
σ_2	**0.964**	**1.000**	**0.986**	**1.000**	**0.950**	**1.000**	**0.979**	**1.000**
	(0.059)	-	(0.160)	-	(0.142)	-	(0.094)	-
ρ	**0.837**	**0.900**	**0.882**	**0.900**	**0.790**	**0.900**	**0.872**	**0.900**
	(0.409)	-	(0.418)	-	(0.542)	-	(0.463)	-

Table D.5: Monte Carlo Simulation: The table reports QML estimates averaged over $M = 1'000$ simulation runs for the endogenous estimator. Time series length is $T = 800$ and $\rho = 0.9$. Averaged standard errors are given in parentheses and are based on numerically evaluating second order derivatives of the log-likelihood function.

D.1.2 Performance Endogenous Estimator: $T = 8'000$

	M_1		M_2		M_3		M_4	
	Estimate	True value	Estimate	True value	Estimate	True value	Estimate	True value
a_1	**2.503**	**2.500**	**2.508**	**2.500**	**2.506**	**2.500**	**2.504**	**2.500**
	(0.015)	-	(0.011)	-	(0.009)	-	(0.009)	-
a_2	**-2.195**	**-2.200**	**-2.195**	**-2.200**	**-2.191**	**-2.200**	**-2.195**	**-2.200**
	(0.019)	-	(0.015)	-	(0.011)	-	(0.010)	-
μ	**-**	**-**	**-**	**-**	**0.100**	**0.100**	**-**	**-**
	-	-	-	-	(0.000)	-	-	-
λ	**-**	**-**	**-**	**-**	**-**	**-**	**0.050**	**0.050**
	-	-	-	-	-	-	(0.001)	-
μ_1	**0.100**	**0.100**	**-**	**-**	**-**	**-**	**0.100**	**0.100**
	(0.000)	-	-	-	-	-	(0.000)	-
μ_2	-0.149	**-0.150**	**-**	**-**	**-**	**-**	**-0.152**	**-0.150**
	(0.005)	-	-	-	-	-	(0.002)	-
λ_1	**-**	**-**	**0.050**	**0.050**	**0.049**	**0.050**	**-**	-
	-	-	(0.001)	-	(0.001)	-	-	-
λ_2	**-**	**-**	**-0.199**	**-0.200**	**-0.200**	**-0.200**	**-**	-
	-	-	(0.002)	-	(0.002)	-	-	-
σ_1	**0.200**	**0.200**	**0.200**	**0.200**	**0.200**	**0.200**	**0.200**	**0.200**
	(0.000)	-	(0.000)	-	(0.000)	-	(0.000)	-
σ_2	**0.999**	**1.000**	**1.001**	**1.000**	**1.000**	**1.000**	**0.999**	**1.000**
	(0.003)	-	(0.001)	-	(0.001)	-	(0.001)	-
ρ	**0.102**	**0.100**	**0.096**	**0.100**	**0.098**	**0.100**	**0.102**	**0.100**
	(0.025)	-	(0.015)	-	(0.012)	-	(0.014)	-

	M_5		M_6		M_7		M_8	
	Estimate	True value	Estimate	True value	Estimate	True value	Estimate	True value
a_1	**2.502**	**2.500**	**2.505**	**2.500**	**2.506**	**2.500**	**2.503**	**2.500**
	(0.013)	-	(0.013)	-	(0.013)	-	(0.012)	-
a_2	**-2.199**	**-2.200**	**-2.192**	**-2.200**	**-2.196**	**-2.200**	**-2.197**	**-2.200**
	(0.018)	-	(0.015)	-	(0.015)	-	(0.015)	-
μ	**-**	**-**	**0.100**	**0.100**	**-**	**-**	**0.100**	**0.100**
	-	-	(0.000)	-	-	-	(0.000)	-
λ	**-**	**-**	**-**	**-**	**0.050**	**0.050**	**0.050**	**0.050**
	-	-	-	-	(0.001)	-	(0.001)	-
μ_1	**-**	**-**	**-**	**-**	**-**	**-**	**-**	**-**
	-	-	-	-	-	-	-	-
μ_2	**-**	**-**	**-**	**-**	**-**	**-**	**-**	**-**
	-	**-**	-	**-**	-	**-**	-	**-**
λ_1	**-**	**-**	**-**	**-**	**-**	**-**	**-**	**-**
	-	-	-	-	-	-	-	-
λ_2	**-**	**-**	**-**	**-**	**-**	**-**	**-**	**-**
	-	-	-	-	-	-	-	-
σ_1	**0.207**	**0.200**	**0.200**	**0.200**	**0.200**	**0.200**	**0.200**	**0.200**
	(0.000)	-	(0.000)	-	(0.000)	-	(0.000)	-
σ_2	**0.993**	**1.000**	**1.000**	**1.000**	**1.000**	**1.000**	**1.000**	**1.000**
	(0.002)	-	(0.002)	-	(0.002)	-	(0.002)	-
ρ	**0.100**	**0.100**	**0.098**	**0.100**	**0.099**	**0.100**	**0.101**	**0.100**
	(0.018)	-	(0.016)	-	(0.016)	-	(0.018)	-

Table D.6: Monte Carlo Simulation: The table reports QML estimates averaged over $M = 1'000$ simulation runs for the endogenous estimator. Time series length is $T = 8'000$ and $\rho = 0.1$. Averaged standard errors are given in parentheses and are based on numerically evaluating second order derivatives of the log-likelihood function.

	M_1		M_2		M_3		M_4	
	Estimate	True value	Estimate	True value	Estimate	True value	Estimate	True value
a_1	**2.502**	**2.500**	**2.476**	**2.500**	**2.506**	**2.500**	**2.501**	**2.500**
	(0.007)	-	(0.006)	-	(0.008)	-	(0.007)	-
a_2	**-2.195**	**-2.200**	**-2.193**	**-2.200**	**-2.189**	**-2.200**	**-2.192**	**-2.200**
	(0.009)	-	(0.009)	-	(0.008)	-	(0.010)	-
μ	**-**	**-**	**-**	**-**	**0.100**	**0.100**	**-**	**-**
	-	-	-	-	(0.000)	-	-	-
λ	**-**	**-**	**-**	**-**	**-**	**-**	**0.049**	**0.050**
	-	-	-	-	-	-	(0.001)	-
μ_1	**0.100**	**0.100**	**-**	**-**	**-**	**-**	**0.100**	**0.100**
	(0.000)	-	-	-	-	-	(0.000)	-
μ_2	**-0.151**	**-0.150**	**-**	**-**	**-**	**-**	**-0.150**	**-0.150**
	(0.001)	-	-	-	-	-	(0.002)	-
λ_1	**-**	**-**	**0.050**	**0.050**	**0.050**	**0.050**	**-**	-
	-	-	(0.001)	-	(0.001)	-	-	-
λ_2	**-**	**-**	**-0.200**	**-0.200**	**-0.200**	**-0.200**	**-**	-
	-	-	(0.001)	-	(0.001)	-	-	-
σ_1	**0.200**	**0.200**	**0.200**	**0.200**	**0.200**	**0.200**	**0.200**	**0.200**
	(0.000)	-	(0.000)	-	(0.000)	-	(0.000)	-
σ_2	**1.001**	**1.000**	**1.000**	**1.000**	**1.000**	**1.000**	**0.999**	**1.000**
	(0.001)	-	(0.001)	-	(0.001)	-	(0.001)	-
ρ	**0.500**	**0.500**	**0.501**	**0.500**	**0.500**	**0.500**	**0.500**	**0.500**
	(0.009)	-	(0.006)	-	(0.008)	-	(0.009)	-

	M_5		M_6		M_7		M_8	
	Estimate	True value	Estimate	True value	Estimate	True value	Estimate	True value
a_1	**2.505**	**2.500**	**2.507**	**2.500**	**2.508**	**2.500**	**2.506**	**2.500**
	(0.009)	-	(0.010)	-	(0.009)	-	(0.008)	-
a_2	**-2.194**	**-2.200**	**-2.197**	**-2.200**	**-2.196**	**-2.200**	**-2.192**	**-2.200**
	(0.012)	-	(0.010)	-	(0.011)	-	(0.009)	-
μ	**-**	**-**	**0.100**	**0.100**	**-**	**-**	**0.100**	**0.100**
	-	-	(0.000)	-	-	-	(0.000)	-
λ	**-**	**-**	**-**	**-**	**0.050**	**0.050**	**0.050**	**0.050**
	-	-	-	-	(0.001)	-	(0.001)	-
μ_1	**-**	**-**	**-**	**-**	**-**	**-**	**-**	**-**
	-	-	-	-	-	-	-	-
μ_2	**-**	**-**	**-**	**-**	**-**	**-**	**-**	**-**
	-	-	-	-	-	-	-	-
λ_1	**-**	**-**	**-**	**-**	**-**	**-**	**-**	**-**
	-	-	-	-	-	-	-	-
λ_2	**-**	**-**	**-**	**-**	**-**	**-**	**-**	**-**
	-	-	-	-	-	-	-	-
σ_1	**0.201**	**0.200**	**0.200**	**0.200**	**0.200**	**0.200**	**0.200**	**0.200**
	(0.000)	-	(0.000)	-	(0.000)	-	(0.000)	-
σ_2	**0.999**	**1.000**	**1.000**	**1.000**	**1.000**	**1.000**	**1.000**	**1.000**
	(0.001)	-	(0.001)	-	(0.001)	-	(0.001)	-
ρ	**0.499**	**0.500**	**0.497**	**0.500**	**0.503**	**0.500**	**0.499**	**0.500**
	(0.008)	-	(0.008)	-	(0.008)	-	(0.008)	-

Table D.7: Monte Carlo Simulation: The table reports QML estimates averaged over $M = 1'000$ simulation runs for the endogenous estimator. Time series length is $T = 8'000$ and $\rho = 0.5$. Averaged standard errors are given in parentheses and are based on numerically evaluating second order derivatives of the log-likelihood function.

	M_1		M_2		M_3		M_4	
	Estimate	True value	Estimate	True value	Estimate	True value	Estimate	True value
a_1	**2.505**	**2.500**	**2.501**	**2.500**	**2.501**	**2.500**	**2.502**	**2.500**
	(0.003)	-	(0.003)	-	(0.003)	-	(0.003)	-
a_2	**-2.194**	**-2.200**	**-2.197**	**-2.200**	**-2.195**	**-2.200**	**-2.196**	**-2.200**
	(0.004)	-	(0.003)	-	(0.003)	-	(0.004)	-
μ	**-**	**-**	**-**	**-**	**0.100**	**0.100**	**-**	**-**
	-	-	-	-	(0.000)	-	-	-
λ	**-**	**-**	**-**	**-**	**-**	**-**	**0.049**	**0.050**
	-	-	-	-	-	-	(0.000)	-
μ_1	**0.100**	**0.100**	**-**	**-**	**-**	**-**	**0.100**	**0.100**
	(0.000)	-	-	-	-	-	(0.000)	-
μ_2	**-0.152**	**-0.150**	**-**	**-**	**-**	**-**	**-0.151**	**-0.150**
	(0.001)	-	-	-	-	-	(0.001)	-
λ_1	**-**	**-**	**0.050**	**0.050**	**0.050**	**0.050**	**-**	-
	-	-	(0.000)	-	(0.000)	-	-	-
λ_2	**-**	**-**	**-0.200**	**-0.200**	**-0.199**	**-0.200**	**-**	-
	-	-	(0.000)	-	(0.000)	-	-	-
σ_1	**0.200**	**0.200**	**0.200**	**0.200**	**0.200**	**0.200**	**0.200**	**0.200**
	(0.000)	-	(0.000)	-	(0.000)	-	(0.000)	-
σ_2	**1.000**	**1.000**	**1.000**	**1.000**	**1.000**	**1.000**	**1.000**	**1.000**
	(0.000)	-	(0.000)	-	(0.000)	-	(0.000)	-
ρ	**0.902**	**0.900**	**0.902**	**0.900**	**0.901**	**0.900**	**0.902**	**0.900**
	(0.000)	-	(0.000)	-	(0.000)	-	(0.000)	-

	M_5		M_6		M_7		M_8	
	Estimate	True value	Estimate	True value	Estimate	True value	Estimate	True value
a_1	**2.500**	**2.500**	**2.501**	**2.500**	**2.502**	**2.500**	**2.502**	**2.500**
	(0.003)	-	(0.004)	-	(0.003)	-	(0.008)	-
a_2	**-2.198**	**-2.200**	**-2.195**	**-2.200**	**-2.198**	**-2.200**	**-2.192**	**-2.200**
	(0.004)	-	0.004	-	(0.004)	-	(0.009)	-
μ	**-**	**-**	**0.100**	**0.100**	**-**	**-**	**0.100**	**0.100**
	-	-	(0.000)	-	-	-	(0.000)	-
λ	**-**	**-**	**-**	**-**	**0.050**	**0.050**	**0.050**	**0.050**
	-	-	-	-	(0.000)	-	(0.001)	-
μ_1	**-**	**-**	**-**	**-**	**-**	**-**	**-**	**-**
	-	-	-	-	-	-	-	-
μ_2	**-**	**-**	**-**	**-**	**-**	**-**	**-**	**-**
	-	-	-	-	-	-	-	-
λ_1	**-**	**-**	**-**	**-**	**-**	**-**	**-**	**-**
	-	-	-	-	-	-	-	-
λ_2	**-**	**-**	**-**	**-**	**-**	**-**	**-**	**-**
	-	-	-	-	-	-	-	-
σ_1	**0.200**	**0.200**	**0.200**	**0.200**	**0.200**	**0.200**	**0.201**	**0.200**
	(0.000)	-	(0.000)	-	(0.000)	-	(0.000)	-
σ_2	**1.000**	**1.000**	**1.000**	**1.000**	**1.000**	**1.000**	**0.999**	**1.000**
	(0.000)	-	(0.000)	-	(0.000)	-	(0.001)	-
ρ	**0.902**	**0.900**	**0.900**	**0.900**	**0.902**	**0.900**	**0.900**	**0.900**
	(0.001)	-	(0.001)	-	(0.000)	-	(0.008)	-

Table D.8: Monte Carlo Simulation: The table reports QML estimates averaged over $M = 1'000$ simulation runs for the endogenous estimator. Time series length is $T = 8'000$ and $\rho = 0.9$. Averaged standard errors are given in parentheses and are based on numerically evaluating second order derivatives of the log-likelihood function.

D.1.3 Efficiency: Endogenous vs Exogenous Estimator

	M_1		M_2		M_3		M_4	
	Endo	Exo	Endo	Exo	Endo	Exo	Endo	Exo
a_1	**2.503**	**2.503**	**2.507**	**2.503**	**2.503**	**2.503**	**2.503**	**2.503**
	(0.014)	(0.004)	(0.010)	(0.004)	(0.009)	(0.003)	(0.007)	(0.004)
a_2	**-2.194**	**-2.195**	**-2.194**	**-2.195**	**-2.192**	**-2.195**	**-2.187**	**-2.195**
	(0.015)	(0.005)	(0.014)	(0.005)	(0.011)	(0.005)	(0.008)	(0.005)
μ	**-**	**-**	**-**	**-**	**0.100**	**0.100**	**-**	**-**
	-	-	-	-	(0.000)	(0.000)	-	-
λ	**-**	**-**	**-**	**-**	**-**	**-**	**0.050**	**0.050**
	-	-	-	-	-	-	(0.001)	(0.000)
μ_1	**0.100**	**0.100**	**-**	**-**	**-**	**-**	**0.100**	**0.100**
	(0.000)	(0.000)	-	-	-	-	(0.000)	(0.000)
μ_2	**-0.151**	**-0.149**	**-**	**-**	**-**	**-**	**-0.150**	**-0.149**
	(0.004)	(0.001)	-	-	-	-	(0.002)	(0.000)
λ_1	**-**	**-**	**0.050**	**0.049**	**0.050**	**0.049**	**-**	**-**
	-	-	(0.001)	(0.000)	(0.001)	(0.000)	-	-
λ_2	**-**	**-**	**-0.201**	**-0.199**	**-0.201**	**-0.199**	**-**	**-**
	-	-	(0.002)	(0.000)	(0.002)	(0.001)	-	-
σ_1	**0.201**	**0.200**	**0.200**	**0.200**	**0.200**	**0.200**	**0.200**	**0.200**
	(0.000)	(0.000)	(0.000)	(0.000)	(0.000)	(0.000)	(0.000)	(0.000)
σ_2	**0.999**	**1.000**	**1.000**	**1.000**	**0.999**	**1.000**	**1.000**	**1.000**
	(0.002)	(0.000)	(0.001)	(0.000)	(0.001)	(0.000)	(0.001)	(0.000)
ρ	**0.002**	**-**	**-0.001**	**-**	**0.000**	**-**	**0.000**	**-**
	(0.021)	-	(0.013)		(0.014)	-	(0.010)	-

	M_5		M_6		M_7		M_8	
	Endo	Exo	Endo	Exo	Endo	Exo	Endo	Exo
a_1	**2.503**	**2.500**	**2.504**	**2.504**	**2.507**	**2.503**	**2.505**	**2.503**
	(0.013)	(0.004)	(0.013)	(0.004)	(0.014)	(0.004)	(0.011)	(0.004)
a_2	**-2.198**	**-2.198**	**-2.193**	**-2.195**	**-2.192**	**-2.195**	**-2.195**	**-2.195**
	(0.024)	(0.005)	(0.014)	(0.005)	(0.015)	(0.005)	(0.013)	(0.005)
μ	**-**	**-**	**0.100**	**0.100**	**-**	**-**	**0.100**	**0.095**
	-	-	(0.000)	(0.000)	-	-	(0.000)	(0.000)
λ	**-**	**-**	**-**	**-**	**0.050**	**0.050**	**0.050**	**0.050**
	-	-	-	-	(0.001)	(0.000)	(0.001)	(0.000)
μ_1	**-**	**-**	**-**	**-**	**-**	**-**	**-**	**-**
	-	-	-	-	-	-	-	-
μ_2	**-**	**-**	**-**	**-**	**-**	**-**	**-**	**-**
	-	-	-	-	-	-	-	-
λ_1	**-**	**-**	**-**	**-**	**-**	**-**	**-**	**-**
	-	-	-	-	-	-	-	-
λ_2	**-**	**-**	**-**	**-**	**-**	**-**	**-**	**-**
	-	-	-	-	-	-	-	-
σ_1	**0.206**	**0.200**	**0.200**	**0.200**	**0.200**	**0.200**	**0.200**	**0.200**
	(0.000)	(0.000)	(0.000)	(0.000)	(0.002)	(0.000)	(0.000)	(0.000)
σ_2	**0.994**	**1.000**	**1.000**	**1.000**	**1.000**	**1.000**	**1.000**	**1.000**
	(0.002)	(0.000)	(0.002)	(0.000)	(0.000)	(0.000)	(0.001)	(0.000)
ρ	**-0.002**	**-**	**0.004**	**-**	**-0.001**	**-**	**0.000**	**-**
	(0.022)	-	(0.014)	-	(0.016)	-	(0.015)	-

Table D.9: Monte Carlo Simulation: The table reports QML estimates averaged over $M = 1'000$ simulation runs for the endogenous estimator. Time series length is $T = 8'000$ and $\rho = 0$. Averaged standard errors are given in parentheses and are based on numerically evaluating second order derivatives of the log-likelihood function.

	M_1		M_2		M_3		M_4	
	Endo	Exo	Endo	Exo	Endo	Exo	Endo	Exo
a_1	**2.548**	**2.500**	**2.541**	**2.500**	**2.535**	**2.500**	**2.535**	**2.500**
	(0.115)	(0.046)	(0.078)	(0.049)	(0.067)	(0.052)	(0.105)	(0.044)
a_2	**-2.093**	**-2.200**	**-2.108**	**-2.200**	**-2.116**	**-2.200**	**-2.118**	**-2.200**
	(0.154)	(0.064)	(0.163)	(0.067)	(0.081)	(0.066)	(0.103)	(0.059)
μ	**-**	**-**	**-**	**-**	**0.100**	**0.100**	**-**	**-**
	-	-	-	-	(0.001)	(0.000)	-	-
λ	**-**	**-**	**-**	**-**	**-**	**-**	**0.048**	**0.050**
	-	-	-	-	-	-	(0.006)	(0.001)
μ_1	**0.100**	**0.100**	**-**	**-**	**-**	**-**	**0.099**	**0.100**
	(0.001)	(0.000)	-	-	-	-	(0.001)	(0.001)
μ_2	**-0.144**	**-0.150**	**-**	**-**	**-**	**-**	**-0.144**	**-0.150**
	(0.051)	(0.008)	-	-	-	-	(0.022)	(0.009)
λ_1	**-**	**-**	**0.052**	**0.050**	**0.047**	**0.050**	**-**	-
	-	-	(0.006)	(0.003)	(0.006)	(0.005)	-	-
λ_2	**-**	**-**	**-0.191**	**-0.200**	**-0.195**	**-0.200**	**-**	-
	-	-	(0.030)	(0.019)	(0.012)	(0.012)	-	-
σ_1	**0.200**	**0.200**	**0.202**	**0.200**	**0.203**	**0.200**	**0.203**	**0.200**
	(0.001)	(0.001)	(0.000)	(0.002)	(0.001)	(0.001)	(0.001)	(0.001)
σ_2	**0.992**	**1.000**	**0.983**	**1.000**	**0.988**	**1.000**	**0.985**	**1.000**
	(0.016)	(0.004)	(0.011)	(0.006)	(0.008)	(0.006)	(0.013)	(0.004)
ρ	**-0.009**	-	**-0.014**	-	**-0.003**	-	**-0.006**	-
	(0.117)	-	(0.112)	-	(0.080)	-	(0.133)	-

	M_5		M_6		M_7		M_8	
	Endo	Exo	Endo	Exo	Endo	Exo	Endo	Exo
a_1	**2.520**	**2.476**	**2.525**	**2.500**	**2.528**	**2.500**	**2.518**	**2.500**
	(0.183)	(0.070)	(0.081)	(0.048)	(0.142)	(0.047)	(0.064)	(0.055)
a_2	**-2.113**	**-2.142**	**-2.106**	**-2.200**	**-2.125**	**-2.200**	**-2.118**	**-2.200**
	(0.130)	(0.111)	(0.128)	(0.065)	(0.154)	(0.062)	(0.089)	(0.072)
μ	**-**	**-**	**0.100**	**0.100**	**-**	**-**	**0.100**	**0.100**
	-	-	(0.001)	(0.000)	-	-	(0.001)	(0.000)
λ	**-**	**-**	**-**	**-**	**0.048**	**0.050**	**0.049**	**0.050**
	-	-	-	-	(0.006)	(0.001)	(0.003)	(0.002)
μ_1	**-**	**-**	**-**	**-**	**-**	**-**	**-**	**-**
	-	-	-	-	-	-	-	-
μ_2	**-**	**-**	**-**	**-**	**-**	**-**	**-**	**-**
	-	**-**	-	**-**	-	**-**	-	**-**
λ_1	**-**	**-**	**-**	**-**	**-**	**-**	**-**	**-**
	-	-	-	-	-	-	-	-
λ_2	**-**	**-**	**-**	**-**	**-**	**-**	**-**	**-**
	-	-	-	-	-	-	-	-
σ_1	**0.211**	**0.236**	**0.206**	**0.200**	**0.220**	**0.200**	**0.211**	**0.200**
	(0.003)	(0.001)	(0.003)	(0.012)	(0.001)	(0.000)	(0.001)	(0.008)
σ_2	**0.984**	1.011	**0.978**	**1.000**	**0.972**	**1.000**	**0.982**	**1.000**
	(0.013)	(0.011)	(0.013)	(0.005)	(0.018)	(0.005)	(0.007)	(0.012)
ρ	**-0.010**	**-**	**0.000**	**-**	**0.001**	**-**	**0.010**	**-**
	(0.101)	-	(0.089)	-	(0.116)	-	(0.074)	-

Table D.10: Monte Carlo Simulation: The table reports QML estimates averaged over $M = 1'000$ simulation runs for the endogenous estimator. Time series length is $T = 800$ and $\rho = 0$. Averaged standard errors are given in parentheses and are based on numerically evaluating second order derivatives of the log-likelihood function.

D.1.4 Bias Analysis

	M_1			M_2			M_3			M_4		
ρ	0.1	0.5	0.9	0.1	0.5	0.9	0.1	0.5	0.9	0.1	0.5	0.9
a_1	**2.519**	**2.516**	**2.505**	**2.507**	**2.508**	**2.503**	**2.504**	**2.505**	**2.507**	**2.509**	**2.518**	**2.503**
	(0.072)	(0.180)	(0.062)	(0.054)	(0.077)	(0.065)	(0.051)	(0.065)	(0.101)	(0.049)	(0.054)	(0.064)
a_2	**-2.096**	**-2.091**	**-2.102**	**-2.095**	**-2.097**	**-2.103**	**-2.088**	**-2.092**	**-2.103**	**-2.091**	**-2.094**	**-2.101**
	(0.158)	(0.168)	(0.066)	(0.078)	(0.114)	(0.064)	(0.069)	(0.077)	(0.086)	(0.071)	(0.069)	(0.087)
μ	**-**	**-**	**-**	**-**	**-**	**-**	**0.100**	**0.099**	**0.097**	**-**	**-**	**-**
	-	-	-	-	-	-	(0.000)	(0.000)	(0.001)	-	-	-
λ	**-**	**-**	**-**	**-**	**-**	**-**	**-**	**-**	**-**	**0.048**	**0.050**	**0.050**
	-	-	-	-	-	-	-	-	-	(0.002)	(0.001)	(0.002)
μ_1	**0.099**	**0.103**	**0.098**	**-**	**-**	**-**	**-**	**-**	**-**	**0.102**	**0.096**	**0.100**
	(0.013)	(0.107)	(0.030)	-	-	-	-	-	-	(0.033)	(0.002)	(0.039)
μ_2	**-0.131**	**-0.093**	**-0.065**	**-**	**-**	**-**	**-**	**-**	**-**	**-0.128**	**-0.092**	**-0.054**
	(0.012)	(0.075)	(0.013)	-	-	-	-	-	-	(0.036)	(0.027)	(0.060)
λ_1	**-**	**-**	**-**	**0.048**	**0.047**	**0.046**	**0.047**	**0.044**	**0.042**	**-**	**-**	**-**
	-	-	-	(0.003)	(0.022)	(0.006)	(0.008)	(0.009)	(0.012)	-	-	-
λ_2	**-**	**-**	**-**	**-0.194**	**-0.194**	**-0.192**	**-0.194**	**-0.194**	**-0.191**	**-**	**-**	**-**
	-	-	-	(0.013)	(0.038)	(0.014)	(0.014)	(0.014)	(0.085)	-	-	-
σ_1	**0.212**	**0.215**	**0.220**	**0.217**	**0.218**	**0.222**	**0.235**	**0.227**	**0.237**	**0.238**	**0.240**	**0.250**
	(0.001)	(0.004)	(0.002)	(0.001)	(0.001)	(0.001)	(0.001)	(0.002)	(0.022)	(0.002)	(0.002)	(0.005)
σ_2	**1.030**	**1.047**	**1.027**	**1.026**	**1.034**	**1.042**	**1.024**	**1.025**	**1.046**	**1.030**	**1.015**	**1.017**
	(0.005)	(0.013)	(0.006)	(0.005)	(0.021)	(0.016)	(0.006)	(0.010)	(0.020)	(0.007)	(0.011)	(0.007)
SrB	**0.2047**	**0.2105**	**0.2652**	**0.1663**	**0.1685**	**0.1749**	**0.1804**	**0.1957**	**0.191**	**0.2203**	**0.2348**	**0.2714**
$\rho = 0$	**0.1963**			**0.1676**			**0.1742**			**0.1977**		

	M_5			M_6			M_7			M_8		
ρ	0.1	0.5	0.9	0.1	0.5	0.9	0.1	0.5	0.9	0.1	0.5	0.9
a_1	**2.474**	**2.465**	**2.470**	**2.511**	**2.510**	**2.507**	**2.502**	**2.508**	**2.493**	**2.512**	**2.515**	**2.495**
	(0.140)	(0.207)	(0.138)	(0.124)	(0.144)	(0.048)	(0.129)	(0.085)	(0.061)	(0.066)	(0.052)	(0.062)
a_2	**-2.155**	**-2.154**	**-2.147**	**-2.104**	**-2.094**	**-2.106**	**-2.103**	**-2.107**	**-2.122**	**-2.103**	**-2.092**	**-2.110**
	(0.211)	(0.145)	(0.143)	(0.172)	(0.183)	(0.060)	(0.104)	(0.102)	(0.074)	(0.075)	(0.071)	(0.064)
μ	**-**	**-**	**-**	**0.100**	**0.098**	**0.097**	**-**	**-**	**-**	**0.095**	**0.094**	**0.093**
	-	-	-	(0.000)	(0.001)	(0.000)	-	-	-	(0.000)	(0.000)	(0.000)
λ	**-**	**-**	**-**	**-**	**-**	**-**	**0.050**	**0.048**	**0.049**	**0.048**	**0.047**	**0.047**
	-	-	-	-	-	-	(0.002)	(0.001)	(0.001)	(0.001)	(0.001)	(0.001)
μ_1	**-**	**-**	**-**	**-**	**-**	**-**	**-**	**-**	**-**	**-**	**-**	**-**
	-	-	-	-	-	-	-	-	-	-	-	-
μ_2	**-**	**-**	**-**	**-**	**-**	**-**	**-**	**-**	**-**	**-**	**-**	**-**
	-	-	-	-	-	-	-	-	-	-	-	-
λ_1	**-**	**-**	**-**	**-**	**-**	**-**	**-**	**-**	**-**	**-**	**-**	**-**
	-	-	-	-	-	-	-	-	-	-	-	-
λ_2	**-**	**-**	**-**	**-**	**-**	**-**	**-**	**-**	**-**	**-**	**-**	**-**
	-	-	-	-	-	-	-	-	-	-	-	-
σ_1	**0.237**	**0.243**	**0.243**	**0.215**	**0.222**	**0.218**	**0.227**	**0.219**	**0.225**	**0.214**	**0.215**	**0.231**
	(0.000)	(0.001)	(0.001)	(0.002)	(0.069)	(0.003)	(0.001)	(0.001)	(0.001)	(0.000)	(0.000)	(0.001)
σ_2	**1.006**	**1.010**	**1.016**	**1.025**	**1.047**	**1.052**	**1.031**	**1.021**	**1.021**	**1.035**	**1.039**	**1.043**
	(0.005)	(0.005)	(0.005)	(0.006)	(0.020)	(0.006)	(0.015)	(0.006)	(0.005)	(0.010)	(0.007)	(0.006)
SrB	**0.0966**	**0.101**	**0.1072**	**0.164**	**0.1792**	**0.1735**	**0.148**	**0.1617**	**0.1473**	**0.1738**	**0.1704**	**0.1753**
$\rho = 0$	**0.0876**			**0.1632**			**0.1279**			**0.1727**		

Table D.11: Monte Carlo Simulation: The table reports QML estimates (in boldface) averaged over $M = 1'000$ simulation runs for the exogenous estimator when the state is endogenous, i.e. $\rho \in \{0.1, 0.5, 0.9\}$. Time series length is $T = 800$. Averaged standard errors are given below the averaged Monte Carlo estimates and are based on numerically evaluating second order derivatives of the log-likelihood function. The row '$\rho = 0$' refers to the SrB test statistics when there is no endogeneity in the data generated process.

	M_1			M_2			M_3			M_4		
ρ	0.1	0.5	0.9	0.1	0.5	0.9	0.1	0.5	0.9	0.1	0.5	0.9
a_1	**2.503**	**2.501**	**2.497**	**2.513**	**2.499**	**2.497**	**2.503**	**2.499**	**2.497**	**2.510**	**2.501**	**2.497**
	(0.004)	(0.003)	(0.001)	(0.003)	(0.004)	(0.005)	(0.003)	(0.003)	(0.004)	(0.007)	(0.004)	(0.002)
a_2	**-2.194**	**-2.196**	**-2.199**	**-2.194**	**-2.194**	**-2.197**	**-2.194**	**-2.194**	**-2.197**	**-2.194**	**-2.195**	**-2.199**
	(0.005)	(0.002)	(0.003)	(0.008)	(0.006)	(0.006)	(0.007)	(0.006)	(0.002)	(0.003)	(0.002)	(0.005)
μ	**-**	**-**	**-**	**-**	**-**	**-**	**0.100**	**0.098**	**0.097**	**-**	**-**	**-**
	-	-	-	-	-	-	(0.000)	(0.000)	(0.000)	-	-	-
λ	**-**	**-**	**-**	**-**	**-**	**-**	**-**	**-**	**-**	(0.050)	(0.052)	(0.053)
	-	-	-	-	-	-	-	-	-	(0.000)	(0.000)	(0.000)
μ_1	**0.099**	**0.098**	**0.096**	**-**	**-**	**-**	**-**	**-**	**-**	**0.099**	**0.097**	**0.096**
	(0.000)	(0.000)	(0.000)	-	-	-	-	-	-	(0.001)	(0.000)	(0.000)
μ_2	**-0.142**	**-0.113**	**-0.084**	**-**	**-**	**-**	**-**	**-**	**-**	**-0.142**	**-0.111**	**-0.080**
	(0.000)	(0.002)	(0.001)	-	-	-	-	-	-	(0.001)	(0.001)	(0.001)
λ_1	**-**	**-**	**-**	**0.049**	**0.049**	**0.050**	**0.049**	**0.049**	**0.049**	**-**	**-**	**-**
	-	-	-	(0.001)	(0.002)	(0.001)	(0.001)	(0.002)	(0.000)	-	-	-
λ_2	**-**	**-**	**-**	**-0.199**	**-0.199**	**-0.196**	**-0.199**	**-0.199**	**-0.196**	**-**	**-**	**-**
	-	-	-	(0.002)	(0.001)	(0.003)	(0.001)	(0.002)	(0.001)	-	-	-
σ_1	**0.199**	**0.199**	**0.196**	**0.200**	**0.199**	**0.197**	**0.199**	**0.199**	**0.197**	**0.200**	**0.199**	**0.196**
	(0.002)	(0.001)	(0.000)	(0.002)	(0.002)	(0.003)	(0.002)	(0.001)	(0.002)	(0.004)	(0.002)	(0.003)
σ_2	**1.000**	**0.999**	**0.999**	**1.000**	**1.000**	**1.002**	**1.000**	**1.000**	**1.002**	**1.000**	**0.999**	**0.999**
	(0.001)	(0.002)	(0.001)	(0.001)	(0.001)	(0.003)	(0.001)	(0.004)	(0.001)	(0.002)	(0.001)	(0.003)
SrB	**0.0172**	**0.0468**	**0.0789**	**0.011**	**0.0111**	**0.0153**	**0.011**	**0.013**	**0.0189**	**0.0181**	**0.0514**	**0.0858**
$\rho = 0$	**0.0098**			**0.0107**			**0.011**			**0.0106**		

	M_5			M_6			M_7			M_8		
ρ	0.1	0.5	0.9	0.1	0.5	0.9	0.1	0.5	0.9	0.1	0.5	0.9
a_1	**2.520**	**2.496**	**2.494**	**2.503**	**2.499**	**2.497**	**2.503**	2.499	**2.496**	**2.503**	**2.499**	**2.497**
	(0.004)	(0.002)	(0.001)	(0.003)	(0.004)	(0.005)	(0.004)	(0.003)	(0.002)	(0.004)	(0.005)	(0.005)
a_2	**-2.197**	**-2.197**	**-2.200**	**-2.194**	**-2.194**	**-2.197**	**-2.194**	**-2.194**	**-2.197**	**-2.194**	**-2.194**	**-2.197**
	(0.006)	(0.004)	(0.005)	(0.005)	(0.004)	(0.003)	(0.004)	(0.006)	(0.007)	(0.007)	(0.004)	(0.004)
μ	**-**	**-**	**-**	**0.100**	**0.098**	**0.097**	**-**	**-**	**-**	**0.095**	**0.093**	**0.092**
	-	-	-	(0.000)	(0.001)	(0.003)	-	-	-	(0.003)	(0.002)	(0.000)
λ	-	-	-	-	-	-	(0.050)	(0.049)	(0.050)	(0.050)	(0.049)	(0.050)
	-	-	-	-	-	-	(0.000)	(0.001)	(0.002)	(0.002)	(0.000)	(0.002)
μ_1	**-**	**-**	**-**	**-**	**-**	**-**	**-**	**-**	**-**	**-**	**-**	**-**
	-	-	-	-	-	-	-	-	-	-	-	-
μ_2	**-**	**-**	**-**	**-**	**-**	**-**	**-**	**-**	**-**	**-**	**-**	**-**
	-	-	-	-	-	-	-	-	-	-	-	-
λ_1	**-**	**-**	**-**	**-**	**-**	**-**	**-**	**-**	**-**	**-**	**-**	**-**
	-	-	-	-	-	-	-	-	-	-	-	-
λ_2	**-**	**-**	**-**	**-**	**-**	**-**	**-**	**-**	**-**	**-**	**-**	**-**
	-	-	-	-	-	-	-	-	-	-	-	-
σ_1	**0.199**	**0.199**	**0.197**	**0.200**	**0.199**	**0.197**	**0.200**	**0.199**	**0.197**	**0.199**	**0.199**	**0.197**
	(0.001)	(0.000)	(0.001)	(0.001)	(0.002)	(0.001)	(0.000)	(0.000)	(0.001)	(0.001)	(0.002)	(0.001)
σ_2	**1.000**	**1.000**	**1.002**	**1.000**	**1.000**	**1.002**	**1.000**	**1.000**	**1.002**	**1.000**	**1.000**	**1.002**
	(0.001)	(0.000)	(0.001)	(0.001)	(0.002)	(0.001)	(0.000)	(0.001)	(0.001)	(0.002)	(0.002)	(0.001)
SrB	**0.0031**	**0.0086**	**0.0123**	**0.0092**	**0.0106**	**0.0148**	**0.0093**	**0.0095**	**0.0119**	**0.0147**	**0.0165**	**0.0202**
$\rho = 0$	**0.003**			**0.0091**			**0.0091**			**0.0145**		

Table D.12: Monte Carlo Simulation: The table reports QML estimates (in boldface) averaged over $M = 1'000$ simulation runs for the exogenous estimator when the state is endogenous, i.e. $\rho \in \{0.1, 0.5, 0.9\}$. Time series length is $T = 8'000$. Averaged standard errors are given below the averaged Monte Carlo estimates and are based on numerically evaluating second order derivatives of the log-likelihood function. The row '$\rho = 0$' refers to the SrB test statistics when there is no endogeneity in the data generated process.

D.1.5 Empirical Estimation Results

	M_1		M_2		M_3		M_4	
	Endo	Exo	Endo	Exo	Endo	Exo	Endo	Exo
a_1	**2.8474**	**2.7852**	**2.7834**	**2.699**	**2.7823**	**2.7377**	**2.7863**	**2.7265**
	0.0374	0.0185	0.1146	0.0047	0.0126	0.0167	0.068	0.0618
a_2	**-1.4589**	**-1.5311**	**-1.6106**	**-1.3837**	**-1.6166**	**-1.5436**	**-1.4084**	**-1.3385**
	0.009	0.0142	0.0186	0.0013	0.0522	0.0184	0.003	0.00692
μ	-	-	-	-	**-0.0001**	**-0.0001**	-	-
	-	-	-	-	1.82E-06	1.27E-06	-	-
λ	-	-	-	-	-	-	**-0.2694**	**-0.2835**
	-	-	-	-	-	-	0.0095	1.85E-05
μ_1	**-0.0001**	**-0.0001**	-	-	-	-	**-0.0001**	**-0.0001**
	4.29E-05	1.76E-05	-	-	-	-	4.70E-06	0.012
μ_2	**-0.0036**	**-0.0008**	-	-	-	-	**-0.0024**	**0.1246**
	0.0007	0.0003	-	-	-	-	0.0002	0.0227
λ_1	**-**	**-**	**-0.2818**	**-0.2692**	**-0.2818**	**-0.2764**	**-**	**-**
	-	-	0.0184	0.0003	0.0003	0.0113	-	-
λ_2	**-**	**-**	**0.094**	**0.1838**	**0.0929**	**0.1034**	**-**	**-**
	-	-	0.0193	0.0049	0.0032	0.0149	-	-
σ_1	**0.0083**	**0.0085**	**0.0081**	**0.0083**	**0.0081**	**0.0099**	**0.0081**	**0.0091**
	2.33E-05	1.08E-06	0.001	5.74E-07	4.53E-06	6.72E-06	0.0001	2.16E-05
σ_2	**0.0206**	**0.0194**	**0.0177**	**0.0259**	**0.0178**	**0.0181**	**0.0216**	**0.0201**
	0.0002	0.0001	0.0001	7.60E-06	0.0001	1.50E-05	0.0052	0.0009
ρ	**0.3517**	**-**	**-0.2805**	**-**	**-0.2888**	**-**	**0.2162**	**-**
	0.0361	-	0.0124	-	0.038	-	0.005247	-
$\log(\hat{\mathcal{L}})$	**-26'822.6**	**-26'225.8**	**-26'761.0**	**-26'758.4**	**-26'763.0**	**-26'760.3**	**-26'816.0**	**-26'832.0**

	M_5		M_6		M_7		M_8	
	Endo	Exo	Endo	Exo	Endo	Exo	Endo	Exo
a_1	**3.8252**	**2.7802**	**3.9592**	**2.7318**	**2.7038**	**2.7769**	**2.7989**	**2.7592**
	0.018	0.0099	0.0022	0.2786	0.0168	0.005	0.0588	0.1248
a_2	**-0.1243**	**-1.114**	**-0.5246**	**-1.2507**	**-1.21**	**-1.5197**	**-1.5798**	**-1.2315**
	0.0632	0.0054	0.0014	0.01426	0.0232	0.0022	0.0271	0.48
μ	-	-	**0.0003**	**1.00E-06**	**-**	**-**	**-0.0002**	**-0.0001**
	-	-	1.93E-07	0.04385	-	-	1.76E-05	9.11E-09
λ	-	-	-	-	**-0.2468**	**-0.2621**	**-0.2647**	**-0.2694**
	-	-	-	-	0.0007	0.0007	0.0009	0.0125
μ_1	-	-	-	-	-	-	-	-
	-	-	-	-	-	-	-	-
μ_2	-	-	-	-	-	-	-	-
	-	-	-	-	-	-	-	-
λ_1	-	-	-	-	-	-	-	-
	-	-	-	-	-	-	-	-
λ_2	-	-	-	-	-	-	-	-
	-	-	-	-	-	-	-	-
σ_1	**0.0147**	**0.0088**	**0.0146**	**0.0086**	**0.0084**	**0.0081**	**0.0081**	**0.0081**
	2.82E-06	1.34E-06	1.35E-06	0.0232	5.36E-06	1.15E-06	1.36E-05	0.0002
σ_2	**1.9791**	**0.0325**	**2.0032**	**0.0292**	**0.0305**	**0.0202**	**0.0196**	**0.0235**
	0.0112	1.78E-05	3.81E-05	0.1417	0.0001	5.74E-05	4.00E-05	4.69E-06
ρ	**-0.9003**	-	**0.9436**	-	**-0.1406**	**-**	**-0.2594**	-
	0.0214	-	0.0006	-	0.0073	-	0.0315	-
$\log(\hat{\mathcal{L}})$	**-1'682.6**	**-26'225.2**	**-1'684.2**	**-26'188.9**	**-26'434.3**	**-26'714.7**	**-26'739.9**	**-26'804.7**

Table D.13: Estimation results at sampling frequency 10 *sec.* for FX EUR/USD exchange rate. The table reports (quasi-) maximum likelihood estimates (in boldface) with corresponding standard errors given below. The columns labeled 'Endo' ('Exo') refer to the endogenous (exogenous) estimator, respectively. The estimation period starts on January 2nd 5 pm and contains for each model 8′000 observations. $\log(\mathcal{L})$ denotes the estimated log-likelihood value of each model.

	M_1		M_2		M_3		M_4	
	Endo	Exo	Endo	Exo	Endo	Exo	Endo	Exo
a_1	**1.5396**	**1.539**	**1.5014**	**1.4756**	**1.5088**	**1.5086**	**1.5257**	**1.517**
	0.0007	0.0185	0.0815	0.0017	0.0938	0.0007	0.0682	0.0047
a_2	**-0.8373**	**-0.8347**	**-1.0736**	**-1.0361**	**-0.9419**	**-0.9414**	**-0.7793**	**-0.8509**
	0.0003	0.0142	0.2096	0.002	0.0116	0.0015	0.0161	0.0063
μ	-	-	-	-	**-4.13E-05**	**-4.94E-05**	-	-
	-	-	-	-	0.0395	8.29E-07	-	-
λ	-	-	-	-	-	-	**-0.0783**	**0.0003**
	-	-	-	-	-	-	0.0065	1.21E-05
μ_1	**0.0007**	**0.0005**	-	-	-	-	**0.0006**	**-0.122**
	0.0106	1.76E-05	-	-	-	-	0.1146	0.0004
μ_2	**-0.0024**	**-0.0006**	-	-	-	-	**-0.0023**	**0.036**
	0.0025	0.0003	-	-	-	-	0.0204	0.001
λ_1	-	-	**-0.1264**	**-0.1274**	**-0.1265**	**-0.1265**	-	-
	-	-	0.043	0.0003	0.0141	0.0004	-	-
λ_2	-	-	**0.0097**	**0.0057**	**0.0171**	**0.0173**	-	-
	-	-	0.0684	0.0007	0.027	0.0007	-	-
σ_1	**0.0245**	**0.0245**	**0.0242**	**0.0245**	**0.0231**	**0.0231**	**0.0245**	**0.0237**
	3.25E-06	1.08E-06	0.0001	1.13E-05	0.0002	1.27E-05	0.0006	2.36E-05
σ_2	**0.0745**	**0.0746**	**0.0677**	**0.0687**	**0.0662**	**0.0662**	**0.076**	**0.0698**
	1.43E-05	0.0001	0.001	3.16E-05	0.0002	4.51E-05	0.0004	3.66E-05
ρ	**0.0402**	-	**0.0671**	-	**0.0092**	-	**0.0377**	-
	0.0002	-	0.0233	-	0.0036	-	0.0364	-
$\log(\hat{\mathcal{L}})$	**-15'389.4**	**-15'547.2**	**-14'907.1**	**-14'792.9**	**-15'304.1**	**-15'547.2**	**-15'767.2**	**-15'738.5**

	M_5		M_6		M_7		M_8	
	Endo	Exo	Endo	Exo	Endo	Exo	Endo	Exo
a_1	**1.5227**	**1.5399**	**1.5266**	**1.5195**	**1.5279**	**1.4849**	**1.4861**	**1.4845**
	0.0186	0.0027	0.0012	0.0017	0.0094	0.0012	0.0026	0.0013
a_2	**-1.1192**	**-1.0063**	**-1.1069**	**-1.0079**	**-1.0272**	**-1.0532**	**-0.9004**	**-0.898**
	0.0566	0.0045	0.002	0.001	0.0193	0.0008	0.0027	0.0003
μ	-	-	**0.0001**	**1.02E-06**	-	-	**0.0002**	**0.0002**
	-	-	9.29E-06	3.88E-07	-	-	6.57E-07	3.51E-06
λ	-	-	-	-	**-0.0796**	**-0.08**	**-0.0789**	**-0.0786**
	-	-	-	-	0.0004	0.0002	0.0001	0.0002
μ_1	-	-	-	-	-	-	-	-
	-	-	-	-	-	-	-	-
μ_2	-	-	-	-	-	-	-	-
	-	-	-	-	-	-	-	-
λ_1	-	-	-	-	-	-	-	-
	-	-	-	-	-	-	-	-
λ_2	-	-	-	-	-	-	-	-
	-	-	-	-	-	-	-	-
σ_2	**0.0236**	**0.0232**	**0.0232**	**0.0232**	**0.0237**	**0.0245**	**0.0228**	**0.0228**
	0.0001	5.87E-06	9.25E-06	2.06E-05	3.81E-05	1.14E-05	9.52E-06	1.66E-05
σ_2	**0.0662**	**0.0656**	**0.0645**	**0.0647**	**0.066**	**0.0687**	**0.0648**	**0.0648**
	0.0005	3.98E-05	0.0002	4.69E-06	0.0003	3.13E-05	2.34E-05	2.23E-05
ρ	**0.0736**	-	**0.0676**	-	**0.0454**	-	**0.0347**	-
	0.0153	-	0.0018	-	0.0022	-	9.75E-04	-
$\log(\hat{\mathcal{L}})$	**-15'059.5**	**-15'305.3**	**-15'727.5**	**-15'502.6**	**-15'324.6**	**-14'781.9**	**-15'724.3**	**-15'723.7**

Table D.14: Estimation results at sampling frequency 20 *min.* for FX EUR/USD exchange rate. The table reports (quasi-) maximum likelihood estimates (in boldface) with corresponding standard errors given below. The columns labeled 'Endo' ('Exo') refer to the endogenous (exogenous) estimator, respectively. The estimation period starts on January 2nd 5 pm and contains for each model 8′000 observations. $\log(\mathcal{L})$ denotes the estimated log-likelihood value of each model.

Appendix E

Additional Graphs: Higher Order Serial Correlation Plots other Currency Pairs

E.1 EUR/CHF exchange rate

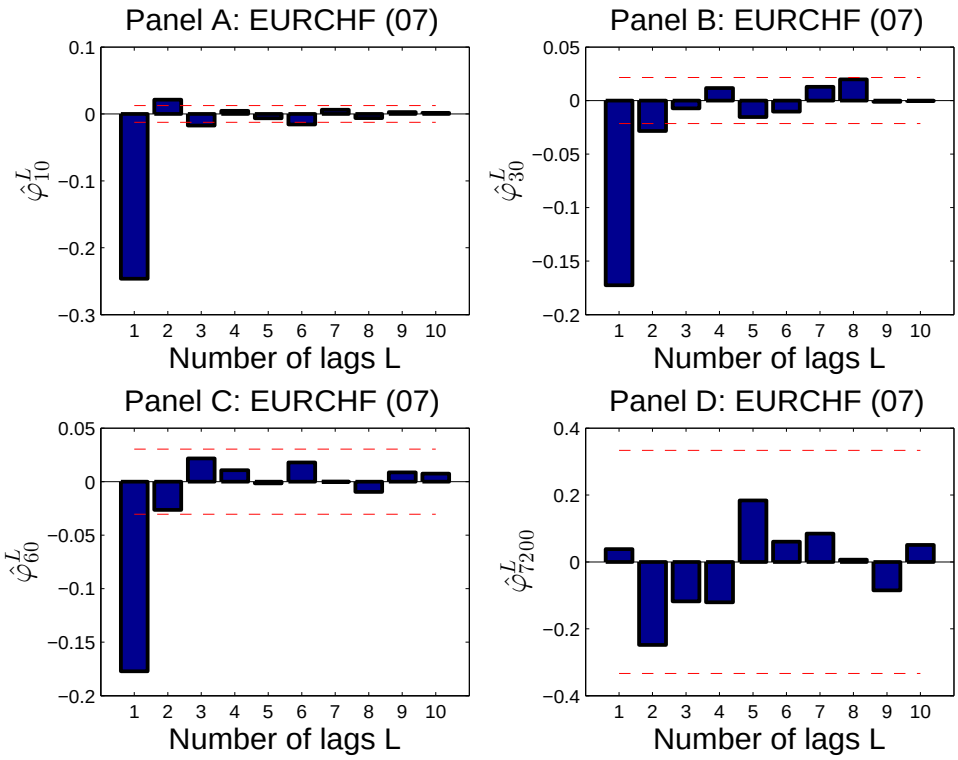

Figure E.1: The figure shows the estimated autocorrelation coefficient $\hat{\varphi}_m^{(L)}$ for lag values $L = 1, \ldots, 10$ for the EUR/CHF spot exchange rate. The selected sampling frequencies are $m = 10sec.$, $30sec.$ $1min.$ and $2hr.$, respectively. Redlines represent approximate $\alpha = 5\%$ confidence intervals as given in Box et al. (1994). Log-return series were constructed using Mid-quotes of the currency pairs EUR/USD, EUR/CHF, EUR/GBP and EUR/JPY of the year 2007 using previous tick price recording, starting on January 2nd 5pm.

E.2 EUR/GBP exchange rate

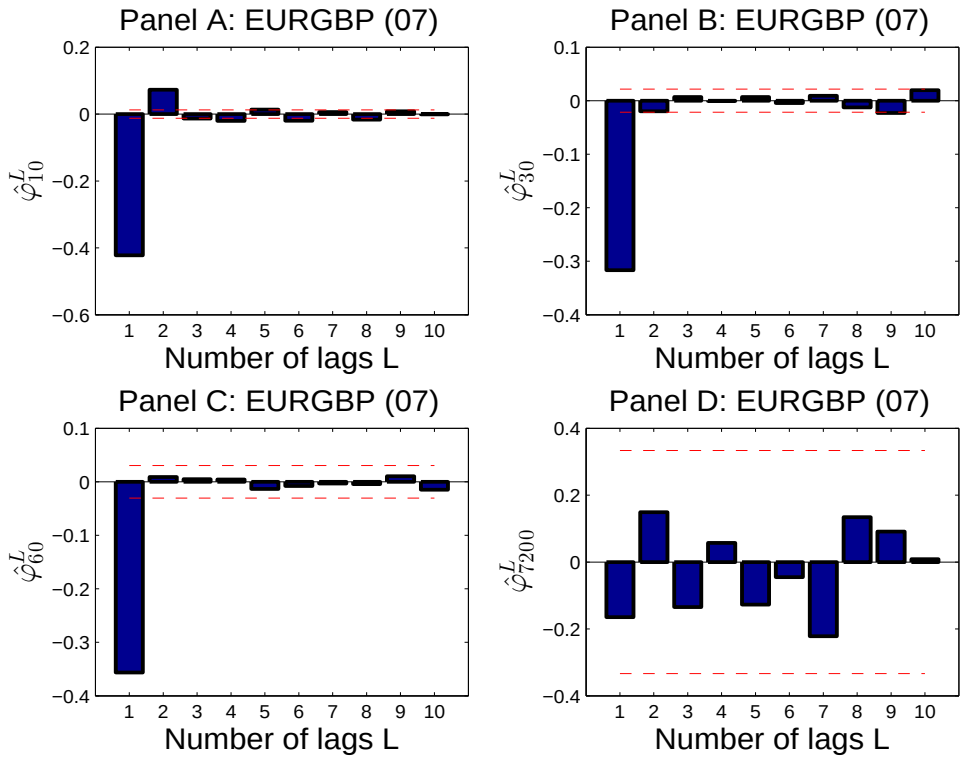

Figure E.2: The figure shows the estimated autocorrelation coefficient $\hat{\varphi}_m^{(L)}$ for lag values $L = 1, \ldots, 10$ for the EUR/GBP spot exchange rate. The selected sampling frequencies are $m = 10sec.$, $30sec.$ $1min.$ and $2hr.$, respectively. Redlines represent approximate $\alpha = 5\%$ confidence intervals as given in Box et al. (1994). Log-return series were constructed using Mid-quotes of the currency pairs EUR/USD, EUR/CHF, EUR/GBP and EUR/JPY of the year 2007 using previous tick price recording, starting on January 2nd 5pm.

E.3 EUR/JPY exchange rate

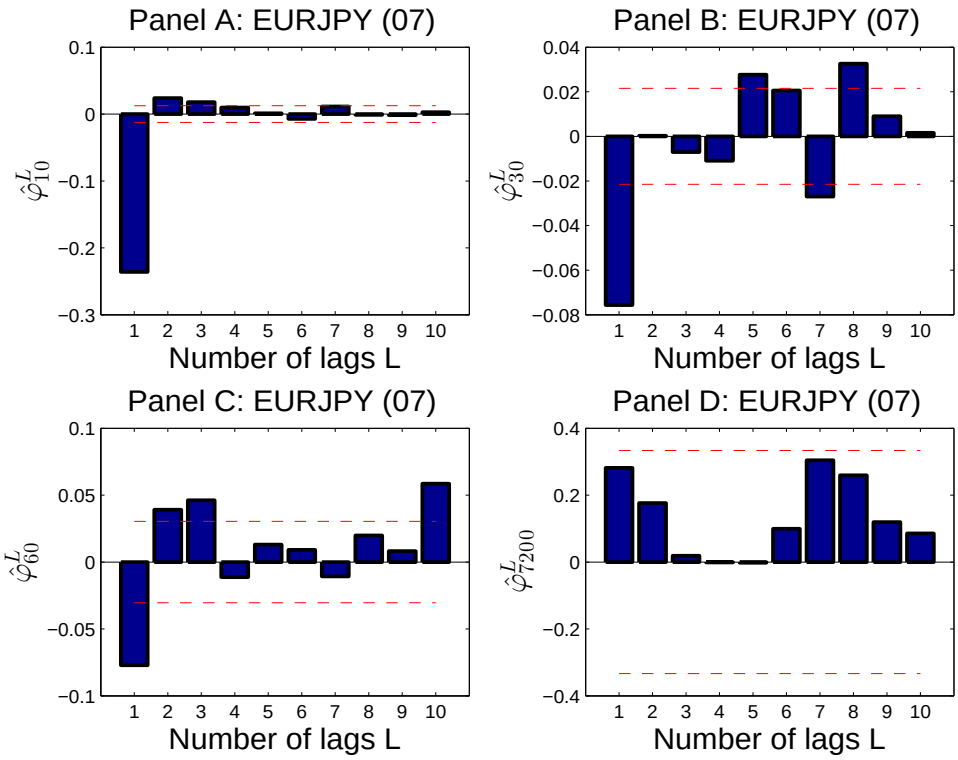

Figure E.3: The figure shows the estimated autocorrelation coefficient $\hat{\varphi}_m^{(L)}$ for lag values $L = 1, \ldots, 10$ for the EUR/JPY spot exchange rate. The selected sampling frequencies are $m = 10sec.$, $30sec.$ $1min.$ and $2hr.$, respectively. Redlines represent approximate $\alpha = 5\%$ confidence intervals as given in Box et al. (1994). Log-return series were constructed using Mid-quotes of the currency pairs EUR/USD, EUR/CHF, EUR/GBP and EUR/JPY of the year 2007 using previous tick price recording, starting on January 2nd 5pm.

Appendix F

Additional Graphs: Endogeneity Plots for other Currency Pairs

F.1 EUR/CHF exchange rate

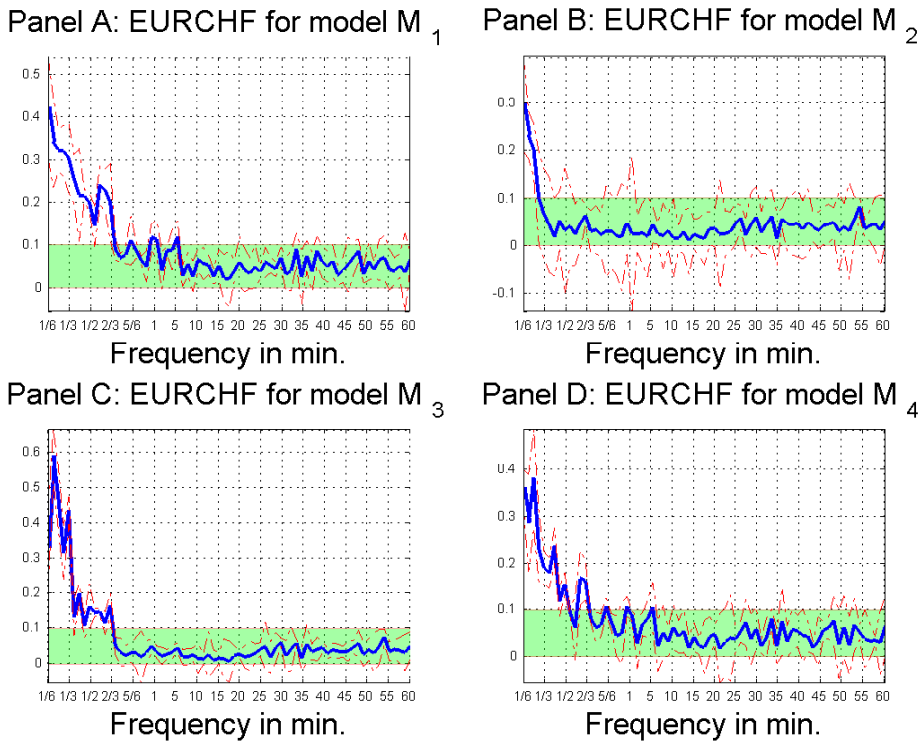

Figure F.1: EUR/CHF spot exchange rate: Average absolute endogeneity level $\bar{\hat{\rho}}^{W}_{m,T} = \frac{1}{\mathcal{S}} \sum_{s=1}^{\mathcal{S}} |\hat{\rho}^{W}_{m,L,s}|$ for models $M_1 - M_4$ with corresponding 95% confidence intervals. The estimation period starts on January 2nd 5 pm and contains for each model 8'000 observations with rolling window of $\mathcal{W}$=200 for a given sampling frequency $m = \{5sec, \ldots, 55sec, 1min, 2min, \ldots, 1hr\}$.

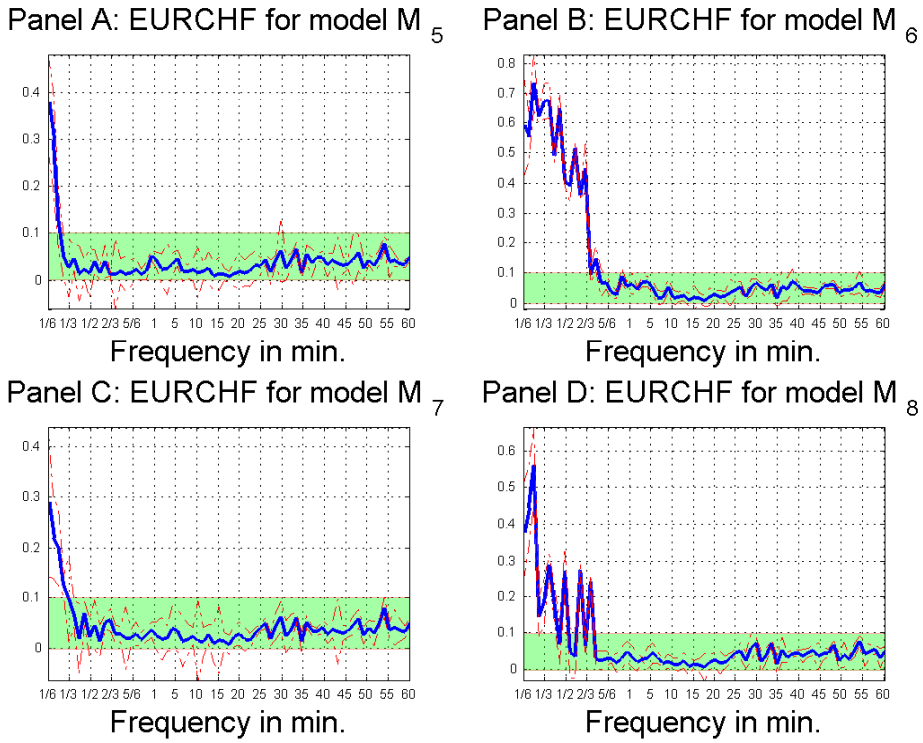

Figure F.2: EUR/CHF spot exchange rate: Average absolute endogeneity level $\bar{\hat{\rho}}^{W}_{m,T} = \frac{1}{\mathcal{S}} \sum_{s=1}^{\mathcal{S}} |\hat{\rho}^{W}_{m,L,s}|$ for models $M_5 - M_8$ with corresponding 95% confidence intervals. The estimation period starts on January 2nd 5 pm and contains for each model 8'000 observations with rolling window of $\mathcal{W}$=200 for a given sampling frequency $m = \{5sec, \ldots, 55sec, 1min, 2min, \ldots, 1hr\}$.

F.2 EUR/GBP exchange rate

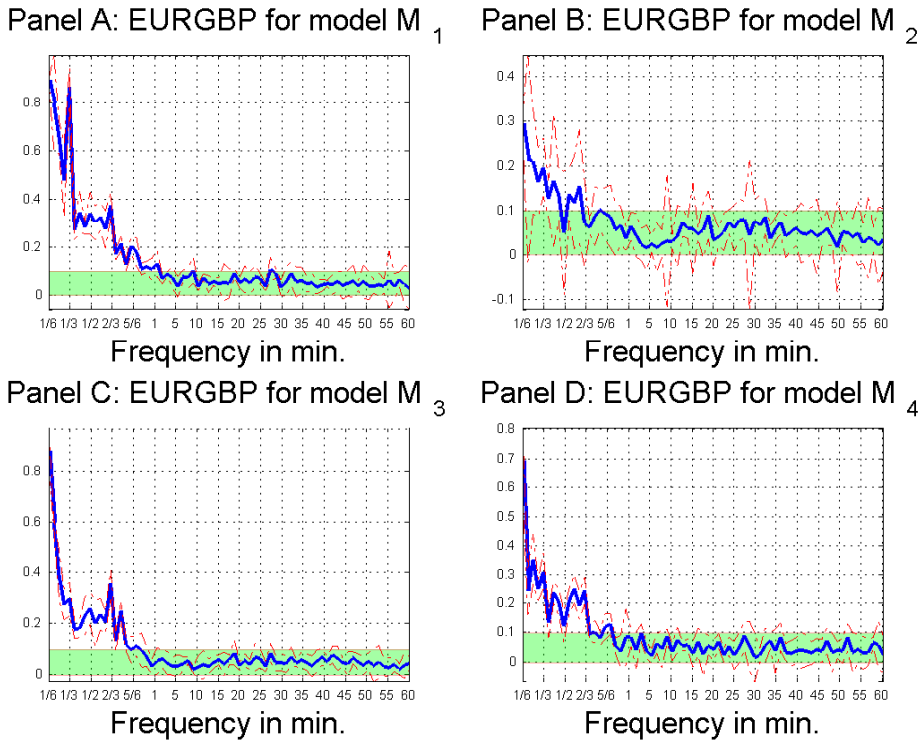

Figure F.3: EUR/GBP spot exchange rate: Average absolute endogeneity level $\bar{\hat{\rho}}^{W}_{m,T} = \frac{1}{\mathcal{S}} \sum_{s=1}^{\mathcal{S}} |\hat{\rho}^{W}_{m,L,s}|$ for models $M_1 - M_4$ with corresponding 95% confidence intervals. The estimation period starts on January 2nd 5 pm and contains for each model 8'000 observations with rolling window of $\mathcal{W}$=200 for a given sampling frequency $m = \{5sec, \ldots, 55sec, 1min, 2min, \ldots, 1hr\}$.

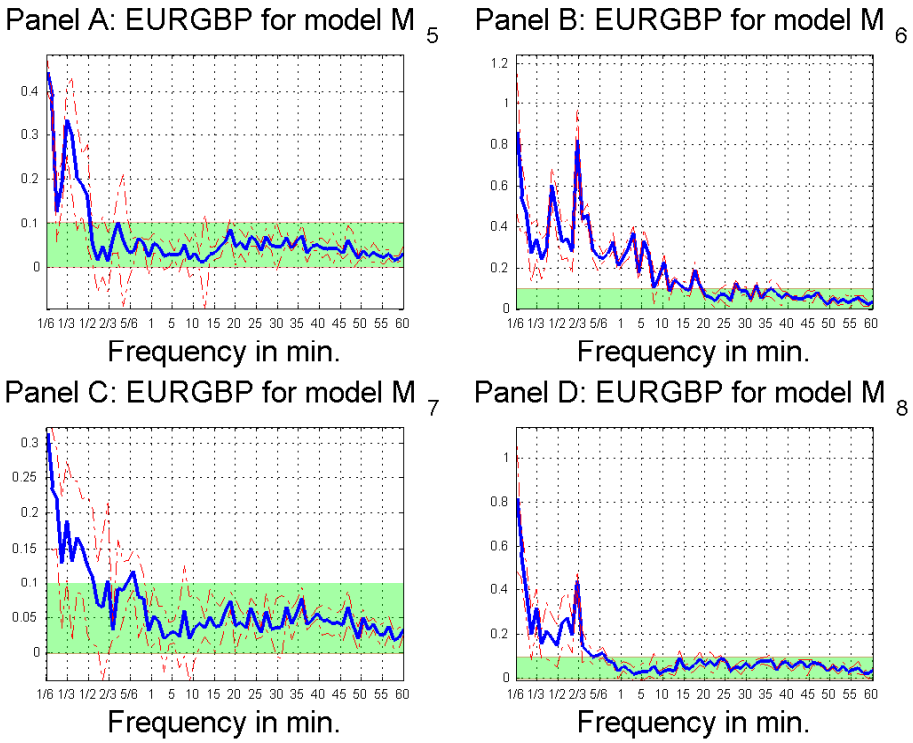

Figure F.4: EUR/GBP spot exchange rate: Average absolute endogeneity level $\bar{\hat{\rho}}^{W}_{m,T} = \frac{1}{\mathcal{S}} \sum_{s=1}^{\mathcal{S}} |\hat{\rho}^{W}_{m,L,s}|$ for models $M_5 - M_8$ with corresponding 95% confidence intervals. The estimation period starts on January 2nd 5 pm and contains for each model 8'000 observations with rolling window of $\mathcal{W}$=200 for a given sampling frequency $m = \{5sec, \ldots, 55sec, 1min, 2min, \ldots, 1hr\}$.

F.3 EUR/JPY exchange rate

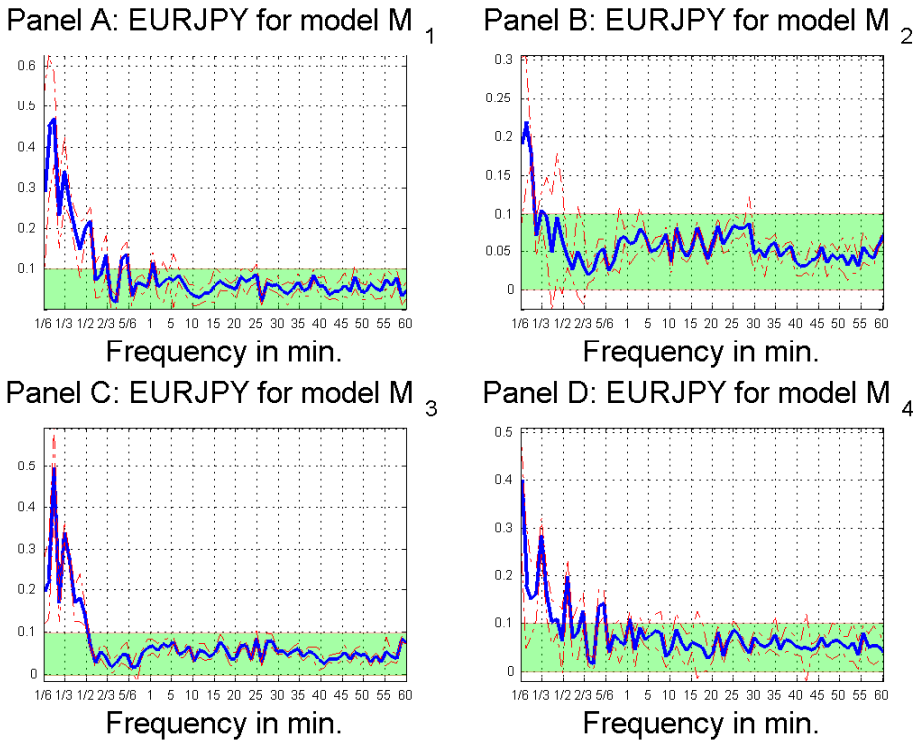

Figure F.5: EUR/JPY spot exchange rate: Average absolute endogeneity level $\bar{\hat{\rho}}^{W}_{m,T} = \frac{1}{\mathcal{S}} \sum_{s=1}^{\mathcal{S}} |\hat{\rho}^{W}_{m,L,s}|$ for models $M_1 - M_4$ with corresponding 95% confidence intervals. The estimation period starts on January 2nd 5 pm and contains for each model 8'000 observations with rolling window of $\mathcal{W}$=200 for a given sampling frequency $m = \{5sec, \ldots, 55sec, 1min, 2min, \ldots, 1hr\}$.

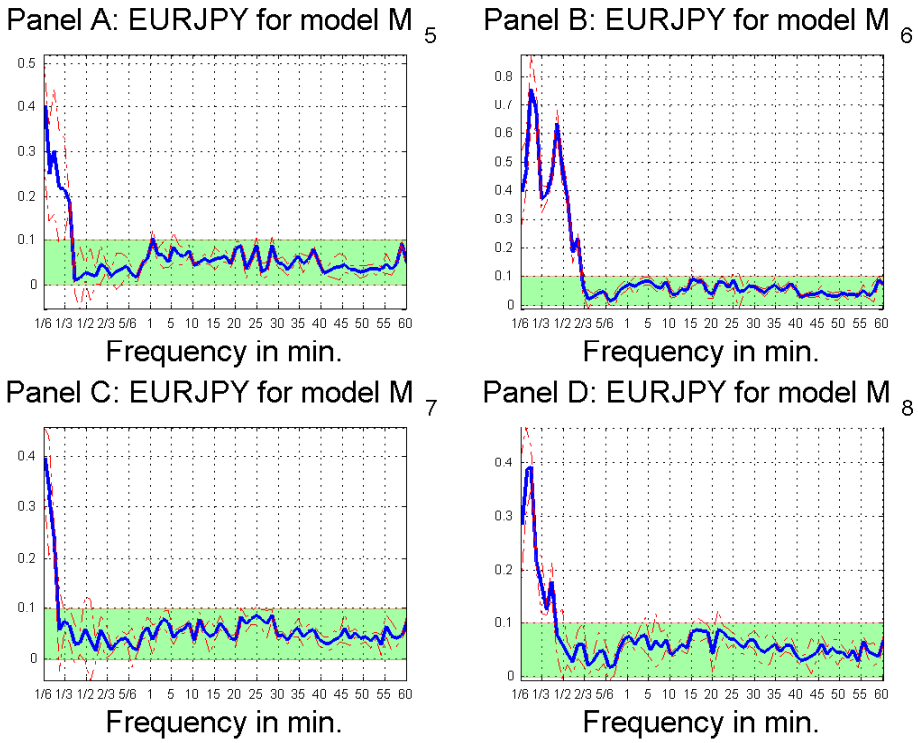

Figure F.6: EUR/JPY spot exchange rate: Average absolute endogeneity level $\bar{\hat{\rho}}^{W}_{m,T} = \frac{1}{\mathcal{S}} \sum_{s=1}^{\mathcal{S}} |\hat{\rho}^{W}_{m,L,s}|$ for models $M_5 - M_8$ with corresponding 95% confidence intervals. The estimation period starts on January 2nd 5 pm and contains for each model 8'000 observations with rolling window of $\mathcal{W}$=200 for a given sampling frequency $m = \{5sec, \ldots, 55sec, 1min, 2min, \ldots, 1hr\}$.

Appendix G

Additional Graphs: Endogeneity Plots for shorter Time Series Length

G.1 EUR/USD exchange rate

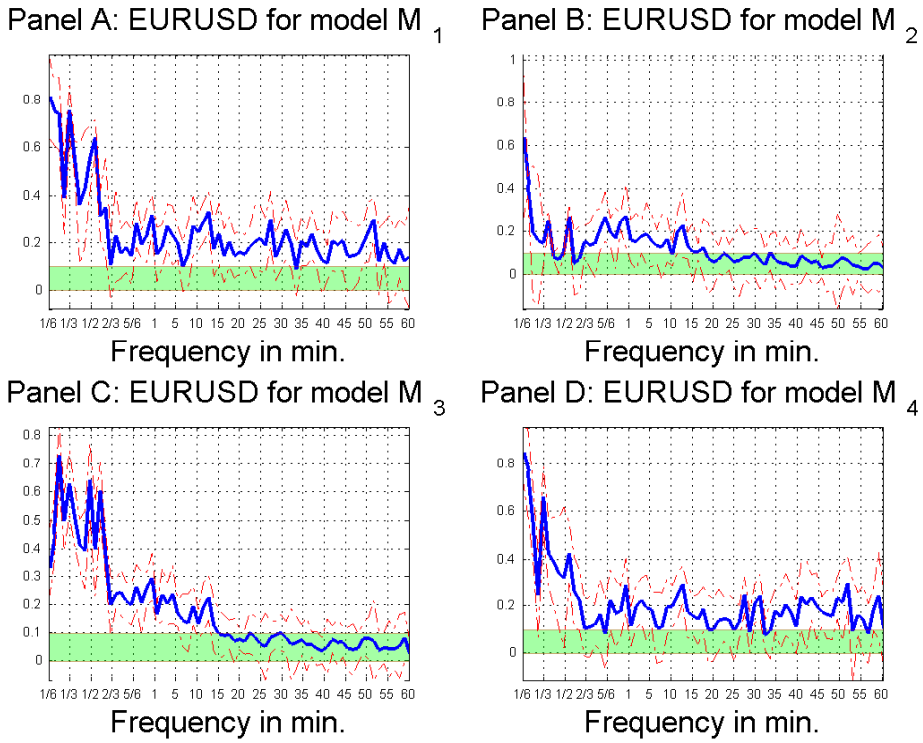

Figure G.1: EUR/USD spot exchange rate: Average absolute endogeneity level $\bar{\hat{\rho}}^{W}_{m,T} = \frac{1}{\mathcal{S}} \sum_{s=1}^{\mathcal{S}} |\hat{\rho}^{W}_{m,L,s}|$ for models $M_1 - M_4$ with corresponding 95% confidence intervals. The estimation period starts on January 2nd 5 pm and contains for each model 800 observations with rolling window of $\mathcal{W}$=20 for a given sampling frequency $m = \{5sec, \ldots, 55sec, 1min, 2min, \ldots, 1hr\}$.

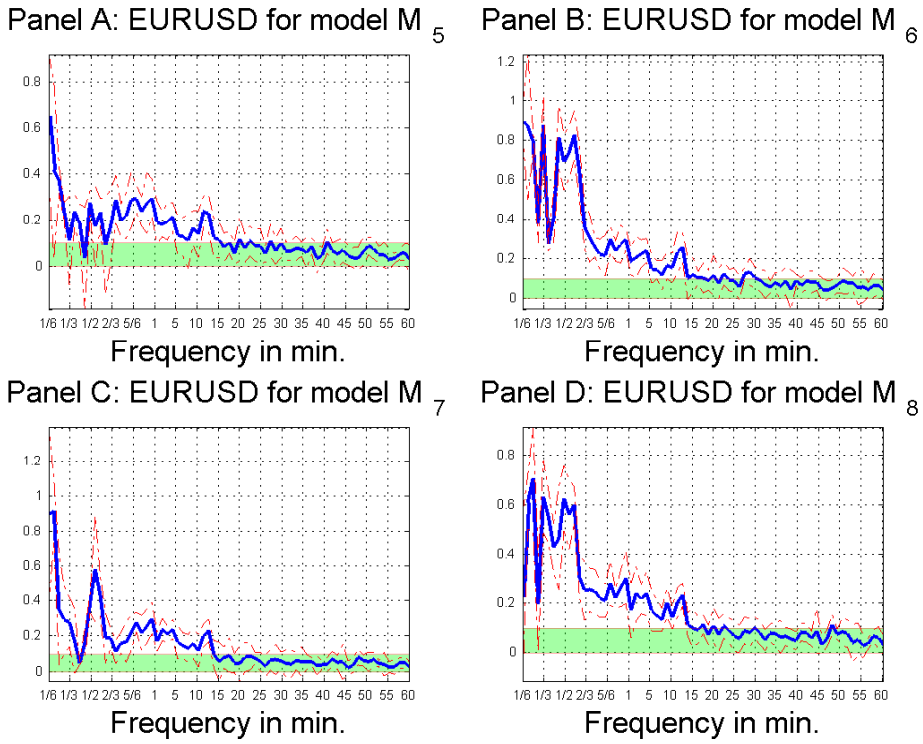

Figure G.2: EUR/USD spot exchange rate: Average absolute endogeneity level $\bar{\hat{\rho}}_{m,L} = \frac{1}{\mathcal{S}} \sum_{s=1}^{\mathcal{S}} |\hat{\rho}_{m,L,s}|$ for models $M_5 - M_8$ with corresponding 95% confidence intervals. The estimation period starts on January 2nd and contains for each model 8'000 observations with rolling window of $\mathcal{W}$=20 for a given sampling frequency $m = \{5sec, \ldots, 55sec, 1min, 2min, \ldots, 1hr\}$.

G.2 EUR/CHF exchange rate

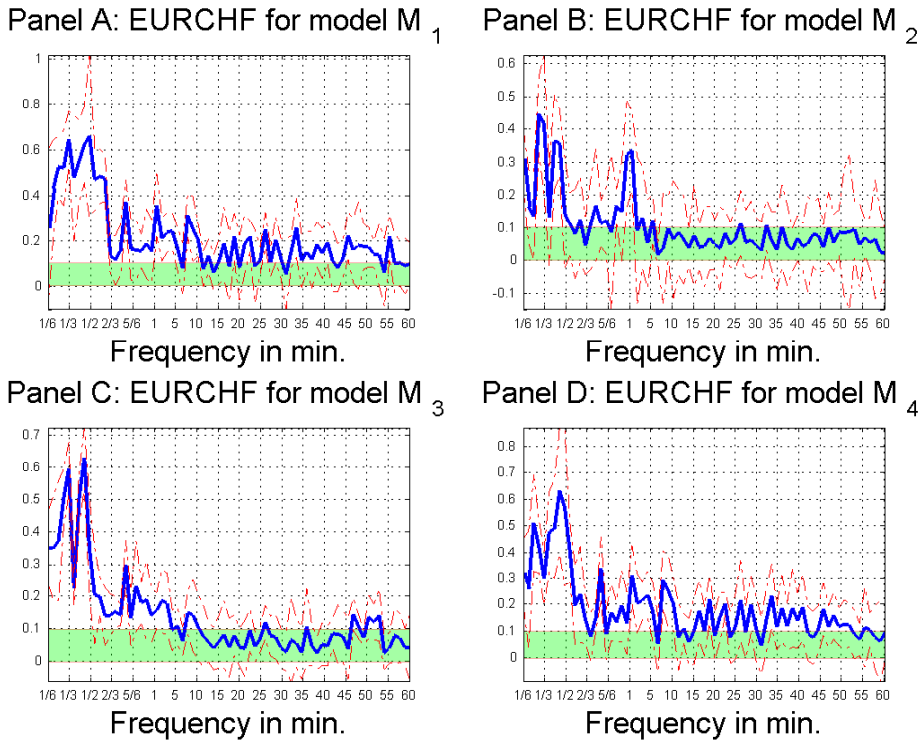

Figure G.3: EUR/CHF spot exchange rate: Average absolute endogeneity level $\bar{\hat{\rho}}^{W}_{m,T} = \frac{1}{\mathcal{S}} \sum_{s=1}^{\mathcal{S}} |\hat{\rho}^{W}_{m,L,s}|$ for models $M_1 - M_4$ with corresponding 95% confidence intervals. The estimation period starts on January 2nd 5 pm and contains for each model 8000 observations with rolling window of $\mathcal{W}$=20 for a given sampling frequency $m = \{5sec, \ldots, 55sec, 1min, 2min, \ldots, 1hr\}$.

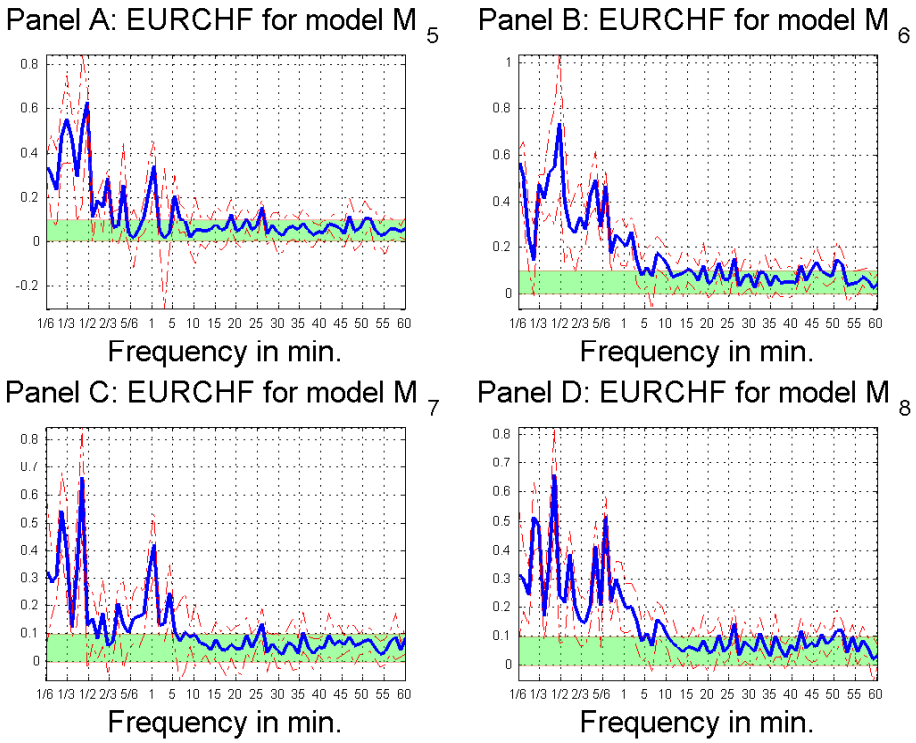

Figure G.4: EUR/CHF spot exchange rate: Average absolute endogeneity level $\bar{\hat{\rho}}^{W}_{m,T} = \frac{1}{\mathcal{S}} \sum_{s=1}^{\mathcal{S}} |\hat{\rho}^{W}_{m,L,s}|$ for models $M_5 - M_8$ with corresponding 95% confidence intervals. The estimation period starts on January 2nd 5 pm and contains for each model 8000 observations with rolling window of $\mathcal{W}$=20 for a given sampling frequency $m = \{5sec, \ldots, 55sec, 1min, 2min, \ldots, 1hr\}$.

G.3 EUR/GBP exchange rate

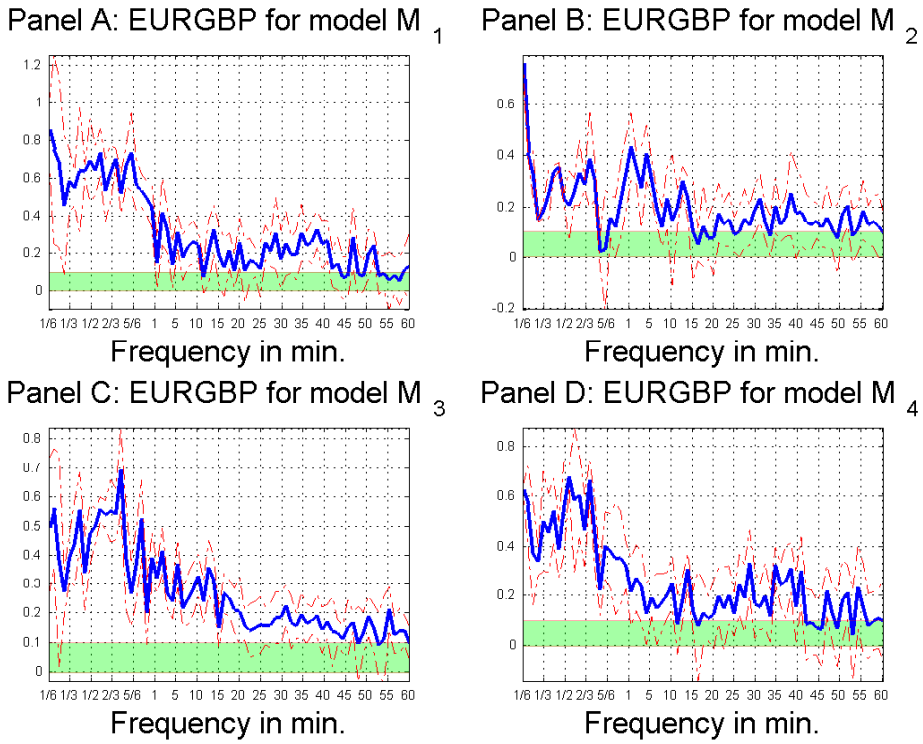

Figure G.5: EUR/GBP spot exchange rate: Average absolute endogeneity level $\bar{\hat{\rho}}^{W}_{m,T} = \frac{1}{\mathcal{S}} \sum_{s=1}^{\mathcal{S}} |\hat{\rho}^{W}_{m,L,s}|$ for models $M_1 - M_4$ with corresponding 95% confidence intervals. The estimation period starts on January 2nd 5 pm and contains for each model 8000 observations with rolling window of $\mathcal{W}$=20 for a given sampling frequency $m = \{5sec, \ldots, 55sec, 1min, 2min, \ldots, 1hr\}$.

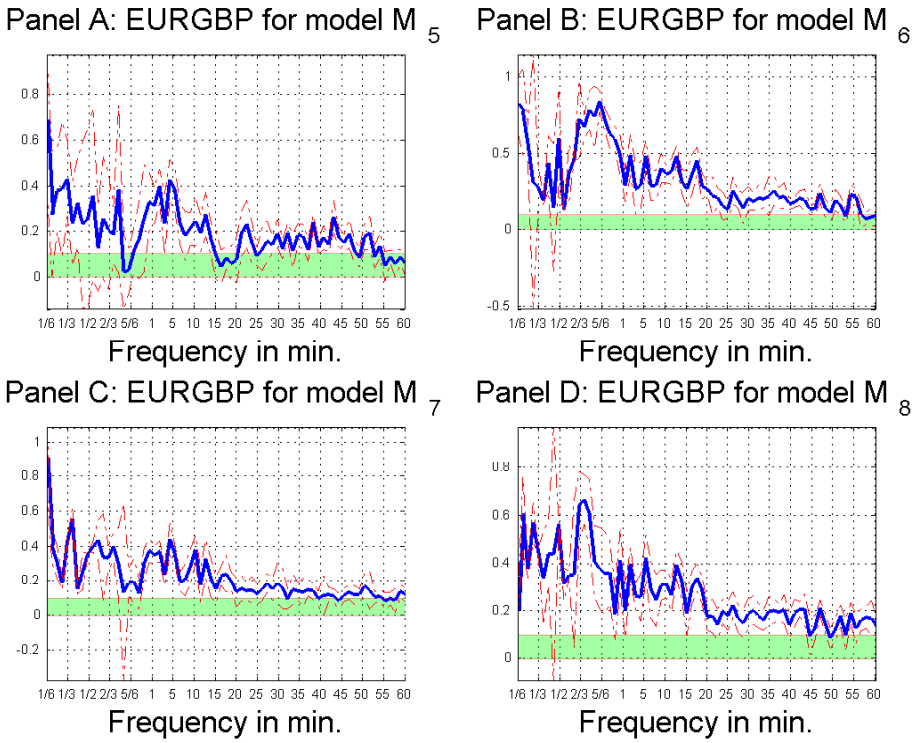

Figure G.6: EUR/GBP spot exchange rate: Average absolute endogeneity level $\bar{\hat{\rho}}^{W}_{m,T} = \frac{1}{\mathcal{S}} \sum_{s=1}^{\mathcal{S}} |\hat{\rho}^{W}_{m,L,s}|$ for models $M_5 - M_8$ with corresponding 95% confidence intervals. The estimation period starts on January 2nd 5 pm and contains for each model 800 observations with rolling window of $\mathcal{W}$=20 for a given sampling frequency $m = \{5sec, \ldots, 55sec, 1min, 2min, \ldots, 1hr\}$.

G.4 EUR/JPY exchange rate

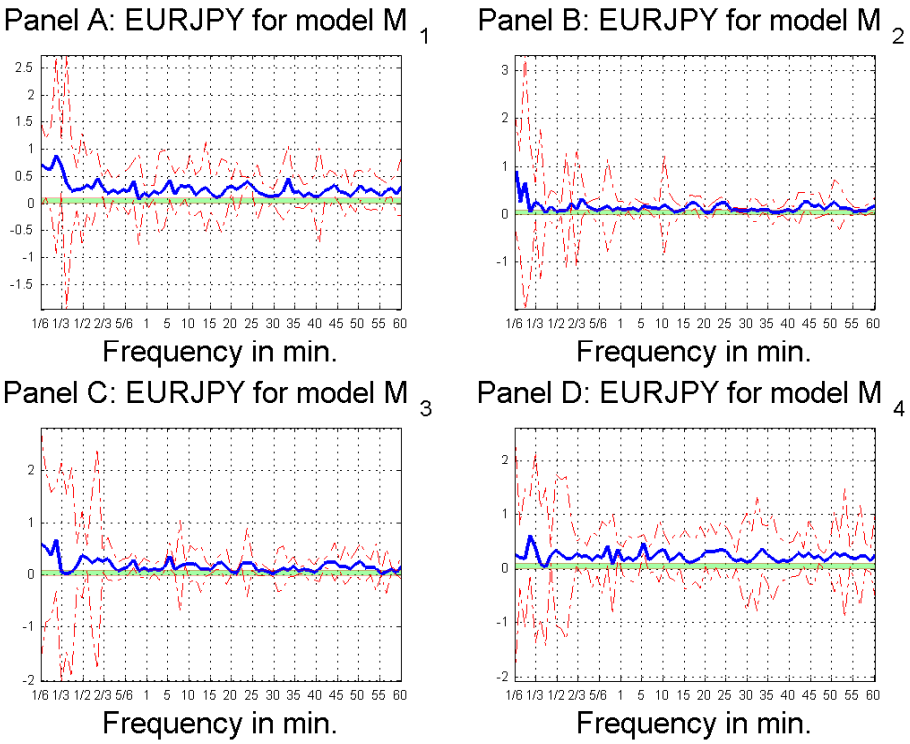

Figure G.7: EUR/JPY spot exchange rate: Average absolute endogeneity level $\bar{\hat{\rho}}^{W}_{m,T} = \frac{1}{\mathcal{S}} \sum_{s=1}^{\mathcal{S}} |\hat{\rho}^{W}_{m,L,s}|$ for models $M_1 - M_4$ with corresponding 95% confidence intervals. The estimation period starts on January 2nd 5 pm and contains for each model 8000 observations with rolling window of $\mathcal{W}$=20 for a given sampling frequency $m = \{5sec, \ldots, 55sec, 1min, 2min, \ldots, 1hr\}$.

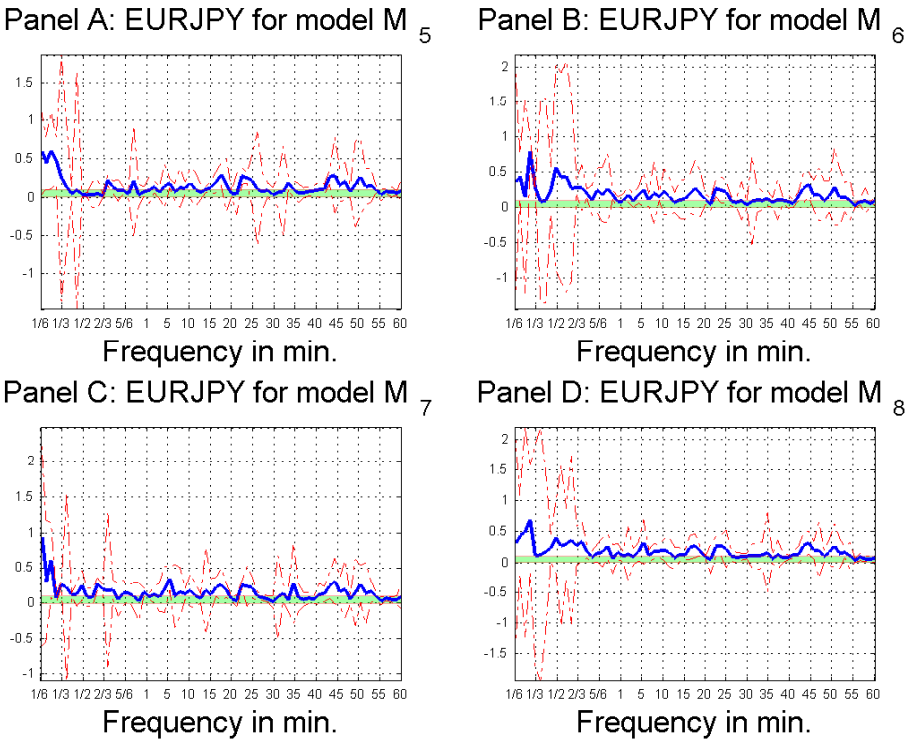

Figure G.8: EUR/JPY spot exchange rate: Average absolute endogeneity level $\bar{\hat{\rho}}^{W}_{m,T} = \frac{1}{\mathcal{S}} \sum_{s=1}^{\mathcal{S}} |\hat{\rho}^{W}_{m,L,s}|$ for models $M_5 - M_8$ with corresponding 95% confidence intervals. The estimation period starts on January 2nd 5 pm and contains for each model 800 observations with rolling window of $\mathcal{W}$=20 for a given sampling frequency $m = \{5sec, \ldots, 55sec, 1min, 2min, \ldots, 1hr\}$.

Bibliography

Aase, K. (1984), 'Optimum portfolio diversification in a general continuous-time model', *Stochastic Processes and Their Applications* **18**, 81–98.

Aït-Sahalia, Y., Cacho-Diaz, J. & Hurd, T. (2009), 'Portfolio choice with jumps: A closed-form solution', *Annals of Applied Probability* **19**, 556–584.

Aït-Sahalia, Y. & Hurd, T. R. (2016), 'Portfolio choice in markets with contagion', *Journal of Financial Econometrics* **14**, 1–28.

Amihud, Y. & Mendelson, H. (1987), 'Trading mechanisms and stock returns: An empirical investigation', *Journal of Finance* **42**(3), pp. 533–553.

Andersen, T., Bollerslev, T., Diebold, F. & Labys, P. (2000b), 'Great realizations', *Risk* **13**, 105–108.

Andersen, T., Bollerslev, T., Diebold, F. X. & Ebens, H. (2001), 'The distribution of realized stock return volatility', *Journal of Financial Economics* **61**(1), 43–76.

Andersen, T. G. & Bollerslev, T. (1997), 'Answering the Skeptics: Yes, Standard Volatility Models Do Provide Accurate Forecasts', *International Economic Review* **39**, 885–905.

Andersen, T. G., Bollerslev, T., Diebold, F. X. & Labys, P. (1999), '(understanding, optimizing, using and forecasting) realized volatility and correlation', *Manuscript, Northwestern University, Duke University and University of Pennsylvania.* (99-061).
URL: *http://ideas.repec.org/p/fth/nystfi/99-061.html*

Andersen, T. G., Bollerslev, T., Diebold, F. X. & Labys, P. (2001), 'The distribution of realized exchange rate volatility', *Journal of the American Statistical Association* **96**.

Andersen, T. G., Bollerslev, T. & Meddahi, N. (2011), 'Realized volatility forecasting and market microstructure noise', *Journal of Econometrics* **160**(1), 220–234.

Andersen, T. G., Dobrevb, D. & Schaumburg, E. (2012), 'Jump-robust volatility estimation using nearest neighboor truncation', *Journal of Econometrics* **169**, 75–93.

Anderson, E. W., Hansen, L. P. & Sargent, T. J. (2003), 'A quartet of semigroups for model specification robustness prices of risk and model detection', *Journal of the European Economic Association* **1**, 68–123.

Andreou, E. & Ghysels, E. (2002), 'Rolling-sample volatility estimators: Some new theoretical, simulation, and empirical results', *Journal of Business & Economic Statistics* **20**(3), pp. 363–376.

Ang, A. & Bekaert, G. (1998), 'Regime switches in interest rates', *Journal of Business & Economic Statistics* **20**(6508), 163–182.

Ang, A. & Piazzesi, M. (2003), 'A no-arbitrage vector autoregression of term structure dynamics with macroeconomic and latent variables', *Journal of Monetary Economics* **50**, 745–787.

Aït-Sahalia, Y., Mykland, P. & Zhang, L. (2005), 'How often to sample a continuous-time process in the presence of market microstructure noise', *Review of Financial Studies* **18**, 351–416.

Baker, S., Bloom, N. & Davis, S. J. (2012), 'Measuring economic policy uncertainty', *Manuscript Stanford University* .

Balduzzi, P., Elton, E. & Green, T. (2001), 'Economic news and bond prices: evidence from the u.s. treasury market.', *Journal of Financial and Quantitative Analysis* **36**, 523–543.

Bandi, F. & Russell, J. (2008), 'Microstructure noise, realized variance, and optimal sampling', *Review of Economic Studies* **75**(2), 339–369.

Bansal, R. & Shaliastovich, I. (2013), 'A Long-Run Risks Explanation of Predictability Puzzles in Bond and Currency Markets', *Review of Financial Studies* **26**(1), 1–33.
URL: *http://ideas.repec.org/a/oup/rfinst/v26y2013i1p1-33.html*

Bansal, R. & Yaron, A. (2004), 'Risks for the long run: A potential resolution of asset pricing puzzles', *The Journal of Finance* **59**, 1481–1509.

Barndorff-Nielsen, O. E., Hansen, P. R., Lunde, A. & Shephard, N. (2004), Regular and modified kernel-based estimators of integrated variance: The case with independent noise, Working paper, Stanford University.

Barndorff-Nielsen, O. E., Nielsen, B., Shephard, N. & Ysusi, C. (2002), Measuring and forecasting financial variability using realised variance with and without a model, Economics Papers 2002-W21, Economics Group, Nuffield College, University of Oxford.
URL: *http://ideas.repec.org/p/nuf/econwp/0221.html*

Barndorff-Nielsen, O. E. & Shephard (2002), 'Econometric analysis of realized volatility and its use in estimating stochastic volatility models', *Journal Of The Royal Statistical Society Series B* **64**(2), 253–280.

Barndorff-Nielsen, O. E. & Shephard, N. (2001), 'Non-gaussian ornstein-uhlenbeck-based models and some of their uses in financial economics', *Journal Of The Royal Statistical Society Series B* **63**(2), 167–241.

Bauer, M. D. & Rudebusch, G. D. (2015), 'Resolving the spanning puzzle in macro-finance term structure models'.

Bekaert, G., Engstrom, E. & Xing, Y. (2009), 'Risk, uncertainty, and asset prices', *Journal of Financial Economics* **91**(1), 59–82.

Bekaert, G., Harvey, C. R., Lundblad, C. T. & Siegel, S. (2012), 'Political risk and international valuation', *NBER WORKING PAPER SERIES* .

Belo, F., Gala, V. & Li, J. (2013), 'Government spending, political cycles and the cross section of stock returns', *Journal of Financial Economics* **107**, 305–324.

Bialkowski, J., Gottschalk, K. & Wisnieski, T. (2008), 'Stock market volatility around national elections', *Journal of Banking and Finance* **32**, 1941–1953.

Billingsley, P. (2008), *Convergence of Probability Measures*, Wiley.

Bloom, N. (2009), 'The impact of uncertainty shocks', *Econometrica* **77**(3), 623–685.

Bond, P. & Goldstein, I. (2012), 'Government intervention and information aggregation by prices', *Working Paper* .

Boutchkova, M. K., Doshi, H., Durnev, A. & Molchanov, A. (2012), 'Precarious politics and return volatility', *The Review of Financial Studies* **25**, 1111–1154.

Box, G., Jenkings, G. & Reseinsel, G. (1994), *Time Series Analysis: Forecasting and Control*, third edn, Upper Saddle River NJ: Prentice Hall.

Branger, N., Kraft, H. & Meinerdin, C. (2014), 'Partial information about contagion risk, self-exciting processes and portfolio optimization', *Journal of Economic Dynamics & Control* **39**, 18–36.

Brogaard, J. & Detzel, A. (2012), 'The asset pricing implications of government economic policy uncertainty', *Working Paper* .

Buraschi, A., Carnelli, A. & Whelan, P. (2014), 'Monetary policy and treasury risk premia', *Working Paper* .

Buraschi, A. & Jiltsov, A. (2005), 'Inflation risk premia and the expectation hypothesis', *Journal of Financial Economics* **75**, 429–490.

Buraschi, A. & Jiltsov, A. (2007), 'Habit formation and macroeconomic models of the term structure of interest rates', *The Journal of Finance* **6**, 3009–30063.

Cai, J. (1994), 'A Markov Model of Unconditional Variance in ARCH', *Journal of Business and Economic Statistics* **12**, 309–316.

Campbell, S. D. (2002), Specification testing and semiparametric estimation of regime switching models: An examination of the us short term interest rate, Working papers, Brown University, Department of Economics.

Carr, P., Jin, X. & Madan, D. B. (2001), 'Optimal investment in derivative securities', *Finance and Stochastics* **5**, 33–59.

Chen, F., Diebold, F. & Schorfheide, F. (2013), 'A markov-switching multifractal inter-trade duration model, with application to us equities', *Journal of Econometrics* **forthcoming**.

Chen, Z. & Epstein, L. (2002), 'Ambiguity, risk and asset returns in continuous time.', *Econometrica* **70**, 1403–1443.

Chiogna, M. (1998), 'Some results on the scalar skew-normal distribution', *Statistical Methods and Applications* **7**, 1–13.

Choulli, T. & Hurd, T. R. (2001), The portfolio selection problem via Hellinger processes, Technical report, McMaster University.

Christensen, K. & Podolskij, M. (2007), 'Realized range-based estimation of integrated variance', *Journal of Econometrics* **141**(2), 323–349.

Cochrane, J. & Piazzesi, M. (2005), 'Bond risk premia', *American Economic Review* **95**, 138–160.

Cogley, T., Colacito, R., Hansen, L. P. & Sargent, T. J. (2008), 'Robustness and u.s. monetary policy experimentation', *Journal of Money, Credit and Banking* **40**, 1599–1623.

Cont, R. (2001), 'Empirical properties of asset returns: stylized facts and statistical issues', *Quantitative Finance* **1**, 223–236.

Cox, J., Iingersoll, J. & Ross, S. (1985), 'A theory of the term structure of interest rates', *Econometrica* **53**, 385–408.

Cvitanić, J., Polimenis, V. & Zapatero, F. (2008), 'Optimal portfolio allocation with higher moments', *Annals of Finance* **4**, 1–28.

Dacorogna, M. M., Gencay, R., Müller, U., Olsen, R. B. & Pictet, O. (2001), *An Introduction to High-Frequency Finance*, Academic press.

Das, S. R. & Uppal, R. (2004), 'Systemic risk and international portfolio choice', *The Journal of Finance* **59**, 2809–2834.

David, A. & Veronesi, P. (2014), 'Investors' and central bank's uncertainty embedded in index options', *Review of Financial Studies* **27**(6), 1661–1716.

de Goeij, P. & Marquering, W. (2006), 'Macroeconomic announcements and asymmetric volatility in bond returns', *Journal of Banking and Finance* **30**(10), 2659–2680.

Delong, L. & Klüppelberg, C. (2008), 'Optimal investment and consumption in a Black-Scholes market with Lévy-driven stochastic coefficients', *Annals of Applied Probability* **18**, 879–908.

DeMiguel, V., Garlappi, L., Nogales, F. J. & Uppal, R. (2009), 'Optimal versus naive diversifcation: How inefficient is the $1/n$ portfolio strategy?', *Review of Financial Studies* **55**, 798–812.

Drechsler, I. (2013), 'Uncertainty, time-varying fear, and asset prices', *The Journal of Finance* **68**, 1843–1889.

Duffie, D. & Kan, R. (1996), 'A yield factor model of interest rates', *Mathematical Finance* **6**, 379–406.

Durnev, A. (2010), 'The real effects of political uncertainty: Elections and investment sensitivity to stock prices', *Working Paper* **University of Iowa**.

Dutoit, L. C. (2007), 'Heckman's Selection Model, Endogenous and Exogenous Switching Models, A Survey', *Working Paper* **42**, 27–62.

Ebens, H. (1999), 'Realized stock volatility', Working Paper 420.

Emmer, S. & Klüppelberg, C. (2004), 'Optimal portfolios when stock prices follow an exponential Lévy process', *Finance and Stochastics* **8**, 17–44.

Engle, R. F. & Sun, Z. (2007), When is noise not noise - a microstructure estimate of realized volatility, Working paper, NYU Working Paper No. FIN07-047.

Evans, C. & Marshall, D. (2007), 'Economic determinants of the nominal treasury yield curve', *Journal of Monetary Economics* **54**, 1986–2003.

Fama, E. & French, K. (1989), 'Business conditions and expected returns on stocks and bonds', *Journal of Financial Economics* **25**, 23–49.

Fang, Y. (1996), 'Volatility modeling and estimation of high-frequency data', *Econometric Society* .

Fisher, S. & Modigliani, F. (1978), 'Towards an understanding of the real effects and costs of inflation', *Weltwirtschaftliches Archiv* **114**, 810–832.

Fleming, M. & Piazzesi, M. (2005), 'Monetary policy tick-by-tick', *Working Paper* .

Frijns, B. & Lehnert, T. (2004), Realized variance in the presence of non-iid microstructure noise, Working Paper 04-008, Economics Group, Nuffield College, University of Oxford.

Gallmeyer, M. F., Hollifield, B., Palomino, F. & Zin, S. E. (2007), Arbitrage-free bond pricing with dynamic macroeconomic models, Working Paper 13245, National Bureau of Economic Research.
URL: *http://www.nber.org/papers/w13245*

Ghysels, E., Santa-Clara, P. & Valkanov, R. (2006), 'Predicting volatility: getting the most out of return data sampled at different frequencies', *Journal of Econometrics* **131**(1-2), 59–95.

Gilbao, I. & Schmeidler, D. (1989), 'Maxmin expected utility with a non-unique prior', *Journal of Mathematical Economics* **18**, 141–153.

Goncalves, S. & Meddahi, N. (2008*a*), 'Edgeworth corrections for realized volatility', *Econometric Reviews* **27**.

Goncalves, S. & Meddahi, N. (2008*b*), 'Edgeworth corrections for realized volatility', *Econometric Reviews* **27**, 139–162.

Gray, S. (1996), 'Modelling the conditional distribution of interest rates as a regime - switching process', *Journal of Financial Economics* **42**, 27–62.

Gürkaynak, R. S., Sack, B. & Swanson, E. (2005*a*), 'Do actions speak louder than words? the response of asset prices to monetary policy actions and statements', *International Journal of Central Banking* pp. 55–93.

Gürkaynak, R. S., Sack, B. & Swanson, E. (2005*b*), 'The sensitivity of long-term interest rates to economic news: Evidence and implications for macroeconomic models', *The American Economic Review* **95**, 425–426.

Gulen, H. & Ion, M. (2012), 'Policy uncertainty and corporate investment', *Working Paper* .

Haas, F., Mittnik, S. & Paolella, M. S. (2004), 'A New Approach to Markov - Switching GARCH Models', *Journal of Financial Econometrics* .

Hamilton, J. (1989), 'A New Approach to the Economic Analysis of Nonstationary Time Series and the Business Cycle', *Econometrica* **57**, 357–384.

Hamilton, J. & Susmel, R. (1994), 'Autorgressive Conditional Heteroskedasticity and Changes in Regime', *Journal of Econometrics* **64**, 307–333.

Han, S. & Rachev, S. (2000), 'Portfolio management with stable distributions', *Mathematical Methods of Operations Research* **51**, 341–352.

Hansen, L. P., Heaton, J. C. & Li, N. (2008), 'Consumption strikes back? measuring long?run risk', *Journal of Political Economy* **116**(2), pp. 260–302.

Hansen, L. P., Sargent, T. J., Turmuhambetova, G. & Williams, N. (2006), 'Robust control and model misspecification', *Journal of Economic Theory* **128**, 45–90.

Hansen, L. & Sargent, T. (2001), 'Robust control and model uncertainty', *The American Economic Review* **91**, 60–66.

Hansen, L. & Sargent, T. (2008), *Robustness*, Princeton University Press.

Hansen, L. & Sargent, T. J. (2010), 'Fragile beliefs and the price of uncertainty', *Quantitative Economics* **1**, 129–162.

Hansen, L. & Sargent, T. J. (2011), 'Robustness and ambiguity in continuous time', *Journal of Economic Theory* **146**, 1195–1223.

Hansen, P. & Lunde, A. (2003), 'An optimal and unbiased measure of realized variance based on intermittent high-frequency data', *Mimeo prepared for the CIREQ-CIRANO Conference: Realized Volatility* .

Hansen, P. R. & Lunde, A. (2006), 'Realized variance and market microstructure noise', *Journal of Business & Economic Statistics* **24**(2), 127–161.

Harris, L. (1990), 'Estimation of stock price variances and serial covariances from discrete observations', *Journal of Financial and Quantitative Analysis* **25**(3), pp. 291–306.

Harris, L. (1991), 'Stock price clustering and discreteness', *Review of Financial Studies* **4**(3), pp. 389–415.

Hasbrouck, J. (2004), *Empirical Market Microstructure: Economic and Statistical Perspectives on the Dynamics of Trade in Secuirties Markets*, lecture notes, New York University, Stern School of Business.

Huang, T., Wu, F., Yu, J. & Zhang, B. (2013), 'Political risk and government bond pricing', *Working Paper* .

Jacod, J., Li, Y., Mykland, P. A., Podolskij, M. & Vetter, M. (2009), 'Microstructure noise in the continuous case: The pre-averaging approach', *Stochastic Processes and their Applications* **119**(7), 2249 – 2276.

Jacod, J. & Protter, P. (2012), *Discretization of Stochastic Processes*, Springer Verlag Berlin Heidelberg.

Jacod, J. & Shiryaev, A. (2003), *Limit Theorems for Stochastic Processes*, 2nd ed. edn, Springer.

Jeanblanc-Picqué, M. & Pontier, M. (1990), 'Optimal portfolio for a small investor in a market model with discontinuous prices', *Applied Mathematics and Optimization* **22**, 287–310.

Joslin, S., Priebisch, M. & Singleton, K. (2014), 'Risk premiums in dynamic term structure models with unspanned macro risks', *The Journal of Finance* **69**, 1197–1233.

Joslin, S., Priebsch, M. & Singleton, K. J. (2014), 'Risk Premiums in Dynamic Term Structure Models with Unspanned Macro Risks', *Journal of Finance* **69**(3), 1197–1233.
URL: *http://ideas.repec.org/a/bla/jfinan/v69y2014i3p1197-1233.html*

Julio, J. & Yook, Y. (2012), 'Political uncertainty and corporate investment cycles', *Journal of Finance* **67**, 45–83.

Kallsen, J. (2000), 'Optimal portfolios for exponential Lévy processes', *Mathematical Methods of Operations Research* **51**, 357–374.

Kang, K. (2010), 'State-Space Models with Endogenous Markov Regime Switching Parameters', *Working Paper* **72**, 217—-257.

Karlin, S. & Taylor, H. M. (1981), *A Second Course inStochastic Processes*, Elsevier.

Kelly, B., Pastor, L. & Veronesi, P. (2013), 'The price of political uncertainty: Theory and evidence from the option market', *Working Paper* .

Kim, C. (2004), 'Markov-Switching Models with Endogenous Explanatory Variables', *Journal of Econometrics* **122**(1), 127–136.

Kim, C. (2009), 'Markov-Switching Models with Endogenous Explanatory Variables ii: A two-step MLE Procedure', *Journal of Econometrics* **148**(1), 46–55.

Kim, C. J., Piger, J. M. & Startz, R. (2008), 'Estimation of Markov Regime - Switching Regression Models with Endogenous Switching', *Journal of Econometrics* **143**, 263–273.

Kimhi, A. (1999), 'Estimation of an endogenous switching regression model with discrete dependent variables: Monte-carlo analysis: and empirical application of three estimators', *Empirical Economics* (24), 224–241.

Klaassen, F. (2002), 'Improving GARCH Volatility Forecasts with Regime - Switching GARCH', *Empirical Economics* .

Kleshchelski, I. & Vincent, N. (2007), 'Robust equilibrium yield curves', *Working Paper* .

Kogan, L. & Uppal, R. (2001), Risk aversion and optimal portfolio policies in partial and general equilibrium economies, Working paper, Sloan School of Management, MIT.

Koopman, S. J., Jungbacker, B. & Hol, E. (2005), 'Forecasting daily variability of the s&p 100 stock index using historical, realised and implied volatility measurements', *Journal of Empirical Finance* **12**(3), 445–475.

Kuttner, K. N. (2001), 'Monetary policy surprises and interest rates: Evidence from the fed funds futures market', *Journal of Monetary Economics* **47**, 523–544.

Lawler, G. (1995), *Introduction to Stochastic Processes*, Chapman & Hall Probability Series.

Leippold, M., Trojani, F. & Vanini, P. (2007), 'Learning and asset prices under ambiguous information', *The Reviews of Financial Studies* **21**, 2565–2597.

Litterman, R. B. & Scheinkman, J. (1991), 'Common factors affecting bond returns', *The Journal of Fixed Income* **1**, 54–61.

Liu, J., Longstaff, F. & Pan, J. (2003), 'Dynamic asset allocation with event risk', *The Journal of Finance* **58**, 231–259.

Ludvigson, S. & Ng, S. (2009), 'Macro factors in bond risk premia', *Review of Financial Studies* **22**, 5027–5067.

Lui, J., Pan, J. & Wang, T. (2005), 'An equilibrium model of rare-event premia and its implication for option smirks', *Review of Financial Studies* **18**, 131–164.

Madan, D. B. (2004), Equilibrium asset pricing with non-Gaussian factors and exponential utilities, Technical report, University of Maryland.

Maenhout, P. J. (2004), 'Robust portfolio rules and asset pricing', *The Reviews of Financial Studies* **17**, 951–983.

Maenhout, P. J. (2006), 'Robust portfolio rules and detection-error probabilities for a mean-reverting risk premium', *Journal of Economic Theory* **128**, 136–163.

Maheu, J. M. & McCurdy, T. H. (2002), 'Nonlinear features of realized fx volatility', *The Review of Economics and Statistics* **84**(4), 668–681.

Meddahi, N. (2002), 'A theoretical comparison between integrated and realized volatility', *Journal of Applied Econometrics* **17**(5), 479–508.

Merton, R. C. (1969), 'Lifetime portfolio selection under uncertainty: The continuous-time case', *Review of Economics and Statistics* **51**, 247–257.

Merton, R. C. (1971), 'Optimum consumption and portfolio rules in a continuous-time model', *Journal of Economic Theory* **3**, 373–413.

Mun, F. (1998), 'The Dynamics of DM/L Exchange Rate Volatility: A SWARCH Analysis', *International Journal of Finance & Economics* **3**(1), 59–71.

Mykland, A. & Zhang, L. (2006), 'Anova for diffusions and itÔ processes'.

Newey, W. & West, K. (1994), 'Automatic lag selection in covariance estimation', *Review of Economic Studies* **61**, 631–653.

Norris, J. (1998), *Markov Chains*, Cambrigde Series in Statistical and Probabilistic Mathematics.

O'Hara, M. (1995), *Market Microstructure Theory*, London: Blackwell.

Øksendal, B. (2003), *Stochastic differential equations*, Springer.

Oomen, R. (2002), 'Modelling realized variance when returns are serially correlated', *unpublished manuscript,University of Warwik, Warwik Business School* .

Ortobelli, S., Huber, I., Rachev, S. T. & Schwartz, E. S. (2003), Portfolio choice theory with non-Gaussian distributed returns, *in* S. T. Rachev, ed., 'Handbook of Heavy Tailed Distributions in Finance', Elsevier Science B.V., Amsterdam, The Netherlands, pp. 547–594.

Otranto, E., Calzolari, G. & Iorio, F. D. (2005), Indirect estimation of markov switching models with endogenous switching, Mpra paper no. 22983, Universita' di Firenze.

Owens, J. & Steigerwald, D. G. (2009), Noise reduced realized volatility: A kalman filter approach, University of California at Santa Barbara, Economics Working Paper Series 866293, Department of Economics, UC Santa Barbara.
URL: *http://ideas.repec.org/p/cdl/ucsbec/866293.html*

Pastor, L. & Veronesi, P. (2012), 'Uncertainty about government policy and stock prices', *Journal of Finance* **4**, 1219–1264.

Pastor, L. & Veronesi, P. (2013), 'Political uncertainty and risk premia', *Journal of Financial Economics* **110**, 520–545.

Pennacchi, G. (1991), 'Identifying the dynamics of real interest rates and inflation evidence using survey data', *The Review of Financial Studies* **4**, 53–86.

Piazzesi, M. (2005), 'Bond yields and the federal reserve', *Journal of Political Economy* **112**, 311–344.

Piazzesi, M. & Schneider, M. (2006), 'Equilibrium yield curves', *NBER WORKING PAPER SERIES* .

Pindyck, R. & Solimano, A. (1993), 'Economic instability and aggregate investment', *NBER WORKING PAPER SERIES* .

Protter, P. (2004), *Stochastic Integration and Differential Equations*, Springer.

Rodrik, D. (1991), 'Policy uncertainty and private investment in developing countries', *Journal of Development Economics* **36**, 229–242.

Sbuelz, A. & Trojani, F. (2008), 'Asset prices with locally constraint entropy recursive multiple prior utility', *Journal of Economic Dynamics & Control* **32**, 3695– 3717.

Shiller, R. (1979), 'The volatility of long-term interest rates and expectations models of the term structure', *Journal of Political Economy* **87**, 1190–1219.

Shirakawa, H. (1990), Optimal dividend and portfolio decisions with Poisson and diffusion-type return process, Technical report, Tokyo Institute of Technology.

Sims, C. A. & Zha, T. (2006), 'Were there regime switches in us monetary policy', *American Economic Review* **96**, 54–81.

Timmermann, A. (2000), 'Moments of Markov Switching Models', *Journal of Econometrics* **96**(1), 75–111.

Trojani, F. & Vanini, P. (2000), 'A note on robustness in merton's model of intertemporal consumption and portfolio choice', *Journal of Economic Dynamics & Control* **26**, 423–435.

Trojani, F. & Vanini, P. (2004), 'Robustness and ambiguity aversion in general equilibrium', *Review of Finance* **8**, 279–324.

Turner, C. M., Startz, R. & Nelson, C. R. (1989), 'A Markkov Model of Heteroskedasticity, Risk and Learning in the Stock Market', *Journal of Financial Economics* **25**, 3—-22.

Ulrich, M. (2010), 'Observable long-run ambiguity and long-run risk.', *Working Paper, Columbia Business School* .

Ulrich, M. (2012), 'Economic policy uncertainty & asset price volatility', *Working Paper, Columbia Business School* .

Ulrich, M. (2013*a*), 'Inflation ambiguity and the term structure of u.s. government bonds', *Journal of Monetary Economics* **60**, 295–309.

Ulrich, M. (2013*b*), 'Inflation ambiguity and the term structure of u.s. government bonds', *Journal of Monetary Economics* **60**, 295–309.

Uppal, R. & Wang, T. (2003), 'Model misspecification and under diversification', *The Journal of Finance* **58**, 2465–2486.

Vasicek, O. (1977), 'An equilibrium characterization of the term structure', *Journal of Financial Economics* **5**, 177–188.

Veronesi, P. & Jared, F. (2000), 'Short and long horizon term and inflation risk premia in the us term structure', *Working Paper* .

Wachter, J. A. (2006), 'A consumption-based model of the term structure of interest rates', *Journal of Financial economics* **79**(2), 365–399.

Wasserfallen, W. & Zimmermann, H. (1985), 'The behavior of intraday exchange rates', *Journal of Banking and Finance* **9**, pp.55–72.

Wright, J. (2012), 'What does monetary policy do to long-term interest rates at the zero lower bound?', *The Economic Journal* **122**, 447–66.

X. Bai, Russel J., G. T. (2004), 'Effects of non-normality and dependence on the precision of variance estimates using high-frequency financial data', *Working Paper, University of Chicago, Graduate School of Business* .

Xiong, W. & Yan, H. (2010), 'Heterogenous expectations and bond markets', *Review of Financial Studies* **23**, 1433–1466.

Yin, G. & Zhou, X. Y. (2004), 'Markowitz's mean-variance portfolio selection with regime switching: from discrete-time models to their continuous-time limits', *Automatic Control, IEEE Transactions on* **49**(3), 349 – 360.

Zhang, L. (2004), 'Efficient estimation of stochastic volatility using noisy observations: a multi-scale approach', *bernoulli* **12**(6), 1019–1043.

Zhang, L., Mykland, P. A. & Ait-Sahalia, Y. (2003), A tale of two time scales: Determining integrated volatility with noisy high frequency data, NBER Working Papers 10111, National Bureau of Economic Research, Inc.

Zhou, B. (1996), 'High-frequency data and volatility in foreign-exchange rates', *Journal of Business & Economic Statistics* **14**(1), pp. 45–52.

Felix H. A. Matthys

updated: August 15, 2016

Personal Data

Date of Birth:	22 March 1982
Nationality:	Switzerland
Civil Status:	Single

Employment

Jan 2016 - present	**Assistant Professor** (tenure - track) at the ITAM (Business School)

Education

Oct 2014 - Nov 2015	Postdoctoral Research Fellow (1 year), Finance, **Princeton University** *Bendheim Center For Finance*, Advisor: Prof. Yacine Aït-Sahalia
Nov 2009 - Oct 2014	PhD studies in Finance, *summa cum laude*, **The University of Zurich**, Thesis Title: '*Three Essays in Quantitative Finance*' Supervisor: Prof. Markus Leippold (UZH) Co-Supervisor: Prof. Loriano Mancini (EPFL)
Sep 2009 - Aug 2011	Master of Science in Quantitative Finance, *magna cum laude*, **The ETH and University of Zurich**,
Sep 2007 - Aug 2009	Master of Arts in Banking and Finance, *magna cum laude*, **The University of Zurich**,
Sep 2004 - Aug 2007	Bachelor of Arts in Banking and Finance, *cum laude*, **The University of Zurich**,

Work Experience

Jul 2006 - Nov 2006	Internship at Bank Leu (Credit Suisse) within *Equity Research Devision*, Zurich - Analysis and assessment of relevant macro and micro information on different levels such as stocks, sectors, countries, regions and styles - Provide inputs on sector, country and region level for equity strategy meetings - Compile primary and secondary information on macroeconomic data and writing reports for weekly bank publication
Jul 2004 - present	Member of the board of the real estate company Matthys Immobilien AG, Zurich and since January 2009 president - Strategic and operational guidance of company (corporate strategy) - Financial planning, investment, mortgage and interest risk management - Development of pricing tool for determining market values (rental prices) of apartments - Providing financial reports to Banks and audit company

Grants and Fellowships

Sep 2014	Department of Banking and Finance Fellowship (University of Zurich)
May 2013	Doc.Mobility fellowship from the Swiss National Science Foundation
Dec 2013	Travel Grant (London) Swiss National Science Foundation
Nov 2009	University of Zurich PhD Fellowship

Languages & Computer Skills

English: Fluent, German: Mothertongue, French: Fluent

Good Knowledge: Microsoft Office, Matlab, R, Mathematica

Intermediate Knowledge: C,C++